Paolo Pavone
Massimo Fioranelli
David A. Dowe

CT Evaluation of Coronary Artery Disease

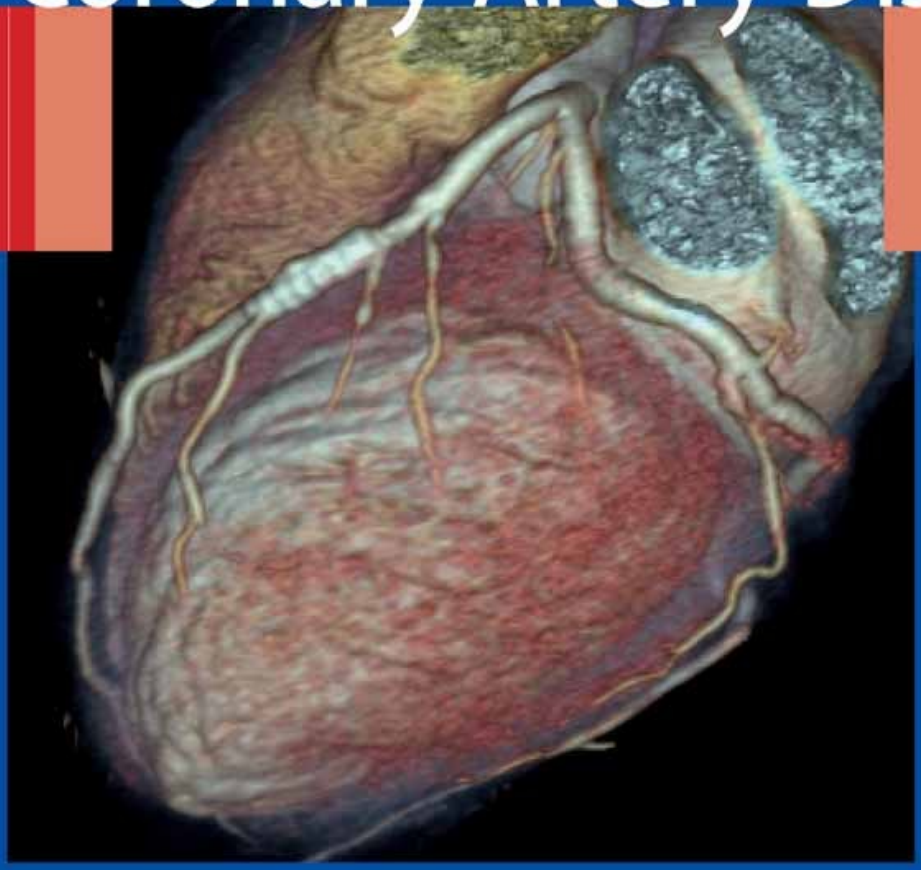

Springer

Paolo Pavone • Massimo Fioranelli • David A. Dowe

CT Evaluation of Coronary Artery Disease

Springer

PAOLO PAVONE
Director, Department of Radiology
"Mater Dei" Hospital
Rome, Italy
Former Chairman
Department of Radiology
University of Parma
Parma, Italy
paolo.pavone@materdei.it

MASSIMO FIORANELLI
Department of Cardiology
"Mater Dei" Hospital
Guglielmo Marconi University
Rome, Italy
massimo.fioranelli@fastwebnet.it

DAVID A. DOWE
Coronary CTA Program Director
Atlantic Medical Imaging
Galloway, NJ, USA

Originally published as:
Malattia coronarica
Fisiopatologia e diagnostica non invasiva con TC
Paolo Pavone, Massimo Fioranelli

Library of Congress Control Number: 2008938918

ISBN 978-88-470-1125-0 Springer Milan Berlin Heidelberg New York
e-ISBN 978-88-470-1126-7

Springer is a part of Springer Science+Business Media
springer.com

Typesetting: C & G di Cerri e Galassi, Cremona, Italy
Printing and binding: Arti Grafiche Nidasio, Assago (MI), Italy

Printed in Italy
Springer-Verlag Italia S.r.l., Via Decembrio 28, I-20137 Milan, Italy

Preface

Coronary CT angiography (CTA) is rapidly changing the patient-care algorithms used to detect coronary artery disease, as well as the approach we take in risk-factor assessment and in the triage of patients. The rapid adoption of coronary CTA into clinical practice has been fueled by significant yearly advances in CT technology, which have improved the spatial and temporal resolution of this technique while simultaneously decreasing radiation exposure.

The growing utilization of coronary CTA has created a need for comprehensive didactic texts that explain the numerous applications of this new technology with respect to the pathophysiology of coronary artery disease, while also providing information on the approach to patients who have undergone previous bypass surgery or percutaneous coronary intervention. I believe this book accomplishes both of these goals, and does so in a reader-friendly format. The image quality of the many figures that accompany each chapter is excellent and reflects the use of state of the art technology. The techniques described for plaque detection and characterization represent the current thinking pervasive in the coronary CTA community. The comprehensive reference list at the end of the book offers the reader a wealth of resources for further study.

There is no doubt that this book will be popular with radiologists, cardiologists, CT technologists and anyone else seeking to acquire a comprehensive understanding of coronary artery disease and its depiction using coronary CTA.

Galloway, October 2008 *David A. Dowe, MD*

Contents

Contributors

Fabrizio Clementi
Interventional Cardiology Unit
"Tor Vergata" University
Rome, Italy

Marcello De Santis
Department of Radiology
"Mater Dei" Hospital
Rome, Italy

Sara di Michele
Department of Cardiology
"Mater Dei" Hospital
Rome, Italy

Massimo Fioranelli
Department of Cardiology
"Mater Dei" Hospital
Guglielmo Marconi University
Rome, Italy

Carlo Gonnella
Department of Cardiology
"Mater Dei" Hospital
Rome, Italy

Chiara Lanzillo
Department of Cardiology
"Mater Dei" Hospital
Rome, Italy

Roberto Leo
Department of Internal Medicine
"Tor Vergata" University
Rome, Italy

Antonio Lucifero
Department of Cardiology
"Mater Dei" Hospital
Rome, Italy

Enrica Mariano
Interventional Cardiology Unit
"Tor Vergata" University
Rome, Italy

Vincenzo Pasceri
Interventional Cardiology Unit
San Filippo Neri Hospital
Rome, Italy

Paolo Pavone
Department of Radiology
"Mater Dei" Hospital
Rome, Italy

Francesco Peverini
Department of Internal Medicine
"Mater Dei" Hospital
Rome, Italy

Maddalena Piro
Department of Cardiology
"Mater Dei" Hospital
Molecular and Cellular Cardiology
Sacred Heart University
Rome, Italy

Giuseppe M. Sangiorgi
Interventional Cardiology Unit
Emo Centro Cuore Columbus
San Raffaele Hospital
Milan, Italy

Francesca Sbandi
Department of Cardiology
"Mater Dei" Hospital
Rome, Italy

Paolo Sordini
Heart Surgery Unit
San Filippo Neri Hospital
Rome, Italy

Giulio Speciale
Interventional Cardiology Unit
San Filippo Neri Hospital
Rome, Italy

Stefano Tonioni
Interventional Cardiology Unit
Fatebenefratelli, San Pietro Hospital
Rome, Italy

1

Clinical Anatomy of the Coronary Circulation

Massimo Fioranelli, Carlo Gonnella, Stefano Tonioni

In the anatomic evaluation of the coronary arteries by multi-slice computed tomography (MSCT), the classification of the American Heart Association, which divides these vessels into 15–16 segments, including those segments with diameters > 1.5 mm, is often used (Fig. 1.1). In this chapter, a more complex classification will be applied as it provides a more detailed anatomic picture.

The right coronary artery (RCA) takes origin from the right aortic sinus of Valsalva and then divides to form two terminal branches, the posterior descending artery (PDA) and the posterolateral (PLV) branches. Along its

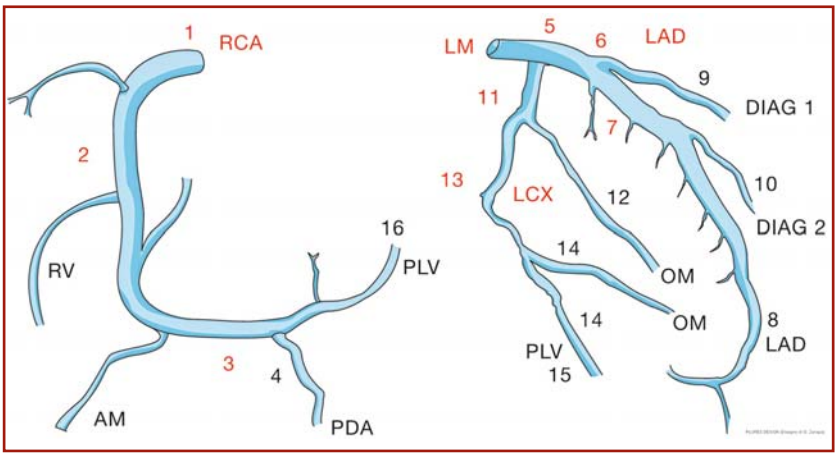

Fig. 1.1. The American Heart Association divides the coronary tree into *15–16* segments. *RCA* Right coronary artery, *RV* right ventricular branch, *AM* acute marginal branch, *PLV* posterolateral ventricular branch, *PDA* posterior descending artery, *LCA* left coronary artery, *LM* left main artery, *LAD* left anterior descending artery, *DIAG 1* 1st diagonal branch, *DIAG 2* 2nd diagonal branch, *LCx* left circumflex artery, *OM* obtuse marginal branches

P. Pavone, M. Fioranelli, D.A. Dowe, *CT Evaluation of Coronary Artery Disease*.

course, the RCA gives off several branches: the sinus node artery, right ventricular (RV) branches, acute marginal (AM) branch, and the atrioventricular node artery.

The left coronary artery (LCA) arises from the left aortic sinus; the left main (LM) branch of the LCA ends in a bifurcation, giving rise to the left anterior descending artery (LAD) and the left circumflex artery (LCx); sometimes, a third ramus intermedius is present between these two branches. The LAD gives off septal (SP) and diagonal (DIAG) branches and ends at the the apex of the heart, sometimes reaching the posterior interventricular groove. The LCx has two or three marginal branches (OM), before either terminating or, in the case of left-dominant or balanced circulation, giving off a posterolateral branch or ending in the posterior atrioventricular groove. Figure 1.1 shows the myocardial areas perfused by the RCA, LAD, and LCx.

Angiographic Anatomy of the Coronary Circulation

In the following, the coronary anatomy is described using the classification proposed in the *Bypass Angioplasty Revascularization Investigation* (BARI) trial reported by Alderman and Stadius (1992), in which the coronary arteries are separated into 29 segments (Fig. 1.2).

The coronary trees have two principal components: (1) the arteries and the veins, which course and ramify on the surface of the heart (subepicardial system), and (2) their perforating branches (intramyocardial system).

The subepicardial system is formed by the right and left coronary arteries, arising from the right and left aortic sinus of Valsalva, respectively. The RCA is divided into three segments. The first segment (BARI 1) extends from the coronary ostium to the first RV branch; if the latter is not present, the segment is usually identified between the ostium and the acute margin of the heart. The second segment (BARI 2) extends from the first RV branch to the acute margin of the heart, which usually coincides with the origin of the AM branch (BARI 10). This vessel is the most constant branch of the RCA and it runs on the surface of the free wall of the right ventricle in the direction of the apex, at an angle proportional to the proximity of its origin. The third segment (BARI 3) begins at the acute margin of the heart and courses to the origin of the PDA (BARI 4), at the level of the crux cordis. At this level, in right-dominant circulation (85% of cases), the RCA divides into two terminal branches, the PDA and PLV branches (BARI 5), perfusing the diaphragmatic wall of the left ventricle. In the remaining 15% of cases, the circulation may be left-dominant or balanced: in left-dominant circulation, the PLV and PDA originate from the LCx; in balanced circulation, the PDA originates from the RCA, and the PLV from the LCx.

The concept of dominance is defined by the relationship between the RCA and LCx, according to the origin of the PDA and in relation to the arterial supply of the inferior wall of the left ventricle, but not in relationship to the extent of the circulatory system.

The PDA, also called the posterior interventricular branch, with its septal branches (BARI 9), is the most important branch of the RCA; it courses in the

homonymous groove without reaching the apex of the heart, which is usually supplied by the recurrent branch of the LAD. The PLV immediately originates after the PDA, at the level of the crux cordis. It courses along the posterior atrioventricular sulcus, branching with its collateral vessels (BARI 6–8) at the diaphragmatic and inferioposterior wall of the left ventricle.

The RCA furnishes smaller branches such as the conus artery, sinus node artery, RV branches, and atrioventricular node artery (Fig. 1.3). The conus artery is the first vessel originating from the RCA. In 40% of the cases it directly originates from the right aortic sinus or from the aorta. The sinus node artery arises from the RCA (2/3 of the cases); in the 25% of cases, it may originate from the LCx, while in 10% the two vessels arise from both coronary arteries. The RV branches originate in the second segment of the RCA and run along the surface of the RV, anterior to the interventricular groove. The number

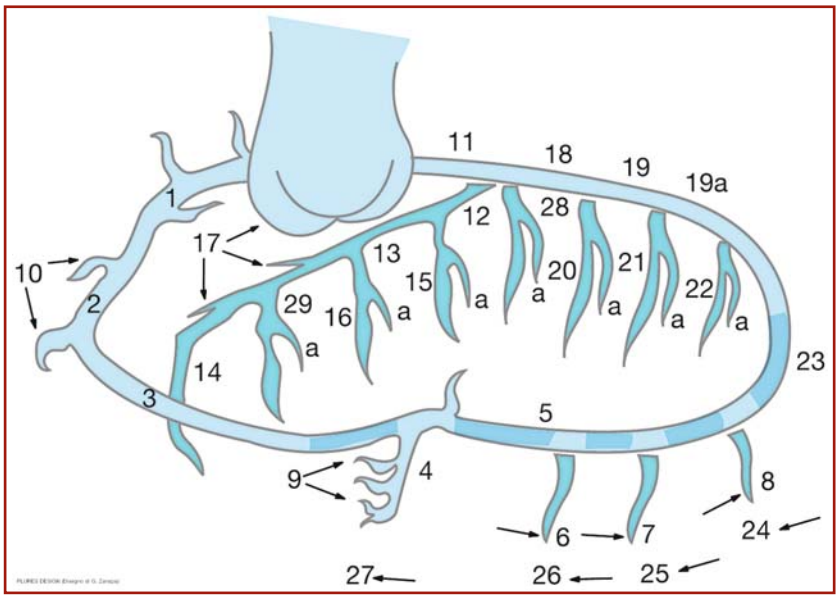

Fig. 1.2. Map of the coronary arterial tree according to the BARI Study Group. This map was used in CASS (Coronary Artery Surgery Study) and includes the diagonal, marginal, and Valsalva branches. The coronary arteries are divided into 29 segments: *1* Proximal segment of the right coronary artery (RCA), *2* middle segment of the RCA, *3* distal segment of the RCA, *4* posterior descending artery (PDA), *5* posterolateral branch of the RCA (PLV), *6* 1st posterolateral branch of the RCA, *7* 2nd posterolateral branch of the RCA, *8* 3rd posterolateral branch of the RCA, *9* inferior septal branches, *10* acute marginal branches of the RCA, *11* left main of the left coronary artery (LM), *12* proximal segment of the left anterior descending artery (LAD), *13* middle segment of the LAD, *14* distal segment of the LAD, *15* 1st diagonal branch (DIAG), *15a* lateral 1st diagonal branch, *16* 2nd diagonal branch, *16a* lateral 2nd diagonal branch, *17* septal branches of the LAD (SP), *18* proximal segment of the left circumflex artery (LCx), *19* middle segment of the LCx, *19a* distal segment of the LCx, *20* 1st obtuse marginal branch (OM), *20a* lateral 1st obtuse marginal branch, *21* 2nd obtuse marginal branch, *21a* lateral 2nd obtuse marginal branch, *22* 3rd obtuse marginal branch, *22a* lateral 3rd obtuse marginal branch, *23* LCx continuing as the left atrioventricular branch, *24* 1st left posterolateral branch, *25* 2nd left posterolateral branch, *26* 3rd left posterolateral branch, *27* left posterior descending artery (PD) (in left-dominant circulation), *28* ramus intermedius, *28a* lateral ramus intermedius, *29* 3rd diagonal branch, *29a* lateral 3rd diagonal branch

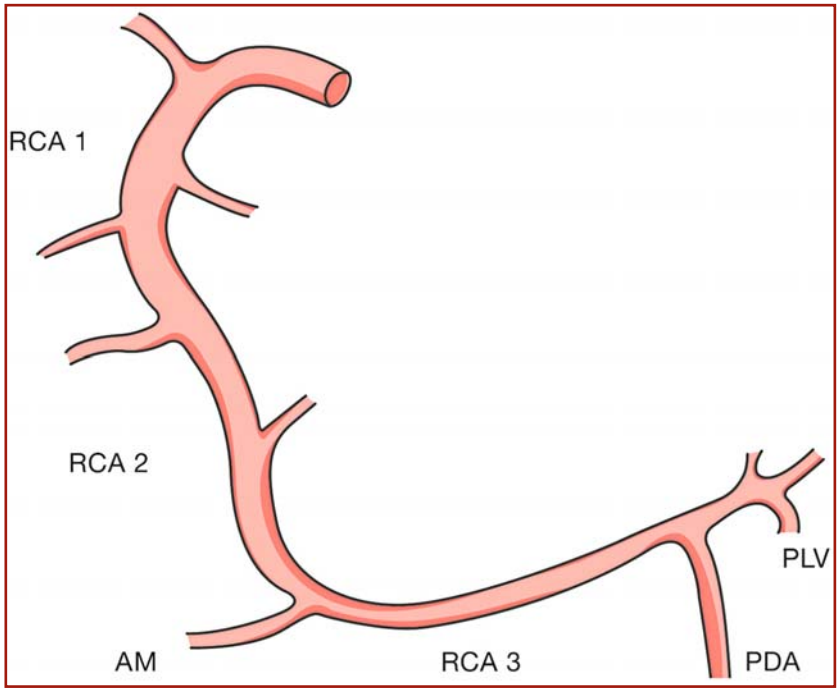

Fig. 1.3. Right coronary artery in left anterior oblique (LAO) view. *RCA* Right coronary artery (segments *1–3*), *AM* acute marginal branch, *PLV* posterolateral branch, *PDA* posterior descending artery

of these branches varies greatly and is inversely proportional to the diameter of such vessels. In 99% of the cases of right-dominant circulation and in 75% of the cases of balanced circulation, the atrioventricular node artery arises at the end of the third segment of the RCA. It is important in the angiographic identification of the crux cordis. In individuals with left-dominant circulation, it originates from the distal segment of the LCx. At the level of Koch's triangle is the subendocardial artery, situated between the septal cuspid of the tricuspid valve and the coronary sinus; it furnishes branches to the posterior interventricular septum and the atrioventricular node.

The LCA arises from the left aortic sinus, at a higher level than the RCA, and is divided into three segments (Fig. 1.4). The LM branch of the LCA (BARI 11) extends for a varying length (generally 2 cm, diameter 3–6 mm) from the ostium to the bifurcation of the LAD and LCx. In 30–37% of the cases, the LM artery gives off three branches, one of which, the ramus intermedius (BARI 28), runs toward the apex and supplies the anterolateral wall of the left ventricle.

The LAD is the most constant, in origin and distribution, among all the coronary vessels. It originates from the LM artery and runs in the anterior interventricular groove to the apex of the heart. In 70% of the cases, the LAD extends up to the posterior interventricular groove such that it furnishes branches for perfusion of the inferior interventricular septum and the apex; otherwise, these arise along the length of the PDA. The first segment of the LAD (BARI 12) runs from the bifurcation of the LM artery to the origin of

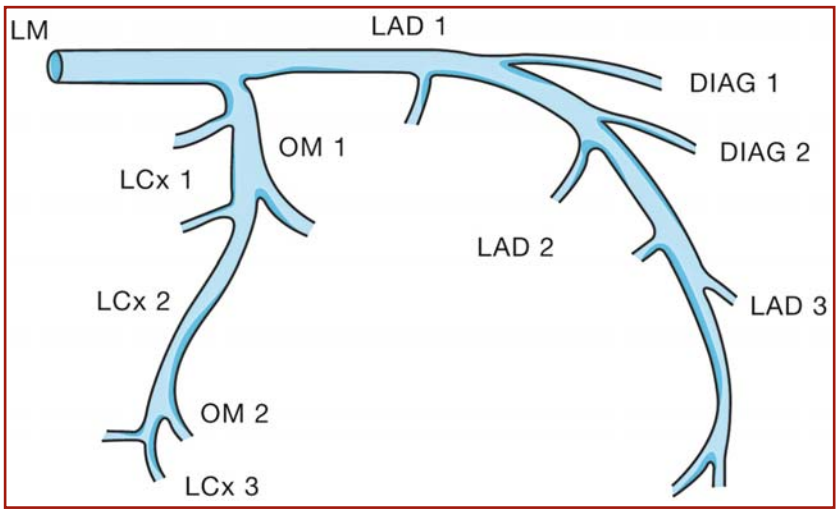

Fig. 1.4. Left coronary artery in caudal right anterior oblique (RAO) view. *LM* Left main artery, *LAD* left anterior descending artery (segments *1–3*), *DIAG 1* 1st diagonal branch, *DIAG 2* 2nd diagonal branch, LCX left circumflex artery (segments *1–3*), *OM 1* 1st obtuse marginal branch, *OM 2* 2nd obtuse marginal branch

the first septal branch (SP, BARI 17). The second segment (BARI 13) extends from the origin of the first septal branch to the origin of the third septal or second DIAG branch. The third segment (BARI 14) ends at the apex, surrounding and sometimes traveling up to the posterior wall. When the third SP or second DIAG branch is not identified, the end of the second segment of the LAD is conventionally defined as the half-length between the first SP and the apex. The LAD furnishes branches for the anterior interventricular septum and the anterolateral wall of the left ventricle. There are generally three SP branches and they originate at right angles from the LAD.

The first SP branch is constant in its origin and course; thus, it is important to identify its passage between the proximal and middle segments of the LAD. Some segments may run intramyocardially, but generally they develop caudally, along the interventricular septum, and supply the proximal two-thirds of the anterior septum. The second and third SP branches are more variable, with narrow diameters; they supply the distal third of the anterior septum. There are usually three DIAG branches (BARI 15, 16–29), each of which originates at an acute angle from the LAD; their pathway is to the anterolateral wall of the left ventricle. The diameter of these vessels is inversely proportional to the number of branches.

The LCx develops from the LM artery and runs in the posterior atrioventricular groove; after a short tract under the left atrium, it continues in the left posterior atrioventricular groove and contacts the mitral annulus. The LCx splits into three segments. The first (BARI 18) extends from the origin to the first marginal branch (OM, BARI 20). If the first OM is absent or not clearly identifiable, the zone of transition among the first and second segments is conventionally identified by a point corresponding to the half-length between the origin of the LCx and the origin of the second OM (BARI 21). The second

segment (BARI 19) runs from the origin of the first OM to the origin of the second OM. If the second marginal branch is absent, the zone of transition is defined by the half-length between the origin of the first OM and the point where the circumflex artery terminates. The third segment (BARI 19a), in right-dominant circulation, extends from the origin of the second OM to the termination point of the vessel; in left-dominant or balanced circulation, to the point of origin of the left ventricular branch or the posterolateral branch in the posterior atrioventricular groove (BARI 23). In left-dominant circulation, the LCx gives rise to the left ventricular branch or PLV, with its side branches (BARI 24–26) and to the PDA (BARI 27), with its septal branches (BARI 9).

The LCx gives rise to the sinus node artery, left atrial branch, and marginal branches. In 25% of the cases, the sinus node artery arises from the proximal segment of the LCx, near the ostium. The atrial branch originates at the end of the proximal segment and runs to the inferoposterior wall of the left atrium. Of the three OM branches, the first one is usually larger and constant; it terminates on the posterolateral wall of the left ventricle toward the apex. Its development is inversely proportional both to the extent of the RCA on the posterolateral surface of the left ventricle and to the number and development of the diagonal branches of the LAD.

Intramyocardial Vascularization and the Venous Circulation

After oxygen and nutritional substrates have been extracted by the myocardium, a portion of the desaturated blood is transported directly into the ventricles through the Thebesian veins. Nevertheless, most of the blood, through the venules and myocardial veins, goes to the epicardial veins, which drain in the coronary sinus, located in the inferoposterior region of the right atrium.

The epicardial arteries are muscular vessels with a wall thickness of about 100 μm; they are made up of three overlapping layers: intima, media, and adventitia. These arteries, which transport oxygenated blood to the arteries, arterioles, and capillaries, traverse the surface of the heart covered by epicardium or sometimes by subepicardial adipose tissue. Muscular bridges of variable length, in which the epicardial vessels become intramyocardial, are present in 5–22% of the cases at the anterior LAD and in 86% in the other coronary arteries (Fig. 1.5).

Normal embryological development of the coronary circulation involves the formation of collateral vessels, that link the different sections of the arterial circulation. The collateral circulation consists of four types of vessels: intramyocardial vessels originating from the same vessel (intracoronary circulation), intramyocardial vessels originating from two or more coronary arteries (intercoronary circulation), atrial vessels connecting with the vasas vasorum of the aorta or other arteries (extracardiac circulation), and intramyocardial vessels that directly communicate with the ventricles (arteriolar luminal circulation). In the normal adult myocardium, the collateral circulation consists of small-caliber vessels (< 50 μm in diameter) that contribute only marginally to coronary flow. In the presence of obstruction or myocardial ischemia, the diameter of the collateral vessels expands to 200–600 μm; the growth of a medial layer allows a significant quantity of blood flow. The development of collaterals results in the formation of connections among proximal and distal segments of a vessel crossing a stenosis.

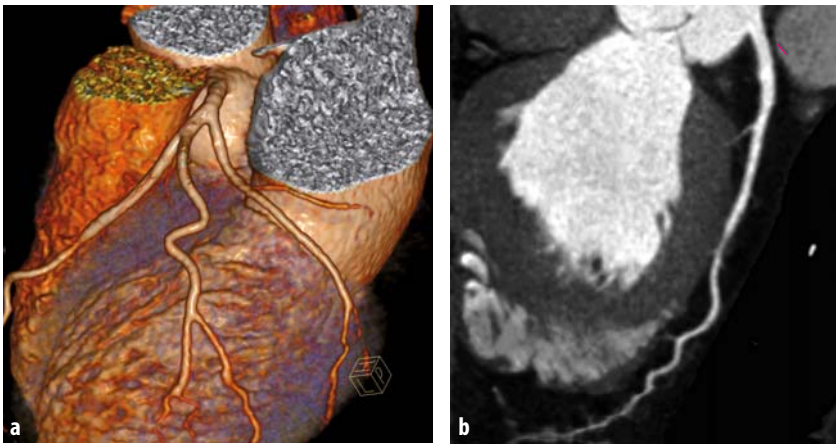

Fig. 1.5 a, b. Myocardial bridging of the left anterior descending artery reduces the arterial diameter

Variability of the Coronary Artery Circulation

The above-described anatomic scheme is highly variable. This is in contrast to other arterial vascular districts, which have a constant, readily identifiable anatomy, such as the carotid, or iliac-femoral arteries, where, except for differences of caliber, the morphology, origin, and anatomic course are the same between individuals. Variations in the coronary arteries include the type of dominance, differences in caliber, and alternative branch morphologies. This aspect of the coronary circulation must be kept in mind during diagnostic evaluation of the arteries, to avoid considering an artery that is small and poorly developed as a stenosis.

The variability of the coronary circulation is such that two patients rarely have the same coronary vascular anatomy. In this context, the use of terminology such as "strongly developed branch" or "hypoplastic vessel" identifies the development of the vessel but does not denote the presence or absence of atherosclerotic lesions. For example, in some patients, the course and caliber of the LCx are highly developed, while in others the artery may be small and perfuse only a small portion of the myocardium. These differences are compensated for by the development of other vessels, which balance the perfusion of a myocardial region by a hypoplastic artery perfusion. The morphology of an artery and the extent of the territory it perfuses are very important considerations in therapeutic planning. The larger the myocardial region perfused by an artery, the greater the justification for a myocardial revascularization procedure in the presence of a critical stenosis.

As shown in Figure 1.6, there are some cases in which the LAD is more developed than the LCx, but in other situations the LCx is more developed and perfuses the largest part of the left ventricle. The caliber of the branches originating from these two arteries depends on the size of the artery from which they derive; that is, the DIAG branches will be of larger caliber than the OM branches when the LAD is more developed than the LCx, while the OM branches will be more developed if the caliber of the LCx is larger.

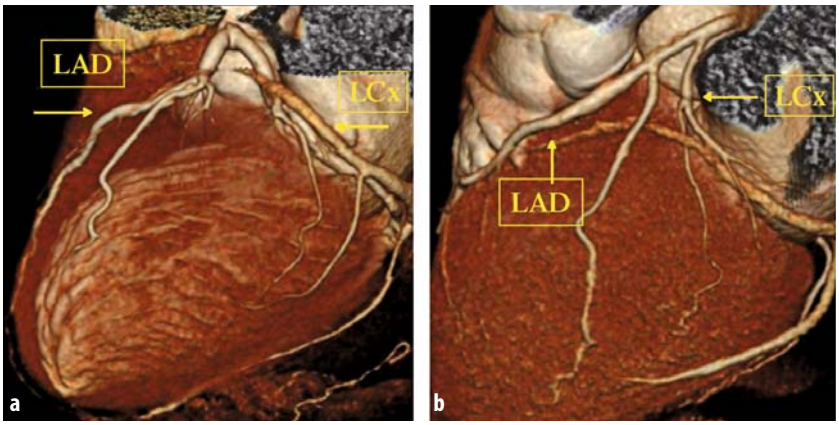

Fig. 1.6 a, b. **a** Hypertrophic left circumflex artery (LCx). **b** Hypoplastic LCx. *LAD* Left anterior descending artery

If the RCA is highly developed, its distal branches (PDA and PLV), in addition to vascularizing the right ventricle, will also perfuse the posterior wall of the left ventricle. In other cases, including right-dominant circulation, the PLV are poorly developed and the great part of the left ventricle is perfused by the LCx (Fig. 1.7).

Finally, the RCA can be hypoplastic, giving rise only to the conus artery after a single AM branch (Fig. 1.8).

These anatomic variations are normal and are not related to ischemic damage. In the presence of atherosclerotic stenosis in a small vessel, the ischemic portion of the myocardium will be correspondingly small. However, when atherosclerosis develops in a main vessel of greater caliber, especially in the proximal segments, the clinical symptoms will be important and the ischemic area large.

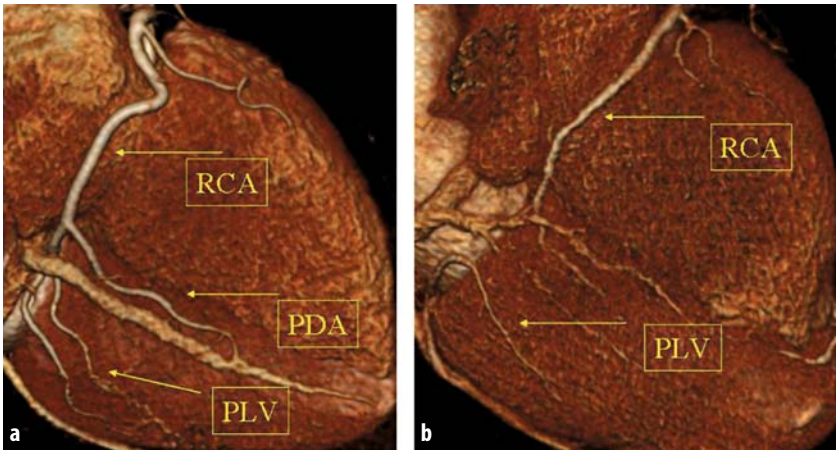

Fig. 1.7 a, b. **a** Right-dominant circulation. **b** Balanced circulation. *RCA* Right coronary artery, *PLV* posterolateral branches, *PDA* posterior descending artery

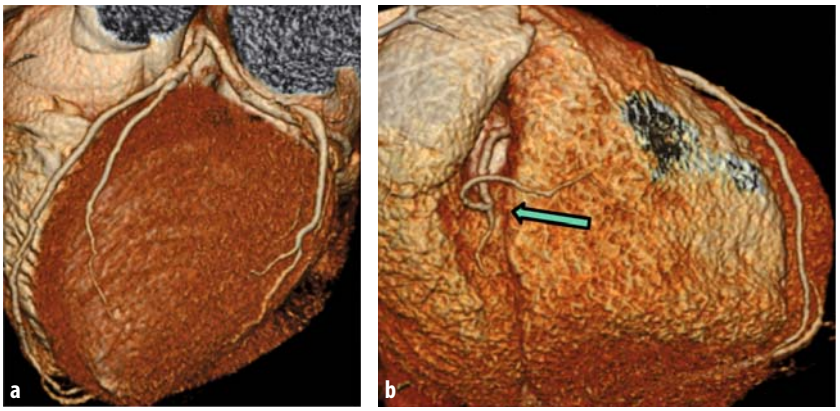

Fig. 1.8 a, b. **a** Left-dominant circulation. The left anterior descending and circumflex arteries are hypertrophic. **b** The right coronary artery (*arrow*) is hypoplastic and branches derive from the acute marginal branch

The classical definition of single-, double-, or triple-vessel disease, referring to the number of vessels with critical stenosis, is tightly correlated to the prognosis and to therapeutic planning; nevertheless, the presence of coronary stenosis must be assessed in the context of the global coronary anatomy. Two-vessel coronary disease is similar to three-vessel disease if the third vessel is a hypoplastic or small artery rather than atherosclerotic.

Anomalous Coronary Arteries

An anomalous coronary artery can be found in 0.64–5.60% of patients who undergo coronary angiography (Fig. 1.9). Some of these variations have no clinical relevance, while others may represent an important pathology. Separate origins of the RCA and conus artery occur in 40–50% of the cases and a

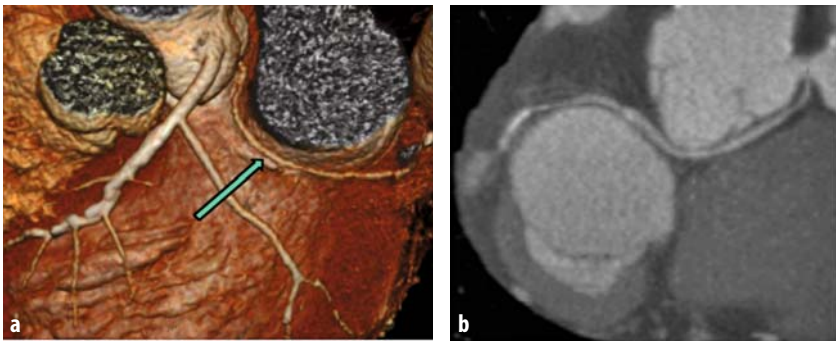

Fig. 1.9 a, b. Anomalous origin of the left circumflex artery from the right coronary artery. In 3D view (**a**) the anomalous vessel (*arrow*) runs between the aorta and the pulmonary artery. In 2D view (**b**) the origin and anomalous and tortuous course of the vessel are visible

separate origins of the LAD and LCx in 1%. The most important anomaly is a LM artery originating from the right sinus of Valsalva or from the RCA. The course between the pulmonary artery and the aorta can be the cause of vessel compression, and therefore of ischemia and sudden death, during or following physical effort. The same is true when the LAD originates from the RCA or from the right aortic sinus. By contrast, a circumflex artery originating from the RCA has no clinical consequences because of its posterior course.

Some congenital cardiopathies are often associated with anomalous coronary arteries.

In the tetralogy of Fallot, an anomalous coronary artery is present in 9% of the cases. The most common variation is a great conus artery, an anomalous LAD originating from the RCA or right sinus of Valsalva. In transposition of the great vessels (D-type), the most frequent (60% of the cases) anomaly is a RCA that originates from the posterior surface of the right aortic sinus and a LAD originating from the posterior surface of the left aortic sinus. In 20% of the cases, the circumflex artery arises from the RCA. In 3–9% of the cases, the RCA arises from the left aortic sinus and the LCA from the right sinus or there is a single coronary artery that takes off from the right or left sinus, of Valsalva; an intramyocardial course is frequent. In the L-type transposition, the coronary arteries can derive from the originating sinus or from the perfused ventricle. In this case, the RCA perfuses the left ventricle on the right side and divides into the LAD and LCx, and the LCA runs in the interventricular groove like the RCA. The anomaly of one or more coronary arteries arising from the pulmonary artery is seen in 0.4% of patients with congenital cardiopathies. The most frequent anomalous coronary artery is the LAD originating from the pulmonary artery (Bland-White-Garland syndrome).

Further coronary anomalies are aneurysms and fistulas. Aneurysm is an expansion of the coronary diameter by at least 1.5-fold more than an adjacent segment. Coronary fistulas are communications between the coronary arteries and the cardiac cavities: these can be congenital or acquired following thoracic traumas, electrocatheter implantation, endomyocardial biopsies, etc. The most frequent location is the RCA (55%), LCA (35%), or both (5%); in 40% of these patients, the fistula is in the right ventricle, in 26% in the right atrium, and in 17% in the pulmonary artery.

Factors Determining Coronary Artery Size

Numerous independent factors, including age, sex, body surface area, physical activity, and some pathologies, influence the caliber of the coronary arteries. For instance, with increasing age there is a reduction of the caliber of the coronary vessels, whereas in patients with myocardial hypertrophy the arteries are of increased caliber.

Generally, in females, the coronary arteries are narrower than in males, probably due to the difference in body surface area.

The reduction in the caliber of the coronary arteries that occurs with age has many explanations: firstly, there is a high prevalence of concentric athero-

sclerosis—not visible with coronary angiography—that causes a homogeneous reduction of the arterial lumen. In most elderly subjects, there is also subendothelial and medial hypertrophy. Angiographic examination of the diameter of the coronary arteries often requires the use of nitrates to resolve vasospasm; however, with increasing patient age, there is a reduction of the effects of nitrates. Furthermore, reduced physical activity and a prevalence of connective tissue in the myocardium are associated with a reduction in the caliber of the coronary arteries.

Physical exercise is a strong stimulus for increasing the caliber of the vessels and it potentiates the effects of nitroglycerine or endothelial-derived relaxing factor (EDRF).

Cardiac pathologies that increase work by the heart and that produce an increase in coronary flow increase of the caliber of the coronary arteries. Thus, in the evaluation of the coronary anatomy it is useful to obtain anamnestic information from the patient.

Figures 1.10–1.13 provide examples of the coronary anatomy, as visualized by CT (Fig. 1.10) or with traditional angiographic projections (Figs. 1.11–1.13), including the cardiac regions perfused by the larger coronary branches.

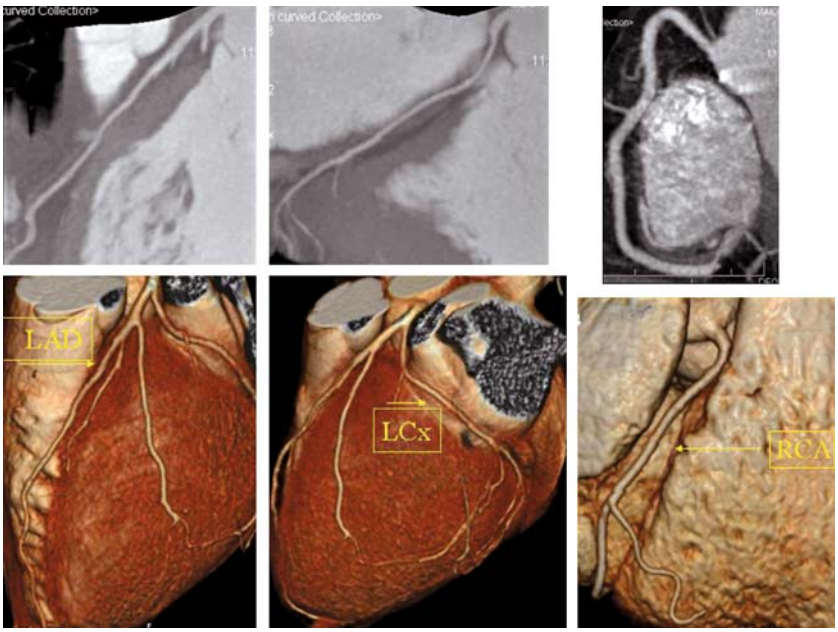

Fig. 1.10. Evaluation of the coronary anatomy with multi-slice computed tomography. *RCA* Right coronary artery, *LAD* left anterior descending artery, *LCX* left circumflex artery

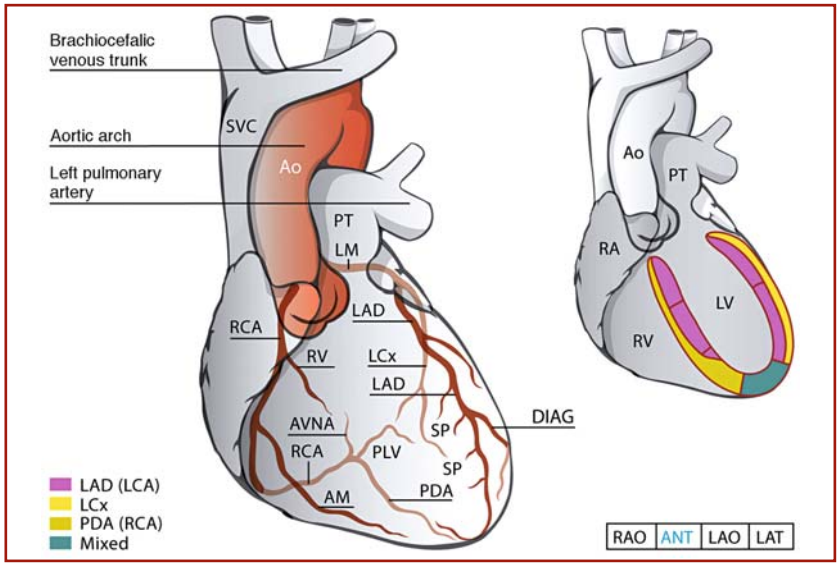

Fig. 1.11. Angiographic evaluation of the coronary circulation; anterior (ANT) view. The classification used by the BARI Study Group Investigatigators is shown in parentheses. *RCA* Right coronary artery (*1*), *RVB* right ventricular branches (*10*), *AM* acute marginal branches (*10*), *PDA* posterior descending artery (*4*), *PLV* posterolateral branches (*5*), *AVNA* atrioventricular nodal artery, *LCA* left coronary artery, *LM* left main artery (*11*), *LAD* left anterior descending (1st segment *12*, 2nd segment *13*, 3rd segment *14*), *SP* septal branches (*17*), *DIAG* diagonal branches (15, 16, 29), *LCX* left circumflex artery (1st segment *18*, 2nd segment *19*, 3rd segment *19a*), *OM* obtuse marginal branches (*20–22*), *Ao* aorta, *LV* left ventricle, *PT* pulmonary trunk, *RA* right atrium, *RV* right ventricle

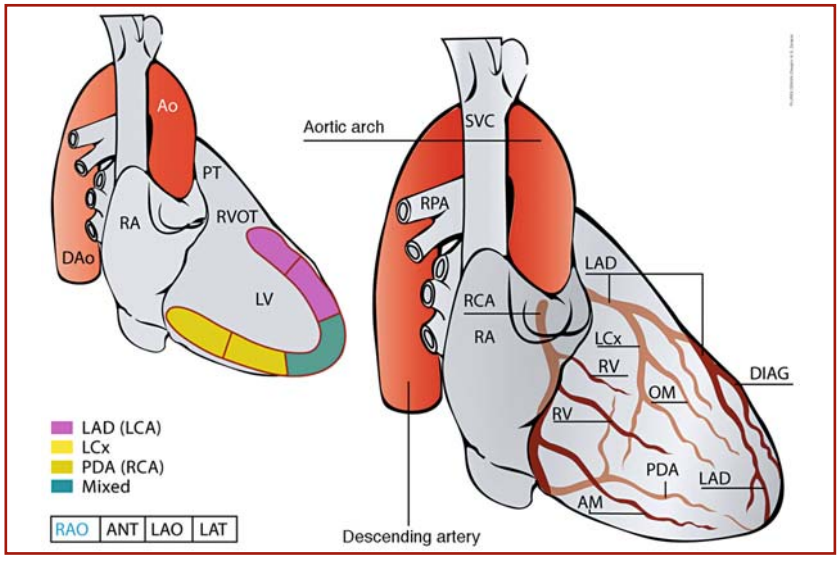

Fig. 1.12. Angiographic evaluation of the coronary circulation; right anterior view (RAO). *RCA* Right coronary artery, *RV* right ventricular branches, *AM* acute marginal branches, *PDA* posterior descending artery, *PLV* posterolateral branches, *LM* left main artery, *LAD* left anterior descending artery, *DIAG* diagonal branches, *LCX* left circumflex artery, *OM* obtuse marginal branches, *Ao* aorta, *Dao* descending aorta, *LV* left ventricle, *PT* pulmonary trunk, *RA* right atrium, *RPA* right pulmonary artery, *RVOT* right ventricular outflow tract, *SVC* superior vena cava

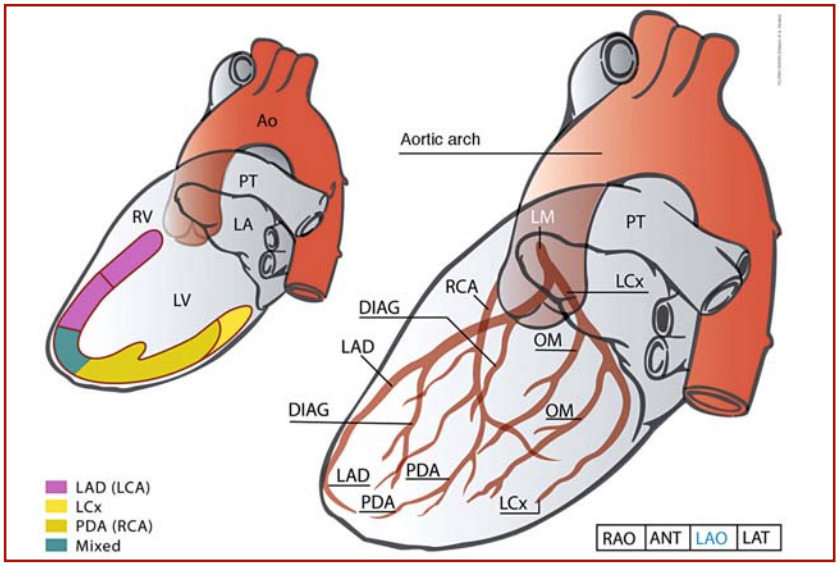

Fig. 1.13. Angiographic evaluation of the coronary circulation; left anterior oblique (LAO) view. *RCA* Right coronary artery, *RV* right ventricular branches, *PDA* posterior descending artery, *LCA* left coronary artery, *LM* left main artery, *LAD* left anterior descending artery, *DIAG* diagonal branches, *LCX* left circumflex artery, *OM* obtuse marginal branches, *Ao* aorta, *LA* left atrium, *LV* left ventricle, *PT* pulmonary trunk, *RV* right ventricle

2

Basic Techniques in the Acquisition of Cardiac Images with CT

Paolo Pavone

Computed tomography angiography (CTA) of the coronary arteries is a very quick and the most advanced imaging technique. Using a multislice imaging approach together with specialized and dedicated software, CTA "freezes" cardiac movement thereby acquiring static images of the rapidly moving heart. In addition, the same approach produces contrast-agent-enhanced images of the coronary arteries, by employing a three-dimensional technique with high spatial and temporal resolution. The aim of this chapter is to educate the non-experienced reader about the CTA modalities that allow these images to be acquired. We evaluate: (a) the basic concepts of the equipment employed, (b) the technical procedures needed to image the coronary arteries, (c) the modalities for proper reconstruction of the three-dimensional images, and (d) the procedures allowing diagnostic analysis and image reproduction.

Technical Principles in the Acquisition of Cardiac Images by CT

"Freezing" moving organs has been one of the main goals of CT since its introduction. All of the apparatuses employed thus far are based on a simple principle: an X-ray tube (the same as employed elsewhere in radiology) rotates around the patient, who lies on a radio-transparent bed. Collimated X-ray (thin beam) is sent towards the patient from one side while sensors (detectors) are located on the other. The amount of X-ray radiation absorbed by the patient at that anatomic level examined is then computed. Thus, from a simple perspective, CT consists (Fig. 2.1) of a large box, the gantry, which contains a circular track that allows fast rotation of the X-ray tube. On the other side of the tube, positioned along the same track, are the detectors, which rotate synchronously with the X-ray tube. The detectors transform the received signal (i.e., the X-ray beam after it has passed through the patient's body) into a weak but consistent electrical signal that is proportional to the amount of X-rays detected. Accordingly, the greater the absorption of the X-ray beam by the patient, the smaller the number of X-rays that hit the detector, and the weaker the electrical signal transformed and trans-

P. Pavone, M. Fioranelli, D.A. Dowe, *CT Evaluation of Coronary Artery Disease*.

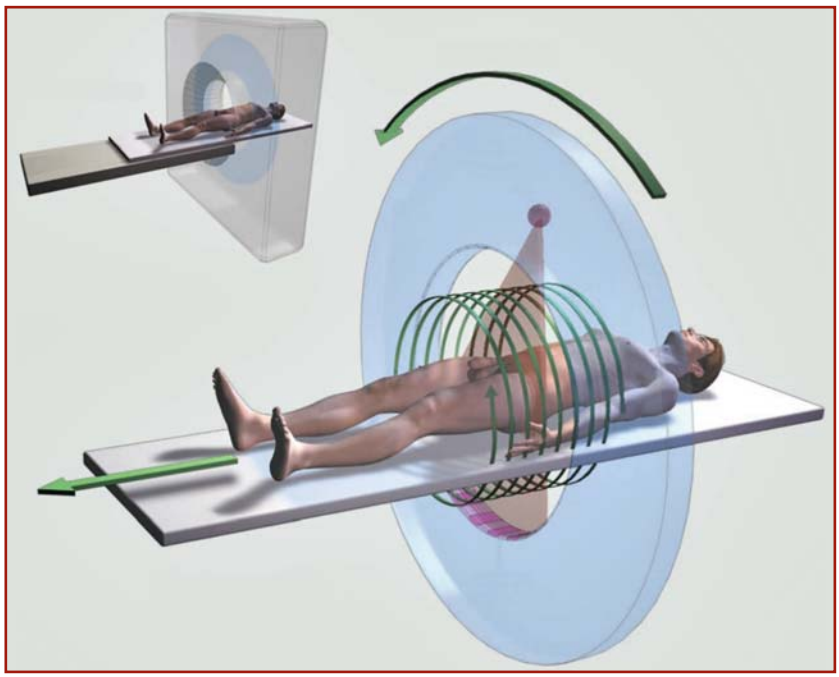

Fig. 2.1. Computed tomography (CT) equipment: basic principles. Reproduced from Brenner and Hall, 2007. © 2008 Massachusetts Medical Society, with permission

mitted by the detector. Therefore, the electrical signal created by the detector is a direct measure of X-ray beam absorption. If the beam crosses an area containing bone (e.g., the vertebrae), X-ray absorption will be consistent and a weak signal will be produced by the detector (Fig. 2.2). If an anatomic area containing air (e.g., the lungs) is evaluated, X-ray absorption will be less and a strong, consistent signal will result as very little of the radiation is absorbed by the lungs.

At the same time that information on X-ray absorption is collected by the CT detectors during rotation of the tube around the patient's body, the detectors are also continuously and rapidly sending electrical signals to a computer. In the process, these weak but significant electrical signals are immediately transformed into digital data that can be analyzed by the appropriate software. Complex reconstruction algorithms ultimately produce a series of diagnostic images, which are displayed on the console monitor and are thus readily accessible by the clinician.

As simple clinical users, it is not necessary to understand the mechanics of these analyses. It is important, however, to acknowledge those scientists who have been able to resolve the numerous technical problems such that CT image quality has constantly improved. Of interest is that the 'inventor' of CT, Sir Hounsfield, succeeded in his efforts thanks in part to the Beatles, since EMI Records financed CT research and the construction of the first "commercial" CT unit. The volumetric (spiral) revolution was a product of the work of Willi A. Kalender. The results of these and related scientific activities are that, today, CT is used almost as easily as digital photography. Indeed, the acquisition principles are the same: in CT, X-rays are absorbed by the anatomic

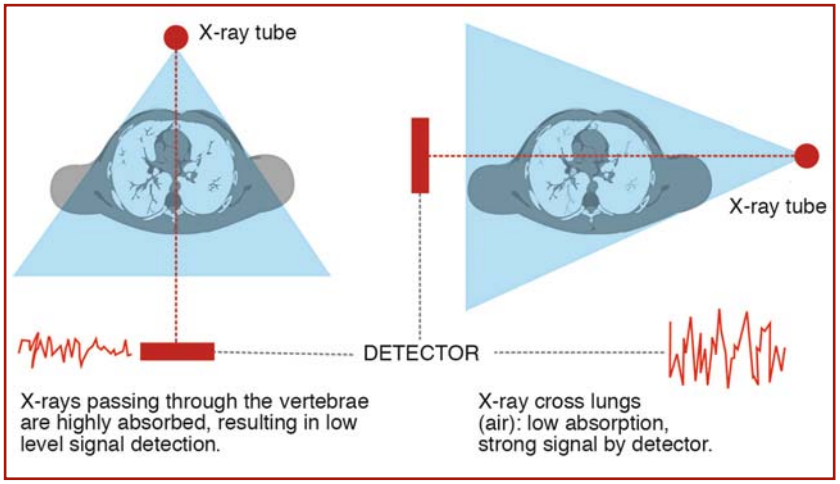

Fig. 2.2. X-ray absorption and signal detection. X-ray absorption is higher or lower depending on the anatomic area crossed by the X-rays. For example, when X-rays pass through the strongly absorbing vertebrae, the detector receives a weak signal. When they pass through the lungs, there is less absorption and the detector receives a much stronger signal

region of interest; in digital photography, the brightness of the object is assessed by a kind of detector, the CCD (charge-coupled device) such that the light signal is transformed into numerical (digital) information.

From Conventional to Spiral CT

The speed of data acquisition in CT depends on two different factors: how fast the tube rotates around the patient and the amount of information that can be analyzed at the same time. Early CT machines needed 18–20 s for a single rotation of the tube around the patient; thus, the waiting time, in which the tube returned to its initial position ready to begin a new rotation, was as long as 1 min. A revolution in CT imaging of the abdomen occurred in the early 1980s, with a tube able to rotate around the body in 2 s, thereby minimizing all artifacts arising from motions of the abdominal organs. As a result, excellent static images of the liver, pancreas, and adjacent vessels could be obtained.

The next step was the introduction of spiral systems, in which the tube is able to move freely in the track contained in the gantry and does not return to its initial position after each rotation. In these machines, introduced in the early 1990s, the electrical power that supplies the X-ray tube is transmitted along the same rotational track, thus avoiding both the need for long cables and a return to the start position after each rotation. "Spiral" refers to the fact that, once a continuous rotation of the tube around the patient is started, movement of the bed along the longitudinal axis creates a spiral acquisition of images along the human body (Fig. 2.1) instead of the axial images acquired in conventional CT. There is dramatic improvement of image quality with spiral CT in terms of speed of data acquisition and the consistency of the diagnostic information. This is due to the fact that images are not acquired on a single imaging plane

(axial); rather, data representative of an entire volume are reconstructed on the axial, coronal, sagittal, and curved planes of the target organ. The information provided by these three-dimensional images facilitates diagnostic evaluation of the internal organs of the human body. Moreover, the development of spiral CT has allowed the development of other techniques, such as virtual endoscopy and CTA, which nowadays are routine tools in clinical practice.

From Spiral to Multislice CT

Despite the advances made with the introduction of spiral CT, the acquisition times were still too long to allow cardiac imaging. The rotation time of the tube was about 1 s, not short enough to "freeze" cardiac movement. Moreover, the need remained to acquire more data within the same time frame, in order to include the anatomic area surrounding the heart. With multislice CT (MSCT) (Fig. 2.3) , which became commercially available at the beginning of

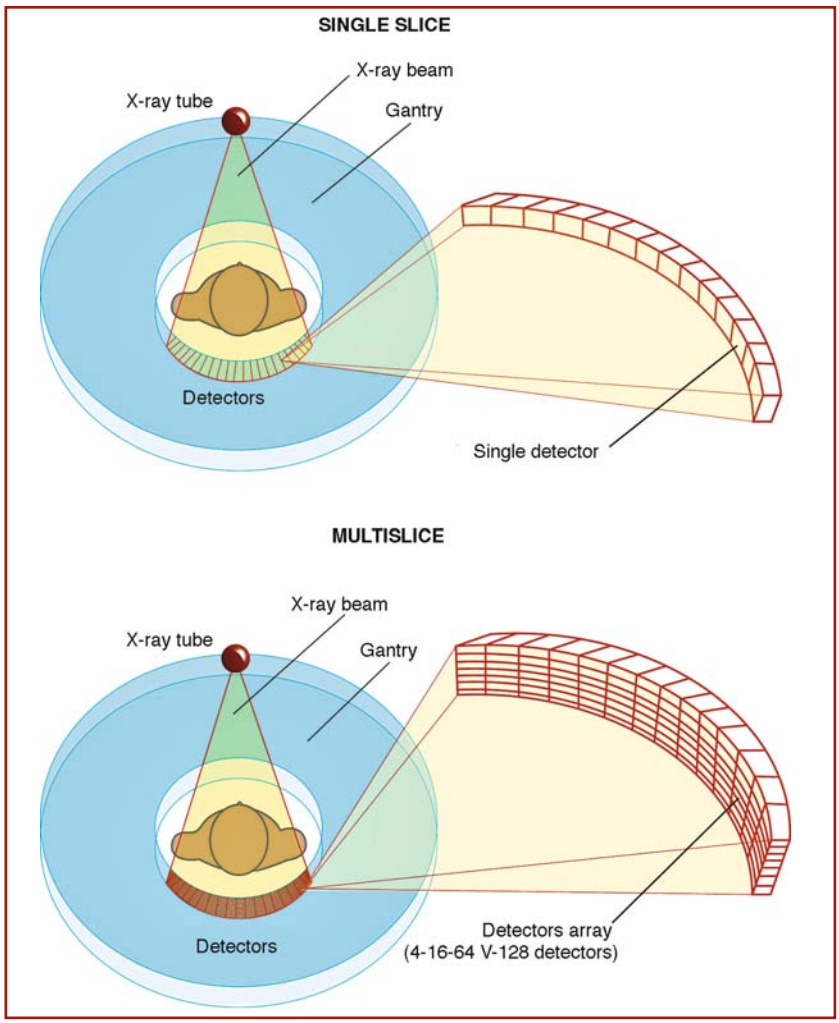

Fig. 2.3. Single slice and multislice (multi-row) detector CT

this century, an increase in the speed of data acquisition has been achieved. The principle of MSCT is simple: in conventional CT, a collimated X-ray beam is emitted and data are collected by a row of detectors located on the other side of the patient, after attenuation of the beam through his or her body. In MSCT, there is a large data-acquisition system, composed of an array of detectors arranged in multiple parallel rows along the longitudinal axis. The larger collimation of the X-ray beam is such that all of the detectors are "hit" at the same time, allowing simultaneous evaluation of a larger anatomic area.

The first systems used in cardiac imaging had four rows of detectors, but the real clinical revolution in cardiac imaging was enabled by machines with 16 detector rows, as they were able to generate images of the coronary arteries with limited artifacts and improved resolution.

Currently, the most widely employed systems have arrays of 64 detector rows, although newer systems with 128, 256, and 320 detectors have since been developed. It is easy to understand why the speed of acquisition is proportional to the number of detectors. Coverage of an anatomic volume such as the heart requires a certain number of rotations of the tube around the patient. Clearly, the larger the anatomic area covered by the detector rows, the fewer the number of rotations needed (Fig. 2.4).

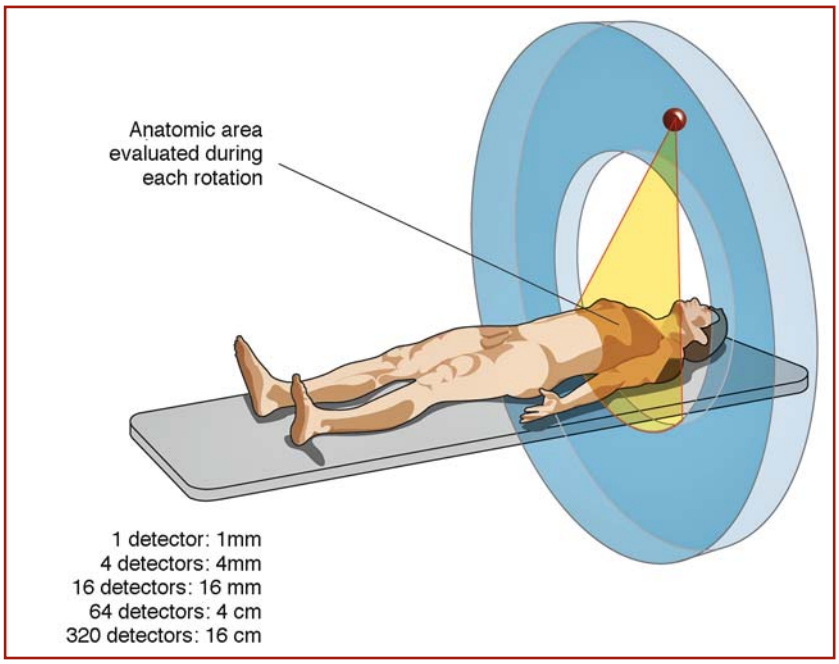

Fig. 2.4. Anatomic area evaluated in a single rotation of the X-ray tube. In MS CT, the higher the number of detectors, the wider the anatomic area evaluated during each rotation of the X-ray tube

Detector Number and Cardiac Imaging

It is worth underlining once more that the number of detectors used in MSCT corresponds to an array of defined width. The volume simultaneously evaluated by the X-ray beam equals the width of the detector array. In a 64-detector-row machine, the detector width and the anatomic area to be explored in a single rotation is 4 cm. Thus, to fully cover the anatomic area of the heart (15–20 cm), four to five rotations are needed during each phase of the cardiac cycle (using cardiosynchronization, as discussed below). With 128 detectors, the number of rotations is reduced by one half, while with 320 detector rows it may be possible to evaluate the entire heart in a single rotation. It should be noted that with 320 detector rows the width of the volume acquired in one rotation corresponds to 16, not 20 cm, due to corrections needed for the so-called cone beam artifact. One rotation, carried out in the telediastolic phase of the cardiac cycle, allows for the simultaneous acquisition of data covering the entire heart. However, multi-cycle images of the heart can also be acquired in a single rotation, with the data reconstructed in the different cardiac phases.

Temporal Resolution in Cardiac Imaging

Together with progress achieved by MSCT regarding the simultaneous acquisition of more data, efforts have been made to reduce the rotation time of the X-ray tube. This technical parameter is of utmost importance, as it represents the real temporal resolution of cardiac CT. In fact, even with the largest detector array (i.e., 320), it would not be possible to "freeze" images of the heart if the rotation time of the X-ray tube was slow (e.g., 1 s, as was the case with the first generation of spiral scanners). In other words, it is not enough to simultaneously obtain as much data as possible; rather, data acquisition must be very fast if the goal is to generate consistent cardiac images.

The rotation time of early MSCT equipment, 0.5 s, was too slow to completely "freeze" cardiac movement. Since the temporal resolution is equal to half of the rotation time, with 250 ms significant artifacts in the diagnostic images were produced and the images were of poor quality.

The rotation time of the X-ray tube has continuously improved with more modern equipment, and currently ranges from 0.4–0.35 s to 0.3–0.27 s (temporal resolution < 150 ms). As would be expected, the faster rotation times have yielded cardiac images of much higher quality, greater reliability, and improved accuracy, as confirmed by world-wide clinical experience. The reason for this improvement lies in the fact that the width of the imaging "window" (Fig. 2.5) in the telediastolic phase (during which the heart is almost completely still) is limited; therefore, the faster the data are acquired, the fewer the movement artifacts.

Another approach to improve temporal resolution is the use of two perpendicular X-ray tubes. In double-source technology, two different X-ray tubes are installed at 90° to each other on the same rotational track, with two perpendicular detector arrays (Fig. 2.6). During X-ray emission and data acquisition, the two tubes and detector arrays operate independently and data are

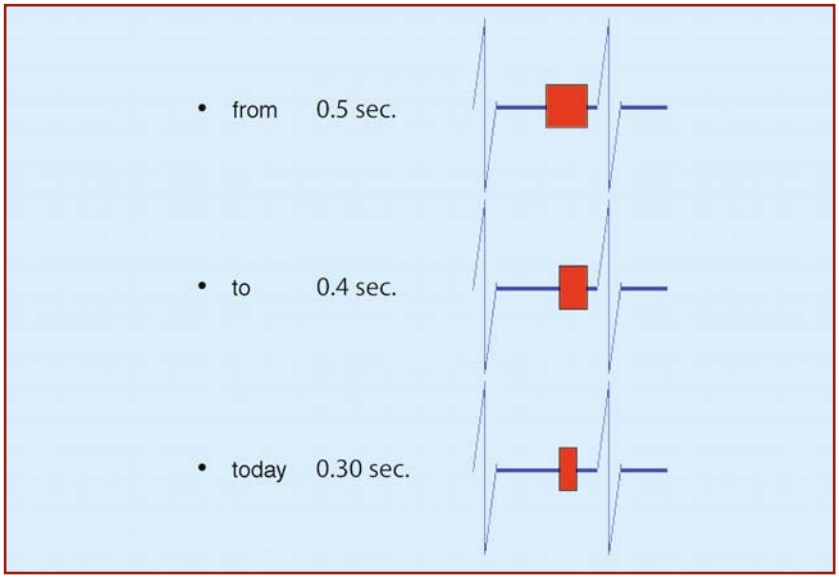

Fig. 2.5. Rotation time of the X-ray tube: during cardiac-gated image acquisition, the width of the red area in telediastole represents the imaging window (time) for data acquisition: the shorter the acquisition time, the fewer the motion artifacts

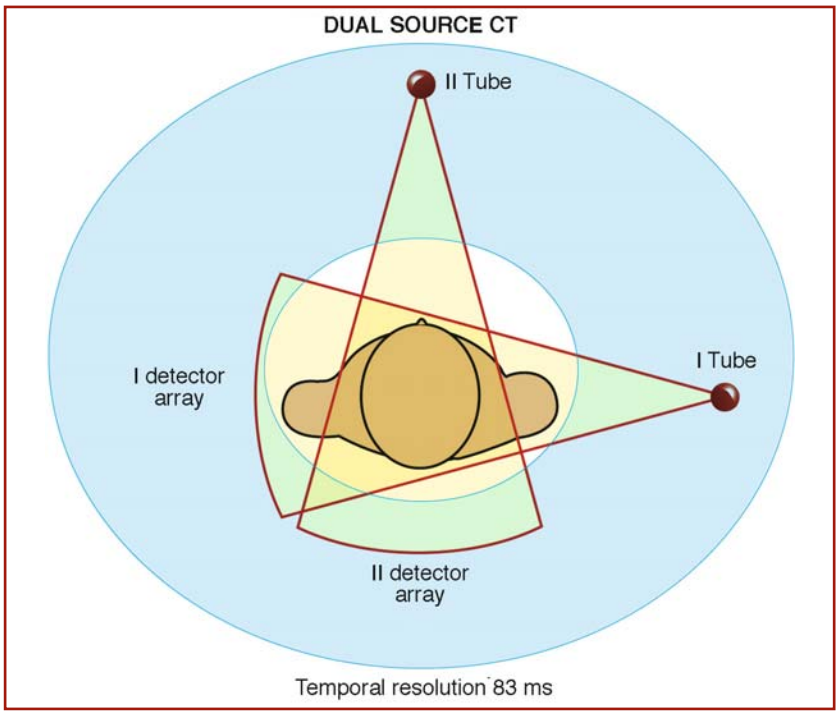

Fig. 2.6. In dual-source CT, the tubes are mounted perpendicular to each other and the data are obtained by two different detector arrays. The acquisition time for each rotation is therefore reduced by one half

collected individually. The computer merges the information produced by the two tubes into a single data package, as if obtained by a single system. The end result is that data from the volume being evaluated are actually obtained in half the time and with a temporal resolution of 83 ms. Only this system generates images of the heart without significant artifacts, even in patients with faster heart rates, and without the need for bradycardic drugs.

Types of Equipment and Their Clinical Uses in Cardiac Imaging

Already following the development of equipment with 4 detectors rows and a rotation time of 0.5 s, CTA of the coronary arteries was proposed. However, because of the long rotation time of the X-ray tube, the data were not satisfactory. Significant artifacts were present in almost all of the resulting images, which were of poor quality and exhibited limited anatomic definition of the coronary circulation. Nonetheless, this technology did find application in the evaluation of cardiac bypass grafts (CABG), since the reduced motion of the extracardiac vascular structures yielded fewer artifacts.

With 16 detectors rows and a rotation time of 0.4 s or less, the situation changed drastically. Clinical experience confirmed the improved accuracy of CT, and CTA of the coronary arteries became an established examination with a high degree of reliability and producing images of great clinical interest. This clearly defined the role of CTA in the assessment of patients with suspected atherosclerotic disease of the coronary arteries.

As noted above, the most widely diffused CT systems for imaging of the coronary arteries are those with 64 rows; however, there has not been the same degree of improvement as that achieved in moving from 4 to 16 slices. In a recent review of papers published in the international literature, the use of 16 and 64 detector rows has corresponded to an improvement in sensitivity (average from 83 to 93%) while there has been little change in the specificity (96%). The newer equipment does feature an improved spatial resolution, with better evaluation of stents (see chapter on this topic).

Newer equipment (128, 256, and 320 detectors rows) provides improved spatial resolution and faster data acquisition, with complete coverage of the anatomic area containing the heart within 5–0.5 s. With an anatomic coverage of 16 cm, it is usually possible to capture the heart in a single rotation of the X-ray tube.

The current goal of CT research is the "imaging plate," that is, a device with 512 detectors. This would provide even more extended anatomic coverage and a definitive improvement in the image quality achieved with CTA. The major problem of imaging research is the cone beam artifact, i.e., conical divergence of the X-ray beam, which causes distortion in image reconstruction.

CT equipment with two X-ray tubes (double-source technology) does not improve resolution, as the acquisition technology is the same as that of machines with 64 detectors rows. However, these systems do offer dramatic and unique improvement in temporal resolution, down to a value of 83 ms. The imaging window in telediastole is very short and for this reason, as discussed elsewhere in this volume, there is no need to give beta-blockers to patients to

induce bradycardia. Use of these systems is therefore recommended mostly in cardiology units with high patient turnover. It is also advised for in the ICU, where patients must be quickly screened for coronary artery disease in cases of acute chest pain (so-called triple rule out) and there is no time or opportunity to wait for the bradycardic effect of beta-blockers.

Other Factors That Improve the Image Quality of CT Technology

So far, our discussion has focused on the two most evident technical parameters of CT technology: the number of detectors in the array (64–320) and the rotation time of the X-ray tube (from < 0.4 to 0.3–0.27 s.). However, there are other ways to improve image quality, an important one being the speed of information capture. Detectors receive information (X-ray absorption through the patient's body) and then send it as an electrical signal to the computer. Since the tube rotates rapidly, the detectors must respond quickly enough to receive and process this information. This speed of data acquisition by the detectors influences an important parameter in spiral CT, the so-called pitch, i.e., the speed at which the patient can be advanced in the gantry, allowing all relevant data to be collected. A 256-detector system may have a slower pitch such that acquisition of the anatomic area containing the heart is achieved in 6 s, while a 128-detector system with faster detectors allows a more rapid pitch, with complete acquisition of the cardiac images in 4 s. Thus, the number of detectors is not the only parameter that determines the speed of data acquisition in CTA of the coronary arteries.

Another parameter currently targeted by industry is the spatial resolution. With more accurate and sensitive detectors along with proper and calibrated emission of the X-ray beam, the spatial resolution has improved from the 0.6–0.5 mm of 64-detector technology to the 0.25–0.33 mm of today's technology. This improvement enables better evaluation of smaller, distal coronary arteries. Consequently, the results achieved with CTA of the coronary arteries may soon be on a par with the spatial resolution of catheter coronary angiography, i.e., < 0.2 mm.

3

CT Examination of the Coronary Arteries

Paolo Pavone

This chapter reviews the techniques needed to obtain high-quality diagnostic images of the coronary arteries by means of CT angiography (CTA). The choice of imaging equipment, discussed in the previous chapter, involves the radiologist only once, at the moment that the CT equipment is purchased. By contrast, the choice of the optimal procedure for imaging of the coronary arteries involves the radiologist or technician in each exam, as the utmost care must be taken to always obtain images of optimal quality. It should be pointed out that this goal is unique for the coronary arteries, since in CT evaluation of the chest, abdomen, musculoskeletal system, or other static organs, suboptimal image quality may nonetheless allow a clinical diagnosis whereas for the coronary arteries the presence of movement artifacts may completely invalidate the diagnostic value of the examination.

Achieving Excellent Image Quality in CT of the Coronary Arteries

In performing CT of the coronary arteries certain goals must be reached. First of all, the images must be obtained as fast as possible, using specific imaging protocols (which differ according to the type of equipment, as discussed in the previous chapter). Second, during the dynamic rapid acquisition of cardiac images there must be a high concentration of contrast agent in the coronary tree. Only the high density provided by the presence of contrast agent in the vessels allows for a proper evaluation of the coronary arteries and their walls. Third, to reduce imaging artifacts, the patient must be properly prepared for the imaging procedure; therefore, good patient cooperation is needed. In addition, in most cases (except with double source technology) the patient will be administered beta-blockers to reduce cardiac frequency, allowing a wider imaging window in telediastole.

In coronary CTA, images of a moving organ are rapidly acquired during the passage of contrast agent at high concentration (bolus). It is therefore crucial to define the procedures, including patient preparation, that will be performed prior to diagnostic CT examination of the coronary arteries.

P. Pavone, M. Fioranelli, D.A. Dowe, *CT Evaluation of Coronary Artery Disease*.

Patient Preparation

Informed Consent

Although CTA of the coronary vessels is a non-invasive procedure (no catheterization or other invasive modality is required), proper information must be obtained from the patient prior to the examination. The patient should not only fill out the informed consent documents (similar to those of any CT procedure using contrast agent), but should also be informed personally about the procedure, i.e., the cardiologist and radiologist must provide the appropriate information in person, clearly explaining the type of examination being performed, the indications for this procedure, whether it is aimed at ruling out a known clinical problem or serves as a screening procedure, as may be the case in mildly or non-symptomatic at-risk patients.

The informed consent documents contain generic information regarding, for example, the possibility that contrast agent may be the cause of allergic reactions; however, this information is very general and often not well-explained. Thus, the clinician must specify that, with the iodinated non-ionic contrast agent currently in use, such allergic reactions are extremely rare, as opposed to the situation 15–20 years ago, when ionic agents were employed. Furthermore, since patients are often scared by the prospect of iodine injection, the radiologist must reassure him or her that the iodine is encapsulated in a closed molecule of the contrast agent, and therefore does not react with the human body, i.e., it does not affect iodine metabolism in the thyroid gland. For this reason, there are no contraindications for patients with thyroid gland disease; the contrast agent and its iodine component are rapidly eliminated through the kidneys after i.v. injection. Those allergic reactions that do occur are not related to iodine but to the molecule itself, and, as noted above, there has been a dramatic decrease in the incidence of allergic reactions following the switch from ionic to non-ionic, i.e., less reactive, molecules, despite the fact that both formulas contain three atoms of iodine per molecule. There is also no absolute contraindication to the use of contrast agent in patients with known allergic problems or in patients with previous allergic reactions to contrast agent. In these cases, however, pre-medication 3 days before the examination is indicated (usually corticosteroids per os).

In informing the patient, the clinician must also state that the examination is performed using ionizing radiation. Patient should be advised that X-ray exposure, mostly if repeated a short time after previous exposures, carries some risk. This topic is discussed in detail in the chapter on X-ray exposure in coronary CTA.

As for any other procedure involving contrast agent, patients undergoing CTA of the coronary arteries must fast for at least 5 h prior to the examination. Furthermore, the radiologists (or the anesthesiologist, who may be present during the examination) will review blood-test data (mostly referring to renal function) and evaluate the patient's ECG. The only real contraindications to CTA of the coronary arteries are severe renal dysfunction, which precludes the use of contrast agent, or not pharmaceutically controlled arrhythmia, which prevents "freezing" of cardiac movement during the examination.

Bradycardia

As the heart is a fast-moving organ, CT evaluation can be performed only by "freezing" cardiac motion, using software and protocols allowing rapid image acquisition. The temporal resolution of currently available equipment (150 ms) does not guarantee static images of the heart in three dimensions. Instead, to obtain dynamic images of the coronary arteries, pharmacologically controlled bradycardia, with an optimal cardiac frequency of 55–65 bpm, is required. Only by inducing bradycardia can an adequate temporal window in telediastole, during which the heart is practically completely still, be achieved (Fig. 3.1). In the absence of bradycardia, image quality will be impaired and, as noted above, a proper diagnosis will not be possible. In Figure 3.2a, bi-dimensional image of the anterior descending coronary artery is displayed on the left, with data acquired at 72 bpm. This image does not provide the diagnosis nor can the vessel contours or the presence of parietal pathology be defined. The image on the right was obtained after bradycardia was pharmacologically achieved; there is clear definition of the vessel wall, with identification of the lumen and evidence of parietal thickening due to atherosclerotic involvement.

Bradycardia must be induced if the cardiac frequency is > 65 bpm. While oral or i.v. administration of beta-blocker is possible, we prefer oral administration of a generic beta-blocker formula (i.e. metoprololo 100 mg) in tablet form 45–60 min prior to the examination. Usually, a frequency of 50–60 bpm is easily achieved, without any symptoms experienced by the patients (these drugs are currently widely used by general practitioners without major patient contraindi-

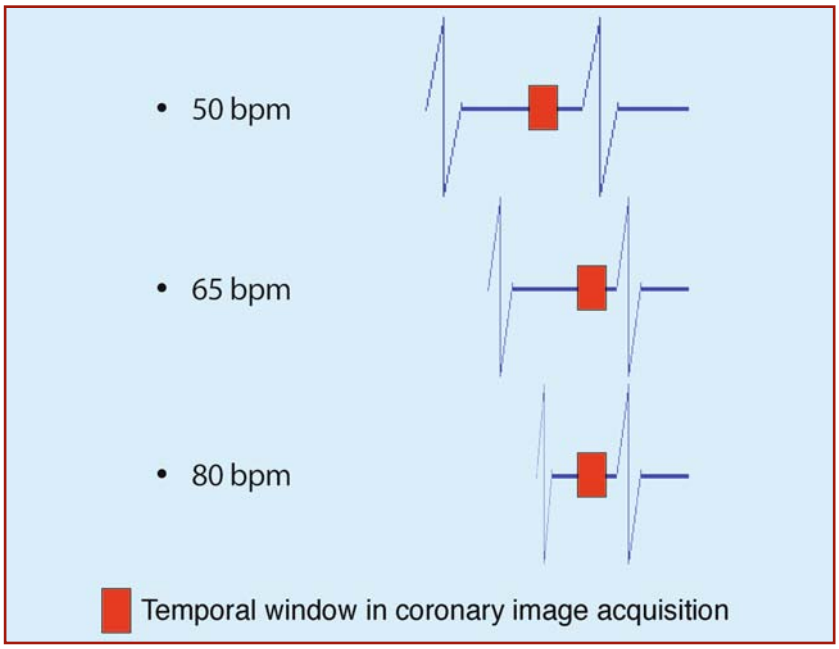

Fig. 3.1. Time imaging window in ECG gating procedures. The lower the heart rate, the larger the time imaging window, leading to a reduction of motion artifacts

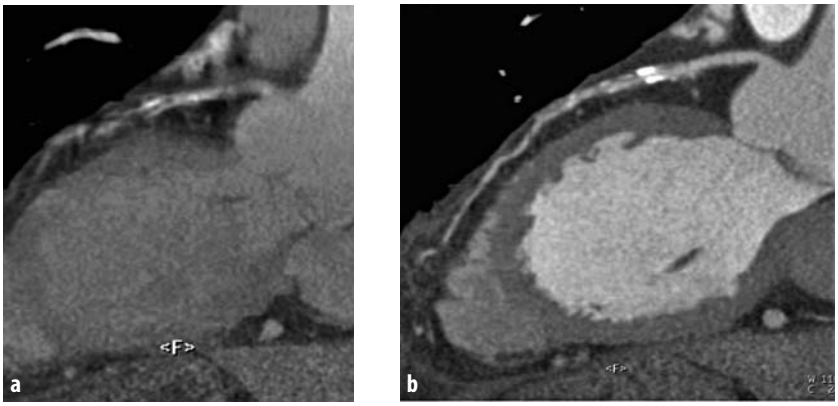

Fig. 3.2 a, b. Image acquired at 75 bpm (**a**) and (**b**), afterwards, at 62 bpm, repeating the injection of contrast agent. Movement artifacts impair image quality and therefore the diagnostic value of the examination

cations). As an alternative or in case of lack of pharmaceutical effect of the oral drug, i.v. formulas can be administered. These are injected at the moment of the examination in the same i.v. cannula prepared for contrast-agent injection, with cardiac frequency evaluated directly in the CT console's monitor.

Cardiac frequency is often influenced by the emotional status of the patient. Despite the efficiency of beta-blockers, once on the CT table and during contrast-agent injection, the patient often becomes tachycardic due to the emotional stress of the examination. We therefore suggest that an anxiolytic drug be provided i.v. just prior to contrast-agent injection. The short-lasting effects of these drugs do not interfere with consciousness at the end of the out-patient examination.

Finally, it should be noted that with double source technology there is no need for bradycardia, as the temporal resolution of 83 ms allows for a consistent image window even in tachycardic patients, without a decrease in the diagnostic quality of the images.

CT Angiography of the Coronary Arteries

Contrast-Agent Injection

The proper contrast-agent injection procedure is very important in CTA of the coronary arteries, as only by ensuring a consistent concentration in the vessels can good image quality be achieved. Visualization of the coronary arteries is made possible by increasing (temporarily, during the passage of the bolus of contrast agent) the radiographic density of the blood plasma (blood mixed with contrast agent) that fills the coronary arteries at that moment. The radiographic density of the blood increases from 40–50 Hounsfield units (HU) to 300–400 and even 500 HU during the passage of contrast agent. Standard HU values are defined to allow the measurement of tissue density in CT, with 0 HU corresponding to the CT density of pure water, -1000 corresponding to that of air, and +1000 to that of compact bone tissue. The higher the CT density of the coronary

contents (blood mixed with contrast agent) during CT image acquisition, the better the quality of the coronary-arteries images obtained.

Contrast-Agent Injection: Role of Resistance and Venous Anatomy

Different parameters determine the success of a consistently high concentration of contrast agent in the arterial lumen during CTA image acquisition, for example, the contrast-agent injection rate. This, in turn, is influenced by the amount of resistance encountered and the venous anatomy of the injection site, i.e., the forearm.

Contrast agent is injected through an automatic injector able to reach high injection rates (Fig. 3.3). In coronary CTA, better results are obtained with a double syringe injector; here, contrast agent is injected with one syringe and, immediately at the end of the injection, the second syringe is activated such that a second bolus, this time of saline, is injected. This saline bolus pushes the contrast-agent bolus towards the right cardiac chamber, thereby "washing" the peripheral veins, where the vascular flow is low; these vessels would otherwise stay filled with contrast agent. In this way, the dispersion of contrast agent in the peripheral veins is guaranteed and the bolus remains compact, thus yielding higher concentrations in the arterial bed. We prefer to inject the saline bolus at the same rate used for contrast-agent injection and in large amount (80–100 ml) ensuring that all the contrast agent is washed out by the saline. In the example shown in Figure 3.4, axial images acquired at the level of the cardiac chambers show the strong opacification of the left cardiac chambers due to high CT density values and a low density of the right chamber, washed out by the saline bolus.

An effective contrast-agent bolus injection speed is also related to the resistance that the bolus encounters during its passage in the i.v. cannula, given the

Fig. 3.3. Contrast-agent power injector (Stellant D, MEDRAD INC., USA), with permission

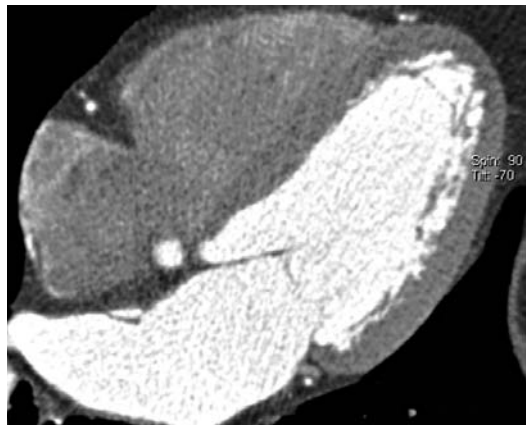

Fig. 3.4. High concentration of contrast agent in the left chambers of the heart causes them to appear bright and hyperdense. The right chambers are "washed" by the chasing bolus and are therefore hypodense

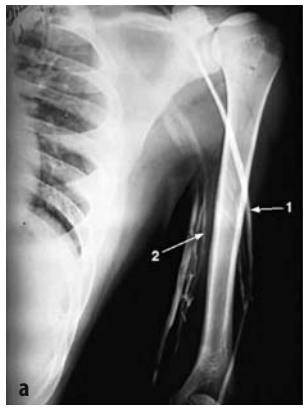

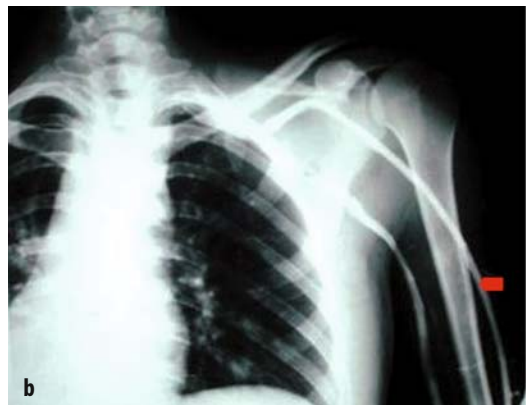

Fig. 3.5 a, b. Anatomy of the veins of the arm. The basilic vein is medial and has a direct course towards the subclavian vein; the cephalic vein is lateral and has a steep angle at the confluence with the subclavian vein . *1* Cephalic vein, *2* basilic vein

high viscosity of these drugs. There are two ways to avoid local resistance: the first is to use a large-bore cannula in the antecubital vein. We always employ a 16G cannula (as opposed to the 18G or even 20G cannula usually proposed in the literature), which allows for a high injection rate without any local resistance. The second is related to the anatomy of the veins of the forearm: the two main venous channels (in most cases) are the basilic vein, medially, and the cephalic vein, laterally. While the basilic vein (Fig. 3.5) follows a straight course, leading directly to the axillary and subclavian veins, the cephalic vein is more tortuous, contains valves, and drains in the axillary vein usually in an arch-wise fashion at an angle of 90°. Considering that the patient's arms are raised during CT examination, it can be readily appreciated that injection into the cephalic vein may cause stagnant flow of contrast agent, leading to a less compact and more diluted bolus and thus a lower concentration in the arterial bed. In Figure 3.6, the effect of bolus dilution during the injection of contrast agent in the cephalic vein is evident. There is persistent opacification of the right chambers and a lower concentration of contrast agent in both the arterial bed and the left cardiac chambers (compare with Fig. 3.4).

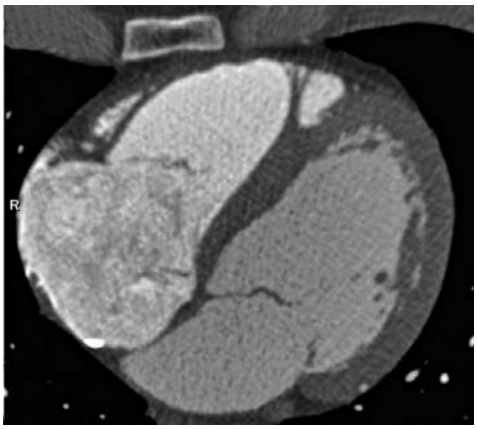

Fig. 3.6. Injection of contrast agent in the cephalic vein. The slower flow leads to a dilution of the contrast-agent bolus. There is evidence of residual opacification of the right chambers during 3D acquisition in an evaluation of the coronary arteries. Note the lower density in the left ventricle

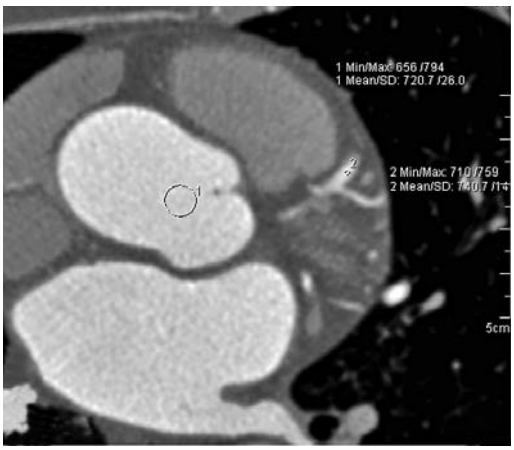

Fig. 3.7. Appropriate contrast-agent injection with high flow in the basilic vein. The CT density evaluated at the level of the aorta is 720 HU

Contrast-Agent Injection: Flow Rate and Amount

Contrast agent can be injected using an automatic injector at different flow rates, usually 3–5 ml/s. However, we routinely use a flow rate of 8 ml/s. This higher injection speed results in a more compact bolus and thus a higher concentration of contrast agent in the arterial bed (after passage through the capillary pulmonary bed and the left cardiac chambers). The average CT density of the coronary arteries as reported in the literature is 300–350 HU. Using faster injection rates and the procedures described above, we have been able to achieve an average density of ≥ 450–500 HU (Fig. 3.7).

Image quality is directly related to a higher concentration of contrast agent in the arterial bed and to a greater difference in density compared with the surrounding tissue. Our data are also in agreement with the results of Schueller et al., published in 2006 . They were able to show that higher injection rates (8 ml/s) improved the evaluation of pancreatic tumors. In coronary CTA, the higher arterial density allows better evaluation of these vessels in three-dimensional reconstructions.

The amount of contrast agent to be injected varies between 70 and 120 ml, depending on the equipment employed. In systems with 16 detector rows, acquisition times are 15–18 s, therefore requiring a longer bolus to completely achieve a high density of contrast agent in these vessels throughout image acquisition (at least 120 ml are required to achieve a prolonged bolus of contrast agent). With faster systems, i.e., those with 64, 128, or 256 detector rows, the acquisition time decreases to 10, 6, and 4 s, respectively, thus necessitating a still compact but shorter bolus (70–80 ml of contrast agent are employed). Data acquisition happens in real time such that, with experience, the radiologist will be able to determine the proper bolus size according to the equipment available and the nature of each case.

Contrast Agents for CT Angiography of the Coronary Arteries: Characteristics and Concentrations

An important element in defining proper image quality of the coronary vessels is the concentration of the contrast agent employed – the higher the concentration of contrast agent, the higher the CT density (measured in HU) of the blood in the coronary arteries. The contrast agent clinically used for i.v. injection is an iodinated non-ionic solution based on a tri-iodated benzene ring; iodated double benzene rings are also available (Fig. 3.8).

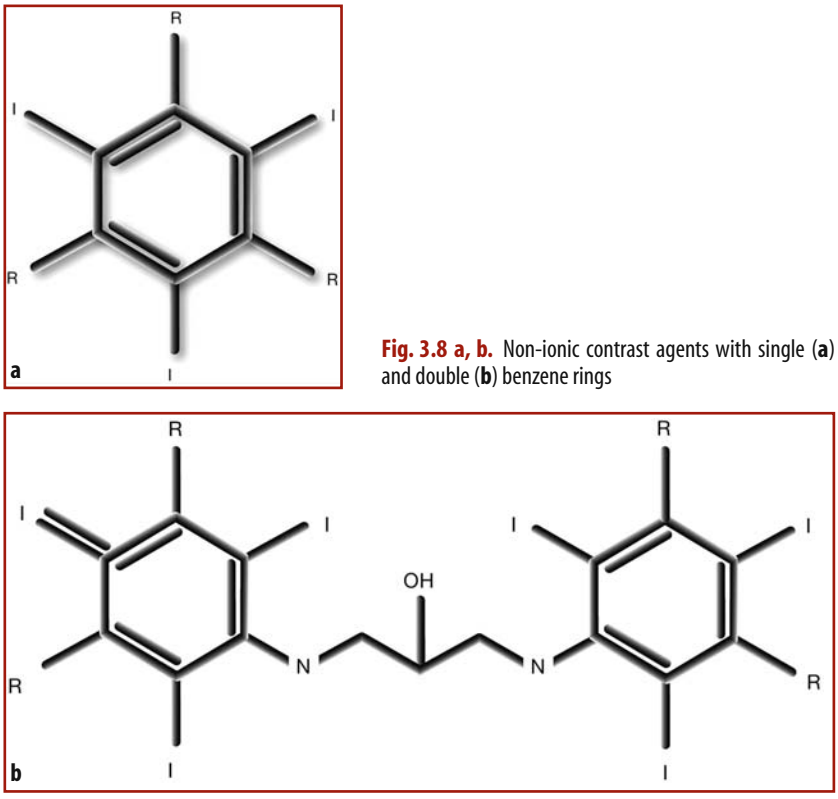

Fig. 3.8 a, b. Non-ionic contrast agents with single (**a**) and double (**b**) benzene rings

The iodine concentration of the contrast agent employed in CTA of the coronary arteries should be in the range of 350–400 mg iodine per 100 ml of solution. A concentration, up to 400 mg of iodine, has been suggested as it provides an even higher CT density in the coronary vessels. In fact, for the same conditions in terms of contrast-agent volume and flow rate of the injection, higher CT densities in the vessels will be reached with higher concentrations of the contrast-agent solution. The viscosity of these solutions increases in parallel with concentration; however, if the proper injection procedure is used and the solution is injected through a large-bore cannula, viscosity should not pose a problem as resistance at the injection site will be minimal.

Currently employed contrast agents are extremely stable and safe molecules; they are rapidly eliminated through the kidney after i.v. injection. Non-ionic contrast agents are also characterized by a low osmolarity (~600 mOsm/l vs. 1200 mOsm/l for the ionic solutions previously employed). The decreased osmolarity has reduced the patient's heat sensation as well as allergic reactions in response to contrast agent. Contrast agents based on an iodated double benzene ring have an even lower osmolarity (300 mOsm/l, similar to that of blood plasma) but have not reduced the incidence of allergic reactions any further. Although they have been successfully used for imaging, their viscosities are definitely higher and resistance at the injection site may be a problem in coronary CTA.

Optimizing the Imaging-Acquisition Window in CT Angiography of the Coronary Arteries

All coronary CTA equipment includes an automated procedure that recognizes the arrival of contrast agent (injected in a peripheral vein) at the level of the coronary arteries. Three-dimensional acquisition of the anatomic area including the heart should in fact start only when the bolus of contrast agent reaches the arterial system and creates a temporary but strong increase in the CT density of the arterial vessels. The automated procedure, referred to as "bolus tracking," requires the placement of a cursor that measures CT density in the center of the ascending aorta, after which single low-dose images are acquired every second following the start of contrast-agent injection. As soon as the cursor measures a density > 100 HU, the acquisition of three-dimensional images is automatically started. This assures that an optimal high density of the vessels is achieved during image acquisition.

Cardiosynchronized Acquisition

Imaging data are acquired in real time, during the dynamic passage of contrast agent through the coronary arteries. In a cardiosynchronized procedure, the ECG data are available to the computer, which synchronizes them with the imaging data (Fig. 3.9). In a second phase, data related only to the telediastole are reconstructed to create artifact-free cardiac images. Data referring to more than one telediastolic phase are needed to completely reconstruct the

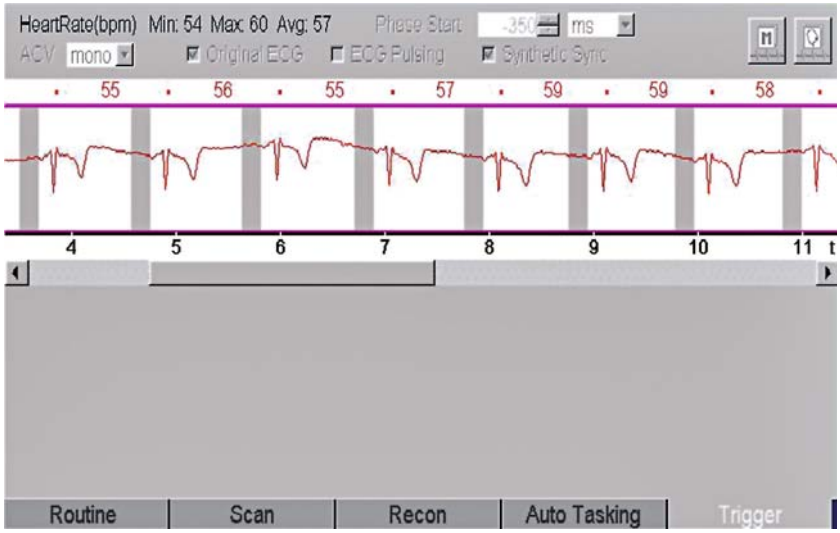

Fig. 3.9. ECG gating as shown on the CT console during data acquisition. Gray vertical lines represent the telediastolic temporal windows of data reconstruction for coronary CT angiography

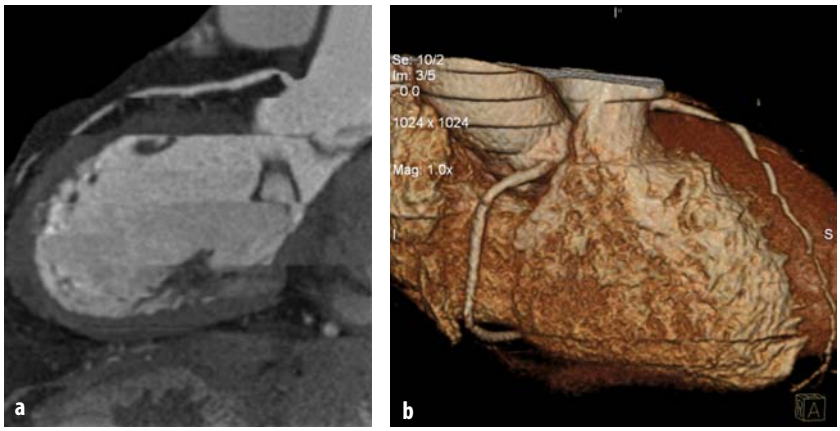

Fig. 3.10 a, b. Images acquired in an arrhythmic patient show typical step artifacts

volume containing the heart. In systems consisting of 64 detectors rows, the volume reconstructed in each telediastolic phase corresponds to the width of the detector array (4 cm); therefore, four to five cardiac cycles must be evaluated for a complete set of information regarding the volume of interest, including the heart (15–20 cm).

A three-dimensional image of the heart is an artificial single volume since in reality it is composed of a number of single smaller volumes placed one over the other and corresponding to succeeding telediastolic phases. Consequently, step artifacts are often present in the area of overlapping single volumes (Fig. 3.10).

As far as the radiation dose is concerned, the procedure described herein has the disadvantage that the patient is irradiated for the entire time of the procedure, during all cardiac cycles, while only data related to telediastole are used for data reconstruction. As will be explained in the chapter on dose exposure, there are a number of way to reduce or eliminate this problem. One of the techniques uses non-spiral data acquisition, with single, small axial volumes (each 4 cm) acquired during telediastole, without X-ray emission in the other cardiac phases. The reduction in X-ray exposure achieved with this procedure is in the range of 80%.

4

Image Reconstruction

Paolo Pavone

Coronary CT angiography (CTA) is a three-dimensional imaging technique. The data obtained during image acquisition, however, are not immediately evident to the radiologist, as the huge amount of digital information acquired is used to reconstruct three-dimensional images of the coronary arteries, according to dedicated and complex software and protocols. The coronary arteries are tortuous, moving objects and are thus often not easily visualized. For this reason, in CTA the movements of these arteries must be "frozen," through cardiosynchronization, during image acquisition.

In order to visualize the coronary arteries in CTA, a very high density of the internal lumen must be created. As specified in the previous chapter, this is accomplished by the dynamic injection of contrast agent. The vessels become evident because of the large difference in the density of the vessel lumen (high density: 300–500 HU, due to the iodine content of the blood during passage of contrast agent) and that of the surrounding tissues, such as epicardial fat (low density: -50–100 HU). The difference is important because, during three-dimensional image reconstruction only structures with very high density will be clearly visualized. The higher the density, the more evident the anatomic structures will be. This is the reason why the first three-dimensional images presented for clinical use were related to bone, a structure with a very high radiologic density.

Starting from volume data, there are two ways to construct three-dimensional images of the anatomic structures of interest: the first is to explore the volume using curved or orthogonal bi-dimensional planes with so-called planimetric technique; the second is to consider and image the entire package of three-dimensional data, using so-called volumetric techniques. In this chapter, we offer a simple explanation of the difference in these visualization techniques and their relative importance in clinical use for the evaluation of coronary artery disease.

P. Pavone, M. Fioranelli, D.A. Dowe, *CT Evaluation of Coronary Artery Disease*.

Planimetric Techniques

Axial Images

During data acquisition in coronary CTA, the console automatically displays axial images of the slices of the anatomic area under investigation, usually at 1-mm intervals (Fig. 4.1). These images confirm that the procedure has been correctly performed and that the acquisition timing, as far as opacification of the vessels by contrast agent is concerned, has been optimally achieved. In fact, segments of the coronary arteries can already be evaluated from these axial images, together with the myocardial walls and the contrast-agent-filled cardiac chambers. For non-experts, these axial images may not offer a clue in the identification of the coronary arteries; however, radiologists are well-acquainted with the CT evaluation of anatomic structures in the axial plane and thus may already gain early information regarding the presence of coronary artery disease simply by evaluating the images reconstructed in these anatomic planes.

Multi-Planar Reformatting

The three-dimensional reconstruction software provides direct access to images displayed in the three orthogonal planes, axial, sagittal, and coronal. This reconstruction technique is generically referred to as multi-planar reformatting (MPR). Moreover, the orthogonal images can be moved within the imag-

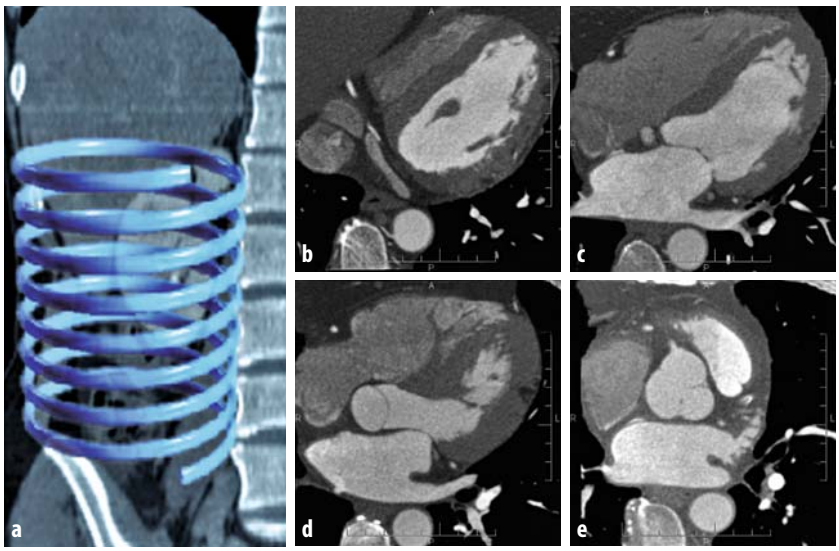

Fig. 4.1 a-e. 3D volume acquisition using spiral technique(**a**). Direct evaluation of single axial images slice by slice. **a** Scheme employed in spiral acquisition. **b–e** Slices reconstructed at different anatomic levels

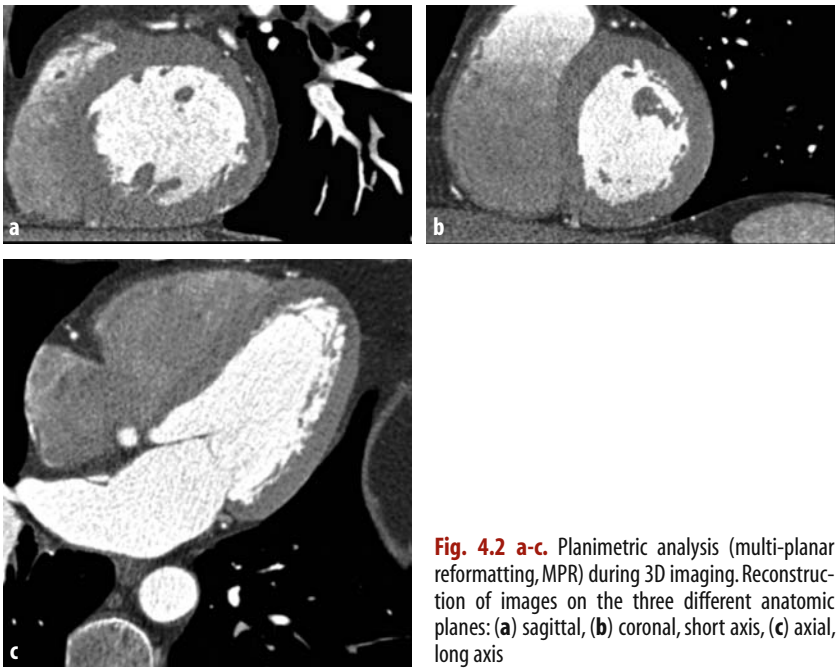

Fig. 4.2 a-c. Planimetric analysis (multi-planar reformatting, MPR) during 3D imaging. Reconstruction of images on the three different anatomic planes: (**a**) sagittal, (**b**) coronal, short axis, (**c**) axial, long axis

ing volume and planes, such as the short or long axis, simplifing, anatomic evaluation of the heart (Fig. 4.2). In the oblique plane, the course and location of the coronary arteries can be identified.

Reconstruction of the Curved Plane: Curved MPR

The same three-dimensional software that enables MPR allows reconstruction of curved planes (curved reformatting), according to the course and location of the coronary arteries. The course of each coronary artery can therefore be followed point by point and image by image. Direct reconstruction of a curved plane yields an image of the vessel of interest, from its origins and extending to its more distal segments, according to specifications that are provided by the radiologist. These images may be obtained manually or automatically, with reconstruction software that identifies the coronary arteries based on their higher CT density (Fig. 4.3).

This image reconstruction technique is essential in the evaluation of coronary artery disease (Fig. 4.4). It allows clear differentiation between the vessel lumen (high density due to contrast agent in the blood and thus bright CT images), the surrounding epicardial fat tissue (darker, due to the lower CT density), and the myocardium (intermediate gray level, intermediate CT density). Furthermore, only these images clearly show the vessel wall, especially in the presence of pathologies such as fibrolipidic plaques (hypodense in CT, dark in reconstructed images) and calcific plaques (hyperdense, bright in CT images).

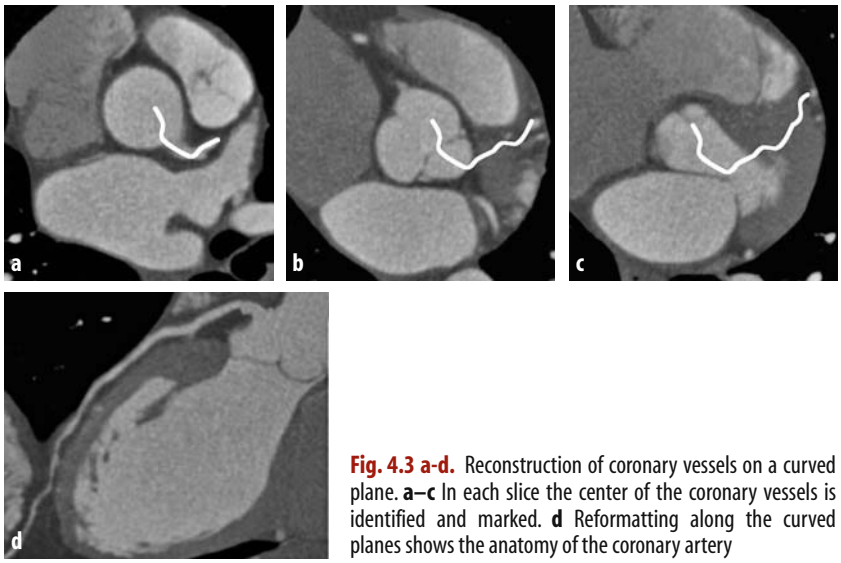

Fig. 4.3 a-d. Reconstruction of coronary vessels on a curved plane. **a–c** In each slice the center of the coronary vessels is identified and marked. **d** Reformatting along the curved planes shows the anatomy of the coronary artery

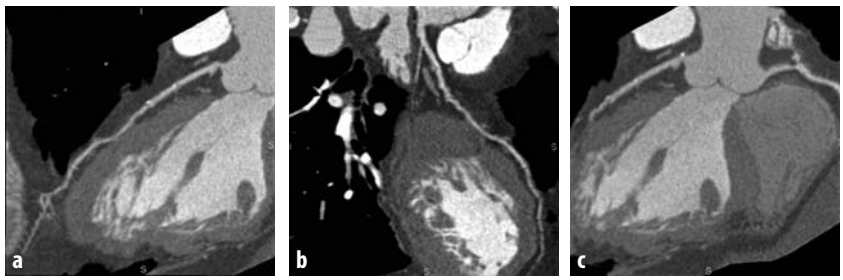

Fig. 4.4 a-c. 3D imaging; planimetric analysis using curved-plane reformatting

Bi-dimensional and planimetric images of the coronary arteries "slice" the vessel lumen in an orthogonal plane. The aim of the evaluation is to identify the vessel wall; therefore it is always important to image the vessels in two perpendicular orthogonal planes. Figure 4.5 very clearly demonstrates that in the case of an eccentric atherosclerotic plaque an orthogonal plane reveals the plaque, while the image reconstructed on a plane passing parallel to the fibrolipidic plaque does not show either the parietal plaque or the lumen stenosis.

At least two planes for each coronary artery must therefore be reconstructed and imaged (six images for three coronary arteries); depending on the specific anatomic variation, orthogonal images of other vessels will also be required, such as the intermediate, diagonal, and obtuse marginal branches.

Together with reconstruction of the vessel in curved longitudinal images, axial images, perpendicular to the imaging plane of the arteries, must be evaluated. Clear evidence of the location of the plaque (concentric or eccentric) and the degree of stenosis can be provided, including information on the presence of remodeling (as discussed later) (Fig. 4.6). Most of the currently

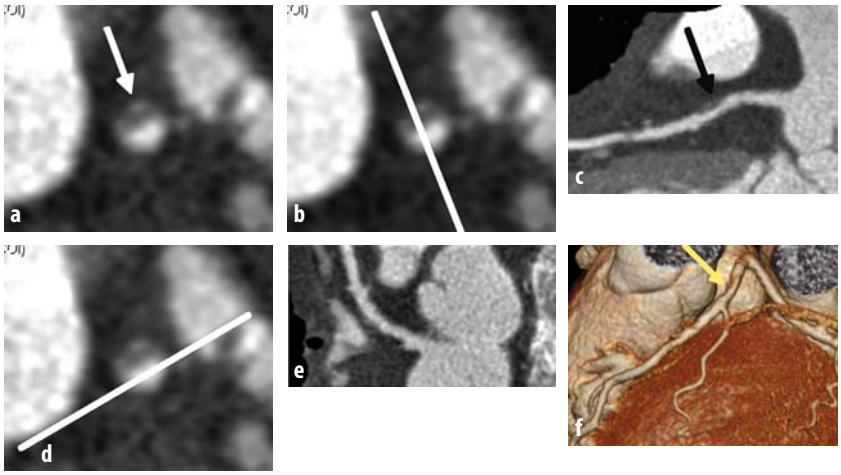

Fig. 4.5 a-f. Marginal eccentric plaque of the left anterior descending artery (LAD). **a** In the axial image, the eccentric fibrolipidic plaque is well evident (*arrows* in **a**, **c**, and **f**); the reduction in caliber is 50%. Visualization is possible only in one reconstruction plane (**b**, *white line* shows the reconstruction plane; **c** is the resulting image). In the orthogonal plane, the vessel seems to be of normal caliber (**d**, *white line* shows the reconstruction plane; **e** is the resulting image). **f** 3D image using volume-rendering technique allows a clear evaluation of the stenosis

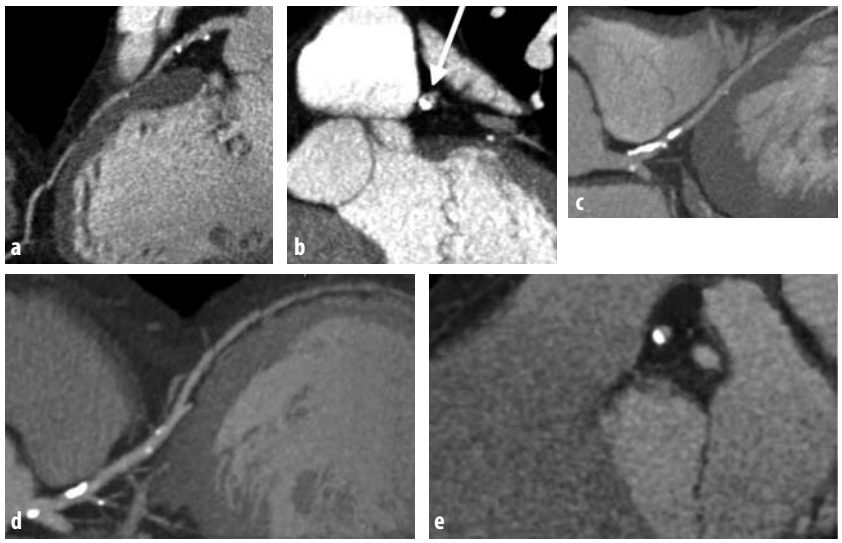

Fig. 4.6 a-e. Marginal plaque of the LAD with a calcific core and fibrolipidic cap (**a, b**), both of which are well-evident in the axial reconstruction (**b**, *arrow*). **c-e** Eccentric calcified plaque without a hypodense component

available software allows direct evaluation of the vessels along their longitudinal axes, in addition to the possibility to interact with the images and rotate them along the different orthogonal planes. At the same time, axial images for the chosen view are displayed on the same console, allowing evaluation of the plaque burden at that specific level.

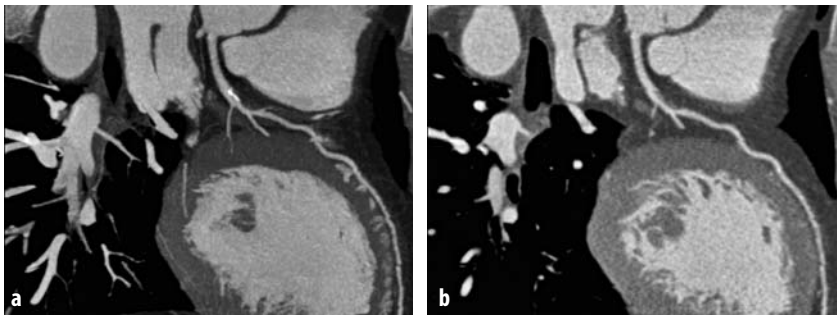

Fig. 4.7 a, b. 3D imaging: planimetric analysis (multi-planar reformatting MPR). **a** Reconstruction with thick slices (5 mm) allows better evaluation of the anatomical course of the left anterior descending artery along the wall of the left ventricle. **b** The same artery evaluated using a thin slice (1 mm)

Usually, MPR curved images have a thickness of 1 mm or less. Depending on the amount of epicardial fat surrounding the arteries, the thickness can be increased to 3–5 mm, yielding anatomically reconstructed images of a more consistent quality (Fig. 4.7). However, these thicker images may hide small parietal plaques, which can be reconstructed and displayed only by the evaluation of thinner slices.

Clinical Use of Planimetric Techniques

Planimetric techniques do not provide direct evidence of the entire data volume acquired, as they are reconstructed according to the three-dimensional data set. These images are very important to define the parietal atherosclerotic plaque burden, identify the plaque, and properly characterize the plaque components. Software that "straightens" the vessels along their longitudinal axes is also available. It can be used to visualize the different sides of the vessel wall, since eccentric plaques may be evident on one side of the artery but not on the other side. Other types of software may also use planimetric images for quantitative evaluation of the vessel lumen, allowing measurement of the degree of stenosis in areas involved by atherosclerosis. Despite these numerous possibilities, in coronary CTA direct evaluation of the coronary vessels by the clinician may be necessary (Fig. 4.8). In calcific plaques, for instance, the so-called blooming artifact leads to an image in which the volume of the plaque is increased such that a false degree of stenosis is estimated by the computer. An expert radiologist, however, is able (using other reconstruction filters) to estimate the real extent and importance of the atherosclerotic involvement. Thus, regardless of the improvements in software for direct evaluation of the coronary vessels, a proper direct interface of the clinician with the console will always be needed to confirm the clinical diagnosis.

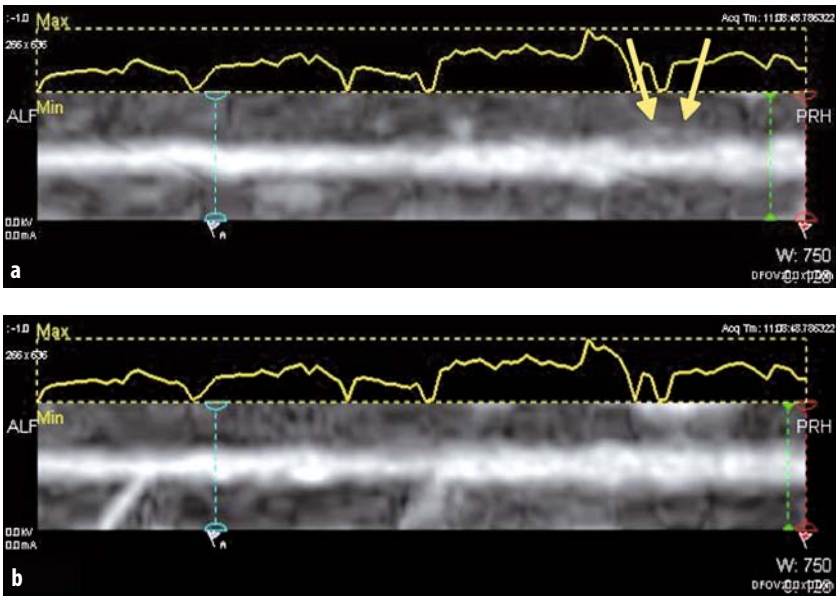

Fig. 4.8 a, b. Coronary artery "straighten" using special software. Rotation along the cental axis reveals evidence of plaque (*arrows*, **a**), wich is not seen in (**b**)

Volumetric Techniques (Volume Rendering)

Image analysis using volumetric techniques creates a color, three-dimensional image that allows direct interactive evaluation of the coronary vessels. The software employed in this application was initially developed mostly for military (aerospace) purposes and was later used in the film industry in virtual reality cartoons. The medical and radiology fields have taken advantage of the progress made in movie animation techniques, as they have contributed to improvements in CT image reconstruction.

Orthogonal and Perspective Imaging

In order to understand the concept of volumetric imaging, a distinction must be made between the traditional concept of images (radiologic, artistic, etc.) and the newer one introduced by 3D imaging. In conventional radiologic images, the anatomic area under evaluation is perceived orthogonally, as if an infinite distance has been created between the viewer and the object being evaluated. In the example shown in Figure 4.9, a series of rounded objects, all of the same diameter, are shown. In orthogonal view they all appear to be of the same size and dimension. In a routine X-ray, the abdomen, kidneys, vertebrae, and all other structures are visualized in a dimension that reflects their original size in the real world. By interacting with a volume data set in 3D imaging, we can move the volume, making it closer to us (the viewer), therefore

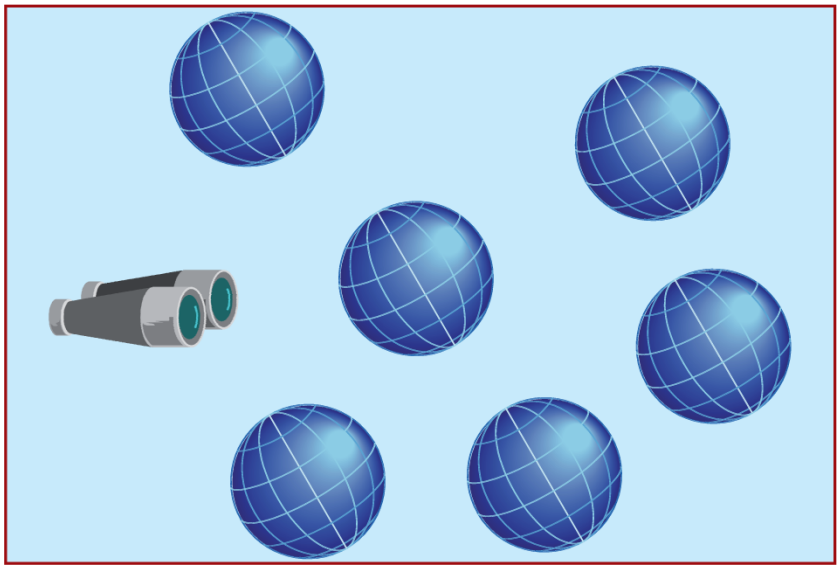

Fig. 4.9. Orthogonal view: all globes are of the same size

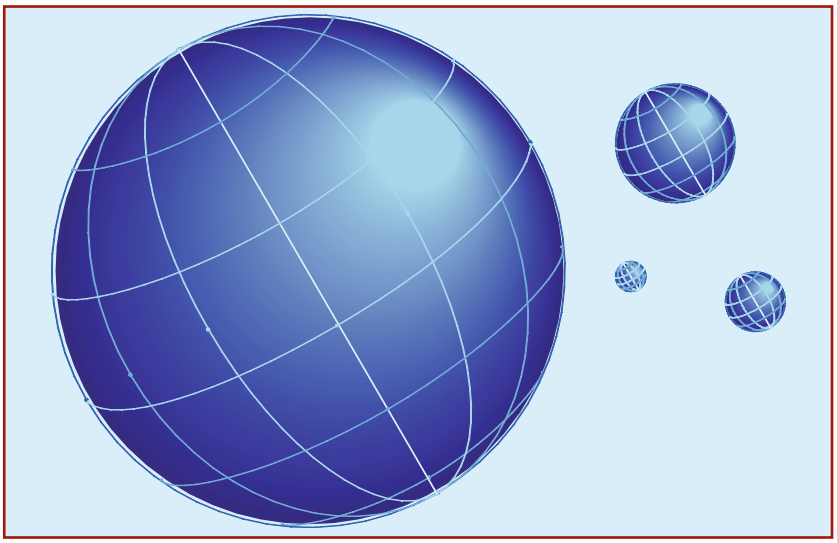

Fig. 4.10. Perspective view. As seen through a virtual eye (the binocular in Fig. 4.9), there is true 3D evaluation of the globes. Those that are closer appear larger than the ones that are more distant, as in real life

modifying our relationship to it, i.e., the closer the object is to us, the larger it will appear. In the example of Figure 4.10, our eye is the binocular, such that the rounded structure is viewed from very near. Thus, objects very close to the binocular (our eye) are very large, while those progressively more distant become proportionally smaller. This phenomenon is referred to as the perspective view of a volumetric object.

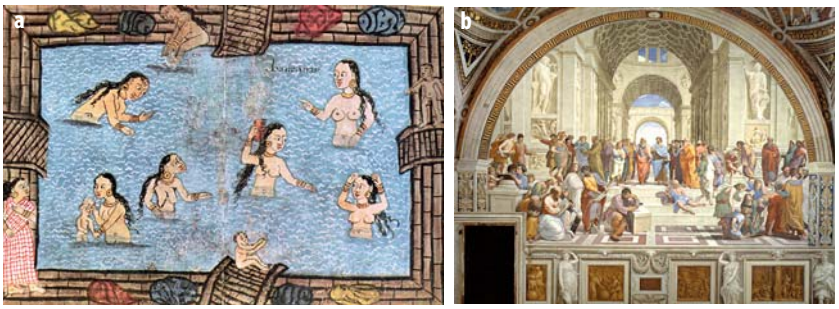

Fig. 4.11 a, b. Orthogonal (**a**) and perspective views in art (**b**). Raffaello's *La scuola di Atene* (Rome, Vatican Museum) is an example of the perspective view in Renaissance art

In early paintings, the figures in a work of art are always of the same size, as if the viewer was at an infinite distance from them. During the Renaissance, painters, particularly Italian painters, became experts in realizing perspective views of human figures and landscapes, with attention to small details that made the depicted objects closer to our visualization of them in the real world (Fig. 4.11). The size of the figures in the painting became proportional to the distance from the painter or the viewer. In the same way, in volumetric CT imaging, a perspective vision is created in which the closer the object, the larger it appears. Moreover, while a painting is a static object, the viewer of a CT image is able to adjust the distance between his or her eyes and the object under evaluation (the 3D volume of images) by direct interaction with the computer console.

Volume Rendering of Human Anatomy

Data sets acquired in CT include all the information contained in the anatomic area under investigation, with the risk that overlapping structures, or structures with different densities may create confusion, e.g., due to distension of the anatomic object (in our case, the coronary vessels) being evaluated. Volume-rendering technique allows the imaging, display parameters to be set so that the structure of interest can be readily identified. For example, to evaluate the surface of the body, the density values are set such that they correspond to those of the skin; by progressively enhancing the density values, muscular structures, internal parenchymal organs, bones or, as in our case, vessels filled with contrast agent (density values of 300–500 HU) are visualized (Fig. 4.12). In effect, the image is restricted to the contrast-agent-filled coronary artery of interest, which is viewed in 3D images that have been reconstructed using volume-rendering techniques. The only overlapping components in the arteries are thus related to the presence of calcified plaques, which have a density even higher than that of the contrast agent. Images of the coronary arteries reconstructed with these techniques are extremely informative and of great diagnostic value, as discussed in the other chapters of this book.

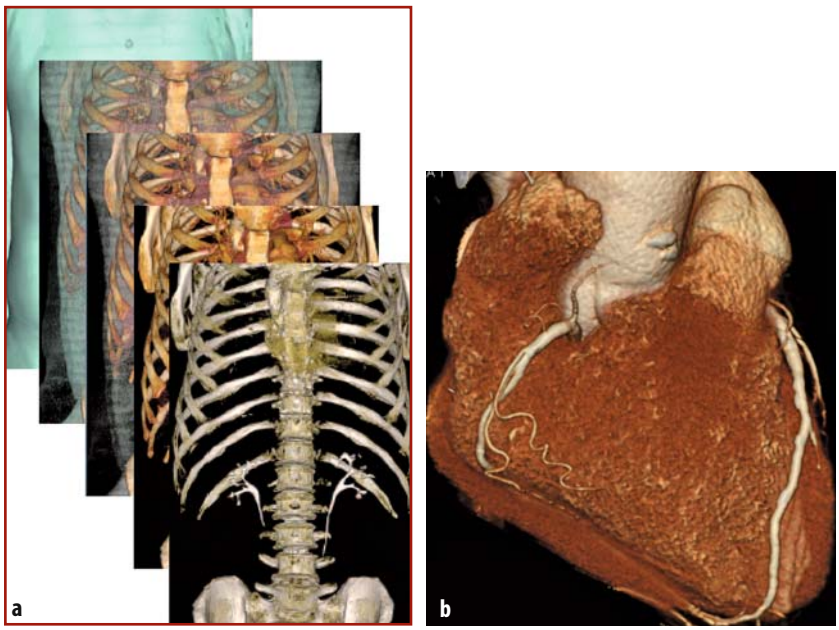

Fig. 4.12 a, b. Volume-rendering technique. **a** In evaluating the body using changing transparency values, deeper structure become evident, from the skin to the bones. **b** In cardiac imaging, a 3D setting is used and is already optimized for evaluating vascular structures opacified by means of contrast agent

Color and Virtual Lighting

Three-dimensional images reconstructed using volume-rendering techniques became more realistic following the introduction of color (albeit, in effect, a false color) and by the use of virtual lighting to create shading effects that enhanced the three-dimensional information. Similar effects (use of color and the proper use of lateral lighting) were used masterfully by the Italian painter Caravaggio, who more than any other artist of his time was an expert in the use of external light to make figures appear more realistic, including in their three-dimensional aspect (Fig. 4.13).

Modern three-dimensional image reconstruction techniques, such as those employed in radiology and in movie animation, are based on the same fundamental concepts, but adapted to be standard, reproducible, and accessible at the computer console. Moreover, there is the additional advantage of direct interaction with the object being evaluated, which allows for a point by point evaluation that enhances the areas of interest in order to define the presence of disease, etc.

Once again, it must be emphasized that is not the coronary arteries that are being seen, but the contrast agent contained within them. Likewise, a surface image of the myocardium and cardiac chambers is achieved only due to the higher density conferred by the presence of contrast agent (Fig. 4.14). Three-dimensional reconstruction of a volume of data acquired at the level of the heart without contrast agent injection would produce a useless evaluation of

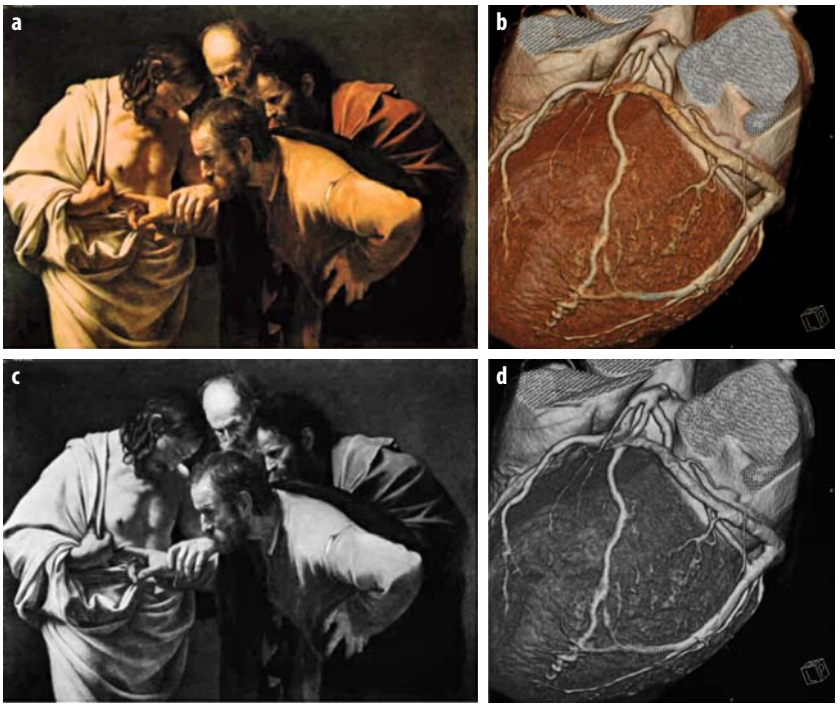

Fig. 4.13 a-d. Use of false color. The 3D effect, both in (**a**) the painting Caravaggio's *Incredulità di Tommaso* (Potsdam, Bildgalerie) and (**b**) the image of the coronary artery is enhanced by use of color, as seen in a comparison with the black and white images (**c, d**)

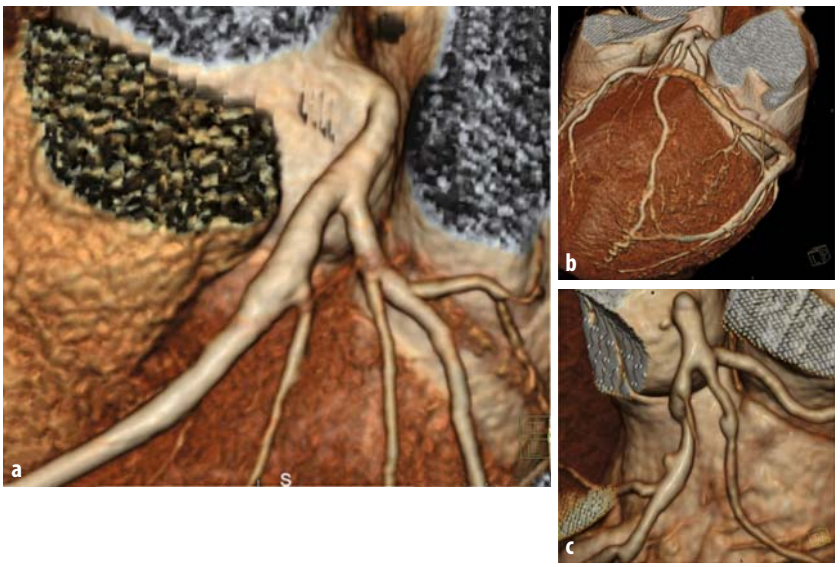

Fig. 4.14 a-c. Examples of coronary vessels evaluated by means of volume-rendering technique

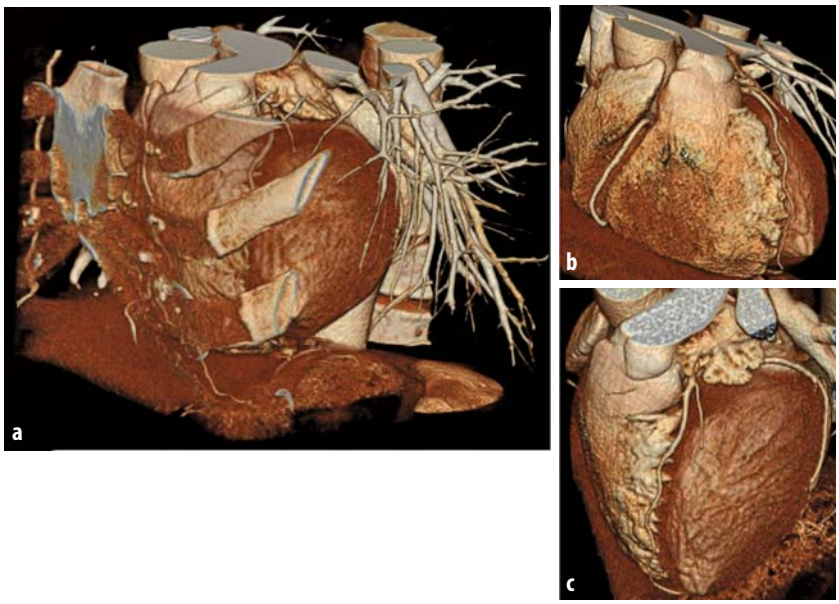

Fig. 4.15 a-c. Thoracic volume evaluated by volume-rendering technique. **a, b** Bones and pulmonary vessels opacified by contrast agent are superimposed on the coronary arteries, limiting anatomic evaluation. Manual or automated editing removes the overlapping structures, revealing the coronary vessels (**c**)

the soft tissues (the myocardium), which would be visible only because they are surrounded by the very low density of the air present in the lungs, but any evidence of the coronary arteries would be absent.

Other structures with high radiologic density overlap the coronary arteries, such as the pulmonary vessels and the bony thoracic cage. These structures can be excluded by "editing" the images (either automatically or manually) thereby providing direct and exclusive evidence of the coronary vessels (Fig. 4.15).

Clinical Use of Volume-Rendering Images

Three-dimensional reconstructed images are foremost important as they provide direct and immediate evidence of the anatomy of the coronary tree (see Chap. 1 for a discussion of the variability of the coronary anatomy). Moreover, this technique allows for a complete and simultaneous evaluation of the entire volume acquired. Nonetheless, care must be taken in evaluating volume images reconstructed with volume rendering techniques as, in fact, they provide a superficial evaluation from outside of the vessels (Fig. 4.16). In a patient with parietal atherosclerotic involvement, stenosis can be visualized only when a fibrolipidic low-density plaque is present; if the plaque is calcific, the higher density of the plaque material will overlap with the density of the vessel lumen, prohibiting proper visualization and analysis of a possible stenosis (in addition to the previously mentioned blooming effect) (Fig. 4.17). Therefore, in every case and for every vessel,

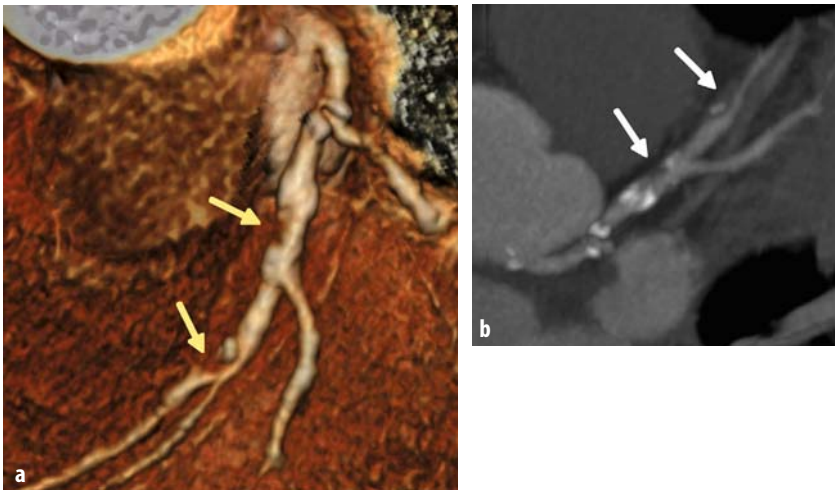

Fig. 4.16 a, b. Fibrolipidic plaque evaluated using three-dimensional volume rendering technique. **a** Evaluation using bi-dimensional technique. Note the central hypodense calcific component of the plaque and the fibrolipidic cap (*arrows*) (**b**)

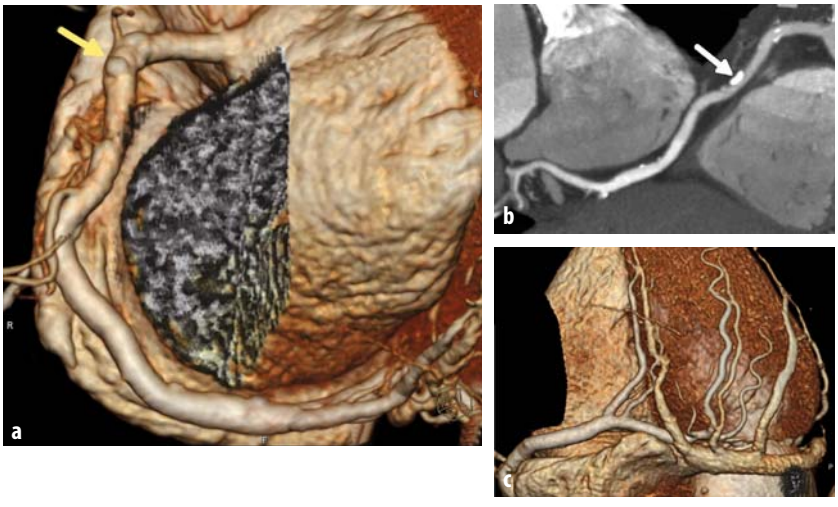

Fig. 4.17 a-c. Calcific plaque evaluated using volume-rendering technique. The plaque is hyperdense (**a**, *arrow*). A detailed evaluation of the vessel lumen is not possible but can be achieved using bi-dimensional images (**b**, *arrow*). There is marked hypertrophy of the right coronary artery (distal branches, **c**)

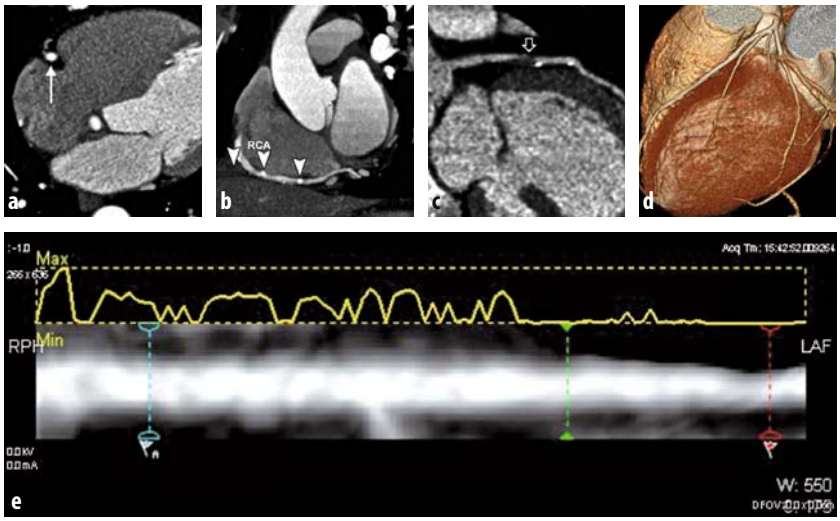

Fig. 4.18 a-e. Different reconstruction techniques: axial (**a**), MPR (**b, c**), volume rendering (**d**), straightened vessel (**e**)

images generated by the two types of reconstruction must be evaluated and compared. This will result in proper anatomic definition and correct identification of the atherosclerotic involvement (Fig. 4.18).

Virtual Endoscopy

We conclude this chapter with a brief discussion of another three-dimensional visualization technique, albeit one that is seldom used to evaluate the coronary arteries, virtual endoscopy. The principles and software needed to acquire virtual endoscopy images are the same as those for volume-rendering images. The difference is that the virtual eye moves from a surface evaluation to an internal examination of the anatomic 3D data sets. To do so, specific settings have to be used, such that the density contained in the lumen (contrast agent) becomes transparent while other densities are made evident. This procedure is carried out by a mouse click at the computer, as these settings are already among the many available to the clinician. Once "inside" the vessel of interest, the viewer can move his or her virtual eyes along the course of the vessels and the area of stenosis, then move on to the origin of the side branches (Fig. 4.19). Although fascinating, this technique does not add any further information to that already provided by the other above-described procedures and is therefore seldom employed. Virtual endoscopy is more useful in other settings, e.g., in the evaluation of pre-cancerous polyps of the colon (virtual colonoscopy) (Fig. 4.20).

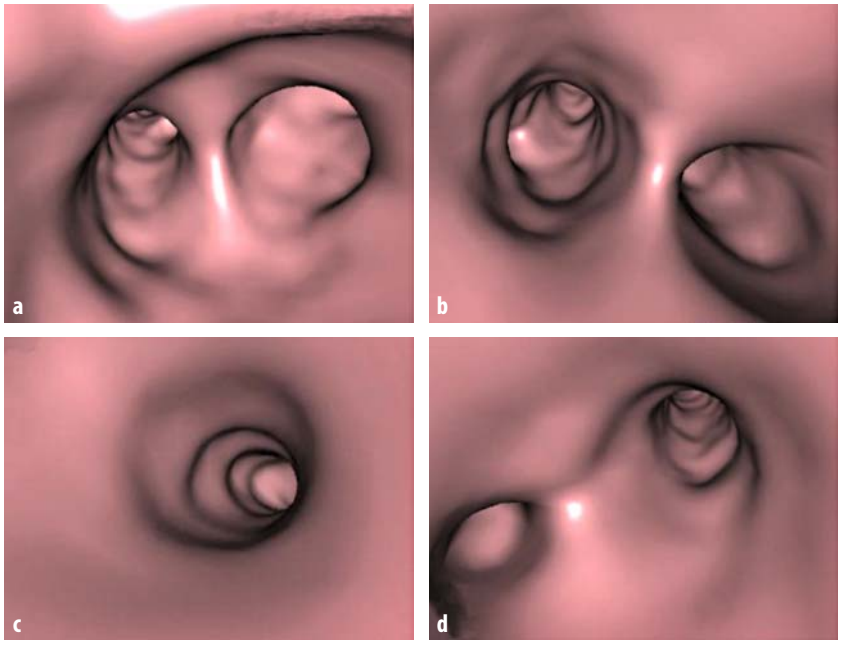

Fig. 4.19 a-d. Virtual endoscopy of the coronary arteries

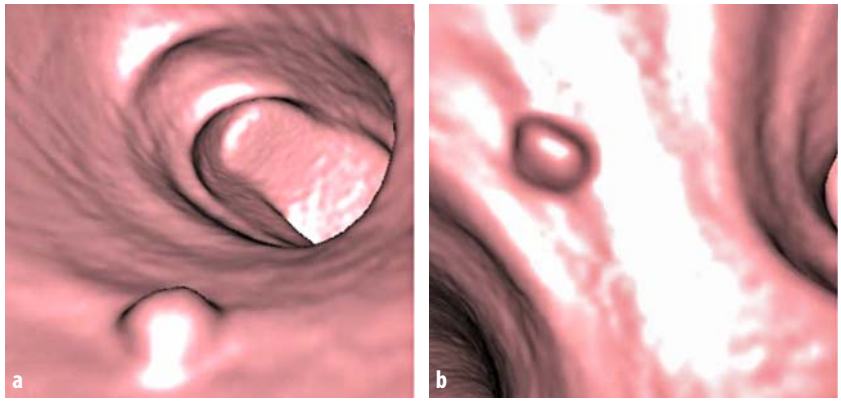

Fig. 4.20 a, b. Virtual endoscopy of the colon (**a**): a parietal 5-mm polyp is easily detected (**b**)

5

Coronary Pathophysiology

Massimo Fioranelli, Chiara Lanzillo, Francesco Peverini

The heart consumes more energy than any other organ. It cycles about 6 kg of ATP every day, which is 20–30 times its own weight. To acquire the energy necessary to carry out cardiac functions, the heart converts chemical energy stored in fatty acids and glucose into mechanical energy, in the form of actin-myosin myofibrillar interactions. The main contributors to ATP synthesis are fatty acids (70%), through β-oxidation, and glucose (30–40%), through aerobic glycolysis.

Energy supplied to the myocardium is used for mechanical activities, i.e., contraction (65%) and relaxation (15%), and for electrical activity (5%); the rest is spent on other cellular functions (20%). Under anoxic or ischemic conditions, the myocardium uses anaerobic glycolysis to produce energy. This consumes a large amount of glucose and leads to the production of lactate and 2 ATP molecules for every molecule of glucose, whereas oxidative phosphorylation produces 36 molecules of ATP for the same amount of glucose. Lactate reduces intracellular pH, which inhibits glycolysis, β-oxidation, and protein synthesis.

Almost all (90%) energy (ATP) derived from substrate utilization is produced in the mitochondrial respiratory chain, through oxidative phosphorylation. During coronary ischemia, ATP is degraded, resulting in the production of ADP and then AMP and adenosine. Consequently, adenosine diffuses from myocytes into the interstitial fluid and the coronary venous effluent. Adenosine is a powerful coronary dilator and the rise in its interstitial concentration parallels the increase in coronary blood flow. Adenosine loss from myocytes can have catastrophic consequences, since as much as 50% of the adenosine reserve may be depleted during prolonged (30 min) ischemia. Adenosine de novo synthesis is very slow; about 2% every hour; thus, during an ischemic event lasting more than 30 min, a large number of myocytes can be permanently injured.

The coronary arteries supply the myocardium with oxygen and nutrients; only the innermost layer of the endocardium (about 0.1 mm thick) is supplied directly from the blood that is inside the heart chambers. From the epicardial

P. Pavone, M. Fioranelli, D.A. Dowe, *CT Evaluation of Coronary Artery Disease*.

coronary arteries, and then via intramuscular and subendocardial vessels, blood flows to the myocardial capillaries. During systole, blood flow in these capillaries is very low due to cardiac contraction and ventricular ejection.

In a normal heart, blood flow is controlled by the vascular tone of the coronary microcirculation (vessels with diameters < 400 μm). A pressure drop across a stenosis causes compensatory vasodilation at rest, thereby diminishing the ability of the coronary circulation to adapt to an increase in oxygen demand. Resting coronary flow is not impeded by mild or moderate stenoses and is maintained by normal vasodilatory regulation of the microcirculation. It remains constant until epicardial coronary constriction exceeds 85–90% of the normal segment diameter. By contrast, maximal hyperemic coronary blood flow begins to decline when the diameter of the stenosis exceeds 45–60%, leading to myocardial ischemia and angina.

Coronary Flow Reserve

The myocardial oxygen supply rises and falls in response to the oxygen demands of the myocardium. Myocardial oxygen extraction at rest is almost maximal (about 70%). In response to physiologic or pharmacologic stimuli, coronary flow to the myocardium is increased from its basal level to a maximal flow, rising to 280 ml for 100 g/min. Coronary flow at rest is 220–250 ml/min (70–90 ml for 100 gr myocardial tissue per min) and is about 5% of cardiac output. An increased metabolic demand can only be met by augmented coronary flow.

Coronary flow reserve is the capacity to increase coronary blood flow in response to a hyperemic stimulus and is defined as the ratio of maximal to basal coronary flow. It is a measure of the ability of the two components of myocardial perfusion, namely, epicardial stenosis resistance and microvascular resistance, to achieve maximal blood flow. Since flow resistance is mainly determined by the microvasculature, coronary flow reserve reflects the microvascular repsonse to a stimulus and therefore presumably the function of the small vessels. Coronary flow reserve is determined by measuring coronary or myocardial blood flow and taking measurements both at rest (basal flow) and with maximal hyperemia, which is achieved with an intracoronary or intravenous infusion of adenosine or an intravenous infusion of dipyridamole.

Normal coronary flow reserve in young patients with normal arteries commonly exceeds 3.0; in patients undergoing cardiac catheterization with angiographically normal vessels, coronary flow reserve averages 2.7±0.6.

In patients with coronary artery disease, the extent of the reduction in coronary flow reserve is directly related to the severity of the stenosis, whereas in individuals with angiographically normal arteries it is a marker of microvascular dysfunction. A coronary flow reserve of <2.0 is often considered abnormal.

Coronary Stenosis: Definition and Evaluation in Coronary Artery Disease

In 1959, the first coronary angiography was performed and the technique soon became the gold standard in the evaluation of coronary artery disease.

Coronary stenosis can be assessed by different approaches: by evaluating lumen reduction (anatomopathological section or CT imaging) or by measuring the reduction in longitudinal diameter (angiography imaging) (Fig. 5.1).

Coronary angiography examines diameter reduction and quantifies coronary lesions in terms of the percentage stenosis and minimal lumen diameter.

The percentage stenosis is given by the relationship between the minimal lumen diameter resulting from the stenosis and the reference diameter upstream or downstream of the lesion, identified as normal. Minimal lumen diameter is calculated in millimeters and is an absolute value; it is more reliable and more consistent than percentage stenosis.

Hyperemic flux, in the animal model proposed by Gould (Fig. 5.2), begins to decrease when an atherosclerotic plaque causes a 50% reduction in diameter; implying a 75% stenosis of the lumenal area (Fig. 5.1). This is why an atherosclerotic plaque is defined as obstructive when the vessel diameter is

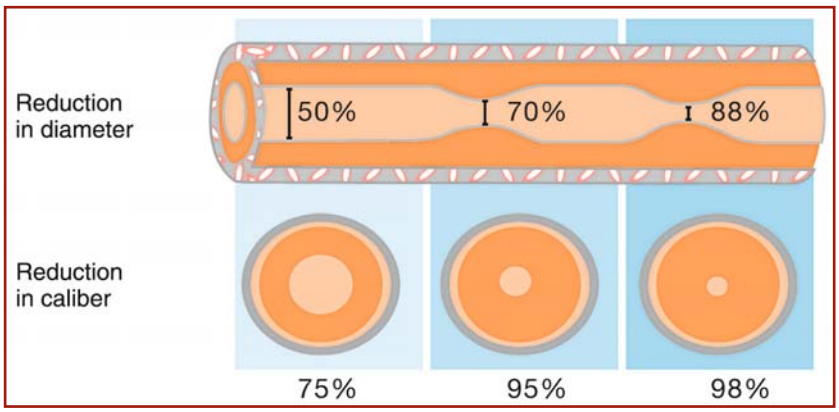

Fig. 5.1. Relationship between diameter and caliber (lumen) reduction in coronary stenosis

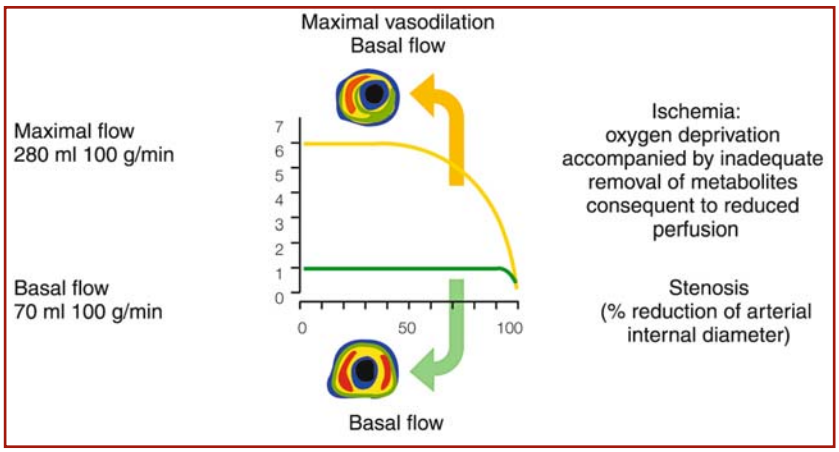

Fig. 5.2. Coronary flow reserve. Relationship between stenosis and microvasculature

decreased by more than 50%. However, this does not mean that the lesion will certainly cause ischemia; rather, it is a threshold value over which the stenosis has ischemic potential.

Coronary blood flow at rest is not significantly decreased until the diameter of the lumen is reduced by about 90%. In the absence of coronary microcirculation dysfunction or hypertrophy, coronary blood flow during exercise is reduced when the stenosis is severe (diameter reduction between 50 and 80%).

In many people with coronary artery disease, any revascularization strategy needs to be discussed not only in anatomic terms but also regarding the functional severity of the stenosis. Thus, it is extremely important to evaluate patients non-invasively, since the angiographic degree of stenosis is not always of prognostic value. When there is moderate stenosis (between 50 and 80%) and non-invasive tests have confirmed myocardial ischemia, if medical therapy is unable to stop the symptoms then the patient is referred for percutaneous revascularization.

If non-invasive testing does not detect myocardial ischemia, even in patients with chest pain, then a functional evaluation of stenosis should be obtained. Among the many functional tests, measurement of fractional flow reserve (FFR) is a good way to evaluate the severity of a stenosis. In the presence of a stenosis, there is a decrement in the distal pressure that is proportional to its severity. To maintain resting myocardial perfusion, arteriolar resistance decreases to compensate for the pressure drop caused by the epicardial stenosis. FFR estimates coronary blood flow through a stenotic artery and is calculated by measuring the coronary pressure distal to a stenosis at constant and minimal myocardial resistances (i.e., maximal hyperemia) obtained during intracoronary adenosine infusion.

FFR is defined as the mean distal coronary pressure divided by the mean proximal coronary or aortic pressure measured during maximal hyperemia. Since it is calculated only at peak hyperemia, FFR differs from coronary flow reserve by being largely independent of basal flow, driving pressure, heart rate, systemic blood pressure, or status of the microcirculation.

A FFR of 1 is considered normal and is anomalous when < 0.75. For example, dividing the pressure value obtained distal to the stenosis, e.g., 52 mmHg, with the value obtained proximal to the stenosis, e.g., 101 mmHg, yields FFR = 0.51, which is obviously anomalous.

Another parameter used to assess stenoses is Doppler flow velocity, in which the velocity of the blood before and after the stenosis is measured using a Doppler probe. The variation in velocity is proportional to the flow changes, assuming that vessel caliber remains the same.

The Limits of Coronary Angiography

Coronary angiography is able to identify the number, extent, and degree of stenosis. However, one of its limitations is that it only visualizes the lumen, whereas coronary artery disease usually affects the arterial wall. In fact, anatomopathological studies and intravascular ultrasound (IVUS) data have shown that angiographically normal coronary artery segments often have an atherosclerotic burden. Moreover, many trials have shown that most coronary

thromboses occur in a non-occluding plaque, and often in mild or moderate stenoses. In addition, positive remodeling, which is caused by an atherosclerotic plaque that extends outwardly from the vessel wall, decreases the accuracy of coronary stenosis evaluation by coronary angiography.

Coronary stenosis is usually evaluated according to the degree of vessel diameter reduction compared to apparently normal proximal and distal vessel segments; but, since coronary artery disease usually extends all along the coronary arteries, there is a high chance that the referring segment also contains plaque. Thus, the amount of stenosis is generally underestimated, as the atherosclerotic burden is present throughout the vessel. In the evaluation of coronary artery disease, it is of pivotal importance to determine the atherosclerotic burden as well as the biological qualitative composition of the plaque. As many vulnerable plaques prone to rupture are non-obstructive, they are often missed by coronary angiography, leading to the increasing need to measure the atherosclerotic burden and to analyze the plaque's composition instead of the degree of stenosis. Thus, the most important prognostic factor is the extent of atherosclerotic disease and not the degree of stenosis, as several studies on patients who died from myocardial infarction or sudden death have clearly established.

6

The Atherosclerotic Plaque

Maddalena Piro, Sara di Michele, Massimo Fioranelli

Even though coronary, cerebral, and peripheral arterial disease represents the most common features of atherosclerosis, it progresses in the absence of any symptoms for most of its developmental course. Generally, the severity of a coronary stenosis is of poor predictive value for cardiac events such as sudden death, myocardial infarction, or unstable angina. For this reason, attention is increasingly being focused on the biology of the atheroma rather than on the severity of the stenosis.

The arterial wall is made up of three layers. The *tunica intima* is 150–200 μm in diameter and consists of endothelial cells. The adjacent smooth muscle cells, extracellular matrix, and internal elastic membrane separate it from the *tunica media*, which is 100–350 μm in diameter and made up of smooth muscle cells, elastin, and collagen. It is encircled by the external elastic membrane. The outermost layer, the *tunica adventitia*, is 100–350 μm in diameter and composed of fibrous tissue. It is surrounded by perivascular connective tissue and epicardial fatty tissue.

The endothelium represents a defensive shield of the vascular wall, acting as a modulator of cellular proliferation as well as inflammatory and thrombotic processes. Its dysfunction plays a crucial role in the progression of atherosclerosis. A single layer of cells comprises the endothelium and serves as the site of contact between the blood and the arterial wall.

The atherosclerotic process develops in the intimal layer, beginning with lipidic striae and ultimately progressing to the fibrolipidic plaque, going through several stages along the way. Initially, oxidized lipoprotein particles accumulate in the intimal layer; subsequently, there is leukocyte infiltration and the transformation of monocytes to macrophages begins. Macrophages phagocytize oxidized LDL, thereby forming cholesterol-rich foam cells that eventually undergo apoptosis. Secondly, smooth muscle cells migrate from the tunica media to the intima, where they secrete extracellular matrix, which provides the structural framework of the plaque. Attracted by cytokines, immunocompetent cells, such as lymphocytes, monocytes, and plasma cells, further accumulate in the plaque. The final process is the formation of a lesion of

P. Pavone, M. Fioranelli, D.A. Dowe, *CT Evaluation of Coronary Artery Disease*.

variable dimensions, that is constituted by a central lipid nucleus (lipid core), a fibroconnective tissue cap (fibrous cap), immunocompetent cell infiltrates, and calcium nodules. Calcium that settles in the coronary arteries is strictly associated with plaque development; its accumulation is an active process that can be observed in all phases of atheroma formation. Histopathological studies and intravascular ultrasound (IVUS) findings have confirmed the close relationship between the atherosclerotic burden and the amount of coronary calcium. The prevalence of calcifications is strongly linked to patient age and consistently rises in men over age 50 and in women over age 60; however, coronary plaques and their calcifications are linked only weakly with stenosis severity. Even though not all plaques show calcifications, typically, the total amount of calcium accounts for about 20% of the entire area of the atherosclerotic plaque. Recently, it has been shown that the calcification pattern differs in patients with acute coronary syndrome (ACS) versus those with stable angina. In patients with ACS and plaque rupture, superficial and deep deposits of small calcium aggregates are seen more frequently; furthermore, the total amount of calcium in the plaques of ACS patients is lower than in those of patients with stable angina. In response to the atherosclerotic insult, the coronary vessel tries to protect itself by preserving the vascular lumen through a process referred to as positive remodeling. In atherosclerotic vessels that have not undergone remodeling, the vascular lumen may be reduced of at least 40% of the perimeter, delineated by the internal elastic membrane, is involved. The degree of reduction affecting the vascular lumen by the atherosclerotic plaque is therefore modulated by the remodeling process, which varies between individuals. Thus, plaque development starts towards the external side of the artery, preserving the vascular lumen. However, while chronic stable angina is associated with a slowly developing plaque, which may affect > 50–70% of the arterial lumen, a quickly developed thrombotic lesion will cause unstable angina or myocardial infarction. Indeed, the complications of an atherosclerotic plaque are essentially rupture of the fibrous cap or erosion of the superficial endothelial layer. These anatomic alterations predispose to thrombus formation and an immediate reduction of the vascular lumen. The atherosclerotic plaque with histopathological characteristics that make it prone to the above-mentioned complications is referred to as a "vulnerable plaque."

The Vulnerable Plaque: Biology and Histology

Atherosclerosis is widely accepted as a chronic inflammatory disease initiated by vascular and extravascular factors. As described above, plaque formation is a long-standing process; it begins with the formation of a fatty streak, followed by increasing lipid and leukocyte infiltration. Initially, the dilation produced by positive remodeling of the diseased artery accommodates the growing plaque, so that the diameter of the vessel lumen is unchanged. Eventually, however, the plaque grows into the vessel, reducing the lumen diameter and, consequently, blood flow. Atherosclerotic plaques typically consist of a lipid-rich core surrounded by an eccentrically thickened intima; the lesion is covered on its luminal aspect by a fibrous cap. A large lipid-rich

core, a thin fibrous cap, and an extensive inflammatory burden identify a vulnerable plaque (Fig. 6.1).

According to recent studies, there is a close relationship between the size of the lipid core and plaque vulnerability; indeed, a large lipid core correlates with a higher probability of plaque rupture and thus of acute coronary thrombosis. It has been observed that plaques with a high lipid content but which are not angiographically significant were more prone to rupture, whereas hemodynamically significant plaques with a small lipid core but a high content of smooth muscle cells and collagen are more stable. Thus, both the lipid core dimension and the composition of the plaque determine its likelihood of rupture. According to some authors, atherosclerotic plaques made up of 40% lipid are at higher risk. This is in line with the observation that cholesterol content affects the plaque mechanical resistance; specifically, plaques rich in cholesterol crystals seem to be stronger than those composed of liquid cholesterol. Among the other factors affecting the probability of rupture is the thickness of the fibrous cap: the greater the thickness of the cap, the smaller the tendency of the plaque to rupture. Generally, atherosclerotic lesions responsible for myocardial infarction have a fibrous cap that is thinner than 60 μm and an underlying well-developed lipid nucleus. At the shoulder region, i.e., at the junction between the plaque and healthy wall, where blood pressure exerts a greater circumferential stress, it is often possible to find fissures, which establish a conduit between the vascular lumen and the underlying lipid pool.

The central, lipid-rich core of the lesion contains many lipid-laden macrophage foam cells derived from blood monocytes. The presence of these cells is of crucial importance in the mechanisms leading to plaque activation and rupture, as they are capable of degrading extracellular matrix by secreting

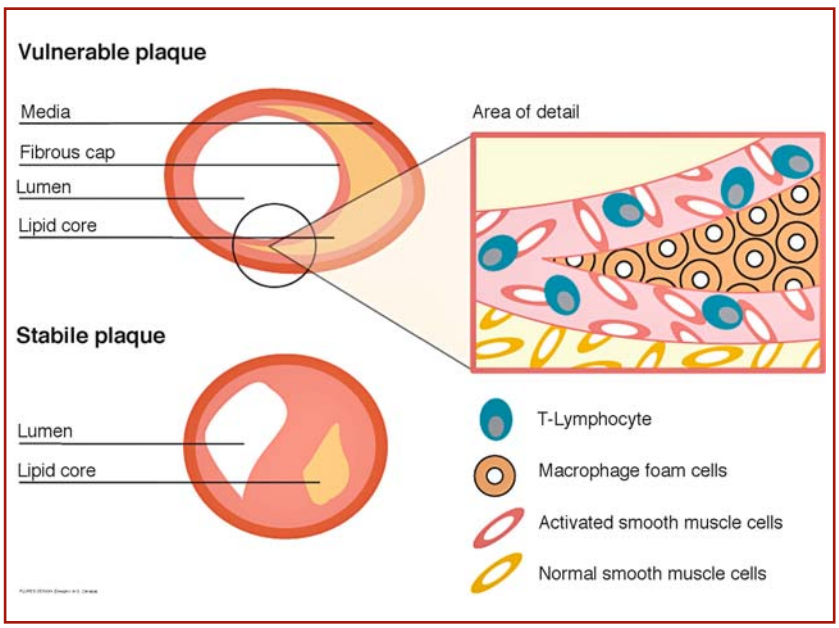

Fig. 6.1. Histological features of the stable and the vulnerable plaque

proteolytic enzymes, such as plasminogen activators and matrix-metalloproteinases, that weaken the fibrous cap. Foam cells also produce large amounts of tissue factor, a powerful procoagulant that stimulates thrombus formation when in contact with the blood. Other cells that comprise the plaque are mast cells, neutrophils, lymphocytes, and, especially, activated lymphocytes. The latter are present in all stages of plaque development, implying their involvement in the pathological process. The activation status corresponds in 65% of cases to memory T cells in a state of chronic activation, suggesting that these T cells are the result of preferential recruitment and/or retention of activated peripheral cells or the local stimulation of resting T cells. It was recently shown that these cells are oligoclonal, primed by specific antigens; however, the specific role played by T lymphocytes is unclear and evidence for specific antigens responsible for their activation is lacking.

Plaque neovascularization, usually secondary to inflammatory stimuli, is relatively frequent in diabetic patients. It may contribute to plaque rupture through the formation of small immature blood vessels within the plaque. Hemorrhage of these vessels into the plaque leads to its destabilization, precipitating acute ischemic events.

More recently, it has been shown that unstable plaques harbor neutrophils with reactivated telomerase activity. The presence of these cells may lead to prolonged local inflammatory activity and the release of factors, such as elastase and myeloperoxidase (MPO), that contribute to cap disruption. As this type of neutrophil is not found in the peripheral circulation, the presence of these cells is likely a local pro-inflammatory process. MPO oxidizes LDL cholesterol, thereby propagating its uptake by macrophages as well as the formation of foam cells. Moreover, MPO activates metalloproteinase, promotes destabilization and rupture of the atherosclerotic plaque, and reduces nitric-oxide bioavailability, impairing the vasodilatory and anti-inflammatory functions of this compound.

In summary, the main characteristics of the vulnerable plaque are:

- Large central lipid pool
- Thin fibrous cap (< 65 μm)
- Abundant inflammatory infiltrate, present at the level of the fibrous cap

Interestingly, there is a peculiar geographic distribution of the high-risk atherosclerotic plaque in that the vulnerable plaque is more likely to occur in the proximal and middle regions of the main coronary arteries. Furthermore, in the same patient there is frequently more than one vulnerable plaque. Thus, the angiographic finding that 80% of ACS patients present with two or more unstable plaques confirms the hypothesis of a widespread inflammatory process involving not only the coronary vascular bed but also the entire vascular system.

The Vulnerable Plaque: Local and Systemic Factors Contributing to Plaque Rupture

Despite several improvements in the treatment and prevention of atherosclerotic coronaropathy, ACS and its complications remain one of the most important causes of morbidity and mortality in industrialized countries. The

clinical presentation of ACS is variable: at one extreme are patients who present with an infarction that has occurred without any previous symptom or evidence of coronary disease, followed by complete stability for years and decades. In these cases, ACS is most likely due to a local mechanical stress that has ruptured a plaque with a thin cap. At the other extreme are patients with a history of primary unstable angina of several weeks duration followed by infarction and then post-infarction angina or by a new infarction within a few weeks or months. These patients often have angiographic evidence of rapid developing or progressing new lesions in previously normal vessels, accompanied by an elevation of inflammatory markers. This persisting recurrent instability is suggestive of a waxing and waning systemic inflammatory process, which may cause multiple plaque fissures and multi-focal plaque instability, with or without rupture. Therefore, identification of the local and systemic mechanisms of plaque rupture is important for understanding ACS and for choosing the appropriate treatment strategy. It is likely that a substantial number of ACS cases are explained by a systemic inflammatory condition, in association with an enhanced coagulation state, activating local hemodynamic, mechanical, and immune reactions.

To date, a growing body of evidence has confirmed the role of inflammation in plaque instability and rupture, and its correlation with both atherogenesis and systemic markers of inflammation. A consistent finding in ACS and a convincing indication that plaque rupture is mediated by systemic inflammation is the presence of elevated levels of inflammatory markers in the peripheral blood of these patients. C-reactive protein (CRP) has been shown to be a stronger predictor of cardiovascular events than other inflammatory markers. A novel finding is the presence of CRP within the plaque, associated with the presence of smooth muscle cells, macrophages, complement activation, and unstable disease. This observation raises the possibility of a direct role for CRP in plaque rupture through the local activation of complement. Moreover, in vivo data support the concept that CRP is able to bind lipids, opsonize native LDL for macrophages present in the atherosclerotic plaque, and directly quench the production of endothelial nitric-oxide synthase, resulting in diminished nitric-oxide bioavailability and thus impaired endothelial function. This finding might explain why the systemic inflammatory response is linked to impaired endothelial function and why systemic endothelial vasoreactivity is blunted in patients with elevated CRP.

Because of the multifocal nature of the plaque, the systemic inflammatory involvement, and the multiple pathways and interrelationships of inflammatory mechanisms, the search for a more coronary-specific marker has intensified. Thus, many markers of inflammation have been investigated in attempts to predict future cardiovascular events and identify patients at risk. These markers include interleukin (IL)-18, tumor necrosis factor (TNF)-alpha, adhesion molecules, matrix metalloproteases, IL-10, IL-6, and, interestingly, heat-shock proteins. The latter are a family of protein chaperones with high immunogenic potential; they have been found in the atherosclerotic plaque and are associated with plaque instability. The enzyme pregnancy-associated plasma protein A (PAPP-A) has also been associated with plaque activity and morphology in patients with ACS. The protein is abundantly expressed in the ruptured and eroded unstable plaque, but absent from or mini-

mally expressed in stable plaques. In plaques with a large lipid core and cap rupture, PAPP-A staining revealed that the enzyme occurred mostly in the inflammatory shoulder region. Placental growth factor-1 (PlGF) has been reported as a specific marker of vascular damage and of coronary events in patients with ACS. It acts as a primary inflammatory instigator of plaque instability.

Since plaque rupture may not lead to dramatic consequences if other, precipitating factors are not simultaneously present, it is reasonable to stress the potential role played by platelets and clotting factors in the transition from a stable to an unstable plaque. The hypothesis of a hypercoagulable state in ACS has been supported by data showing that the levels of coagulation system markers, such as prothrombin factor F1+2, thrombin-antithrombin complex, plasminogen activator inhibitor-1, and D-dimers, are elevated in the blood of ACS patients and may be elevated for months. As mentioned above, the vulnerable plaque is relatively rich in tissue factor; thus, exposure of the pro-thrombotic material contained in the plaque to hypercoagulable blood may lead to the catastrophic event of sudden coronary occlusion. A key molecule in the interplay between inflammation and coagulation is CD40 and its counterpart CD40L (CD145) ligand. CD40 and CD40L are expressed by B lymphocytes but also by endothelial cells, macrophages, monocytes, and platelets. Plaque rupture induces platelet activation through the liberation of collagen, thrombin, and ADP, resulting in an increased surface expression of CD40 ligand, which is subsequently cleaved from the membrane surface. Released soluble CD40 ligand activates CD40 expressed on endothelial cells, thereby inducing a pro-inflammatory cascade in the vessel wall. Moreover, soluble CD40 ligand also activates CD40 expressed on inflammatory cells such as monocytes and T cells. The subsequent activation of these cells and their invasion into the ruptured or eroded plaque results in further inflammatory perturbation of the vessel wall. Moreover, CD40L, by binding to endothelial and smooth muscle cells, also has been implicated in the activation of matrix metalloproteases, possibly inducing apoptosis of core macrophages and the expression of tissue factor. CD40 ligand not only identifies patients who are at highest risk for cardiovascular events but also provides important information on which patients will derive major benefits from anti-platelet treatment with abciximab, a glycoprotein IIb/IIIa receptor antagonist that suppresses monocyte tissue factor through a reduction of monocyte-platelet cross-talk.

Conclusion

Many of the mechanisms in plaque formation are simply physiologic adaptations, which are largely responsible for the remodeling process that accommodates the plaque during its growth. Nonetheless, our ability to identify local and systemic mechanisms of plaque rupture is important in understanding atherogenesis and in choosing the appropriate treatment strategy for patients with ACS. It is likely that a systemic inflammatory condition, in association with an enhanced coagulation state, activates local hemodynamic, mechanical, and immune reactions, which may be more prevalent or more “mature” in

one plaque than in another. This hypothesis explains a substantial number of ACS cases and answers the key question: Why is there usually a "culprit plaque" even when there is evidence of multiple "unstable plaques"?

The report of multiple inflammed coronary plaques at post-mortem in patients who died of ACS and the widespread coronary and myocardial inflammation in patients with severe unstable angina or infarction suggest that inflammation is responsible for the simultaneous development of multi-focal coronary instability, with or without plaque rupture. In line with this observation, the concept of "the vulnerable patient" has been introduced. This distinction is aimed at identifying patients who are at higher risk of ischemic cardiovascular events.

The difficulty in identifying, among asymptomatic individuals, those who are at risk of suffering an acute coronary event underlines the limits of current screening methods. It is well known that angiographic evidence of significant atherosclerotic plaques involving epicardial coronary arteries reliably identifies only a small number of ACS cases. More frequently, the culprit mechanism behind acute coronary thrombosis is represented by the thin fibrous cap rupture (80% of men, 50% of women) or superficial erosion of the intima, with subsequent exposure of thrombogenic substrates and acute thrombosis of the vessel wall (20% in men, around 50% in women). These observations support the concept of the vulnerable or at-risk plaque, which is prone to destabilize, contains a large number of inflammatory cells, and is rich in metalloproteases. This definition of the vulnerable plaque reflects a clinical approach that is more biological than angiographic and is aimed at identifying patients who are at an increased risk of developing thrombosis and rapid stenotic progression. Related to this definition is the inflamed thin-cap fibroatheroma (TCFA), which also refers to a vulnerable plaque.

If all the acute coronary events are linked to the presence of a vulnerable plaque, not all vulnerable plaques cause coronary events, since not all such plaques undergo rupture or erosion and, if they do, the outcome is not necessarily a coronary event. Usually, coronary events happen when a thrombus is formed, obstructing vascular flow, which, in turn, irritates a critical myocardial area where there is insufficient collateral flow. Ventricular fibrillation may ensue, due to the electrical instability of the affected myocardial tissue. Thus, the benefits of understanding the plaque's in vivo characteristics – independent of determining the degree of stenosis – in choosing the proper therapy are clear. Accordingly, the diagnosis of high-risk plaques in vivo could provide a clear indication of the optimal diagnostic and therapeutic pathway, with the goal of stabilizing the plaque through the administration of pharmacologic agents. This should decrease the incidence of sudden death and non-fatal myocardial infarction. In the last few years, several innovative intra-coronary imaging techniques have allowed better histological characterization of the atherosclerotic plaque. Among these, IVUS represents a new approach, one that complements angiographic evaluation of the coronary tree. IVUS provides high-resolution tomographic images – and thus a full-thickness study of the atherosclerotic plaque – that properly define its composition and distribution either in the radial or longitudinal direction.

7

Intravascular Ultrasound: From Gray-Scale to Virtual Histology

Fabrizio Clementi, Giuseppe M. Sangiorgi

Introduction

For over a decade, coronary angiography has represented the "gold standard" in the appraisal of the coronary anatomy and the diagnosis of coronary artery disease. However, the introduction of percutaneous coronary revascularization, along with increasing evidence of the prognostic importance of atherosclerotic plaque composition, fostered the concept that simple coronary angiography is limited in estimating the distribution and extent of coronary pathology. Indeed, angiography simply shows the vessel lumen, a perspective that is insufficient in representing the complex nature of coronary disease.

Since its introduction at the end of the 1980s, intravascular ultrasound (IVUS), as the most modern application of diagnostic ultrasound, has been capable of supplying important information about the composition of atherosclerotic plaques. IVUS is an invasive technique that yields tomographic images of the vascular structures and direct visualization of both the luminal area and vessel wall composition. Since angiography only provides planar, map-like information about the coronary anatomy, it is also limited in estimating the mechanisms and progression of atherosclerotic disease. By contrast, IVUS visualizes the artery in cross-sections through tomographic appraisal of the plaque, its extent, and its composition below the endothelial surface. Moreover, IVUS can also supply qualitative information regarding the risk of plaque progression/destabilization and quantitative data about the dimensions of the lumen and vessel.

The IVUS console is made up of three components: a catheter with a transducer, a pullback system, and a computer containing the software and the hardware able to convert the ultrasound signal into gray-scale imaging. The IVUS catheters currently available for clinical use have external diameters between 2,6 and 3.5 French (0.87- to 1.17-mm coronary and peripheral, respectively). The probe is available either as a mechanical or an electronic device, with the spatial resolution of the latter lower than that of the former. In

P. Pavone, M. Fioranelli, D.A. Dowe, *CT Evaluation of Coronary Artery Disease*.

order to acquire the IVUS image, the target vessel should be selectively cannulated with a guiding catheter. After a 0.014-inch angioplasty wire has been positioned, the IVUS probe is advanced distally to the level of the target area and withdrawn proximally by an automated pullback device (with a speed of 0.5 or 1.0 mm/s) into the ostium of the guiding catheter.

Ultrasound gray-scale images of a normal coronary segment show a circular lumen surrounded by three layers. The inner layer is relatively echolucent and represents the intima and inner elastic lamina in normal arteries, or the atherosclerotic plaque in atherosclerotic arteries. The middle layer is usually transparent and dark, and represents the media. The external layer is more echolucent and represents the external elastic lamina, the adventitia, and the periadventitial tissue. The different echolucencies of these layers are due to their different histological composition; for example, the collagen-rich adventitia is very echolucent whereas the media, rich in smooth muscle cells, is relatively less echolucent.

Validation studies demonstrated that the atherosclerotic plaque can be differentiated according to its prevalent characteristic, i.e., lipidic, fibrotic, or calcific, which can also be distinguished echogeneically Thus, on the basis of the echogenicity of the plaque, three different types of coronary lesions can be distinguished: (1) hyperechoic regions with acoustic shadow corresponding to calcific deposits; (2) hyperechoic regions without acoustic shading corresponding to fibrotic components of the plaque; and (3) hypoechoic regions corresponding to lipid lakes or thrombotic material. However, the sensitivity and specificity for calcific and fibrotic tissues are much higher than for lipidic tissue. Thus, calcium is very well visualized as a highly echolucent, distinct area such that the diagnostic accuracy is much higher than obtained with conventional angiography. Initially, the classic IVUS pattern of a low echolucent area with a sharp border was misinterpreted and sometimes confused with the echotransparency (gradual acoustic shadow) typical of dense fibrous tissue; however, the use of 40-MHz probes has improved the identification of lipid "pools," as documented by in-vitro and in-vivo studies (with a spatial resolution of 150–300 μm).

Gray-scale images provide a relatively precise image of vessel anatomy and, above all, of plaque morphology. Indeed it is possible to obtain detailed information about intimal surface ulcerations, vessel remodeling (compensatory expansion of the media during plaque development), plaque distribution and, especially, the type of plaque composition. All of this information is extremely important in the planning of interventional procedures, such as the choice of stent design, in optimizing acute results (by stent apposition to the arterial wall and uniform circumferential expansion of the stent), and in identifying complications (such as plaque dissection or re-stenosis).

From Gray-Scale to Color-Coded IVUS: The Virtual-Histology Revolution

Today, clinical and laboratory data have challenged our classical notions of the pathogenesis of acute coronary syndromes. Several independent lines of clinical evidence have shown that critical stenosis causes only a fraction of this group of pathologies. Rather, the rupture of a thin fibrous cap covering a

large, lipid-rich, necrotic or superficial intimal erosion frequently triggers acute coronary thromboses at sites of non-critical narrowing of the coronary arteries. This shift in our thinking has fostered the notion of the "vulnerable" or "high-risk" plaque and spawned manifold attempts to develop methods for its detection, a quest predicated on the postulate that local intervention could preclude plaque thrombosis and thus acute coronary syndromes. This approach may prove applicable to patients already targeted for invasive diagnosis or treatment in whom the identification of non-stenotic lesions unseen by traditional angiography might guide a local intervention aimed at the prevention of a coronary event. Patients presenting with acute coronary syndromes are at a high short-term risk of recurrence, which justifies an aggressive approach such as this one.

The typical vulnerable plaque has been clearly defined in autopsies of patients who died of acute myocardial infarction. It is mostly constituted by a necrotic core, rich in cholesterol crystals and lipids, with an overlying thin fibrous cap that separates this highly thrombogenic material from the blood stream. Such lesions are referred to as thin-cap fibroatheromas (TCFAs).

Several imaging modalities, including gray-scale IVUS, are under investigation by extensive clinical testing in order to identify the most reliable in discovering the "vulnerable plaque." However, some studies have reported that, according to gray-scale IVUS analysis stable and unstable plaques share several characteristics, which reduces the ability, of IVUS to clearly differentiate among them. Moreover, IVUS resolution is about 200-300 μm – a threshold far above the thickness of the typical thin fibrous cap of a vulnerable plaque (40–80 μm). Another limitation is that the gray-scale code is not useful for clearly differentiating between the different histological components of the vulnerable plaque (i.e., necrotic core vs. fibrous material and calcium microcrystals), thus reducing the diagnostic accuracy of the methodology in detecting vulnerable TCFAs.

The development of IVUS-virtual histology (IVUS-VH) is a promising step as the technique can be used in the catheterization lab to identify vulnerable plaques. IVUS-VH discriminates among different tissues with high sensibility and specificity, thus improving the diagnostic accuracy for any single plaque and, prospectively, distinguishing between vulnerable (rupture prone) and non-vulnerable (non-rupture prone) atherosclerotic lesions.

IVUS-VH images color-code four different tissue types (Figs. 7.1, 7.2):

- Lipid: displayed in yellow
- Fibrolipids: displayed in green
- Necrotic core: displayed in red
- Calcium: displayed in white

IVUS-VH image acquisition and processing are very different than in standard gray-scale IVUS. VH uses the frequency and amplitude from tissue-reflected ultrasound. Moreover, the analysis, which is performed on backscatter signals and based on all data acquired by the ultrasound beam, uses complex mathematical equations (blind deconvolution, autoregressive modeling, three-component classification algorithm) to extract the required information.

"In vitro" the diagnostic accuracy in identifying the four different tissue types ranges from 93 to 99%. The "in vivo" diagnostic accuracy is also extremely high (Table 7.1, Fig. 7.3). Of note is the observation that a typical vir-

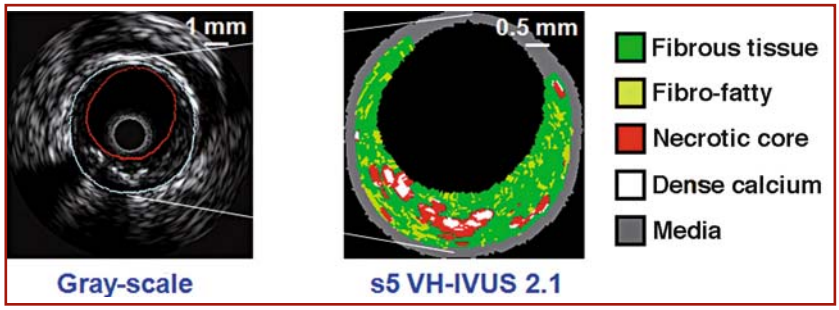

Fig. 7.1. Comparison between gray-scale and virtual-histology. A moderately calcific deposit can be clearly seen in the intravascular ultrasound (IVUS) gray-scale image on the left at 6 and 7 o'clock. In addition, IVUS-virtual histology (IVUS-VH) identifies lipid lakes associated with the calcium deposit. This is sometimes a characteristic of the necrotic core

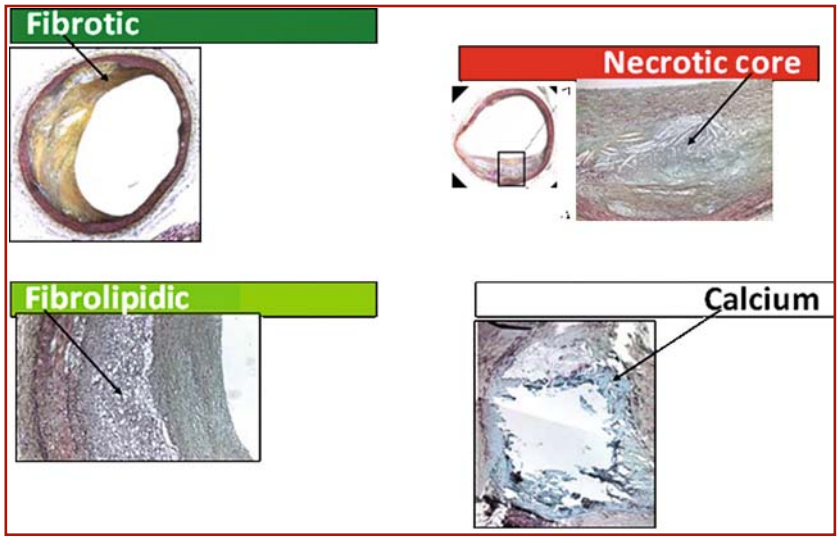

Fig. 7.2. The four color-coded plaque components classified by virtual histology and their corresponding histopathologies. Adapted from Sangiorgi G. et al (2007)

Table 7.1. Sensitivity and specificity of virtual histology (VH) for the different tissue types

	Accuracy	Sensitivity		Specificity	
Type		%	CI	%	CI
Fibrous	93.5%	95.7%	94–98	90.9%	88–94
Fibrolipids	94.1%	72.3%	65–80	97.9%	97–99
Core necrotic	95.8%	91.7%	87–96	96.6%	95–98
Calcific	96.7%	86.5%	81–92	98.9%	98–100

CI confidence interval

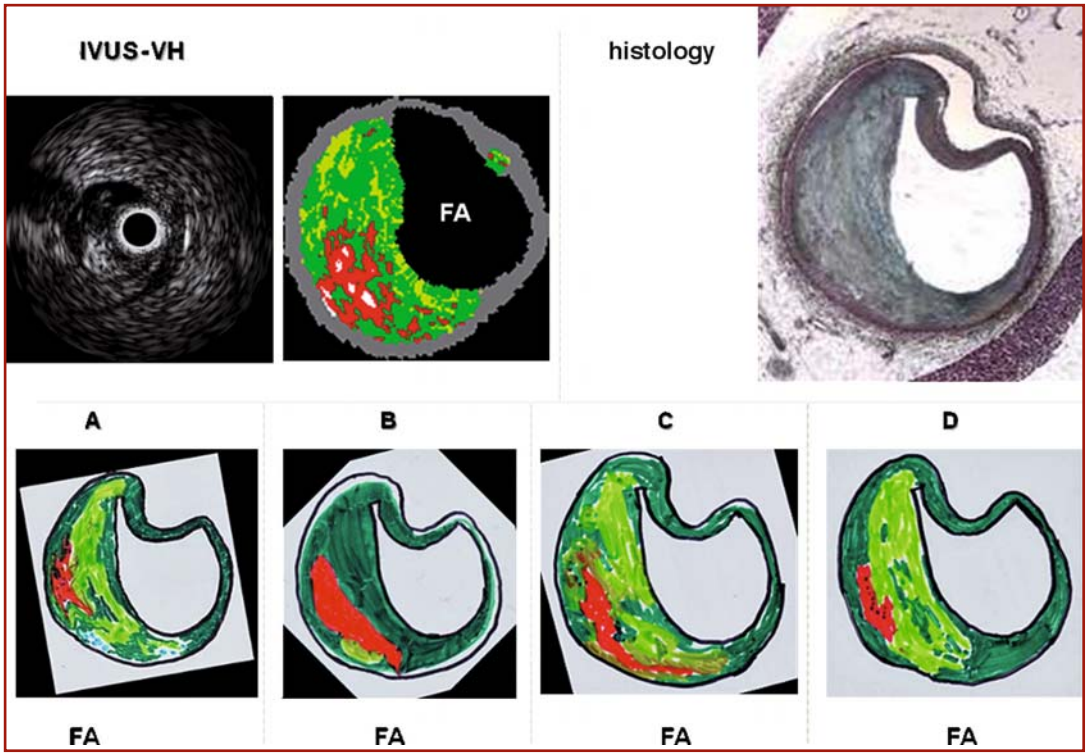

Fig. 7.3. Comparison between histology and IVUS-VH. Hand-drawn reconstructions by four different pathologists (*A-D*) using the same colors as in VH. Note the excellent correlation with the three classifications by VH. The reconstruction of an IVUS-VH image, in which the 300-μm field of interest is essentially the sum of many histological 4-μm slices and therefore is not perfectly super-imposable. *FA* Fibroatheroma

tual histology slice is 3- to 4-μm thick in contrast to the 300-μm thickness of an IVUS slice. This means that slices obtained during IVUS analysis do not perfectly correlate with histological slices; instead, IVUS-VH images represent the mean of values acquired from more than one histological segment (Fig. 7.4a).

Lesion Classification Using IVUS-VH

Coronary lesions can be classified as stable (pathological intimal thickening, fibro-atheroma; calcific fibro-atheroma) and unstable (TCFA, superficial erosions, superficial microcalcifications). The most representative of this latter group, particularly in coronary vessels, is the TCFA. As previously described, the thickness of the cap is far below the threshold of the ultrasound beam. For this reason, conventionally, IVUS diagnosis TCFA when the necrotic core component is in direct contact with the lumen, representing a fibrous cap thinner that 200 μm. Different lesion types are defined by IVUS-VH (Fig. 7.4b), each with its own corresponding sensitivity and specificity. Of note is the high specificity of this technique for TCFA (Table 7.2).

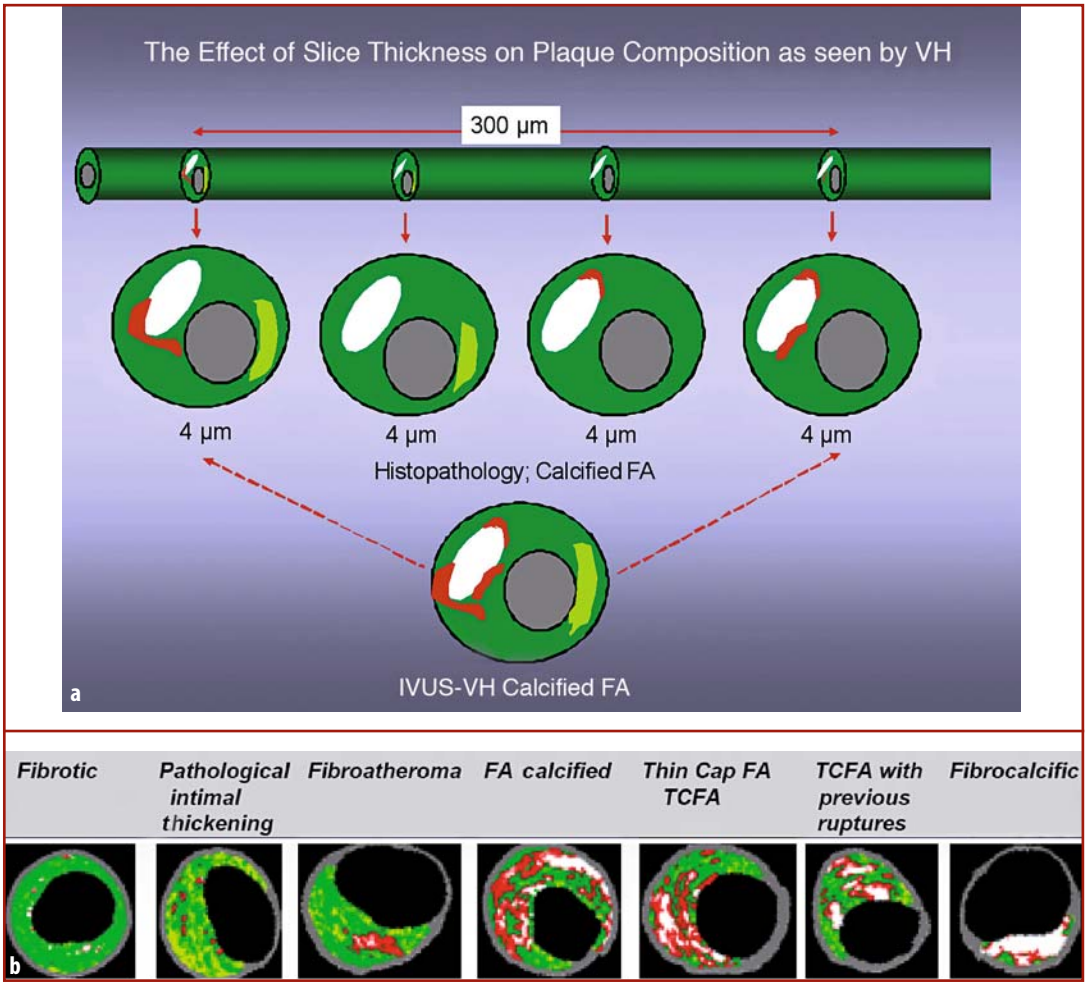

Fig. 7.4 a, b. Comparison between histologic cross-sections and those obtained with virtual histology (VH) (**a**). Since the former are usually 4-µm and the latter 300-µm thick, the two image sets may not perfectly matched. Instead, a single VH image corresponds (when utilized for comparison with histology) to the sum of several histologic cross-sections. **b** Classification of the different atherosclerotic plaque types by intravascular ultrasound (IVUS)-VH. *FA* Fibroatheroma. Figure 7.4b reproduced from Sangiorgi G. et al (2007)

Table 7.2. Specificities, sensitivity, and diagnostic accuracy of virtual histology for different types of atherosclerotic lesions

Type of plaque	Accuracy	Sensitivity	Specificity	Total (n)
FACa	72.4%	32.5%	93.0%	40
TCFACa	96.1%	90.0%	97.1%	20
FA	85.9%	54.1%	96.9%	37
FCa	85.5%	87.1%	84.5%	31
PIT	83.4%	88.5%	82.0%	26
TCFA	99.4%	75.0%	100%	4

FACa fibroatheroma calcified, *TCFACa* thin cap calcific fibroatheroma, *FA* fibroatheroma, *FCa* fibrocalcific, *PIT* pathological intimal thickening, *TCFA* thin-cap fibroatheroma

IVUS-VH Console and Image Interpretation: Tips and Tricks

Figure 7.5 shows a typical screenshot from an IVUS-VH S5 consol. The current software version features automatic, real-time, border detection that is extremely reliable. VH analysis is available only with 20-Mhz probes, which means less spatial resolution than obtained with the recently introduced 40-Mhz mechanical probes. The advantage of the electronic 20-Mhz probe is its lower crossing profile, which allows for easy crossing even of more calcific and compact lesions. Furthermore, the probe is very flexible and can be more easily pushed than mechanical ones. Unfortunately, in the absence of an external layer, during pullback the probe could become entrapped, in the plaque, slowing the speed of the maneuver. This is manifested as a less than perfect reading of the longitudinal axis. Also, unlike what occurs in gray-scale imaging, the need for ECG synchronization prohibits a constant frame-rate to speed ratio. This means that the slice number per length segment varies in every single acquisition, depending on the patient's heart rate – a major drawback in longitudinal studies evaluating, for example, plaque regression.

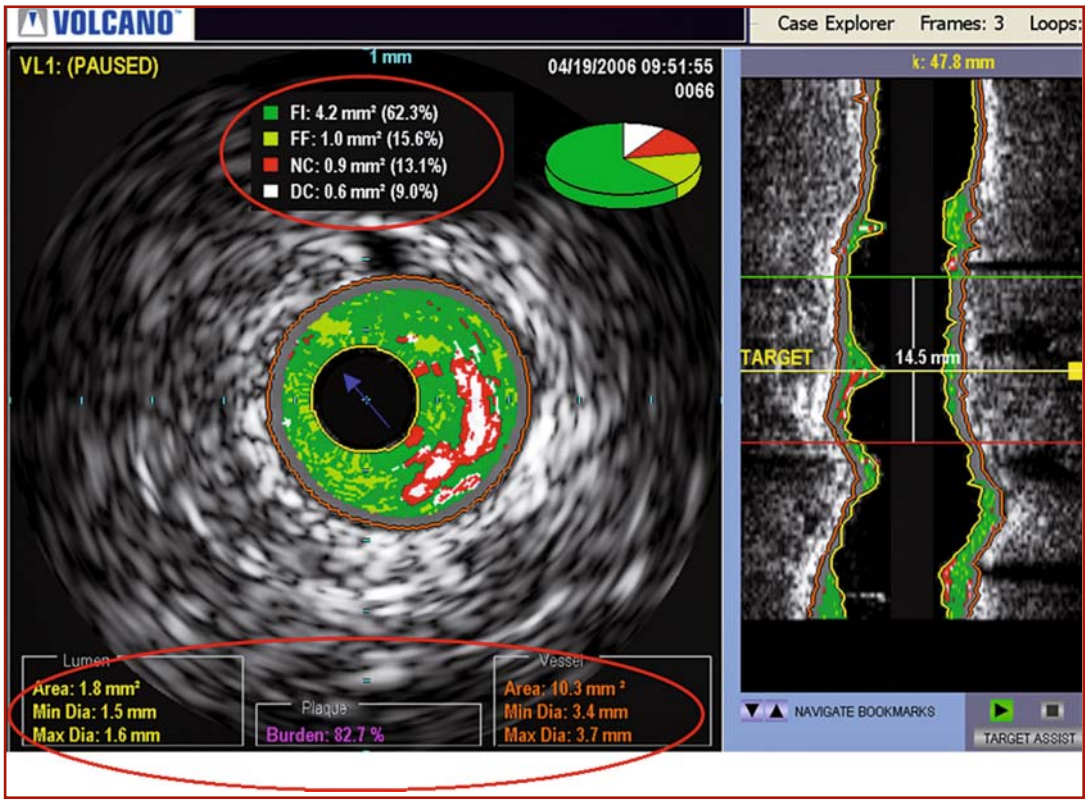

Fig. 7.5. The image displays the VH monitor view after a run acquisition. *Left* One section of the vessel, with the area of the plaque analyzed. In addition, the three panels display, from left to right, lumen area and diameters, plaque burden, and area and diameters of the external elastic lamina. Above, the different plaque components are presented both as volume occupied by the different components and as percentage of the entire region of interest. *Right* A longitudinal section of the vessel. This plaque is classified as calcific fibroatheroma. Reproduced from Sangiorgi G. et al (2007)

Conclusion

Despite the opportunity to identify and treat any critical stenosis directly in the catheterization laboratory, most of the acute events in patients with coronary artery disease cannot be prevented. Conversely, the identification of a vulnerable plaque (often not stenotic, Fig. 7.6), and even of a vulnerable patient (bearing multiple vulnerable asymptomatic plaques in his or her coronary tree) may help target interventions to those plaques most likely to become disrupted and to the prevention of related complications. Refined coronary imaging techniques will eventually corroborate autopsy studies demonstrating the heterogeneity of coronary atherosclerotic lesions, as stratified by individual patient-risk-factor profile. The gap is still large and only prospective observations have reliably identified plaques that are prone to rupture, forcing a change in our approach to the treatment of coronary atherosclerotic disease. However, several prospective studies (SPECIAL, IBIS-2, PROSPECT) are currently ongoing. By means of imaging modalities such as IVUS-VH, this exciting journey has just begun.

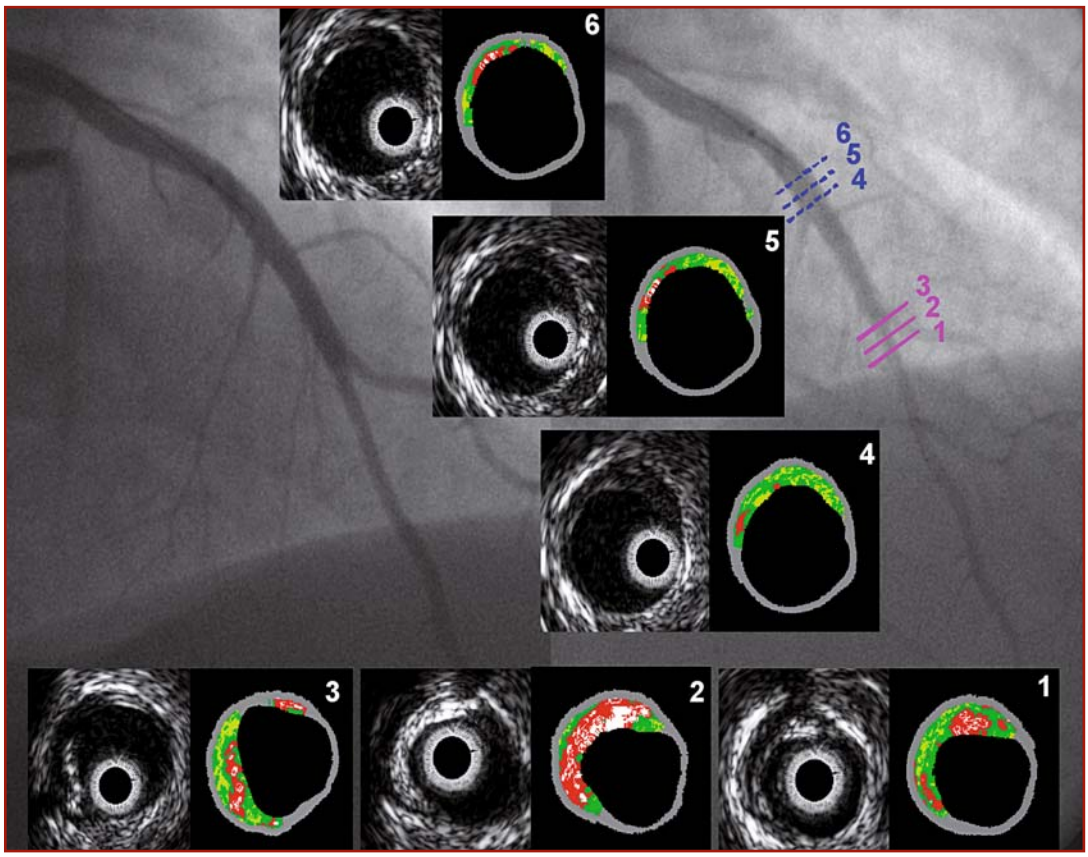

Fig. 7.6. Comparison between angiography, gray-scale IVUS, and IVUS- VH. Note that the left anterior descending artery appears normal along its entire length, according to angiography. The numbers indicate the different coronary segments corresponding to the images acquired by IVUS. A small fibrotic plaque is present in segments *4*, *5*, and *6*. Conversely, a fibrocalcific plaque (segments *2* and *3*) and a vulnerable plaque (segment *1*) are identified by the lipidic content, close to the lumen (in the VH image shown as a red region), with the IVUS-VH technique

8

Identification and Characterization of the Atherosclerotic Plaque Using Coronary CT Angiography

Paolo Pavone, David A. Dowe

Coronary CT angiography (CTA) is the first diagnostic modality that allows simultaneous evaluation of the lumen and wall of these small, rapidly pulsating arteries. Catheter coronary angiography, by contrast, only evaluates the internal, patent lumen of these vessels, without providing direct information on the vessel wall or the extent of vascular parietal involvement by atherosclerosis. While it identifies areas of stenosis or obstruction, it does not show details of the plaque itself, unless heavy calcifications make the atherosclerotic plaque evident on the X-ray image. Intravascular ultrasonography (IVUS) is an excellent method to obtain high-resolution images of the vascular wall, with identification of the different layers and proper characterization of the atherosclerotic plaque; however, it is an invasive procedure, performed in the course of catheter coronary angiography, and does not simultaneously evaluate the vessel lumen. Coronary CTA is therefore the first non-invasive imaging technique that allows evaluation of the lumen and walls of the coronary arteries, a particular advantage in determining the atherosclerotic burden in these arteries. Since atherosclerosis is a disease of the vessel wall, obtaining proper and direct evidence of a coronary plaque is an important new diagnostic possibility. The technique provides morphological information and CT density measurements, with important prognostic and therapeutic implications.

Normal Vascular Wall

Coronary CTA creates an image during dynamic passage of a bolus of contrast agent in the coronary arteries. Thus, in images acquired using three-dimensional analysis, the vessel lumen has a high CT density and is therefore very bright. The vessel wall is not enhanced by contrast agent so that it is hypodense on CT. The normal vessel wall is too thin to be clearly defined in CT images, unless newer systems, which have very high spatial resolution (< 0.3 mm),

P. Pavone, M. Fioranelli, D.A. Dowe, *CT Evaluation of Coronary Artery Disease*.

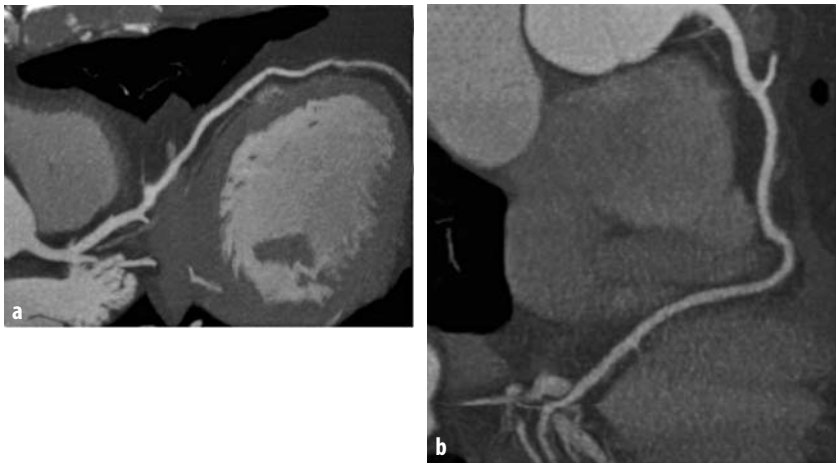

Fig. 8.1 a, b. Normal coronary arteries evaluated using a bi-dimensional technique. **a** Left anterior descending coronary artery. **b** Right coronary artery. The vessel wall is difficult to evaluate due to its normal thickness. The vessels themselves are well-evident, as they are surrounded by very hypodense epicardial fat tissue

are employed, although experience with the most recent technology is still preliminary. The inability to identify the normal parietal vascular wall is not a negative factor in coronary CTA (Fig. 8.1), as non-visibility reflects a normal status and a lack of atherosclerotic involvement.

Identification of the vascular wall should always be performed using bi-dimensional reconstruction techniques (planimetric imaging, see Chap. 4). Only this type of image clearly displays the course of the vessel, with evidence of the hyperdense internal aspect of the patent lumen and the hypodense parietal layers. Care must be taken, as discussed previously, to evaluate the vessels in their longitudinal course and in the transverse, axial plane, to obtain a complete and detailed definition of the vascular wall.

Identification of Atherosclerotic Plaques in Coronary CT Angiography

The atherosclerotic plaque must always be identified by both three-dimensional imaging reconstruction (volume rendering) and bi-dimensional techniques. In the latter images, due to simultaneous visualization of the lumen and wall, atherosclerotic plaques are well-evidenced as areas of focal thickening. Images evaluated in the different orthogonal planes allow clear definition of the relationship between the atherosclerotic plaque and the lumen, and thus proper delineation of the extent of vascular stenosis.

CT Density Values and Plaque Characterization: Fibrolipidic and Calcific Plaques

In addition to its ability to identify atherosclerotic plaque, an intrinsic feature of CT is that the different components of the atherosclerotic plaque have

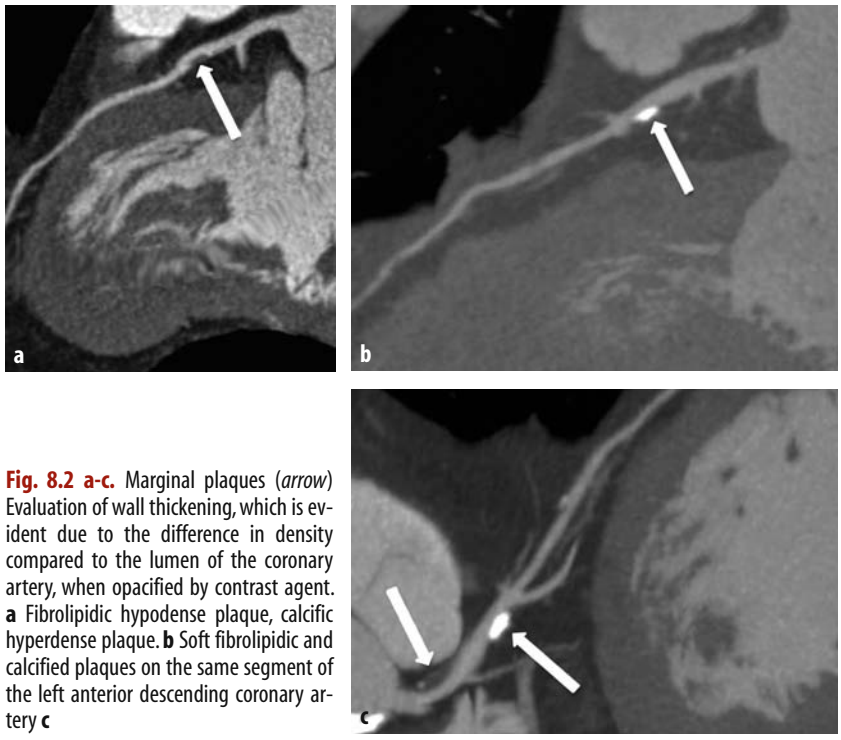

Fig. 8.2 a-c. Marginal plaques (*arrow*) Evaluation of wall thickening, which is evident due to the difference in density compared to the lumen of the coronary artery, when opacified by contrast agent. **a** Fibrolipidic hypodense plaque, calcific hyperdense plaque. **b** Soft fibrolipidic and calcified plaques on the same segment of the left anterior descending coronary artery **c**

different densities: (a) lipidic plaques, with very low density values (< 0 HU); (b) fibrotic plaques, with intermediate tissue density (20–30 HU); and (c) calcific components of the plaque, which because of their high density (500–1000 HU), are always well evident in coronary CTA. Differentiation among these three plaque components is readily obtained by analysis and evaluation of the bi-dimensional images. In the examples shown in Figure 8.2, the low-density plaque can be easily distinguished from the calcific high-density plaque, and different plaques in the same artery are distinctly visualized.

Plaques with a predominantly lipidic component cannot always be discriminated from those that are mostly fibrotic when clinically evaluated by CT. Therefore, during image evaluation and in the report, radiologists refer mostly to a "fibrolipidic" plaque, thereby indicating the absence of calcific components (Fig. 8.3). The difference between fibrolipidic and calcific plaque is always seen by coronary CTA.

Calcific plaques are strongly hyperdense and almost always well-evident in three-dimensional as well as in bi-dimensional images; whereas hypodense, non-calcific, fibrolipidic plaques are less obvious in appearance and require an experienced radiologist, who must make a careful detailed evaluation segment by segment (Fig. 8.4). The accuracy in the identification of non-calcific vs. calcific atherosclerotic plaque may be lower, especially in the more distal segments of the coronary arteries. For proximal segments, there is no difference since both calcific and non-calcific are correctly identified and characterized. The main goal of coronary CT examination is in fact to identify plaque burden, mostly in the proximal segments, while the definition of

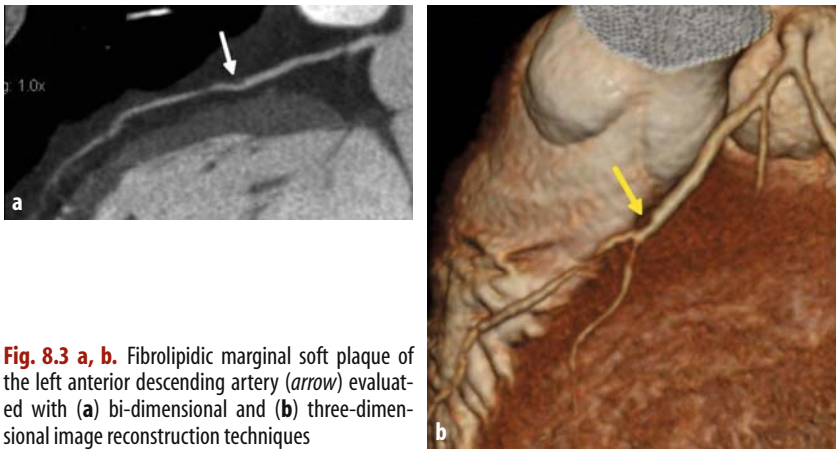

Fig. 8.3 a, b. Fibrolipidic marginal soft plaque of the left anterior descending artery (*arrow*) evaluated with (**a**) bi-dimensional and (**b**) three-dimensional image reconstruction techniques

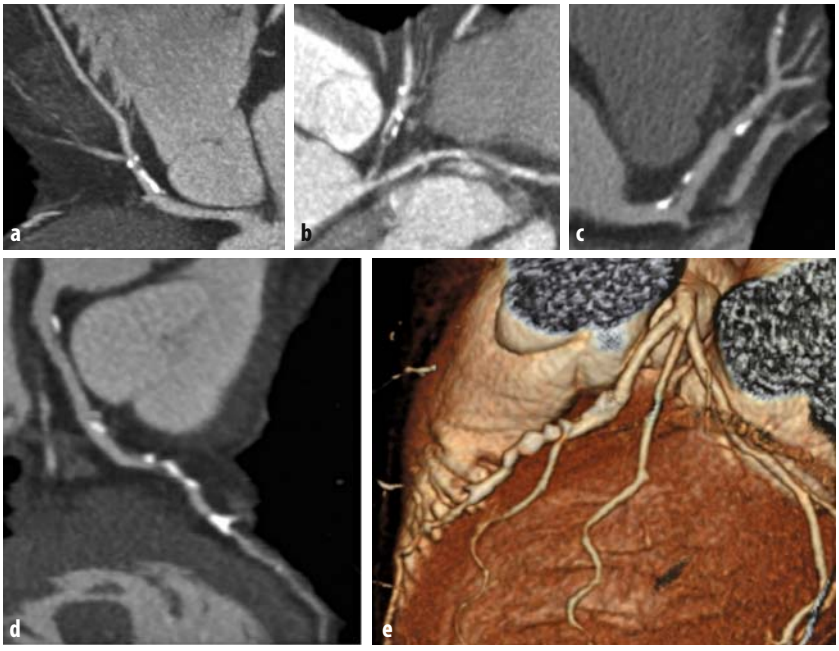

Fig. 8.4 a-e. Marginal calcific and mixed plaques. **a-d** Bi-dimensional image, three-dimensional reconstructed image (**e**)

smaller, more distal, branches is limited. However, for disease prognosis, clinical involvement of the proximal and intermediate segments of the coronary arteries is more important than the involvement of distal segments.

Atherosclerotic Plaque and Disease Evolution

Atherosclerotic disease has a temporal course, with an evolution similar to that of inflammation. In this view, calcification may be considered as the end

stage of pathological vascular involvement. With coronary CTA, eccentric calcific plaques, almost always in an extraluminal location, are frequently encountered. These represent areas of vessel wall with limited and focal atherosclerotic involvement that has reached a final and stable pathological condition, without causing stenosis. Completely calcified plaques have to be considered as "safe" plaques since the atherosclerotic process has terminated. Of course, in the process, the plaque, although calcified and stable, may have caused significant stenosis, as will be discussed in the next chapter.

Identification of a non-calcific fibrolipidic plaque – also when there is eccentric involvement of the vessel wall – that has not caused significant reduction of the lumen diameter (Figs. 8.5, 8.6) indicates to the cardiologist that the atherosclerotic process is still active and that other events may

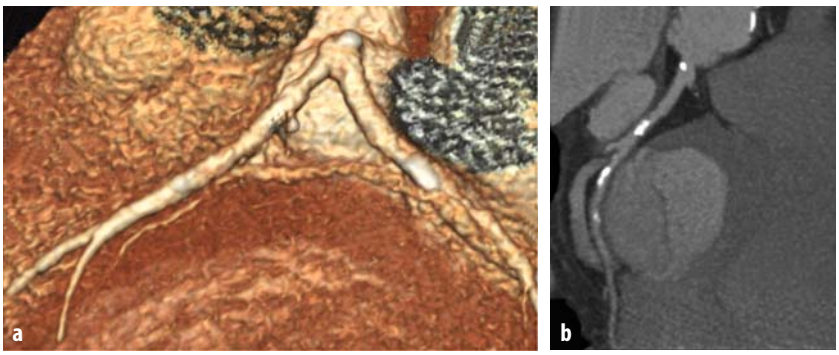

Fig. 8.5 a, b. Diffuse atherosclerotic involvement of the left anterior descending and circumflex coronary arteries

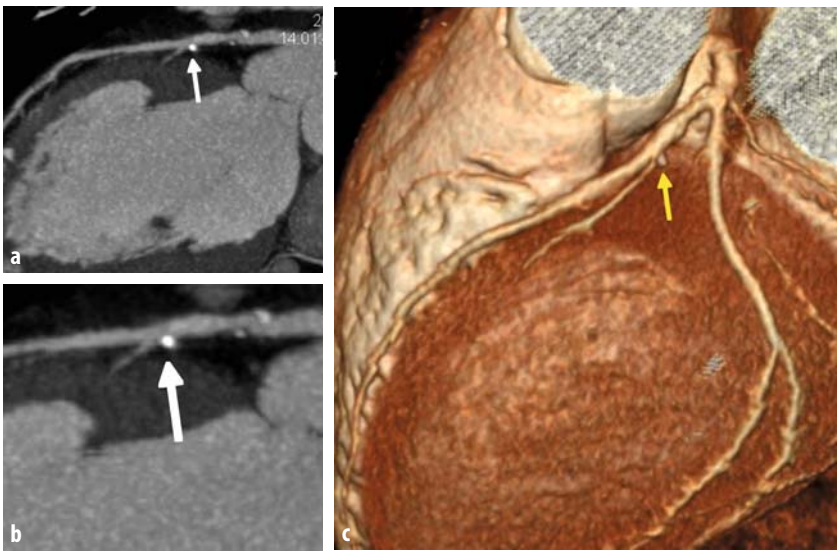

Fig. 8.6 a-c. Small marginal calcific plaque (*arrow*) of the left anterior descending coronary artery (*arrow*) evaluated in orthogonal bi-dimensional planes and in three-dimensional image reconstruction technique

occur, leading to further progression of the disease and to worsening of the patient's clinical condition. These plaques (vulnerable plaques) may also create acute anatomo pathological changes that lead to a sudden cardiac event and infarction. In fact, vulnerable plaques may undergo different types of complications: (a) a further increase in size, with progressive reduction of the vessel lumen; (b) internal hemorrhage, leading to an immediate increase in plaque volume and sudden vascular occlusion, with acute infarction; (c) ulceration, with dispersion into the vessel lumen of atherosclerotic material, resulting in vascular occlusion or turbulent flow in the vaswlar ulcer, with subsequent development of thrombi; (d) intimal dissection at the plaque level, leading to immediate vascular occlusion (Figs. 8.7, 8.8). These potential complications, well-known mostly to pathologists, must always be considered by both the radiologist and the cardiologist carrying out a coronary CTA examination. Knowledge of the morphology and characteristics of the atherosclerotic plaque provide a better and more defined prognostic and therapeutic approach to atherosclerotic disease of the coronary arteries. While in a non-stenosing calcific plaque the diagnosis is always stabilized atherosclerotic disease, in the presence of a non-stenosing fibrolipidic plaque the cardiologist may recommend support therapies, i.e., drugs or lifestyle changes, that limit disease progression while at the same time reducing the possibility of an acute event, which may lead to a further reduction in the diameter of the vessel lumen and to vascular occlusion.

Mixed plaques may be encountered as well; these have to be considered as at-risk, vulnerable plaques if the fibrolipidic component is prevalent, with only small internal, central calcifications (Figs. 8.9–8.11).

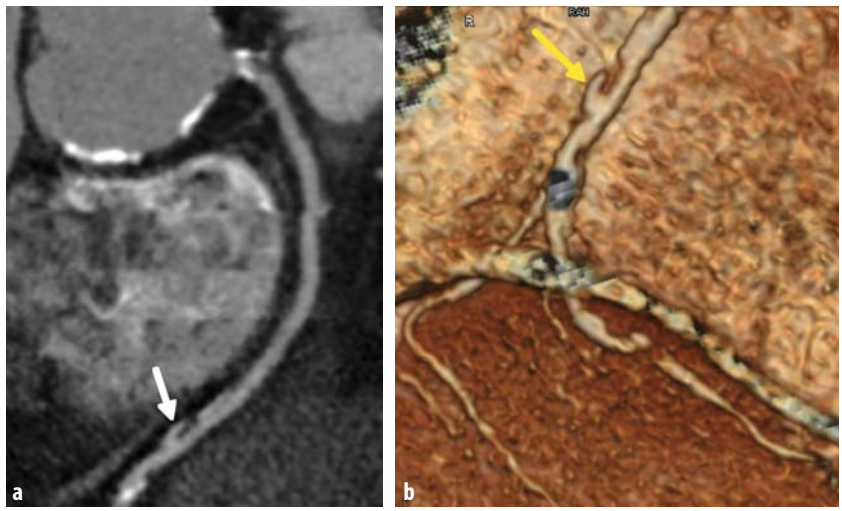

Fig. 8.7 a, b. Ulcerated plaque (*arrow*) of the distal part of the right coronary artery

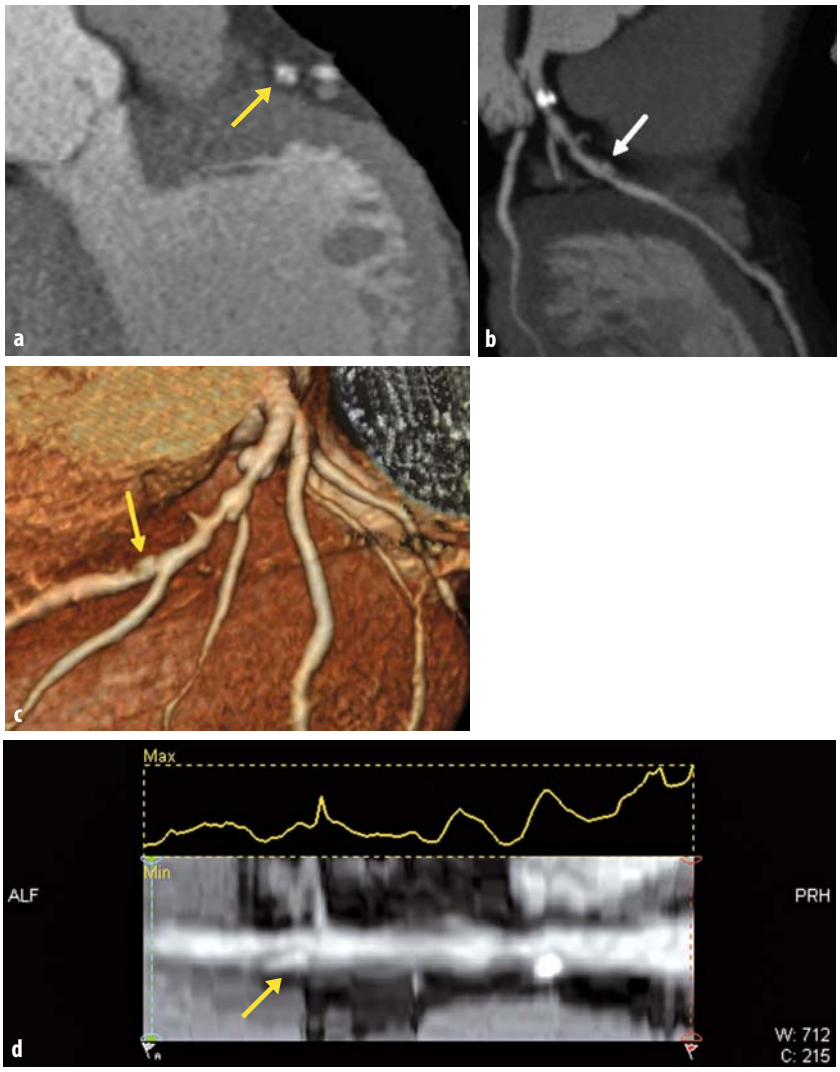

Fig. 8.8 a-d. Plaque dissection (*arrow*) of the left anterior descending coronary artery. **a** Axial image shows the intimal flap; the central component of the plaque is filled with contrast agent (**b, c**). The patient suffered acute clinical symptoms a few hours before CT. **d** Bi-dimensional reconstructed image also shows the intimal flap. There is also a mild reduction in the caliber of the vessel in the proximal segment and a second fibrolipidic plaque (*arrows*)

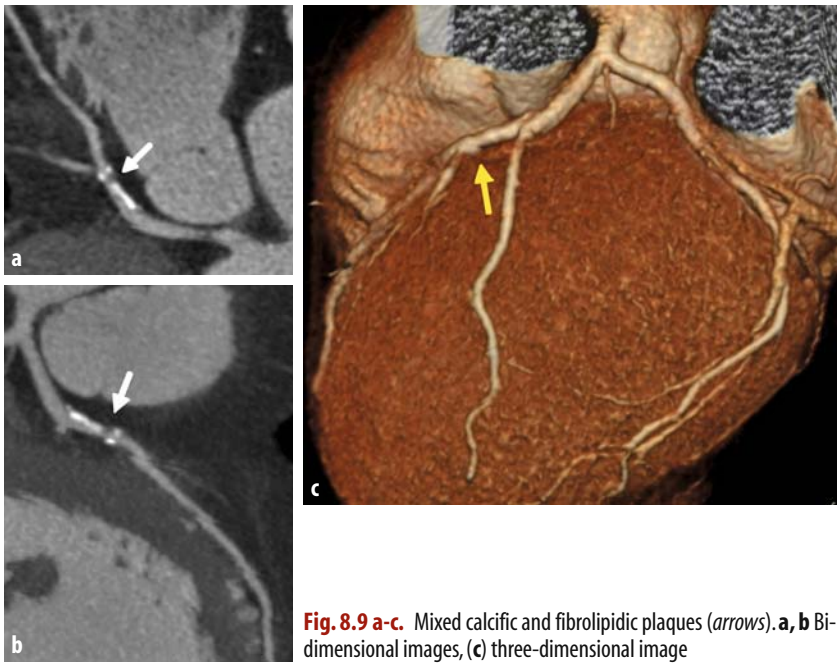

Fig. 8.9 a-c. Mixed calcific and fibrolipidic plaques (*arrows*). **a, b** Bi-dimensional images, (**c**) three-dimensional image

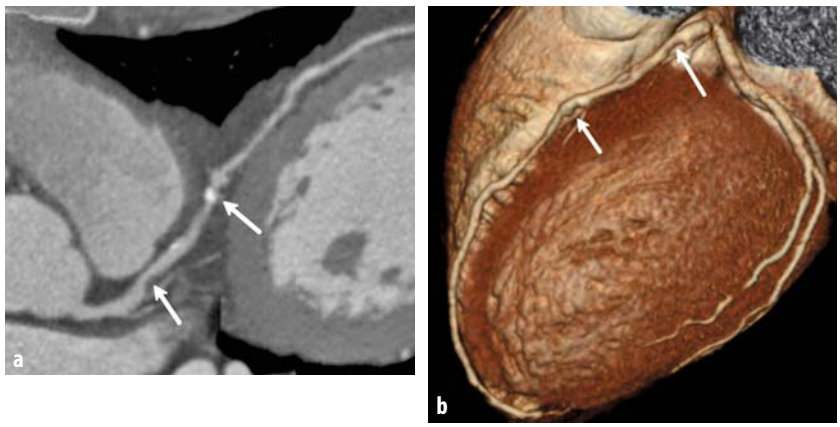

Fig. 8.10 a, b. Mixed plaque involving the proximal segment of the left anterior descending artery and a calcific plaque of the middle third of the same vessel (*arrows*). Both bi-dimensional (**a**) and three-dimensional (**b**) images are displayed

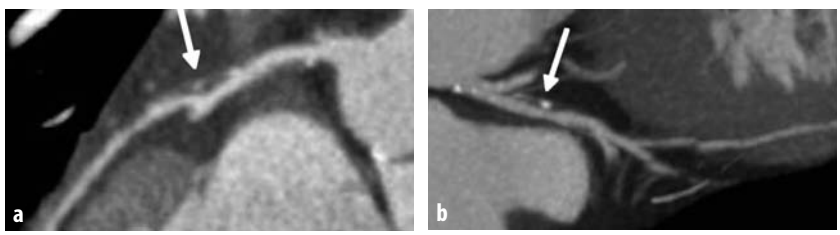

Fig. 8.11 a, b. **a** Mixed plaque (*arrow*) with (**b**) a central hyperdense calcific core and a peripheral fibrolipidic cap. The plaque is eccentric, with non-significant reduction of the vessel lumen

Diagnostic Evaluation of Coronary Disease During Medical Therapy

The development and wide clinical use of drugs aimed at significantly decreasing serum cholesterol levels may lead to a reduction in the size of the atherosclerotic plaques of most patients with coronary artery disease. This, of course, applies only to fibrolipidic plaques, as in the calcific plaque complete stabilization of the atherosclerotic process has been already achieved and the plaque burden of the vessel wall can no longer be reduced.

CT is not only able to identify and characterize the fibrolipidic component of the plaque, but, being a non-invasive procedure, it allows the clinician to monitor plaque evolution over time. For example, the three-dimensional images acquired with CT can show the effect of statins on plaque size (Fig. 8.12, Table 8.1).

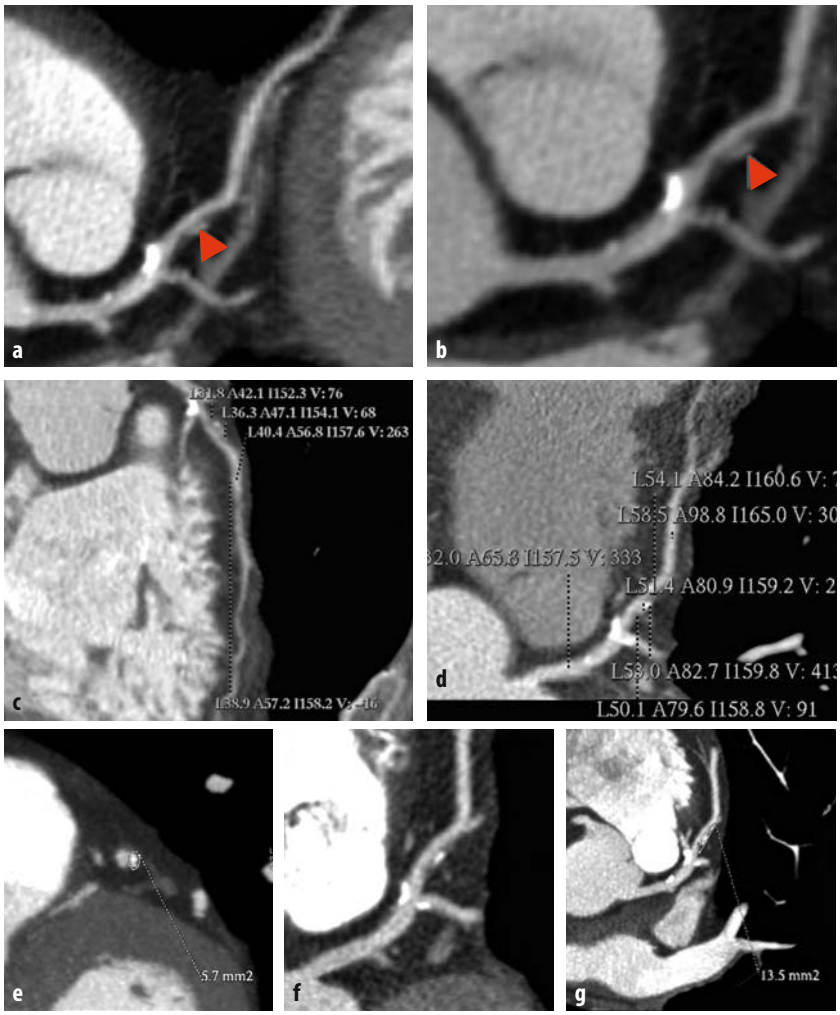

Fig. 8.12 a-g. Reduction of the volume of an atherosclerotic plaque (*arrowheads*). **a** Follow-up controls after statin therapy. **b** 03-04-02, (**c, d**) 09-06-03, (**e-g**) 26-06-04

Table 8.1. Atherosclerotic involvement and volume change of the atherosclerotic plaque over the course of statin therapy

Date	Panels	Plaque lenght (mm)	Plaque area (mm^2)
03.04.2002	b	13,6	19,8
09.06.2003	c, d	13,2	13,7
26.06.2004	e-g	13,2	10,8

The clinical relevance of CT in patients with atherosclerosis of the coronary arteries is that non-calcific, non-stenosing fibrolipidic plaques, which do not require interventional procedures, can be accurately identified. These patients can be started on a therapeutic approach with drugs (statins) that target both plaque volume and the overall atherosclerotic burden on the vessels. At the very least, statins are able to reduce further growth of the plaque, therefore limiting the possibility of sudden anatomic changes in it (see above). A few years after the start of therapy, plaque volume can be monitored in follow-up controls with coronary CTA.

These concepts are new and not completely accepted by clinicians. Some consideration has to be taken regarding the cost-benefit effects. Today, statins are recommended to all at-risk patients with high serum cholesterol levels. The possibility to image the coronary arteries prior to the beginning of therapy would screen for patients with non-calcific fibrolipidic plaques, who may benefit from this type of therapy, distinguishing them from patients with only calcified plaques or with normal arteries, neither of whom would benefit from statins. Long-term monitoring may indicate the proper time to terminate medical therapy and thus lead to important saving in drug and medical costs.

9

Coronary CT Angiography: Evaluation of Stenosis and Occlusion

Paolo Pavone, Roberto Leo

Once an atherosclerotic plaque has been identified and properly characterized by means of coronary CT angiography (CTA), the next step is to define the extent of atherosclerotic involvement, i.e., significant reduction of the lumen by stenosis or complete occlusion of the vessel. A reduction in the caliber of the vessel lumen is associated with a reduction in blood flow and may have significant hemodynamic consequences; however, an important and clearly evident parietal atherosclerotic plaque may be present without significantly reducing lumen caliber. Thus, an exact definition of the extent of lumen reduction by means of coronary CTA is very important from a clinical point of view. In most cases, this diagnostic procedure is employed in not highly symptomatic patients (in patients in whom there is strong clinical suspicion of coronary disease, catheter angiography is directly performed); then, depending on the results of the clinical examination, a decision is made as to whether a more invasive approach (catheter angiography) is required. This decision depends at least in part on the significance of the vessel stenosis. The aim and key role of coronary CTA is to differentiate patients with normal coronary vessels from those with limited atherosclerotic involvement without evidence of stenosis (who may benefit from supportive drug therapy) and from those with significant stenosis. In this latter group, catheter coronary angiography may confirm the significance of the disease and define the therapeutic approach.

The direct evidence of arterial stenosis provided by coronary CTA provides access to additional information. For example, a stenosis > 70% causes a significant hemodynamic reduction of vascular flow. Completely asymptomatic patients, with negative treadmill tests, may present with important and significant stenoses of one or more coronary arteries but with an overall reduction in flow that is less than the 70% threshold.

In clinical practice, a stenosis is considered significant when the vessel caliber is reduced by > 50%. Thus, the goal is to interpret coronary CTA images such that the level of stenotic vascular involvement is precisely determined.

P. Pavone, M. Fioranelli, D.A. Dowe, *CT Evaluation of Coronary Artery Disease*.

Non-Significant Moderate Stenosis

As discussed in the previous chapter, marginal atherosclerotic plaques not causing a significant reduction of the lumen caliber are frequently encountered in coronary CTA images. Once a plaque has been identified, it must be properly analyzed. This requires that the vessel be evaluated in the orthogonal and axial planes, with the aim of trying to define the influence of this marginal plaque on lumen caliber, using qualitative as well as semi-automated quantitative approaches (Figs. 9.1, 9.2). If the non-significance of the lumen reduction is established, no further procedure is necessary, as coronary CTA is

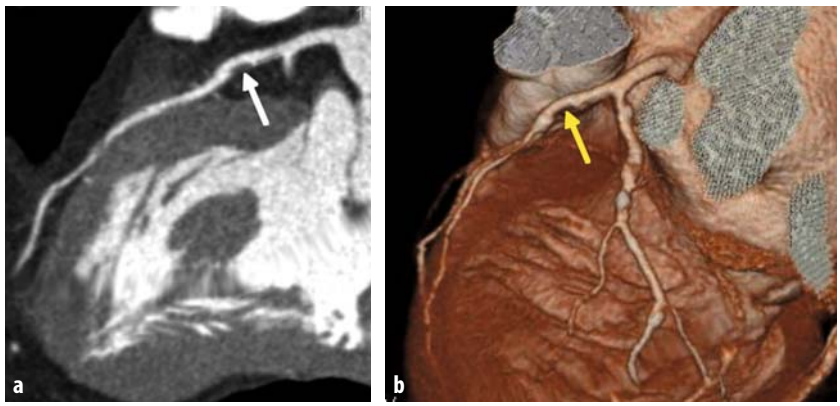

Fig. 9.1 a, b. Marginal fibrolipidic plaque (*arrow)* of the middle third of the left anterior descending artery (LAD), without significant caliber reduction. **a** Bi-dimensional image. **b** Three-dimensional volume-rendered image

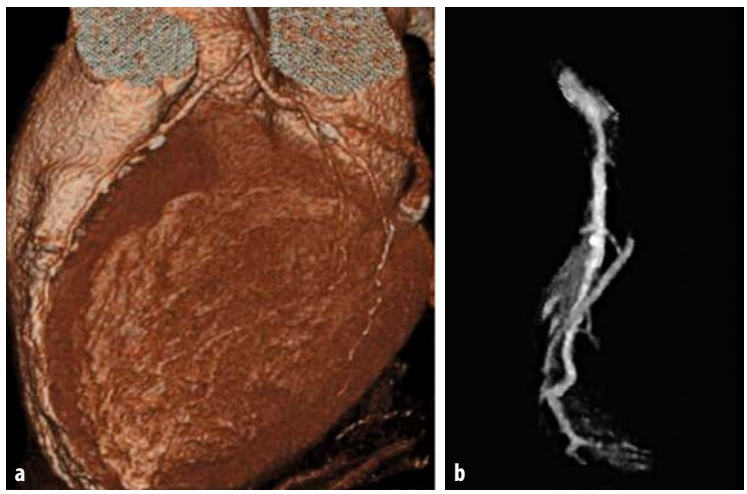

Fig. 9.2 a, b. Mild stenosis of the LAD. **a** Three-dimensional image. **b** Bi-dimensional image showing mild reduction in the caliber of the proximal segment of the LAD

by itself diagnostic, allowing identification and characterization of the plaque as well as definition of the extent of lumen reduction.

The semi-automated approach to analyzing lumen reduction is a fascinating and important alternative to the qualitative, operator-dependent, approach. Specific software analyzes the vessel in a bi-dimensional planimetric image and displays axial, transverse images simultaneous with the longitudinal vascular exploration. The software is able to evaluate the caliber of normal-sized vessels and the area of the lumen in the segment involved by atherosclerotic plaque, providing an estimate of the degree of stenosis. However, while definitely useful, the semi-automated approach is usually combined with a more personalized approach; that is, qualitative definition by the radiologist of the influence exerted by the parietal plaque on the vessel lumen, thus differentiating significant from non-significant stenosis.

Calcified Plaques: Problems in Defining Vascular Stenosis

In a vessel with atherosclerotic calcified plaque involvement, the challenge to the clinician is to define and properly specify the degree of vessel reduction. However, densely calcified plaques create a "blooming" effect on CTA, i.e., in both three and bi-dimensional reconstructed images, the volume of the calcified plaque appears much larger that it is in reality (Fig. 9.3). This CT artifact is similar to that observed when metal objects are present in the area being imaged (for instance, the metallic wires of pacemakers). In the blooming effect, there are large bright streaks and lines surrounding the object, both of which limit the definition of its contours. Calcified plaques create a larger volume, thereby impeding the radiologist's efforts to understand the effective influence of the plaque on the vessel lumen (Figs. 9.4, 9.5). It is then difficult to clearly estimate (even with automated software) the significance of the stenosis. Thus, in the evaluation of calcified plaques, care must be taken in image analysis and reconstruction. Proper reconstruction protocols that limit

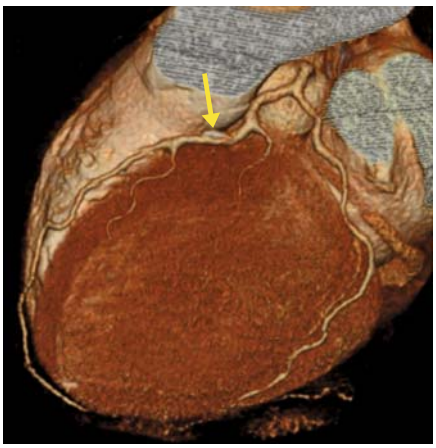

Fig. 9.3. Short segmental isolated plaque of the LAD. Blooming artifacts create a false external expansion of the plaque out of the vessel lumen (*arrow*)

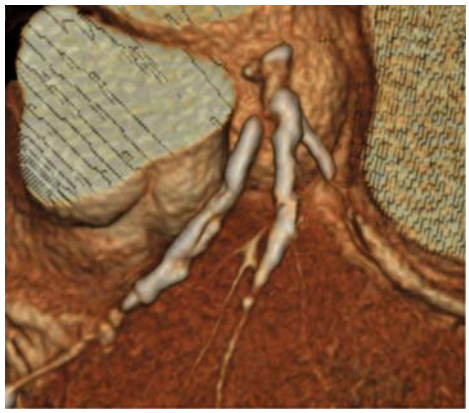

Fig. 9.4. Diffuse atherosclerotic involvement with densely calcified plaques; an artifactual blooming effect is present

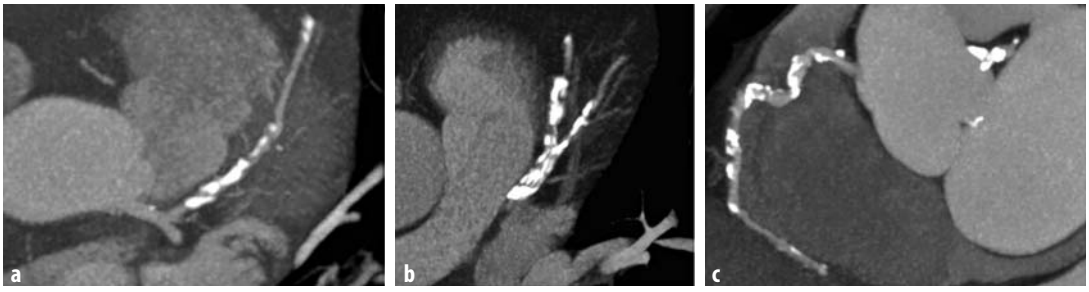

Fig. 9.5 a-c. Bi-dimensional images of densely calcified plaques with artifactual blooming effect. **a, b** Extensive plaques of the left descending coronary artery. **c** Calcified plaque of the circumflex arteries

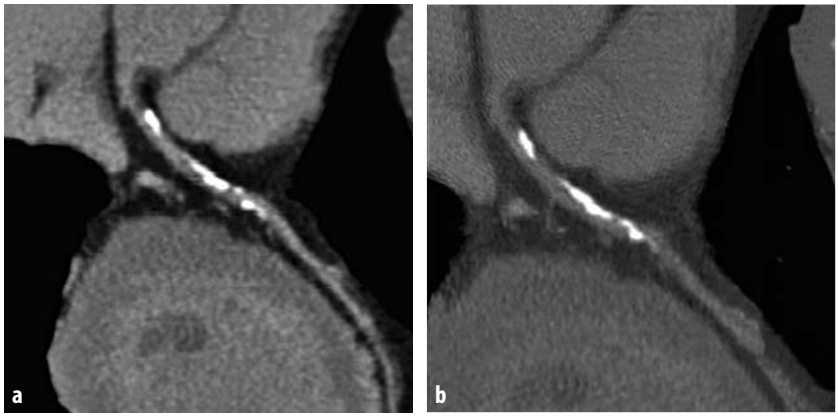

Fig. 9.6 a, b. Diffuse calcified plaques of the LAD. **a** A normal filter (value 30) shows the strong blooming effect, with plaques appearing larger then they actually are. **b** The blooming effect is reduced with a 46-value filter. Calcified parietal plaques with moderate stenosis are shown

the blooming effect have to be employed. In the evaluation of stents, better results are obtained using reconstruction filters of intermediate value (usually a value of 46 is indicated) (Fig. 9.6). Moreover, in bi-dimensional image reconstruction and analysis, images of the vessels must be reviewed in the three

orthogonal planes; for images in the longitudinal axis, the plane located in the most central position of the vessel has to be selected, while avoiding the so-called partial volume effects (well-known to radiologists) that may further lead to overestimation of the stenosis.

Despite these considerations, atherosclerotic calcified plaques remain difficult to evaluate. The real degree of stenosis is frequently overestimated in current clinical practice, leading to the unnecessary use of catheter coronary angiography. Experience with CTA and the development of newer software (using image subtraction) will further improve our diagnostic confidence in this field.

Significant Stenosis

Atherosclerotic plaques that cause significant stenosis may be eccentric, marginally located, or concentric. Coronary CTA images are able to define the influence of the plaque on lumen caliber and to identify patients with significant stenotic involvement. Stenosing plaques may be calcific or fibrolipidic, and proper characterization of the atherosclerotic plaques will result in a more appropriate therapeutic approach (Figs. 9.7–9.9). In the evaluation of 3D images acquired by CT, a complete analysis on three planes has to be performed, as discussed previously, in order to better define the degree of stenosis. Manual reconstruction methods provide qualitative measurement of the degree of stenosis, whereas semi-automated procedures generate quantitative information.

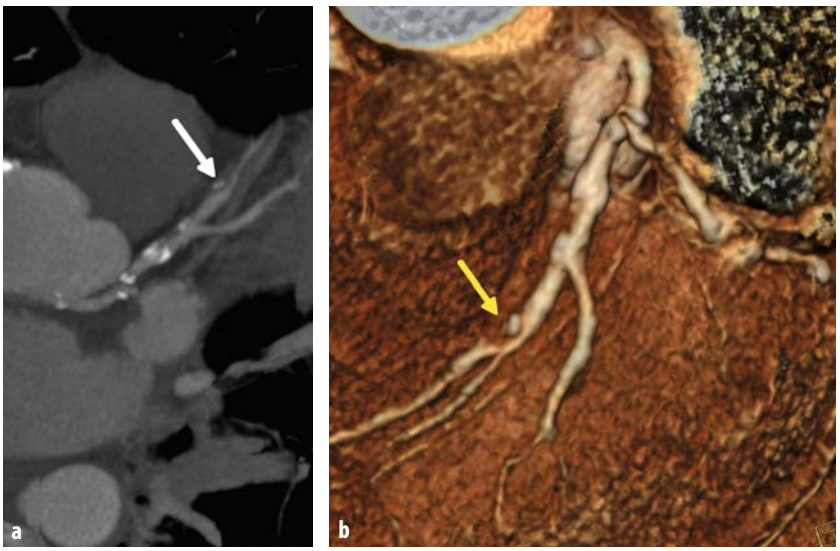

Fig. 9.7 a, b. Significant stenosis caused by a mixed plaque with a central calcific core (*arrow*), as seen in (**a**) bi-dimensional and (**b**) three-dimensional techniques

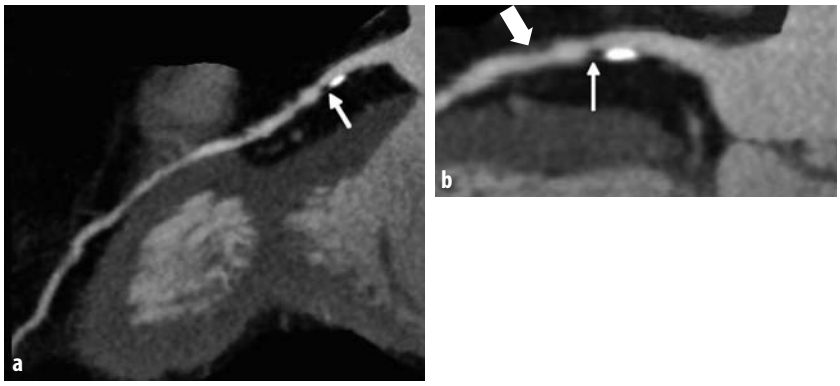

Fig. 9.8 a, b. Bi-dimensional images show (**a**) a marginal calcific plaque and a second, non-calcific fibrolipidic plaque, with 50% vessel stenosis (*arrow*). A third non-calcific plaque is also present (*arrowhead*) (**b**)

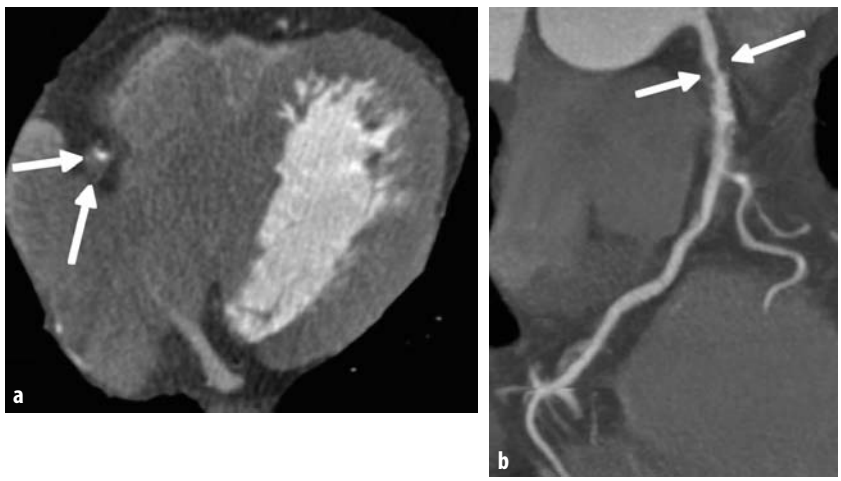

Fig. 9.9 a, b. Severe stenosis caused by a concentric plaque of the proximal segment of the right coronary artery. **a** Axial image shows the plaque involvement and allows analysis of the reduced vessel lumen. **b** Bi-dimensional reconstructed image shows evidence of the stenosis, but with good distal vascular opacification

The extension of the atherosclerotic burden on the coronary bed has to be properly assessed and defined in CTA images, specifically, whether one, two, or three coronary vessels are involved, since multi-vessel involvement influences clinical outcome and the course of coronary atherosclerotic disease (Figs. 9.10–9.12). In addition, patient survival is directly related to the extent of atherosclerotic involvement; being high for non-significant stenosis, low in the presence of significant stenosis of a single vessel (Figs. 9.13–9.15), and even lower when three-vessel disease is evident.

Stenosing atherosclerotic disease of the coronary arteries has to be correlated with the anatomic configuration of the coronary bed. If congenital

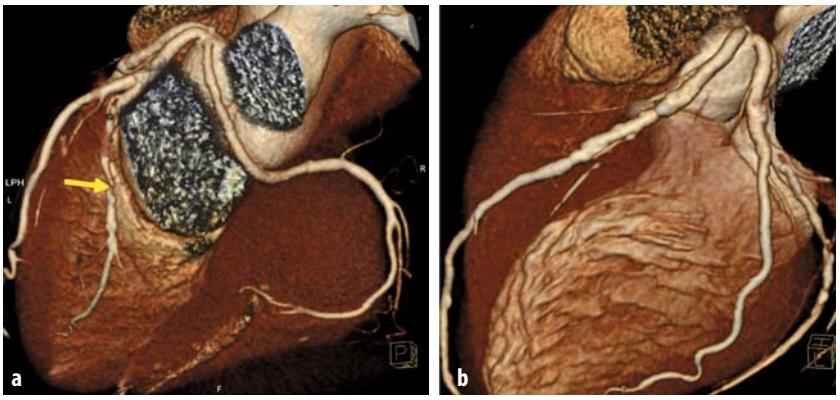

Fig. 9.10 a, b. Anomalous origin of three vessels from the same left coronary sinus. A stenosis of the middle segment of the circumflex artery is also present (*arrow*)

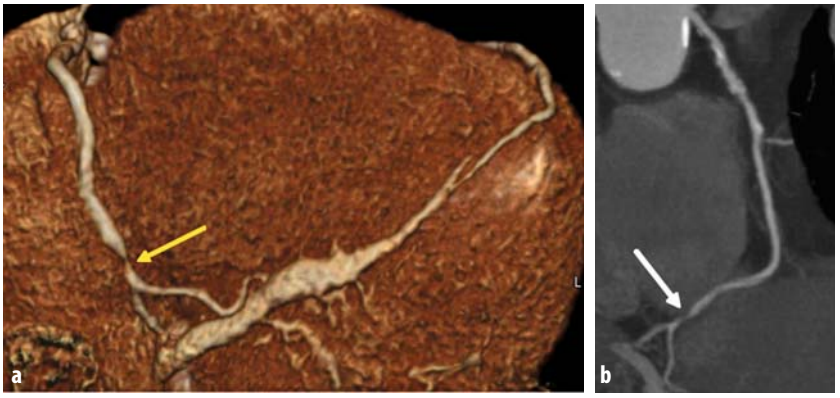

Fig. 9.11 a, b. Significant stenosis of the right coronary artery just proximal to the crux (vascular bifurcation). The stenosis is evident both in three-dimensional (**a**) and bi-dimensional (**b**) images

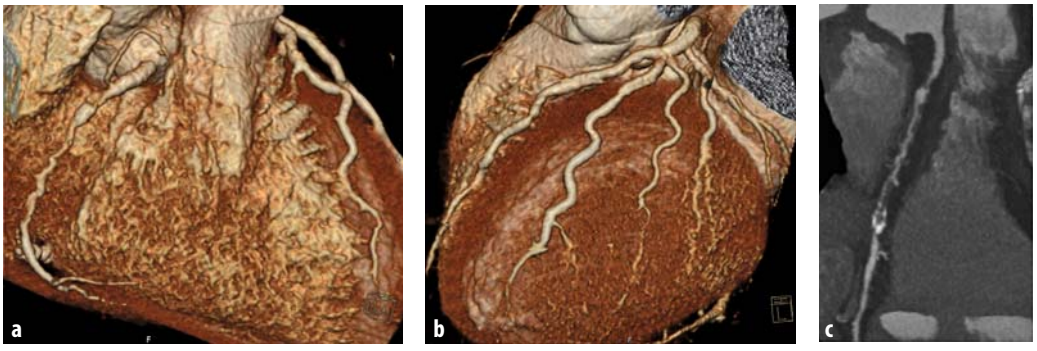

Fig. 9.12 a-c. **a, b** Right coronary artery involved in multiple plaques, with focally significant reduction in the caliber of the arterial lumen. **c** Strong compensatory hypertrophy of the vessels of the left vascular anatomy are well evident in 3D volume-rendering images

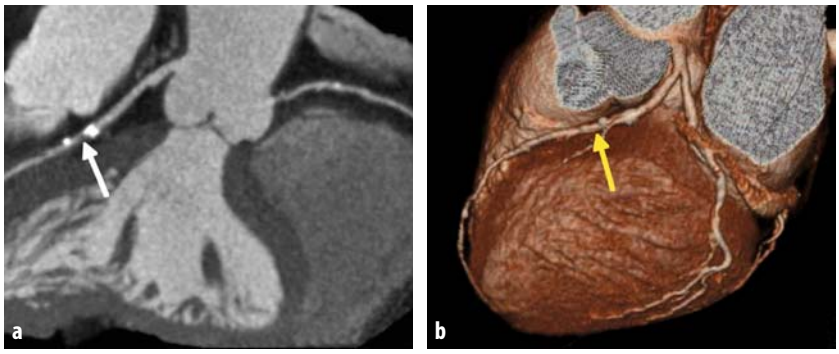

Fig. 9.13 a, b. Significant stenosis of the LAD due to a calcified plaque (*arrow*), as shown in (**a**) bi-dimensional and (**b**) three-dimensional techniques

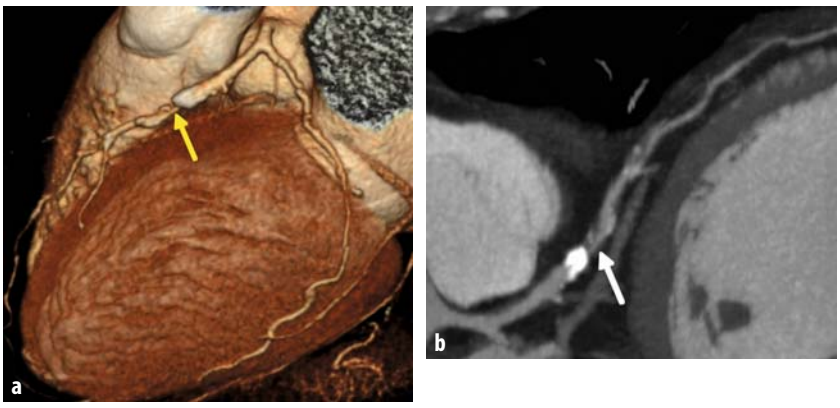

Fig. 9.14 a, b. Significant stenosis of the LAD, evaluated by (**a**) volume-rendering and (**b**) curved multiplanar reformatted (MPR) images

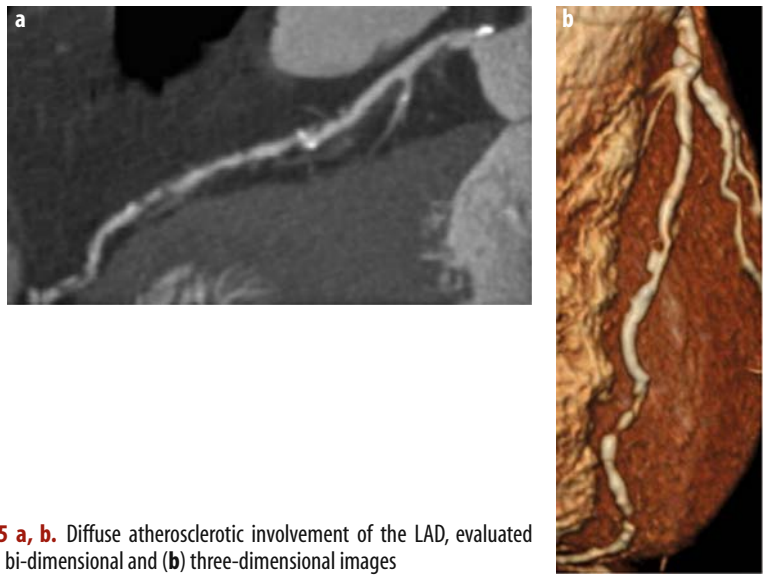

Fig. 9.15 a, b. Diffuse atherosclerotic involvement of the LAD, evaluated using (**a**) bi-dimensional and (**b**) three-dimensional images

hypertrophy of one coronary vessel is present (see chapter on coronary anatomy), stenosis of that single vessel will cause more significant pathological findings, whereas stenosis of a congenitally hypoplastic vessel may have less influence on myocardial perfusion. The same applies to coronary occlusion, which may be compatible with life only if a hypoplastic or non-dominant vessel is involved.

Remodeling

The presence of an atherosclerotic plaque is not always paralleled by vessel stenosis. Coronary arteries are rapidly pulsating vessels with consistent elasticity; significant remodeling of the vessel lumen may reduce the effect of a parietal plaque on vessel caliber and lumen. It is possible to have an important marginal plaque, e.g., 2 mm thick, that does not significantly influence the vessel lumen. This is exclusively found in coronary arteries and does not apply to other vessels in the body. Progression of an atherosclerotic plaque of the carotid arteries will be paralleled by a reduction of the lumen, with an increase of the plaque volume. In the coronary arteries, however, if the vessels retain their elasticity, the volume increase induced by a parietal, eccentric atherosclerotic plaque will lead to distension of the contralateral vessel wall, with deformity of the vessel course but also an increase in the vessel lumen and thus a lack of stenosis. This phenomenon is called vascular remodeling and may be well-evidenced in coronary CTA images (Fig. 9.16). In these cases, coronary CTA may be even more accurate than catheter angiography. In case of remodeling, the caliber of the vessel, as shown by catheter angiography, may be completely normal. Only coronary CTA will correctly demonstrate and characterize the important, eccentric plaque. These findings have important prognostic value; in fact, only CTA is able to show that such patients have coronary artery disease and require treatment (mostly in the presence of fibrolipidic athero-

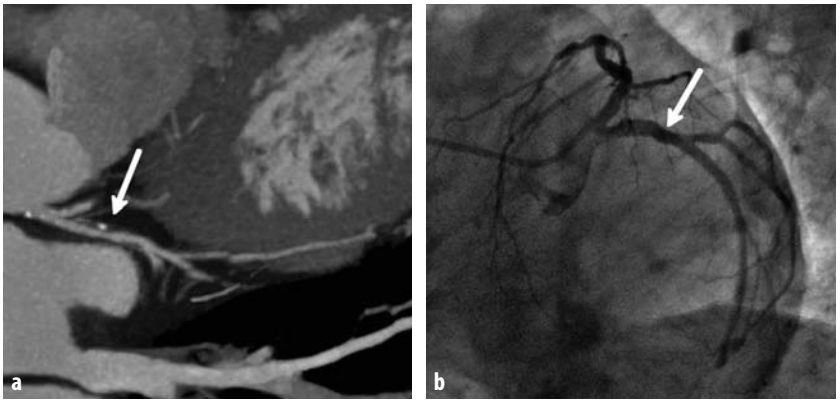

Fig. 9.16 a, b. Vascular remodeling. **a** CT image shows evidence of a thick peripheral marginal and eccentric coronary plaque (*arrow*) of the circumflex coronary artery. **b** Catheter coronary angiography does not show any significant area of lumen reduction, due to vascular remodeling

sclerotic plaque) to limit the possibility of atherosclerotic progress and to reduce the risks of complications of soft plaques (ulceration, hemorrhage), especially the development of acute coronary syndrome.

Occlusion of the Coronary Arteries and the Development of Collateral Circulation

Coronary artery occlusions can be easily evaluated with coronary CTA, due to the fact that distal to an atherosclerotic plaque the lack of visualization of a coronary vessel is diagnostic for coronary occlusion (Fig. 9.17). While complete occlusion of the main left artery is never diagnosed, because it is a fatal condition, it is not rare to find occlusions of the right coronary artery or of a relatively hypoplastic left coronary branch, without concomitant significant clinical findings. In fact, the anatomic configuration (dominant vessels, congenitally hyperplastic arteries) may greatly reduce the influence of vascular occlusion, at least regarding the clinical aspect.

The coronary arterial bed is considered a "terminal" vascular bed in that distal arteries, once occluded, cannot be revascularized by other, contiguous vessels. This is true only for acute coronary occlusions; myocardial infarction will develop if an occlusion occurs acutely, such that contiguous vessels are unable to compensate for the reduced perfusion. However, atherosclerosis is more frequently a slowly progressing chronic disease and there is sufficient time for the development of coronary collateral circulation. Collaterals are very thin, peripheral intramyocardial vessels with an inverted vascular flow that allows revascularization distal to the vascular occlusions (Figs. 9.18–9.20). They are usually too small for their proper and direct demonstration by coronary CTA and may be opacified only at catheter angiography. CTA instead provides indirect evidence of their presence. In complete vascular occlusion, with distal re-filling of the involved vessel, a diagnosis of collateral circulation can be made, thus also providing

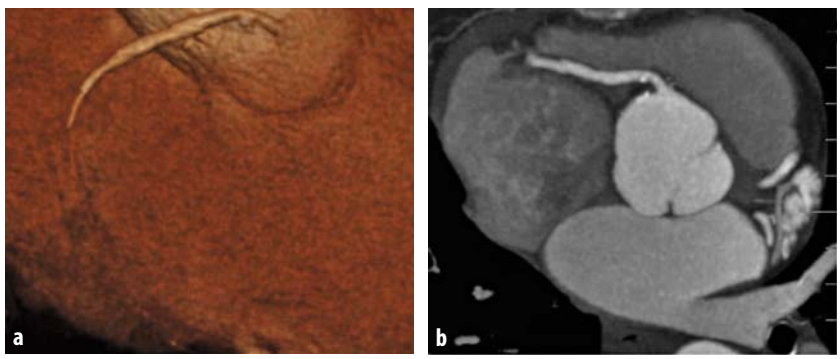

Fig. 9.17 a, b. Occlusion of the right coronary artery without distal re-vascularization and without collateral vessels. **a** Three-dimensional image. **b** Bi-dimensional reconstructed image

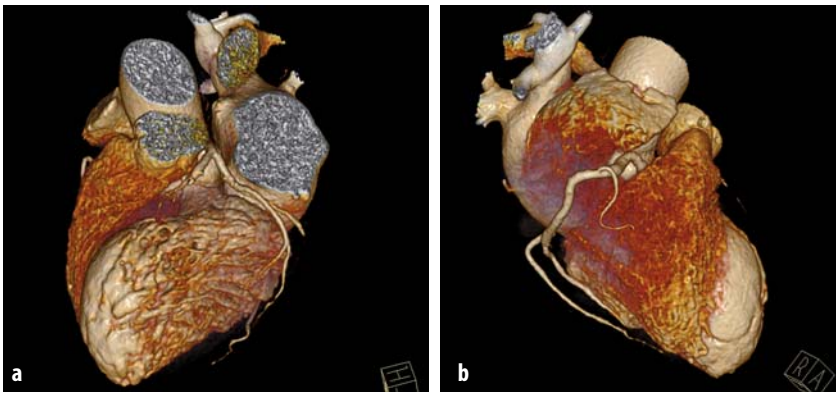

Fig. 9.18 a, b. Complete occlusion of the LAD. **a** Aneurismatica dilatation of the lateral part and the apex of the left ventricle. **b** There is hypertrophy of the right coronary artery and the circumflex artery, supplying vascularization to the remaining part of the left ventricular wall

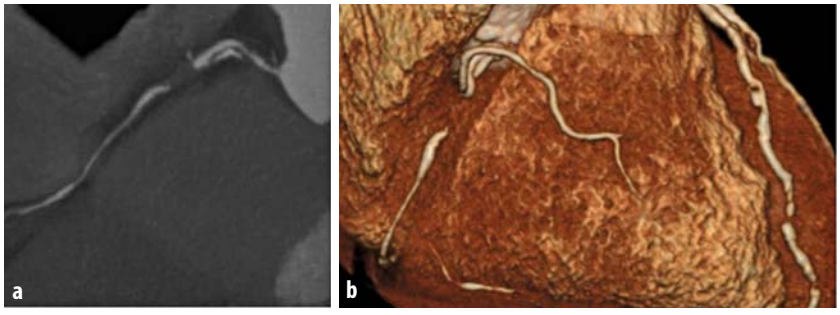

Fig. 9.19 a, b. Occlusion of the right coronary artery, with evidence of collateral circulation providing flow distal to the occluded segment (collateral circulation is not directly evident in acquired CT images). Bi-dimensional (**a**) and three-dimensional images (**b**)

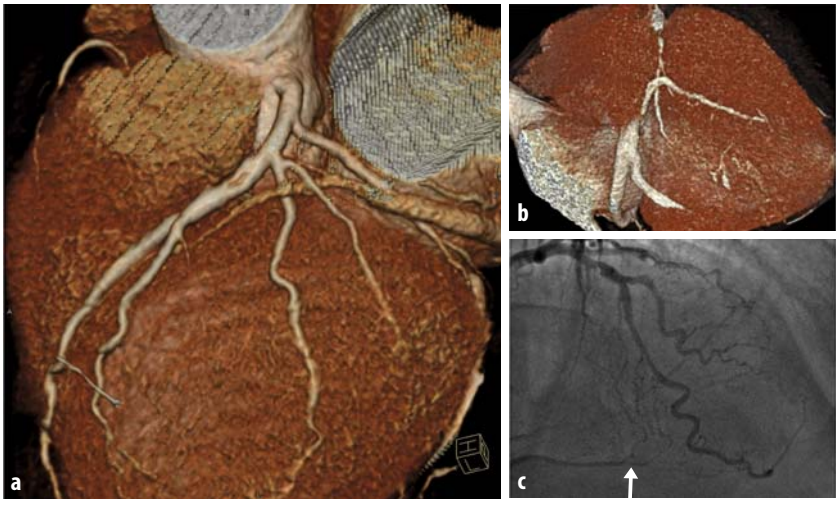

Fig. 9.20 a-c. Collateral circulation from the LAD shows revascularization distal to the occlusion of the right coronary artery. **a, b** Three-dimensional images acquired with CT. **c** Catheter coronary CT angiography shows small collateral vessels and revascularization of the distal right coronary vessel

information on the vessel that is contributing the inverted flow for revascularization. Only in a few instances is it possible to directly evaluate collateral circulation, based on evidence of hypertrophic superficial epicardial vessels or the "corkscrew" appearance of the vessels (Fig. 9.21). In addition, collateral circulation may develop in the same coronary vessel (homo-coronary collateral circulation) (Fig. 9.22).

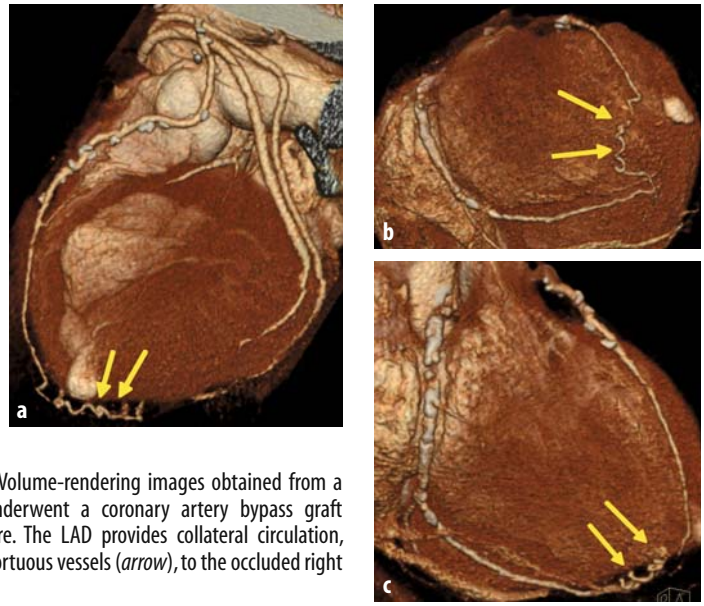

Fig. 9.21 a-c. Volume-rendering images obtained from a patient who underwent a coronary artery bypass graft (CABG) procedure. The LAD provides collateral circulation, with large and tortuous vessels (*arrow*), to the occluded right coronary artery

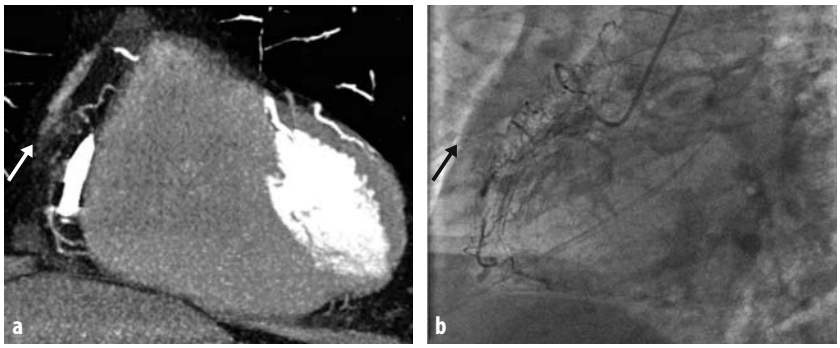

Fig. 9.22 a, b. Ipsilateral collateral circulation. The right coronary artery is occluded (stent occlusion). Both CT (**a**) and catheter coronary angiography (**b**) show the small tortuous vessels providing revascularization of the distal right coronary artery (*arrow*)

Evaluation of Coronary Artery Stenosis: A Review of the Literature

Coronary CTA exhibits a high sensitivity and specificity in the definition of coronary artery stenosis. The sensitivity in defining significant stenosis (> 50% caliber reduction) is 93% for the evaluation of single vessels and even higher on a per patient basis, as shown in a recent meta-analysis of literature data. Not surprisingly, the sensitivity with 64-slice systems is much higher than that of 16-slice systems (83 vs. 93%), a difference that may also be related to methodological improvements (more concentrated contrast agent, better injection protocol) or to the faster rotational speed of the X-ray tube and advances in detector characteristics. Further improvements are expected with technical advances, such as larger and more sensitive detectors arrays and even faster rotation times, leading to reduced acquisition times of coronary images.

As far as specificity is concerned, the current overall value is high, in the range of 96%. Another important issue is related to the negative predictive value, which is 97–98%. The significance of negative predictive value is very important from a clinical point of view; in fact, it defines the ability of coronary CTA to determine whether the vessels are normal, i.e., free of atherosclerotic involvement. Accordingly, if the arteries are normal with respect to the CTA findings, then there is a 98% certainty that the patient does not have coronary atherosclerosis. This stresses the important role that CTA plays (in symptomatic as well as in asymptomatic at-risk patients) in screening patients without or with atherosclerotic involvement. The first group consists of patients with normal coronary arteries, in whom no further diagnostic evaluation is needed. In the second group are patients with coronary artery disease, which needs to be further characterize and staged by CTA, either alone or, in the presence of clearly significant stenosis, by means of catheter angiography. It is estimated that at least 30% of the catheter angiography examinations currently performed identify a normal coronary bed; thus, a large number of these procedures could be avoided. At the same time, once significant coronary disease has been diagnosed at CTA, it is not crucial whether the same method is able to properly address the exact degree of stenosis; rather, further defining and characterizing atherosclerotic vascular involvement are left to catheter angiography.

Saving Lives

Radiologists, especially those who have only recently gained experience in the field of cardiology, should be well aware of the fact that there are a number of truly asymptomatic patients who would have never undergone catheter angiography, due to a lack of clinical indications. In this group, only the use of coronary CTA is able to show the presence of important coronary disease. These patients can thus be regarded as lives saved by CTA.

By being alert to such patients, we hope to overcome the indifference with which some clinicians still regard coronary CTA. Several developments advocate the increased use of coronary CTA: (1) the problem of high radiation exposure has been solved (80% reduction with newer equipment,

i.e., much less than the exposure that occurs in nuclear-medicine procedures); (2) the technology is no longer primitive and the procedures have become standard; and (3) the image quality is consistent, facilitating good professional collaboration between cardiologists and radiologists and thus better-informed clinical diagnoses. The frequency and ease with which CTA can be used should reassure the properly informed patients that he or she is undergoing a standard, routine clinical procedure, not a dangerous examination. CTA is, in this aspect, no different than, e.g., a CT scan of the kidneys for evaluation of kidney stones (which has made I.V.P. almost completely obsolete) or magnetic resonance of the brain (which has totally replaced the very invasive procedures used by neuroradiologists until the 1970s).

"Seeing" the coronary arteries, as is possible with CTA, is the best approach to directly determine whether a patient has coronary artery disease. Every other diagnostic procedure provides only indirect information.

In the following, present three representative cases in which the patients had highly significant CTA findings but either none or limited clinical findings and a negative treadmill test.

Case 1: 40-year-old patient with mild symptoms, related to epigastric area. Negative endoscopy, negative treadmill test. Stenting of the stenotic lesion was performed (Figs. 9.23, 9.24).

Case 2: 70-year-old patient with no symptoms and a negative treadmill test. The only indication for CTA was the fact that his son had died of an acute cardiac arrest while playing football. The patient underwent stenting of a stenotic lesion was performed (Fig. 9.25).

Case 3: 68-year-old asymptomatic patient with a negative treadmill test who requested CTA after learning of the procedure in the media. A coronary artery bypass graft was performed after coronary angiography (Figs. 9.26–9.28).

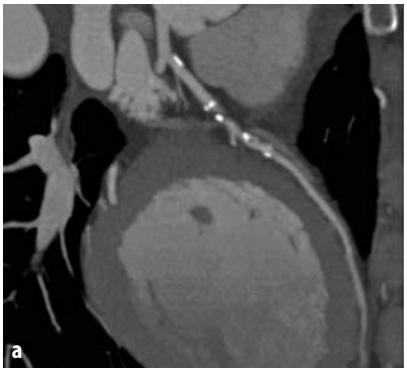

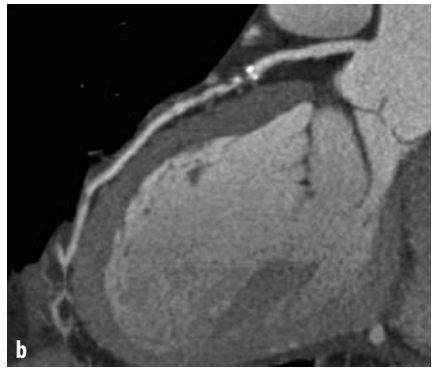

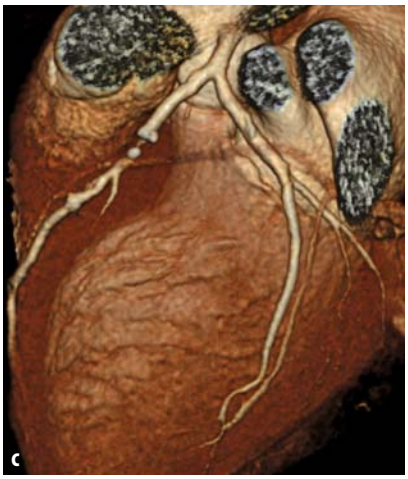

Fig. 9.23 a-c. Case 1. Bi-dimensional MPR images (**a, b**) and 3D images (**c**) show a severe stenosis of the middle segment of the LAD due to a calcified plaque

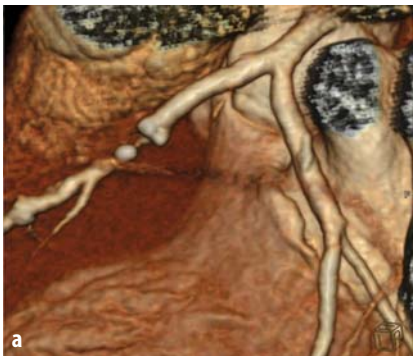

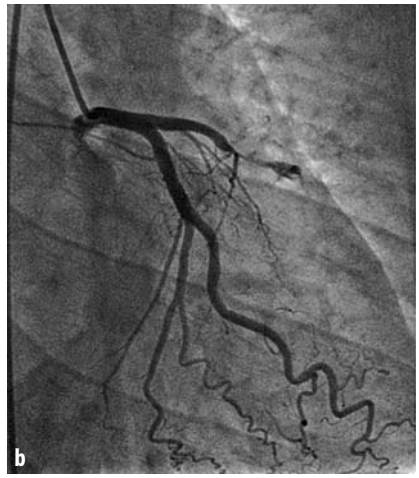

Fig. 9.24 a, b. Case 1. **a** 3D image of the stenosis. Catheter coronary angiography (**b**) confirms the diagnosis and the absence of vascular flow distal to the diseased segment

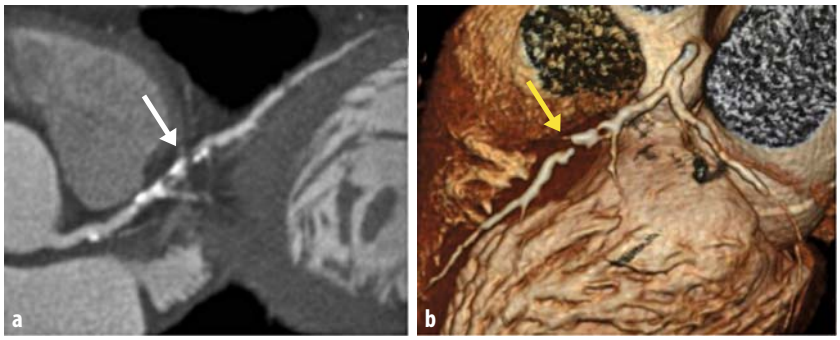

Fig. 9.25 a, b. Case 2. Severe stenosis of the LAD evaluated both in (**a**) bi-dimensional and (**b**) three-dimensional images

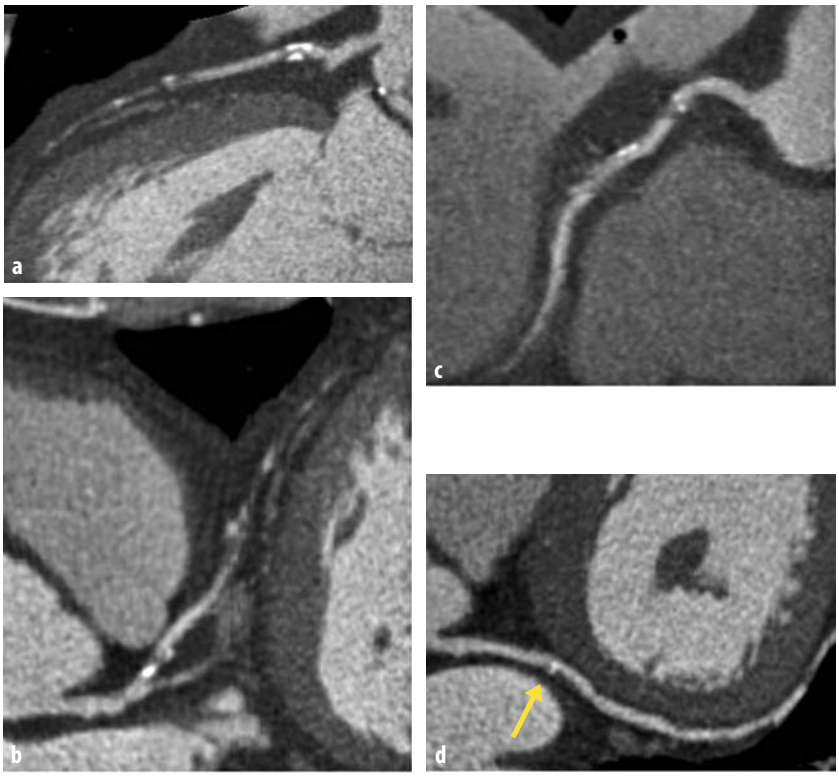

Fig. 9.26 a-d. Case 3. Bi-dimensional images show occlusion of both the right coronary artery and the LAD. There is also a marginal plaque in the middle segment of the cirumflex artery, with significant stenosis (*arrow*)

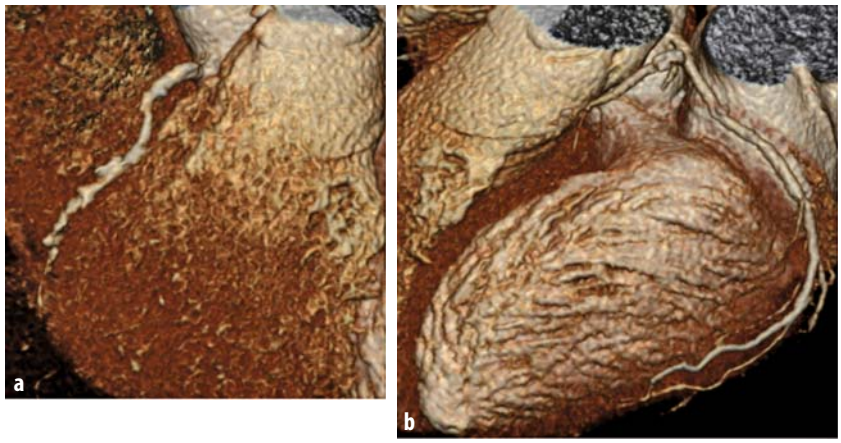

Fig. 9.27 a, b. Case 3. Three-dimensional volume-rendering images show occlusion of (**a**) the middle third of the right coronary artery and (**b**) the LAD. The circumflex artery is hypertrophic

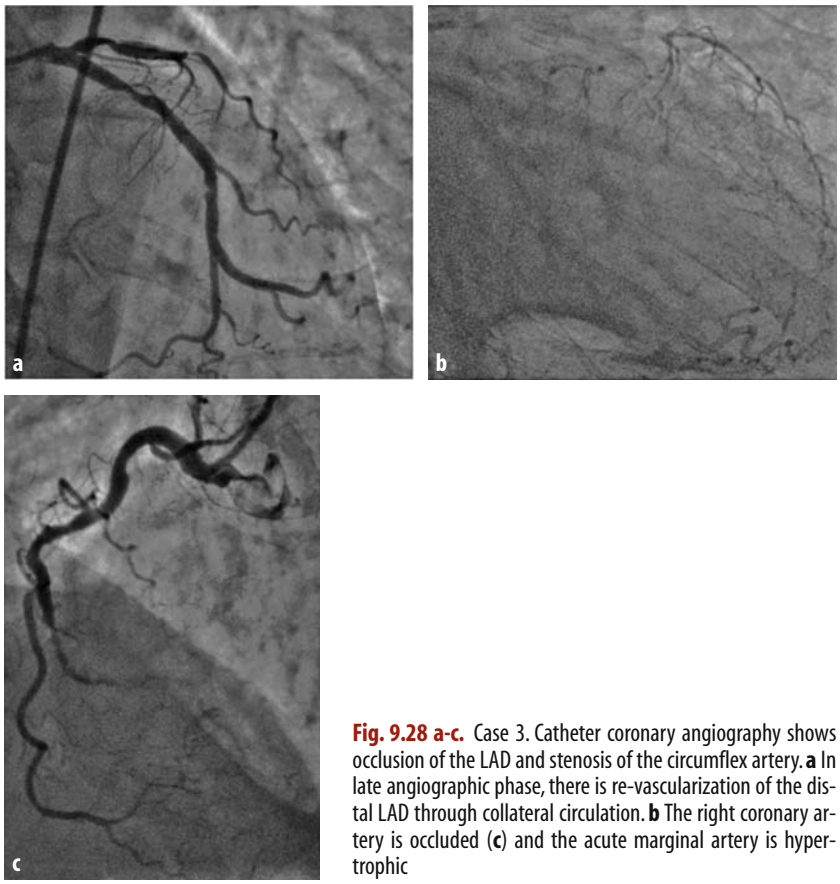

Fig. 9.28 a-c. Case 3. Catheter coronary angiography shows occlusion of the LAD and stenosis of the circumflex artery. **a** In late angiographic phase, there is re-vascularization of the distal LAD through collateral circulation. **b** The right coronary artery is occluded (**c**) and the acute marginal artery is hypertrophic

10

Current Strategies in Cardiac Surgery

Paolo Sordini

Coronary artery bypass grafting (CABG) is a surgical procedure used to divert blood around narrow or clogged arteries. It is more effective than medical management in relieving symptoms such as angina, dyspnea, and fatigue. The 2004 American College of Cardiology/American Heart Association (ACC/AHA) CABG guidelines state that CABG is the preferred treatment for disease of the left main coronary artery and disease of all three coronary vessels (left anterior descending artery, left circumflex artery, right coronary artery). CABG is also advocated for other high-risk patients, including those with severe ventricular dysfunction (i.e., low ejection fraction) or diabetes mellitus.

Standard Grafting Techniques

The two main coronary arteries, the left and right coronary arteries (Fig. 1.1), give rise to important branches. The left coronary artery (LCA) divides into the left anterior descending artery and the circumflex branch. The LCA supplies blood to the left ventricle and left atrium, while the LAD supplies blood to the front of the left side of the heart and the circumflex artery, which encircles the heart muscle, perfusing the lateral side and back of the heart. The right coronary artery (RCA) divides into the right posterior descending and acute marginal arteries; it supplies blood to the right ventricle, right atrium, the sinoatrial node (a cell cluster in the right atrial wall that regulates the heart's rhythmicity), and the atrioventricular node. Smaller branches of the coronary arteries include: acute marginal, posterior descending, obtuse marginal, septal perforator, and diagonals.

The median sternotomy incision is used for most coronary artery bypass surgery. The pericardium is opened longitudinally. During harvesting of the venous grafts, the patient is given heparin to prevent the blood from clotting.

P. Pavone, M. Fioranelli, D.A. Dowe, *CT Evaluation of Coronary Artery Disease*.

In addition, the patient's cardiac and pulmonary requirements are met artificially; hence the term cardiopulmonary bypass (Fig. 10.1). In this procedure, the patient's blood bypasses the heart and lungs, such that the desired bloodless, motionless operative field is achived while the other organs of the body are maintained with a constant supply of oxygen and nutrient-rich blood. Other aspects of cardiopulmonary bypass surgery include aortic clamping and the administration of a potassium-based cardioplegic solution, which is mixed with blood and infused into the coronary circulation to induce and maintain paralysis during the surgical procedure.

Distal anastomoses are performed first, with proximal anastomoses constructed after each distal anastomosis or before removal of the cross-clamp. The long saphenous vein is the most commonly used to bypass a coronary artery obstruction. Previously, the internal thoracic artery was chosen as a coronary bypass graft, but because of the difficulty involved in its mobilization and the resulting patient morbidity it was abandoned. However, with improvements in bypass surgery, results with the internal thoracic artery, radial artery, and right gastroepiploic artery have been encouraging. In fact, current-

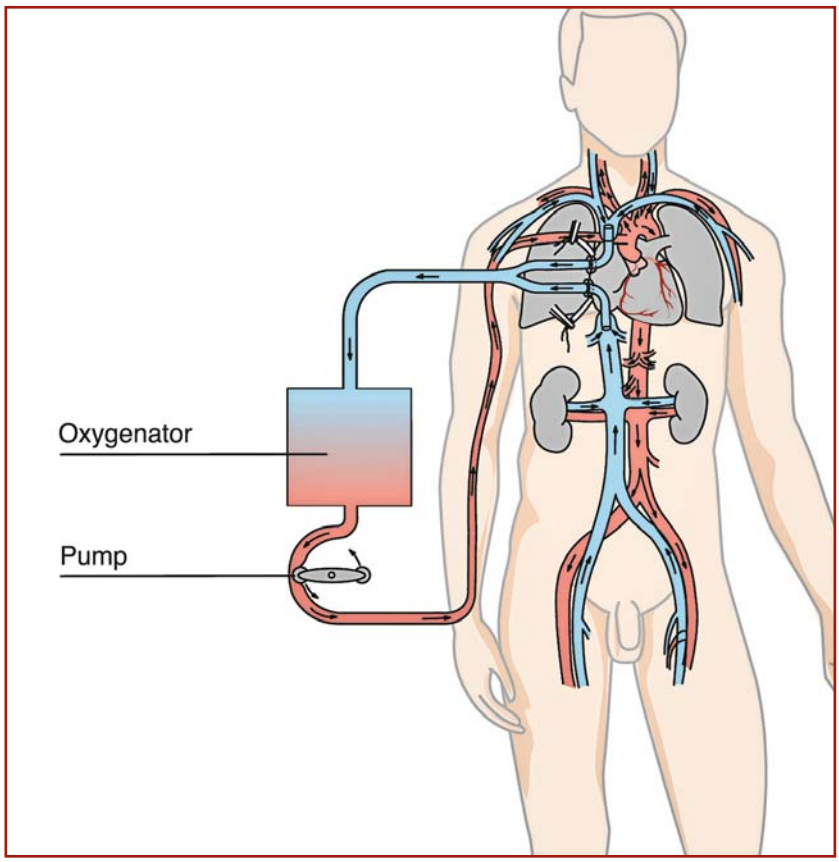

Fig. 10.1. Heart-lung machine

ly, the in-situ left internal thoracic artery is the preferred vascular conduit, followed by the saphenous vein.

At the end of the surgical procedure, the aortic cross-clamp is removed and the cardiopulmonary bypass interrupted. Protamine is given to reverse the effects of heparin and the sternum is closed (Fig. 10.2).

Beating-heart bypass surgery is the newest and most significant advancement in cardiac surgery. It allows the heart to continue beating naturally during the operation, thus eliminating the need for a heart-lung machine or a pump. Many surgeons choose the beating-heart bypass procedure because of its benefits, including less trauma due to the elimination of the heart-lung machine and a reduced need for blood transfusions as there is less bleeding. The limitation is that it is more difficult to perform anastomoses. Indications for off-pump CABG surgery include a heavily calcified aorta.

Minimal extracorporeal circulation (MECC) is a promising perfusion technology. It retains the advantage of extracorporeal circulation but with a significantly reduced priming volume. MECC has proved to be safe, feasible, and superior to standard cardiopulmonary bypass in terms of post-operative complications.

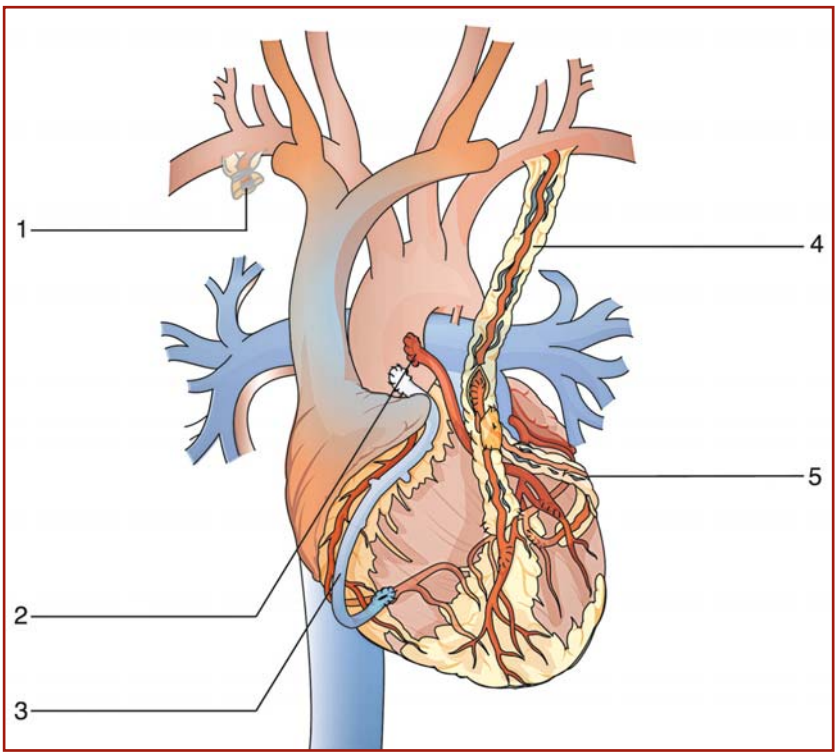

Fig. 10.2. Examples of coronary bypass. *1* Ligation of the right internal mammary artery (RIMA). *2* Radial-artery graft from the aorta to the diagonal coronary artery. *3* Saphenous-vein graft from the aorta to the right coronary artery (RCA). *4* In-situ graft from the left internal mammary artery (LIMA) to the left anterior descending artery (LAD). *5* Radial-artery graft from composite RIMA graft from LIMA graft to left circumflex artery (LCx)

Results

The long-term clinical results of bypass surgery depend upon the combined influence of the following factors: age, extent of cardiac disease, ventricular function, and associated pathology, especially diabetes mellitus, arterial hypertension, renal failure, and bronchitis.

Operative risks were 1–2% in patients with high-quality ventricular function and good general clinical condition. The long-term outcome was related to the rate of atherosclerosis progression.

Percutaneous coronary intervention, commonly known as coronary angioplasty, is a therapeutic procedure to treat graft patency.

The use of arterial grafts in coronary bypass surgery remains the best form of therapy for long-term results and improved life expectancy of patients.

11

Coronary CT Angiography: Evaluation of Coronary Artery Bypass Grafts

Marcello De Santis, Paolo Pavone

Myocardial re-vascularization is one of the fundamental steps in the clinical history of patients with coronary atherosclerotic disease. Solving the symptoms of angina, improving tolerance to effort, and a global gain in terms of reduced morbidity and mortality are the general goals that coronary re-vascularization has tried to achieve since its beginning.

Pre-Operative CT Evaluation

The surgical approach to coronary artery disease has evolved significantly over the past several years, with corresponding improvement in the size of the arterial conduits used for treatment (beside the classical left internal mammary artery, also the right internal mammary, radial, right gastro-epiploic, and inferior epigastric arteries). There is more frequent use of arterial conduits as opposed to grafts consisting of segments of the saphenous vein (leading to better short- and long-term patency). Newer surgical techniques have also been introduced, including off-pump surgery and minimally invasive surgery-coronary artery bypass grafts (MID–CABG). The developments in this field have led to increased interest in the use of newer imaging procedures, before and after graft placement. Radiologists are required to evaluate the course and patency of arterial conduits in order to better plan the surgical approach (Fig. 11.1). At the same time, the potential presence of a major thoracic deformity can be evaluated by CT. Other pre-operative questions of surgeons that can be successfully addressed by CT include definition of the quality, and caliber of the coronary artery site where the distal anastomosis will be placed and whether there is bridging of a segment of the coronary artery, which may prevent placement of a distal anastomosis, if a mini-invasive approach is planned (Fig. 11.2).

P. Pavone, M. Fioranelli, D.A. Dowe, *CT Evaluation of Coronary Artery Disease*.

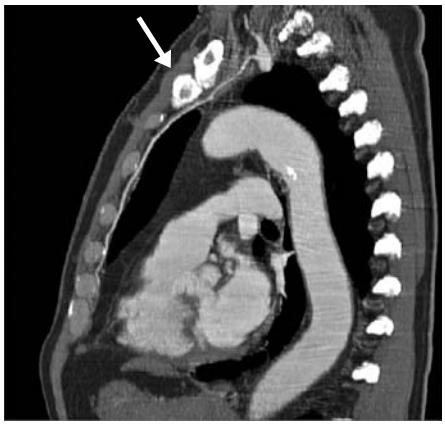

Fig. 11.1. MIP reconstruction of the left internal mammary artery

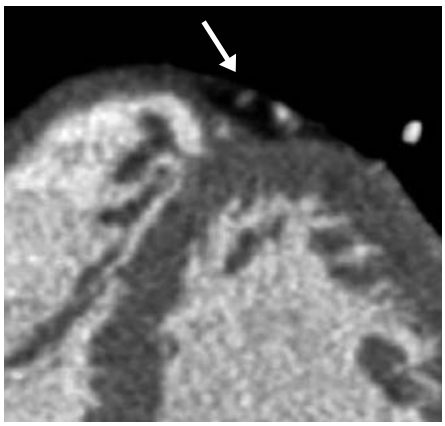

Fig. 11.2. Short-axis reconstruction of the left ventricle. Intramyocardial course of the left anterior descending artery (bridging)

Post-Operative Evaluation of CABG

The goals of postoperative evaluation of CABG are two-fold: (1) to evaluate and monitor graft patency and (2) to identify the possible progression of atherosclerotic disease in native vessels. Either factor may account for the recurrence of ischemic myocardial symptoms.

As noted above, the long-term patency of arterial grafts is better (patency of internal mammary arterial grafts: 85–90% at 10 years) than that of venous bypass grafts (75–80% at 5 years, 61% at 10 years, 50% at 15 years, with a yearly obstruction rate of 2% between the first and sixth year and 4–5% per year in the following years). Venous-graft pathologies account for 53% of angina symptoms occurring within the first 5 years following surgery, 76% of the episodes occurring between 5 and 10 years post-operatively, and 92% of those after more than 10 years. In the same time frame, atherosclerotic progression in native vessels accounts for 47, 24, and 8% of ischemic events, respectively.

Before the introduction of coronary CT angiography (CTA), the post-operative non-invasive evaluation of these patients was performed by the treadmill test, echocardiography, or nuclear medicine procedures (the latter two accompanied by pharmacologic or ergometric stress tests), as for the evaluation of native arteries. Treadmill testing with ECG is considered to be the first level of evaluation, although the sensitivity and specificity are much lower than achieved with second-level tests.

Catheter coronary angiography remains the gold standard in the evaluation of the degree of patency of bypass grafts and for the proper choice of revascularization procedures. However, it is an invasive procedure, carries several risks and is therefore used only in patients with strongly positive second-level stress tests (anomalies of regional parietal motility as seen on echocardiography, or perfusion deficit areas visualized by nuclear medicine procedures). In patients with graft pathology, a decision must be taken regarding the proper further therapeutic approach, either an interventional procedure or a new surgical procedure. The choice, according to the ACC/AHA 2001–2002 guidelines, depends on the location and extent of the disease: stenting of areas involved by new atherosclerotic burden is recommended first, while new surgical procedures are reserved for patients with multiple stenosis and multivessel disease, with reduced ventricular function.

CT Evaluation of CABG: Technique

The technique to be used for the evaluation of CABG is similar to that used to evaluate of native vessels. Beta-blockers are administered to reduce cardiac beats per minute (bpm), as discussed elsewhere in this volume. However, care needs to be taken to widen the cranial aspect of the anatomic area that will be evaluated during coronary opacification with contrast agent. The upper limit of the examination volume has to reach and include the subclavian arteries in order to allow a complete and detailed evaluation of the mammary arteries beginning at their origin. In patients with arterial bypass in which the right gastro-epiploic artery was used, the imaging volume must include the upper abdomen.

Since the acquisition volume is larger than that obtained in the evaluation of native coronary arteries, a larger imaging window (time) is needed. The inflow of contrast agent in the coronary arteries during image acquisition must be continuous and therefore requires a “longer“ bolus, either with a larger amount of contrast agent (20–150 ml) or a reduced flow of the injection (3–4 rather than the suggested 5–8 ml per second).

CT Evaluation of CABG: Results

Since its appearance, coronary CTA has been considered a reliable technique. There are technical reasons for the improved imaging of bypass grafts and the fewer artifacts seen on the images: the larger caliber of the arterial and venous conduits vs. that of native arteries, and the frequently extracardiac course of the grafts. Early studies, in which CT with four detector rows had been used,

reported sensitivity and specificity values of 90 and 75–85%, respectively, for the definition of stenosis. With newer equipment, the sensitivity in the diagnosis of CABG occlusion is 100% and in the evaluation of stenosis, over 96% (Figs. 11.3, 11.4).

Nonetheless, there are limits in the evaluation of CABG, such as in patients with arrhythmia and when surgical clips create significant beam-hardening artifacts (Fig. 11.5). However, in most cases, very high-quality images are obtained and important therapeutic decisions based directly on these images can be made, thus limiting the use of catheter coronary angiography to more complex cases, interventional procedures, or in the immediate preoperative phase, in patients in whom a new re-vascularization procedure is planned.

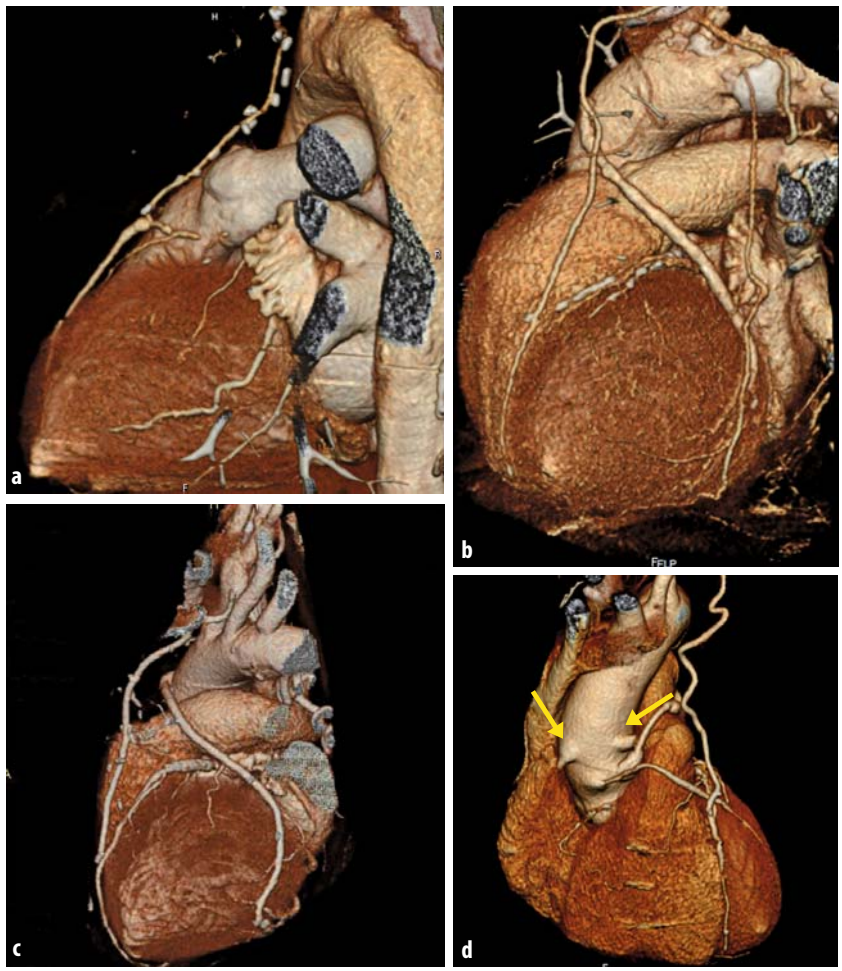

Fig. 11.3 a-d. Examples of CABG evaluated using volume rendering technique

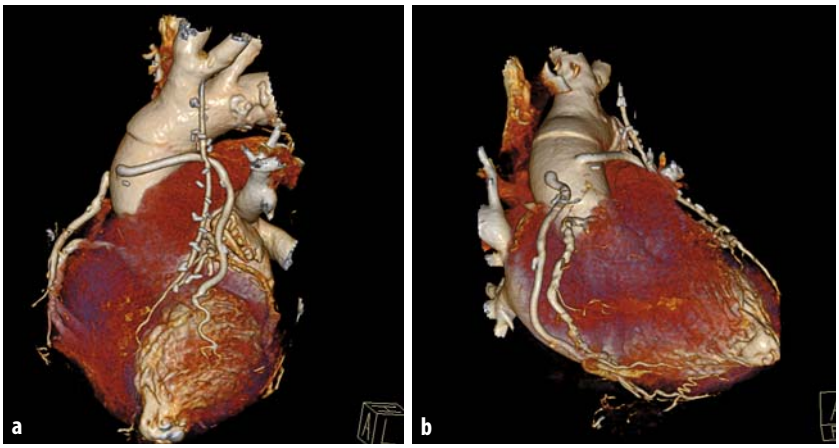

Fig. 11.4 a, b. Patency of the arterial bypass between left internal mammary artery and the left anterior descending artery (**a**). Also the two venous bypasses to the first diagonal branch (**a**) and the right coronary artery (**b**) are patent and well-evident

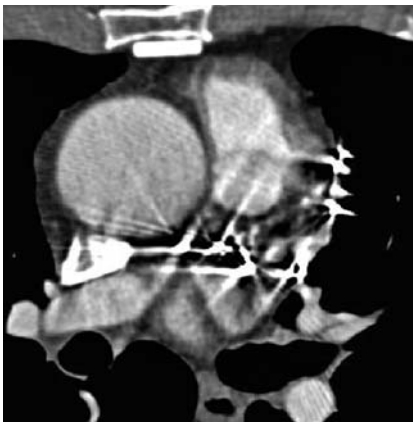

Fig. 11.5. Axial CT image: presence of significant metallic artifacts related to surgical clips

12

Coronary Stents

Enrica Mariano, Giuseppe M. Sangiorgi

Coronary stent technology is a crucial part of most interventional procedures for percutaneous revascularization. Previously, vessel wall injury and plaque fracture were the usual sequelae in response to the mechanical effect of balloon angioplasty. Nowadays, a sophisticated engineering tool serves not only as a scaffolding platform but also as an advanced vector for local anti-proliferative drug delivery to the arterial wall. The wide acceptance of coronary stenting is based on the results of pioneering trials, such as the BENESTENT and STRESS trials, which showed the superiority of stenting over balloon angioplasty in terms of a reduction of angiographic restenosis and the need for repeated intervention. Since then, the growing use of stents in ever more complex lesions and patients has stimulated the introduction of a rapidly increasing number of different stent designs. These have been proposed in order to address physiologic concerns: indeed, a primary aim of stent development is to reduce device profiles and increase flexibility thus facilitating safe delivery of the stent. Percutaneous coronary stent implantation frequently results in significant three-dimensional (3D) changes in the geometry of native coronary arteries. These changes may increase the risk of in-stent re-stenosis due to altered vessel wall compliance and subsequent alterations in shear stress. Additionally, the implantation of a stiff stent within the coronary arteries may result in flexion or hinge points due to the abrupt changes in vessel wall rigidity at the ends of the stent. These hinge points have been associated with increased rates of re-stenosis and may increase the risk of edge dissection and the need for additional stent implantation. Other important issues are lesion coverage, to avoid plaque prolapse, and radial support, to prevent elastic recoil of the artery. Furthermore, the ability to easily access arterial side branches through the struts of a deployed stent in bifurcation lesions has progressively gained importance. Finally, radiologic visibility during angiography is another important element in optimizing the clinical benefits of a stent, especially during placement, while the attenuation index must be considered if, for example, computed tomography will be performed after the procedure.

P. Pavone, M. Fioranelli, D.A. Dowe, *CT Evaluation of Coronary Artery Disease*.

This chapter summarizes the components of stent design that are important in terms of the biological response of the arterial wall and clinical outcome. In addition, new stent platforms, mainly represented by the biodegradable stent, are reviewed since they are expected to provide a more "physiologic" answer to stent implantation, reducing vascular injury and accelerating vessel healing with consequent improvement in clinical outcome.

Types of Stents

In clinical practice, the interventional cardiologist must decide which stent is most appropriate for the patient and, even more importantly, for the lesion to be treated. Albeit the "ideal" stent – one that is tailor-made to treat a given lesion or a particular subset of patients – does not exist, the general characteristics of the "perfect" stent can be summarized as follows:

- Flexible
- Trackable
- Low unconstrained profile
- Radio-opaque
- Thromboresistant
- Biocompatible
- Reliably expandable
- High radial strength
- Circumferential coverage
- Low surface area
- Hydrodynamic compatibility

In general, stents can be classified according to several engineering variables that influence the stent characteristics, biocompatibility, and outcome (Figs. 12.1, 12.2):

- Mechanism of expansion (self-expanding or balloon-expandable)
- Materials (stainless steel, cobalt-based alloy, tantalum, nitinol, inert coating, active coating, or biodegradable)
- Forms (sheet, wire, or tube)

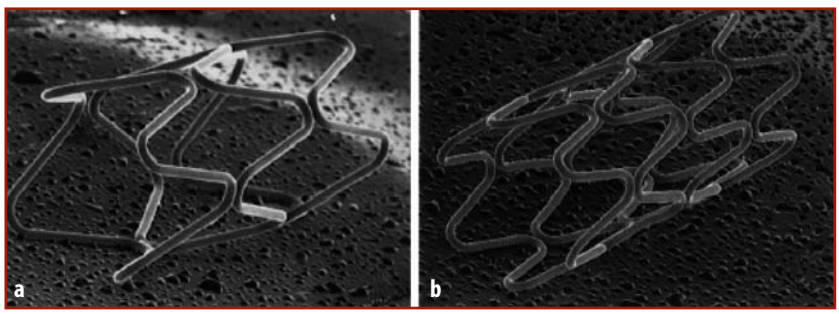

Fig. 12.1. Scanning electron micrographs (magnification ×18) showing stents of (**a**) 8-strut and (**b**) 12-strut design after balloon expansion. Reproduced with permission from Sangiorgi G. et al (2007)

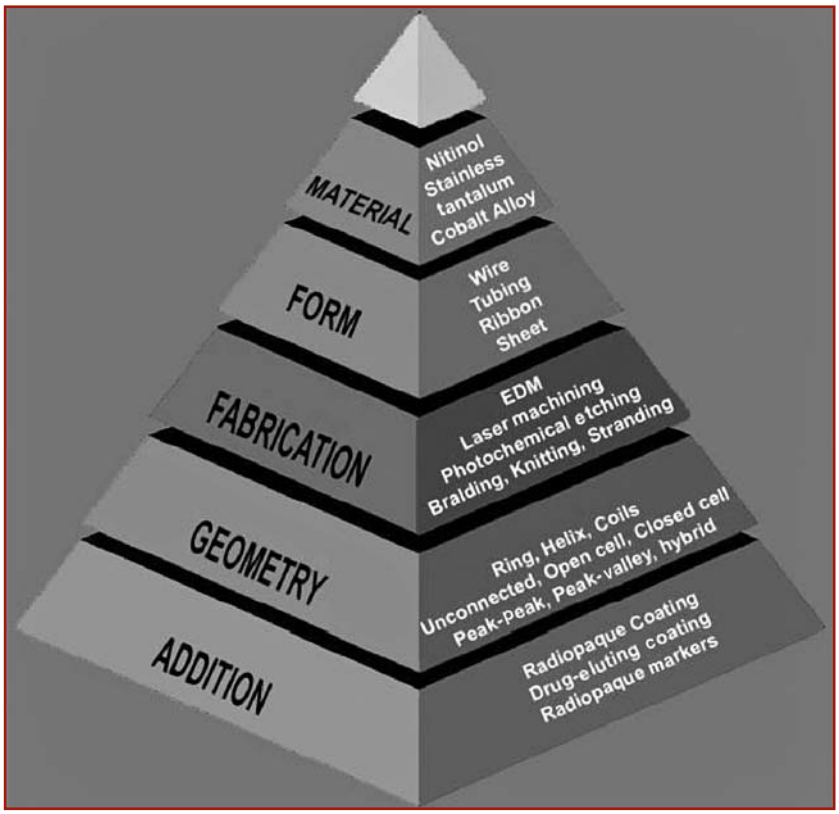

Fig. 12.2. Stent-design pyramid showing different materials and construction characteristics. Reproduced from Garasic J.M. et al (2000)

- Manufacturing methods (laser-cut, water-jet cutting, photo-etching, etc.)
- Geometrical configurations/design (mesh structure, coil, slotted tube, ring, multi-design, or custom design)
- Addition to stent (grafts, radio-opaque markers, coatings, etc.)

Mechanism of Stent Expansion

Balloon-expandable stents are made from materials that can be plastically deformed through the inflation of a balloon; after the balloon is deflated, the stent remains in its expanded shape, except for a slight recoil caused by the elastic portion of the deformation. Self-expanding stents, by contrast, are manufactured in the expanded shape, then compressed and constrained in a delivery system. Upon their release from the delivery system, they spring back, i.e., self-expand, to the pre-set diameter. Indeed, this characteristic of a self-expandable stent can be used when metallic struts are needed to cover a soft plaque, in which case a larger stent can be chosen that will not fully expand in the vessel but will remain compacted among the different cells, producing more lesion coverage.

Materials

Materials for metallic balloon-expandable or self-expanding stents must exhibit excellent corrosion resistance and biocompatibility (Table 12.1); they should be adequately radio-opaque, and create minimal artifacts during magnetic resonance imaging (MRI). For balloon-expandable stents, the ideal material for construction should have a low yield stress (to make it deformable at manageable balloon pressures), high elastic modulus (for minimal recoil), and become hardened following expansion, thus being of high strength.

The most widely used material for balloon-expandable stents is stainless steel, typically 316L, a particularly easily deformable material with low carbon content and additions of molybdenum and niobium. Alternative materials for balloon-expandable stents are tantalum, platinum alloys, niobium alloys, and cobalt alloys. Their advantages are better radio-opacity, higher strength, improved corrosion resistance, and better MRI compatibility.

For self-expanding stents, the ideal material should have a low elastic modulus and a high yield stress for large elastic strains. Currently, the most widely used material is nitinol, a nickel-titanium alloy that can recover from an elastic deformation of up to 10%. This unusually wide elastic range, commonly known as super-elasticity, is the result of a thermo-elastic martensitic transformation.

Raw Material

Stents can be made from sheet, wire (round or flat), or tubing. The latter two account for a large majority of balloon-expandable and self-expanding stents. Stents made from sheet metal have to be rolled into a tubular configuration after the pattern has been created.

Fabrication Methods

The choice of fabrication method depends mainly on the raw material used. Wires can be formed into stents in various ways using conventional wire-forming techniques, such as coiling, braiding, or knitting. The simplest shape for a wire stent is a coil. All coil stents marketed today are balloon-expandable. Wire-mesh stents (such as the self-expanding Wallstent, Boston Scientific, Natick MA) and the coil stent (such as the old Gianturco-Roubin Flex/GR-II, Cook, Bloomington IN; and the Wiktor, Medtronic, Minneapolis MN) have been shown to have a high propensity for thrombosis and re-stenosis and are thus no longer used by cardiologists for coronary interventions.

The vast majority of coronary stents, and probably the majority of peripheral vascular stents, are produced by laser cutting from tubing, typically, Nd:YAG lasers. Balloon-expandable stents are cut in a crimped or near-crimped condition, and only require post-cutting deburring and surface treatment, typically electropolishing.

Self-expanding nitinol stents can be cut either in the ‘small’ configuration, requiring post-cutting expansion and shape-setting, or in the expanded condition.

Table 12.1. Overview of materials used in balloon-expandable and self-expandable stent manufacture, different stent forms, stent fabrication, stent geometry, and additions. Reproduced with permission from Sangiorgi G. et al (2007)

Materials	Balloon-expandable stents	• Stainless steel 316L (vast majority) • Tantalum • Martensitic nitinol • Platinum iridium • Polymers • Niobium alloy • Cobalt alloy	
	Self-expanding stents	• Super-elastic • Nickel-titanium • Nitinol (majority) • Cobalt alloy) • Full hard (stainless steel)	
Form	Wire	• Wallstent (cobalt alloy) • Bridge, S7, S660, (stainless steel, welded rings) • Angiostent (platinum iridium) • Strecker (tantalum) • Expander (nitinol)	
	Tube	• (Vast majority)	
	Sheet	• NIR (stainless steel) • ZR1 (stainless steel) • GRII (stainless steel) • Endotex (nitinol)	
	Ribbon	• Horizon Prostatic (nitinol) • EndoCoil, Esophacoil (nitinol)	
Fabrication	Laser-cutting	• (Vast majority)	
	Photochemical etching	• NIR • Nitinol sheet • Coiled nitinol framework, ePTFE covering	
	Brading	• Wallstent (cobalt alloy)	
	Knitting	• Streaker (tantalum)	
	Vapor deposition		
	Water jet	• SCS, SCS-Z stent	
	Helical spiral	• Periodic peak-to-peak connections • No/minimal connections • Axial spine • Integral with graft	
	Woven	• Braided • Knitted	
	Individual rings		
Stent geometry Slotted tube/coil	Sequential rings	Open cells	• Peak-to-peak connections • Peak-to-valley connections • Midstruts connections • Hybrids • Other
		Closed cells	• Regular peak-to-peak connection • Non-flex connector • Flex connector • Combined connector • Hybrid
		Coil	
Additions	Covering	• WallGraft; coiled nitinol framework, ePTFE covering	
	Radio-opaque markers	• Tabs (tantalum end, gold end, platinum within strut) • Sleeve (gold, platinum) • Welded (tantalum)	
	Radio-opaque coating	• Gold, silicone carbide over gold	
	Biocompatibility coatings	• Tantalum coating, phosphorylcholine, carbon coating, silicone carbide	
	Drug-eluting coating	• Rapamicyn, paclitaxel	

In either case, they have to be deburred and polished. A cutting method that does not produce a heat-affected zone is water-jet cutting, in which a focused jet of water and an abrasive additive is used instead of a laser beam to cut the pattern. Another interesting manufacturing method is photochemical etching.

Geometry

Early designs were generally classified as having either slotted-tube geometries, such as the Palmaz stents, or coil geometries, such as the Gianturco-Roubin Flex stent. While the former had excellent radial strength, they lacked flexibility. The opposite was the case for coil designs. The subsequent evolution of stent design led to the development of a wide variety of stent geometries, which can be classified into five main categories: coil, helical spiral or woven individual rings, or sequential rings.

Closed Cell

In sequential ring construction, all internal inflection points of the structural members are connected by bridging elements. This condition is typically only possible with regular peak-to-peak connections (Fig. 12.3). The primary advantages of closed-cell designs are optimal scaffolding and a uniform surface, regardless of the degree of bending. However, these advantages result in a structure that is typically less flexible than that conferred by a similar open-cell design.

Open Cell

In this type of construction, some or all the internal inflection points of the structural members are not connected by bridging elements. The unconnected structural elements contribute to longitudinal flexibility (Fig. 12.4). Periodically connected peak-to-peak designs are common among self-expanding stents, such as the SMART stent, and balloon-expandable stents, such as the AVE S7.

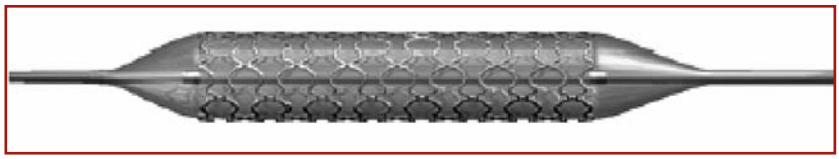

Fig. 12.3. The Skylor is a balloon-expandable cobalt-chromium stent characterized by a closed cell and thin struts pre-mounted on a rapid-exchange-type balloon catheter. Reproduced from Koolen J.J. et al (2007), with permission from Blackwell Publishing

Fig. 12.4. Coroflex Blue™, with its open-cell design, represents a new-generation cobalt-chromium stent endowed with characteristics of high flexibility and thin struts (65 μm). Reproduced with permission from B. Braun Melsungen AG, Germany

Coatings

Several active compounds have been used to cover stents in order to increase their biocompatibility, thereby enhancing their safety and effectiveness. Among the different compounds tested, heparin was one of the first, reducing the coagulation cascade (and thus possibly the thrombogenic risk) after the deployment of a stent. Other coatings, such as phosphorylcholine and silicon-carbide, have been used in order to reduce platelet activation and interaction, with the goal of limiting platelet adhesion to the stent struts during the acute phase of stent re-endothelialization.

Passive coverage also has been shown to be useful. Indeed, covered stents have been created in which a polytetrafluoroethylene (PTFE) layer was placed between two stents (Jostent graft, Jomed) or one stent was covered by an inner and an outer layer of PTFE (Symbiot, Boston Scientific).

Additions

Radio-Opacity Enhancements

To improve the X-ray visibility of stents made from stainless steel or nitinol, gold, platinum, or tantalum markers are added to the stent struts. Electroplating (with gold) is another option, albeit it may induce an inflammatory reaction of the vessel wall.

Drugs

The combination of highly refined metallic stent designs and polymer materials has been the standard approach in several drug-eluting stent (DES) initiatives. Stent-based drug delivery has been accomplished by three distinct mechanisms:

- Bio-absorbable polymeric stents can be loaded with a drug that is eluted slowly over time.
- Metal stents can have a drug bound to their surfaces or embedded within macroscopic fenestrations or microscopic nanopores, thus providing more rapid drug delivery.
- Metal stents coated with an outer layer of polymer (bio-absorbable or non-bio-absorbable) can be drug-loaded, thus providing more controlled and sustained drug delivery and, consequently, more effective drug-tissue interactions.

Recent experimental data suggest that stent-strut configuration directly determines the pattern and degree of drug delivery achieved by the stent. Therefore, maintenance of regular strut spacing despite expansion of the stent under various anatomic circumstances will result in the most regular and predictable drug delivery. For DESs in which the drugs have wide toxic-to-therapeutic ratios, such as those loaded with members of the sirolimus family (e.g., the sirolimus-eluting Cypherstent; Cordis, Johnson & Johnson, Miami Lakes, FL), the regularity of strut spacing might be less important and adequate drug doses can be applied to the stent surface so that, despite broad variability in the delivery location, an adequate dose is uniformly released. For DESs containing drugs with narrower toxic-to-therapeutic ratios (e.g., the paclitaxel-eluting Taxus; Boston Scientific) (Fig. 12.5), inadequate dosing may occur at sites where the stent struts lie far apart and over-therapeutic or toxic dosing at sites where the struts bunch together, owing to vessel curvature or asymmetric expansion.

While Cypher has a closed-cell design, Taxus has a tandem architecture that features neither a closed- nor an open-cell design; instead, there are intervals with a shorter or longer axis to increase radial force. Both stents have inert and non-erodible polymeric coatings. The Endeavor stent (Medtronic, Minneapolis, MN) uses the non-erodible polymer phosphorylcholine to release the sirolimus analogue ABT-578; it is the first DES in which a non-stainless steel alloy serves as the foundation for a polymer-coated DES, i.e., the thin-strut cobalt-chromium alloy (Driver).

The platform of the Xience V stent (7) is a L-605 cobalt chromium (CoCr) balloon-expandable stent that is remarkably similar to its successful bare-metal stent (BMS) equivalent, the Multi-Link Vision (Abbott Laboratories), whose

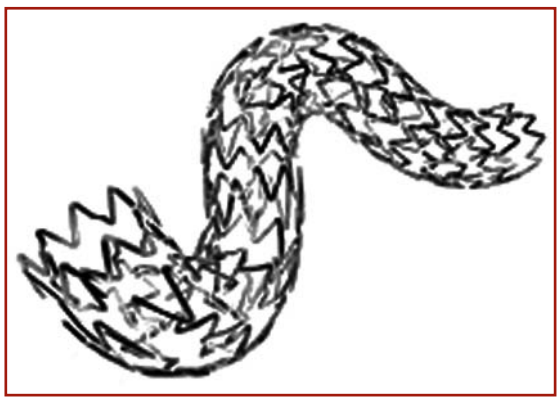

Fig. 12.5. Taxus (paclitaxel-eluting) stent from Boston Scientific (Genoa, Italy). Reproduced with permission

main characteristics are low strut thickness, high flexibility and deliverability, acceptable compliance, recoil, and overall good radio-opacity. Everolimus (Certican, Novartis, Basel, Switzerland) is a sirolimus analogue and it has a useful role in the prevention of allograft rejection after organ transplantation. With its potent suppression of reactive neointimal ingrowth, this drug has been shown to significantly reduce neointimal proliferation. The polymer coating in the Xience V stent is formed by two layers, a primer and a drug reservoir, and by two polymers, an acrylic polymer and a fluoropolymer. A 5- to 6-μm thick layer of everolimus-polymer matrix is applied to the surface of the stent and is loaded with 100 μg of everolimus per cm^2 of stent surface area with no top-coat polymer layer. The safety profile of the Xience V stent has been to date quite satisfactory, despite the duration of dual anti-platelet therapy being limited to the conventional 3–6 months. Specifically, 3-year data from the SPIRIT I trial demonstrated no significant increase in major adverse cardiac events or late stent thrombosis in patients treated with Xience V. Similarly favorable results have been reported from the SPIRIT II (one patient had late stent thrombosis by 6 months in each group) and SPIRIT III (stent thrombosis rates at 270 days 0.5% for Xience V vs. 0% for Taxus) trials. Late incomplete apposition (i.e., stent malapposition), a phenomenon potentially associated with late stent thrombosis, was similarly uncommon with either Xience V or Taxus in the SPIRIT II and III trials.

Impact of Stent Design on Clinical Outcome

Acute Outcome

Lesion-related (vessel diameter and length, ostial or bifurcational position, implantation technique, IVUS guidance), and patient-related (diabetes, clinical presentation) variables are major determinants of acute, sub-acute, and long-term clinical outcomes. Although the immediate performance of the stent may be improved by increasing strut thickness (which increases radio-opacity, radial strength, and arterial-wall support) excessive strut thickness may impart more vascular injury, trigger more intimal hyperplasia, and engender a higher risk for re-stenosis than thinner struts. In recent years, active-drug coating (e.g., with sirolimus or paclitaxel) has emerged as a major determinant in the reduction of angiographic re-stenosis and repeated re-vascularization of the target lesion. The choice of a particular type of stent design is mainly influenced by the specific familiarity of the surgeon with one device or another, and by the potential performance of that device in a specific lesion. Indeed, as different lesions behave in different ways after stent deployment, each type of lesion may require treatment with a different stent. For example, tortuous lesions necessitate the use of particularly conformable and flexible stents, while in ostial lesions stents with strong radial support and good radiologic visibility are often preferred. For bifurcation lesions, the possibility to rewire the side branch through the stent struts after stent deployment in the main branch is a major factor determining a good result, while chronic total occlusions constitute a subset of lesions in which good lesion coverage and favorable radial support are important. Furthermore, small vessels require stents with good flexibility, very thin strut structure, and a good trackability in the case of very distal lesions.

The most threatening acute complication of a stenting procedure, stent thrombosis, has been reduced to <1–2% (compared to 5-7% in the initial trials) due to the introduction of high-pressure deployment of the device and double anti-platelet therapy. However, there are substantial differences in the hemodynamic and wall rheological characteristics of implanted stents of different designs; accordingly, the "hydrodynamic compatibility" of a stent is now recognized as an important feature of ideal stent design.

Long-Term Outcome

The wire-mesh stent, e.g., the self-expanding Wallstent (Boston Scientific), and the coil stent, e.g., the old Gianturco-Roubin Flex/GR-II (Cook) and Wiktor (Medtronic) stents, have been shown to have a high propensity for thrombosis and re-stenosis, because of the high metal to surface area ratio of the former and the high degree of elastic recoil (associated with poor radial strength) and tissue prolapse of the latter. Other stent designs, such as the tubular stent [e.g., the Palmaz-Schatz (Johnson & Johnson, NIR, Boston Scientific) and Crown (Cordis, Johnson & Johnson) stents] and the multicellular model (Multi-Link, Guidant, Boston Scientific), have been shown to attain better results than the wire-mesh and coil stents. However, none of these stents are still used in clinical practice.

The immediate performance of the stent may be improved by increasing strut thickness (which increases radiovisibility, radial strength, and arterial-wall support); however, excessive strut thickness triggers more intimal hyperplasia, and engenders a higher risk for re-stenosis than thinner struts. Clinical studies confirm this direct relationship between strut thickness and arterial-wall reaction. In the ISAR-STEREO-2 trial, the ACS RX Multi-Link stent (Guidant, Advanced Cardiovascular Systems), with 0.05-mm struts, elicited less angiographic and clinical re-stenosis than the BX Velocity stent (Cordis, Johnson & Johnson), with a strut thickness of 0.14 mm.

The ideal DES should have a large surface area of contact with the vascular wall, minimal inter-filament gaps, robust radial support, and symmetrical expansion to ensure uniform drug elution. At the same time, it needs to be slim, flexible, and conformable to enable successful deployment in complex lesions. The potential for long-term adverse effects of the synthetic polymers often used as carriers for anti-mitotic drugs is a major concern. Synthetic polymers may induce an enhanced inflammatory reaction and, possibly, a pro-thrombotic response. Late stent thrombosis, late stent apposition, and coronary aneurysm are thus real possibilities.

Stent Coating

Stents with an active coating of gold, a highly radiovisible and biocompatible material, have been demonstrated to be inferior to plain stainless steel stents in four randomized trials. A higher rate of stent thrombosis and re-stenosis rate was observed with gold-coated stents than with BMS in all trials. Coating stents with silicon carbide, a potentially less thrombogenic and more compatible material

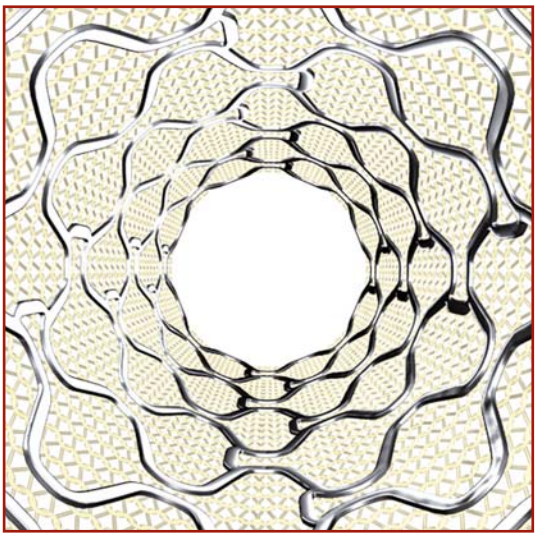

Fig. 12.6. A 3D view of MGuard™ Coronary Stent System (Inspire-MD, Tel-Aviv, Israel). MGuard is a bare metal stent with an ultra-thin PET sleeve designed to protect against an embolic shower during and post-procedure

than stainless steel, also did not improve angiographic and clinical outcomes compared with BMS in two recent randomized trials. Other randomized trials showed similar results with phosphorylcholine- and heparin-coating. Indeed, in all these studies there was no angiographic or clinical benefit compared to BMS.

Passive coverage of stents with PTFE has been assessed in the treatment of degenerated saphenous vein grafts containing a considerable amount of friable athero-thrombotic material. Other useful indications for PTFE-covered stents are coronary aneurysm exclusion and coronary perforation. The MGuard coronary stent (Inspire-MD, Tel-Aviv, Israel) is designed to protect against a post-procedural embolic shower (Fig. 12.16). This device presents a novel combination of a coronary stent and an embolic protection device. The latter consists of an ultra-thin polymer mesh protective sleeve that is wrapped around the stent and anchored to the external surface of the stent. The sleeve is composed of a micron-level-fiber knitted mesh, designed for flexibility while retaining the strength characteristics of the fiber material. In ongoing clinical trials conducted in Germany and Brazil, interim results have shown a procedural success rate of 100% and no report of any major adverse cardiac events. To date, the MGuard coronary stent has shown safety in human coronary and vein graft indications.

Drug Elution

Stent implantation was developed to overcome the acute recoil and high re-stenosis rate of balloon angioplasty, but resulted in the development of chronic in-stent re-stenosis related to specific factors regarding patient, stent, lesion, and procedural characteristics. Some factors are not modifiable, such as patient and lesion characteristics, whereas procedural characteristics may be improved by better implantation technique and stent design. DESs are a novel approach in stent technology and design in which local drug delivery is aimed

at inhibiting intimal thickening by interfering with the pathways involved in inflammation, migration, proliferation, and/or secretion of the extracellular matrix. The breakthrough appearance of stents eluting anti-proliferative drugs with or without a carrier polymer has recently produced unparalleled results, with an overall reduction in the re-stenosis rate of 70–85% and in major adverse cardiac events of about 60% compared with BMS. The overall occurrence of re-stenosis and target lesion revascularization is < 10%.

Both the drug and the delivery vehicle must fulfill pharmacologic, pharmacokinetic, and mechanical requirements. Current successful DESs require a polymer coating for drug delivery. Clinical trials examining several pharmaceutical agents, particularly sirolimus and paclitaxel, have demonstrated a marked reduction in re-stenosis following stenting. Sirolimus is a natural macrocyclic lactone and paclitaxel is a cytotoxic agent effective against many tumors. Both compounds block cell-cycle progression and thus inhibit the proliferation of smooth muscle cells. The ideal drug to prevent re-stenosis must have an anti-proliferative and anti-migratory effect on smooth muscle cells but must also enhance re-endothelialization, in order to prevent late thrombosis. Additionally, it should effectively inhibit the anti-inflammatory response after balloon-induced arterial injury. Stents eluting sirolimus, paclitaxel, and, more recently, ABT-578 and everolimus are commercially available, but ongoing research and clinical trials will result in new stents, with novel designs and loaded with a variety of compounds, coming to market. Further improvements, including expansion of drug-loading capacity, coatings with programmable pharmacokinetic capacity, and the discovery of new drugs, will further enhance the efficacy and safety of these stents. Although DESs have significantly reduced the angiographic re-stenosis rate and improved clinical outcome, late thrombosis and re-stenosis remain an important subject of ongoing research. Synthetic or biological polymers can be used as matrixes for drug incorporation, but concerns have been raised regarding biocompatibility, sterility, or the potential induction of inflammation. Currently, alterations on stent-backbone design (biodegradable, bioabsorbable, nanoporous, etc.) are being explored.

Bioabsorbable and Biocompatible Stents

There is an emerging safety concern regarding the risk of stent thrombosis associated with DES implantation. The clinical and angiographic predictors are represented by the discontinuation of dual anti-platelet therapy, minimal lumen diameter (MLD, mm), stent under-expansion, stent malapposition (either after stent implantation or at follow-up as a result of positive remodelling), stent length, residual untreated dissections, geographic miss of the diseased vessel, left ventricular dysfunction, diabetes mellitus, age, acute coronary syndrome, chronic renal insufficiency, bifurcations, and in-stent re-stenosis.

Promising results have arisen with DESs designed with biodegradable polymer technologies. In addition, an attractive alternative is certainly represented by the bioabsorbable stents; however, it remains to be determined whether this technology will address the issues of delayed endothelialization and late thrombosis, re-stenosis at the edges, unavoidable inflammatory reac-

tion, and impaired vessel healing, all of which are normally encountered after stent implantation.

Novel materials used as stent coatings include biocompatible though not biodegradable phosphorylcholine, a natural component of the cell membrane, and biodegradable polylactic acid (PLA) and poly (lactic-co-glycolic acid (PLGA). The latter two are fully metabolized to water and carbon dioxide, leaving in situ a BMS after the active compound is released. Promising results have been reported in the CREATE and CURAMI trials on three different stainless steel stents covered with PLA and sirolimus (Table 12.2).

Biolimus A9, a potent rapamycin derivative, has been evaluated in two PLA-coated stainless steel stents: the Biomatrix (Biosensors International, Singapore) and the Nobori (Terumo, Japan). In the Nobori study, at 9-month angiographic follow-up there was a benefit for Nobori over Taxus in terms of in-stent late lumen loss (0.11±0.50 vs. 0.32±0.50 mm, $p < 0.001$) and binary re-stenosis (0.4 vs. 4.6%, $p = 0.01$). At 2-year-follow-up, there were no significant differences between the two study groups in the incidence of ARC-defined stent thrombosis, (0% for Nobori vs. 2.4% for Taxus).

Tacrolimus is a macrolide that decreases the expression of pro-inflammatory cytokines (e.g., interleukin-2) and suppresses T-cell proliferation. It has a preferential effect on smooth muscle cells and does not enhance the expression of tissue factor. A cobalt chromium stent containing a PLGA

Table 12.2. Novel biodegradable and biocompatible stents. Reprinted by permission of Edizioni Minerva from Minerva Cardioangiol, Rogacka R. et al (2008)

	Stent name	DES/BMS	Active drug	Stent platform	Manufacturer	Study
Biodegradable/biocompatible polymer						
PLA	Exel	DES	Sirolimus	SS	JW Medical Systems	CREATE
	Cura	DES	Sirolimus	SS	Orbus Neich	CURAMI
	Supralimus	DESSupralimus	Supralimus	Matrix SS	Sahajanand	PAINT
	Infinnium	DES	Placlitaxel	Matrix SS	Sahajanand	PAINT
	Biomatrix	DES	Biolimus A9	SS	Biosensors Int.	UI
	Nobori	DES	Biolimus A9	SS	Terumo	NOBORI
	S-stent	DES	Biolimus A9	SS	Biosensors	
PLGA	CoStar	DES	Paclitaxel	SS	Conor Medsystems	
	Mahoroba	DES	Tacrolimus	CoCr	Keneka	UI
	SymBio	DES	Pimecrolimus+ Paclitaxel	SS	Conor Medsystems	UI
	Synchronnium	DES	Sirolimus+ heparin	SS	Sahajanand	UI
No polymer	Tinox	BMS		SS+Ti/NO alloy		TiNOX
	Nanoporous AlO	DES	Tacrolimus	SS+AlO		UI
	Nanoporous hydroxyapetite	BMS		SS		UI
Biodegradable platform						
No PDLLA	Igaki-Tamai	BMS	Self-expandible	PLLA	Igaki Medical Planning	
	Absorb	DES	Everolimus	PLLA	Abbott	ABSORB
	Dreams	DES	Pimecrolimus	Mg	Biotronik	UI
PDTECI	REVA	DES	Paclitaxel	Tyrosine poly-carbonate	REVA	RESORB

polymer that releases tacrolimus (Mahoroba, Kaneka, Japan) and the association in another stent of its analogue pimecrolimus with paclitaxel (SymBio, Conor Medsystems, Menlo Prak, California) are currently under investigation. The Synchronnium stent (Sahajanand Medical Technologies, India) incorporates sirolimus and heparin, with the goal of decreasing thrombogenicity.

Modern technologies have also made use of the well-known properties of flavonoids. A combination of genistein, a natural isoflavonoid phytoestrogen that inhibits collagen-induced platelet aggregation, and sirolimus is delivered by heparinized biodegradable polymers (PLA, PLGA, and polyvinyl pyrrolidone) in the Coronnium stent platform. This design is currently being tested.

Polymer-Free Solutions

Data on the possible pro-thrombotic effect, by delayed endothelial healing, of the permanent polymers of the first generation of DESs, has forced research into new stent platforms into two directions: the development of biocompatible polymers and of modern stent platforms that do not include polymer coating. In a randomized trial examining the titanium – nitric – oxide-coated stent *(TiNOX)*, 92 patients received TiNOX stent or a BMS of identical design. Quantitative coronary angiography at 6 months revealed lower late loss (0.55 ± 0.63 vs. 0.90 ± 0.76 mm, $p = 0.03$) and percent diameter stenosis (26 ± 17% vs. 36 ± 24%, $p = 0.04$) in lesions treated with TiNOX-coated than control stents. Binary re-stenosis was reduced from 33% in the control group to 15% in the TiNOX stent group ($p = 0.07$).

To avoid application of a polymer, micro- and nanoporous stent platforms have been designed with the aim of allowing impregnation with active drug, thus customizing drug doses and/or combinations of different drugs. Nanoporous hydroxyapetite (a biocompatible crystalline derivative of calcium phosphate) coating is currently under investigation.

Biodegradable Platforms

Fully degradable stents represent an attractive alternative to stents with a novel polymer coating. However, important characteristics need to be fulfilled in order to meet the expectations of modern interventional cardiology, such as the ability of controlled, sustained drug release and sufficient mechanical strength to prevent negative vessel re-modeling and avoid stent deformity/strut fractures. Late positive re-modeling with vessel expansion associated with a not fully endothelialized or malapposed stent would no longer be a problem if that stent could dissolve as the vessel remodeled. The major theoretical advantage of this type of stent should hopefully be a lower risk of stent thrombosis and subsequently the possibility to eliminate prolonged dual anti-platelet therapy. In addition, vasomotion is restored after stent degradation, which may be an advantage in case of the necessity for repeat percutaneous or surgical re-vascularization.

In 2000, Tamai et al. published the first data on a fully degradable PLLA Igaki-Tamai stent (Igaki Medical Planning, Japan). The 6-month results of 15 patients treated with 25 stents confirmed the safety and feasibility of this device.

Tyrosine-Derived Polycarbonate

Another device currently under investigation is the REVA stent (REVA Medical, San Diego, CA). This radio-opaque stent has a unique structure that allows it to expand in the artery with sliding, locking parts rather than through material deformation. The preliminary data from animal studies were presented at the Scientific Sessions of Cardiovascular Revascularization Therapeutics (CRT) Congress in 2007. Due to its "slide and lock" design, the REVA stent is characterized by a steel-like performance with low acute recoil (< 1%) and high radial strength. The unique chemistry of the polymer platform allows adjustable degradation over 7–12 months. At 1 month, complete endothelialization of the stent was observed and no thrombotic events occurred. These preliminary data are to be confirmed in the ongoing "REVA Endovascular Study of a Bioresorbable Coronary Stent" (RESORB). The first patients were recently enrolled in the two study sites in Germany and Brazil.

Magnesium Alloy

An absorbable metal stent (AMS, Biotronik, Bülach, Switzerland) composed of a magnesium alloy is a promising alternative to polymer platforms. Dissimilar to traditional metallic stents, it is completely radiolucent, with two radio-opaque markers at its ends, and erodes completely in 30–60 days. The results of the First in Man study, with non-drug-eluting AMS, were disappointing. In the "Biotronik Absorbable Metal Stent Below the Knee" (BEST-BTK) trial, the rate of re-stenosis in peripheral arteries was approximately 50%.

Conclusion

Although stents are currently considered the gold standard for the treatment of narrowed coronary arteries, there is experimental and clinical evidence to indicate that "a stent is not just a stent." Different stent models have different structural properties, with their own inherent advantages. Tubular or corrugated stents are better than coil or wire-mesh stents, in terms of a better acute and mid-term outcome. Stents with thinner struts and lower metal density yield a lower risk of re-stenosis than stents with thicker struts and should be used for high-risk lesions, such as those located in small vessels, where the risk of re-stenosis is often magnified. The availability of new, highly biocompatible, and more radiovisible alloys with the same if not superior tensile strength as stainless steel will enable the production of low metal density stents that may further improve the anatomic and clinical outcomes obtained with current stainless steel stents. Furthermore, stents

coated with anti-proliferative agents, in particular sirolimus and paclitaxel, have opened a new era in interventional cardiology. The re-stenosis rates of these stents are unrivaled by other BMS models. However, several important questions regarding their cost-effectiveness, long-term safety, and durability need to be addressed in order to clearly understand their potential impact on daily practice. Moreover, as these devices may be unsuccessful, an understanding of the causes of their failures and of their different performances in various anatomic and biochemical settings becomes of pivotal importance. As scientists and companies continue to develop new types of stents containing different anti-proliferative drugs, it is entirely foreseeable that most interventional procedures will eventually involve DESs – containing sirolimus, paclitaxel-or even more effective drugs with both anti-mitotic and anti-thrombotic actions – impregnated onto highly biocompatible carrier vehicles and mounted onto a stent design with uniform expansion and with programmable, controllable drug-eluting capability. It is also possible that a co-action of different drugs, i.e., a paclitaxel-eluting stent and oral rapamycin given systemically, may further improve the clinical outcome in terms of re-stenosis. Finally, new stent platforms, such as biodegradable stents or endothelial progenitor cell capturing stents may soon provide a more "physiologic" answer to stent implantation, thus reducing vascular injury, accelerating vessel healing, and consequently improving clinical outcome. With the wide variety of devices currently under investigation and the prompt response of the industry to the requests of interventional cardiologists looking for their "Holy Grail", the road to finding the "ideal stent" may gradually becoming shorter.

13

CT Angiography of Coronary Stents

Marcello De Santis, Paolo Pavone

Coronary stenting is the most widely used non-surgical coronary re-vascularization procedure (537,000 interventional procedures in the USA in 2002) and completes the dilatation performed during angioplasty. Despite the use of newer and more sophisticated stents and drug-eluting stents, the risk of long term re-stenosis arising from in-stent development of neointimal hyperplasia is high, varying between 4 and 40%. This high incidence justifies the use of diagnostic procedures to re-evaluate the stent in follow-up examinations.

Non-invasive monitoring can be achieved using treadmill ECG testing, echocardiography, and stress tests monitored by nuclear medicine procedures. Of course, in case of a strong suspicion of re-stenosis, catheter coronary angiography is the gold-standard procedure, since, prior to the development of coronary CT angiography (CTA), it was the only technique able to directly evaluate the vessel lumen.

Coronary CTA has been proposed in the non-invasive re-evaluation of stents and re-stenosis: however, the metallic mesh composing the stent wall has the same CT appearance as a highly calcific atherosclerotic plaque, resulting in overestimates of plaque size. This "blooming effect" prohibits the accurate evaluation of the inner lumen–a limitation that is particularly evident in smaller size vessels.

Technological improvements have resulted in better stent imaging. The higher spatial resolution of newer equipment (0.3 mm) is close to that of catheter coronary angiography (0.2 mm), allowing better visualization of the vessel, the stent, and the inner lumen and limiting the number of artifacts. CT devices with more than 64 slices are optimal for these purposes, as they provide more detailed imaging of smaller vessels (Fig. 13.1). Our early experience with 128-row detector CT confirmed the improved evaluation of the inner lumen of the stents, as long as an optimal contrast-agent injection protocol had been used in which the contrast agent thoroughly opacified the coronary lumen, thereby revealing potential intimal hyperplasia along the stent.

P. Pavone, M. Fioranelli, D.A. Dowe, *CT Evaluation of Coronary Artery Disease*.

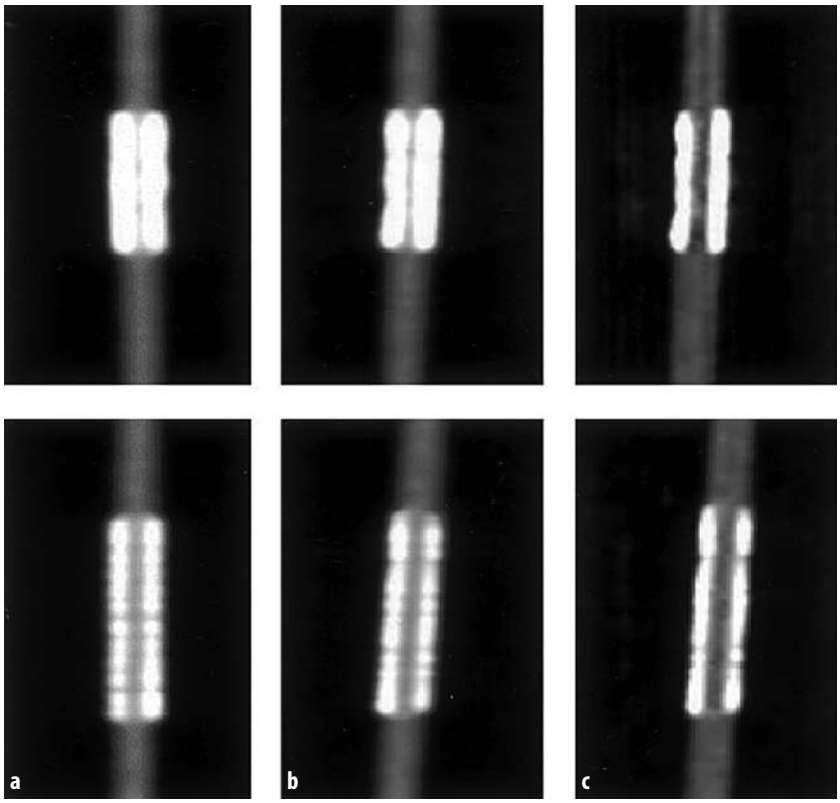

Fig. 13.1 a-c. In vitro images of coronary stents evaluated using CT with 4, 16, and 64 detector rows. An improvement in spatial resolution is obtained using newer and more detailed equipment

In evaluating stents (as well as in the evaluation of densely calcified plaque) it is important to reconstruct coronary images using an intermediate type of filter algorithm. Whereas for native vessels a low filter is used (usually 25–30), stents should be evaluated with higher-level filters. The most appropriate filter and the one routinely employed by radiologist for this purpose has a value of 46 (Fig. 13.2).

Most of the literature reports refer only to the use of 64-row detector CT and there are, as yet, essentially no data available for higher-level equipment (128, 256, 320 rows). According to published data, stents 3 mm in diameter can be well-evaluated. The accuracy for stents ≥ 3 mm or larger is 85% but it drops to as low as 26% for smaller stents. However, these data need to be revised once the results obtained with larger series and using more detailed imaging systems, with a higher spatial resolution, have been obtained. With equipment of higher resolution, only the assessment of very small stents located in distal coronary arteries will remain difficult (Figs. 13.3–13.6).

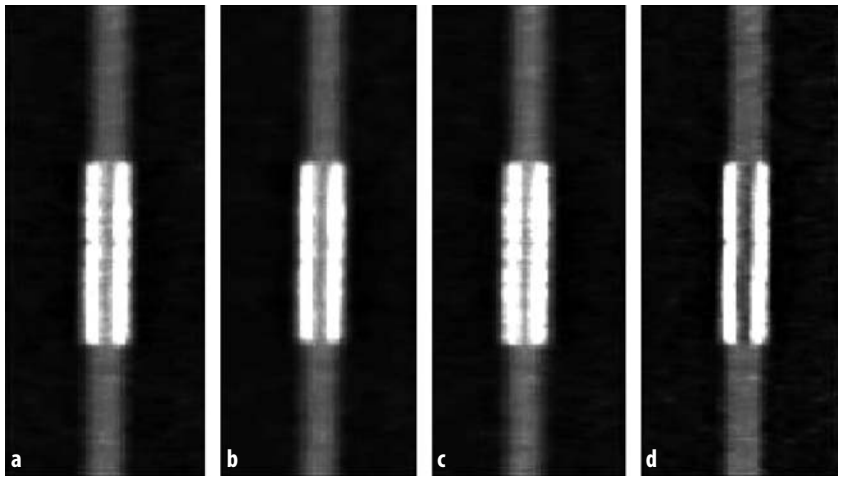

Fig. 13.2 a-d. In vitro images of coronary stents evaluated using different filter algorithms (**a** B20f, **b** B25f, **c** B30f, **d** B64f). Improvement of stent evaluation using filter B 46

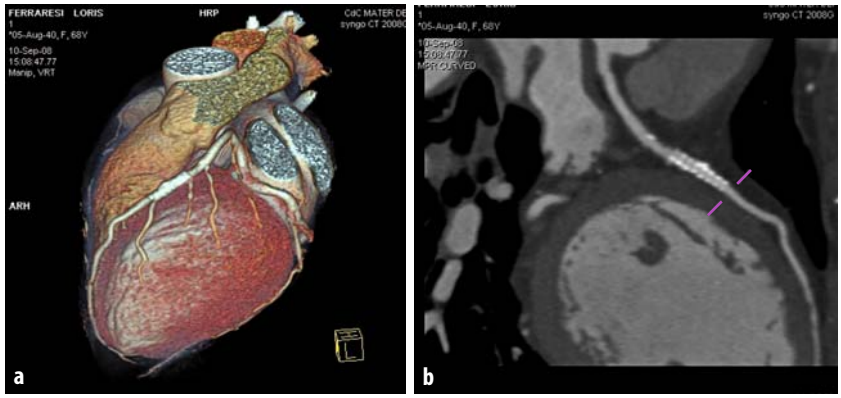

Fig. 13.3 a, b. Stent in the left anterior descending coronary artery. The stent is well evident in the 3D images (**a**). Bi-dimensional evaluation clearly shows stent patency with good evaluation of the contrast-enhanced internal lumen and no evidence of neointimal hyperplasia

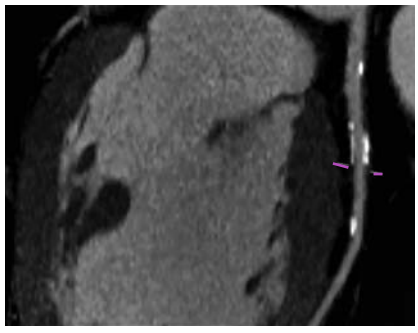

Fig. 13.4. Short stent of the left anterior descending artery. In bi-dimensional evaluation the patent lumen is evident: note the displaced calcified plaque, external to the stent

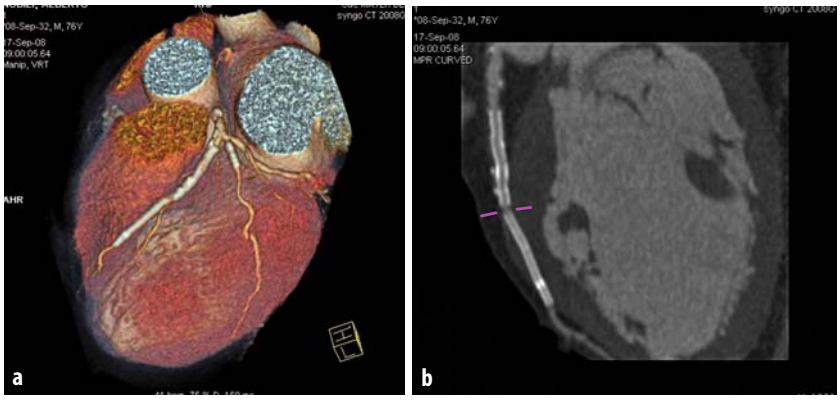

Fig. 13.5 a, b. Two long stents are present in the left anterior descending artery (LAD) and one in an intermediate coronary artery (**a**, 3D evaluation). Bi-dimensional evaluation (**b**) of the LAD shows stent extent and patency. The more distal stent has a smaller caliber and its internal evaluation is made somewhat difficult due to the limited spatial resolution (0.33 mm in the example shown)

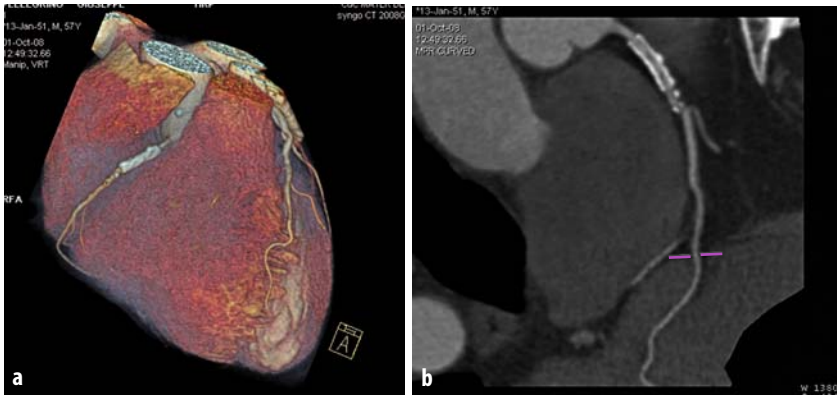

Fig. 13.6 a, b. Stent in the right coronary artery: **a**, 3D evaluation. In bi-dimensional imaging, (**b**) the presence of two darker, hypodense areas in the stent lumen is clearly depicted, leading to the diagnosis of stent re-stenosis due to neointimal hyperplasia

14

X-ray Exposure in Coronary CT Angiography

Paolo Pavone

In coronary CT angiography (CTA), X-ray radiation is delivered through an X-ray tube from which the amount of radiation emitted can be carefully controlled. Recently, the use of X-rays for diagnostic purposes has been the subject of important and renewed attention, with the aim to limit exposure and thus its negative consequences on human health. The potential oncological impact of X-rays is well-known. Earlier generations of radiologists used diagnostic equipment often without the protection that has since become routine. Consequently, they often suffered dermatological problems on their hands as well as an increased frequency of tumors, mostly of the hematopoietic series. In the following, we focus on the unintentional exposure that occurs during a diagnostic evaluations, i.e., for coronary artery disease.

Damage from Ionizing Radiation

The damage induced by ionizing radiation can lead to tumor development. While this is a well-known fact, neither a definitive and consistent cause-effect relationship nor the incidence of tumors induced by exposure to diagnostic examinations can be measured or defined properly. In fact, the low amount of X-rays used in diagnostic examinations cannot have an immediate effect on human tissues (unless there has been continuous exposure, as in repeated and prolonged exposure during cardiac catheterizations). Direct damage by ionizing radiation can, however, be exactly forecasted and documented for therapeutic irradiation in radiotherapy, in the use of nuclear weapons (Hiroshima and Nagasaki), and in the course of unforeseen events at nuclear power stations (Chernobyl). In these cases, the immediate or delayed effect of ionizing radiation can be defined with precision, with more radiosensitive organs, i.e., those with more active metabolism and high cellular turnover, being the most vulnerable.

In the diagnostic use of ionizing radiation, the damage is hypothetical and cannot be evaluated immediately. Brenner and Hall, in a study pub-

P. Pavone, M. Fioranelli, D.A. Dowe, *CT Evaluation of Coronary Artery Disease*.

lished in 2007, concluded that, following the atomic bombing of Hiroshima, approximately 25,000 people who were far from the central area of atomic fall-out were exposed to an amount of radiation similar to that used during diagnostic CT. However, the comparison is not entirely valid, since radiation exposure due to atomic fall-out is continuous in time and involves the entire body uniformly; the exposure during diagnostic CT, by contrast, is controlled, with X-ray exposure of only a limited part of the body (collimated exposure) and for a very short time (in the range of seconds). Thus, such claims have to be evaluated with extreme care, and scientific proof of the damage caused by diagnostic exposure to X-rays remains to be definitively determined.

X-ray Dose During CT

Table 14.1 provides a direct comparison of the X-ray dose used in frequently performed cardiac diagnostic procedures, including coronary CTA, as measured in mSievert (m Sv). Overall, coronary CTA exposes patients to a high dose of X-rays, in the range of 7–13 mSv. In fact, with current procedures, X-rays are emitted throughout cardiac image acquisition, despite the fact that the computer, during image reconstruction, utilizes only a small portion of the data acquired, i.e., those obtained in the telediastolic part of the ECG. Therefore, for clinical purposes, a consistent part of cardiac irradiation is unnecessary and corresponds to an excess X-ray dose of over 80%.

Techniques for Limiting X-ray Exposure in Coronary CT Angiography

New techniques aimed at drastically reducing the amount of X-ray exposure during coronary CTA have recently been proposed. Here, we consider three that have been used successfully proposed.

The first technique is available as part of every type of CT equipment and allows a proportional reduction of X-ray exposure according to the patient's size and weight. The procedure is fully automated and evaluates body thickness and tissue consistency (in terms of X-ray penetration) in order to reduce, slice by slice and moment by moment, the amount of X-rays emitted, in terms of milliamperes. For example, higher doses are required for the abdomen than

Table 14.1. Typical organ radiation dose from various cardiological diagnostic examinations. From Dowe D. Radiological Society of North America (2006)

Procedure	Dose (mSv)
Coronary catheter angiography	6-9
Coronary CTA	7-13
Interventional coronary procedure	20
SPECT Thallium, Persinakis et al (2002)	25,3
SPECT sesta-MIBI, Persinakis et al (2002)	12,2

for the chest, which contains air. This technique reduces unnecessary X-ray exposure by 30–40%. Furthermore, for thinner patients, the radiologist can manually reduce X-ray exposure by reducing the kV values.

In the second, recently proposed technique, X-ray exposure is controlled and it is limited to the telediastolic phase through the use of a prospective gating procedure. In this so-called snap and shoot approach, each data packet, corresponding to an anatomic area containing a thick slice of the heart (4 cm for 64-slice CT), is acquired during an axial rotation of the X-ray tube, with emission only in the telediastolic phase. Immediately afterwards, the table is moved to the next anatomic area and the data are again acquired (the spiral procedure is therefore not used during data acquisition). These steps are repeated four to five times until the entire anatomical area containing the heart has been scanned (Fig. 14.1). This technique reduces the X-ray dose from 15–20 mSv to 2–3 mSv, according to patient configuration. Its one major limitation is that it excludes the use of spiral acquisition and instead requires single axial acquisitions, possibly leading to overlap artifacts in the single thick slices acquired during each telediastolic phase.

An alternative to this technique uses a prospective gating procedure, but rather than obtaining axial slices with stepwise movement of the patient table, it allows spiral acquisition of the data. The X-ray tube continuously emits radiation during the acquisition procedure, but emission is very low during the cardiac cycle (only 4% of the standard emission) and increases to the amount needed for diagnostic imaging only in the telediastolic phase (Fig. 14.2). There are no artifacts arising from the overlap of each thick volume (as in the

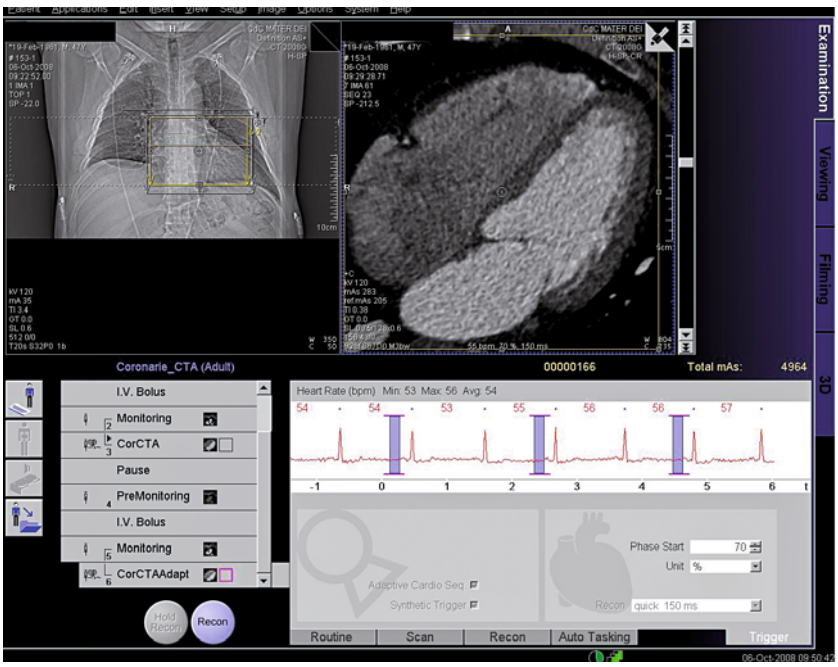

Fig. 14.1. Snap and shoot axial acquisition: X-rays are emitted by the tube only during telediastole (blue stripe in the ECG gating scheme of the console)

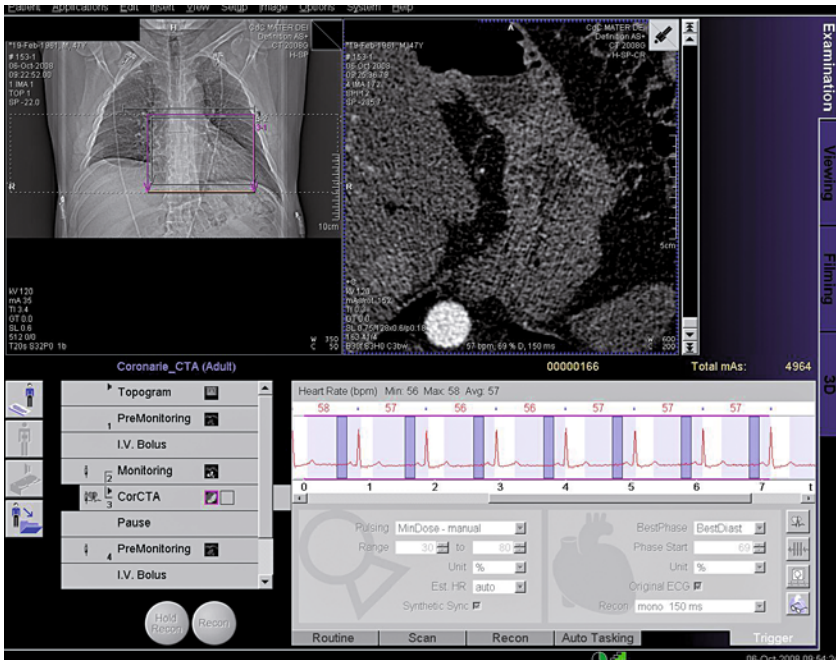

Fig. 14.2. Spiral acquisition with reduced X-ray exposure. During systole, 4% of the radiation dose is emitted, whereas during the time frame when telediastole is expected (light blue area in the scheme) the full dose is emitted. Thus, it is possible to define the width of the area of maximal exposure

previous technique), since the acquisition is fully spiral. A dose reduction of 50–60% has been estimated.

In Fig. 14.3 a case is shown in which, with the patient's consent, a snap and shoot acquisition was followed by a second acquisition using spiral technique with dose reduction. In the three-dimensional and bi-dimensional images, there are no major differences in the image quality and diagnostic evaluation of the coronary arteries. The dose exposure was 2 mSv with snap and shoot and 12 mSv using the spiral procedure.

Large-array detectors, with single-slice acquisition of the entire anatomic area containing the heart, modulate X-ray emission, limiting patient exposure to the telediastolic phase and avoiding overlap-type artifacts in the acquisition of thick volumes.

X-ray Exposure and Patient Age

The damage caused by X-rays is directly related to the age of the patient. In children, the radiosensitivity of growing organs and the fact that exposure has occurred before the patient reaches his or her adult years, together with the fact that he or she will almost inevitably undergo further X ray diagnostic procedures in the future, allow a more definitive cause-effect relationship to be established. Pediatric radiologists are fully aware of this problem and thus

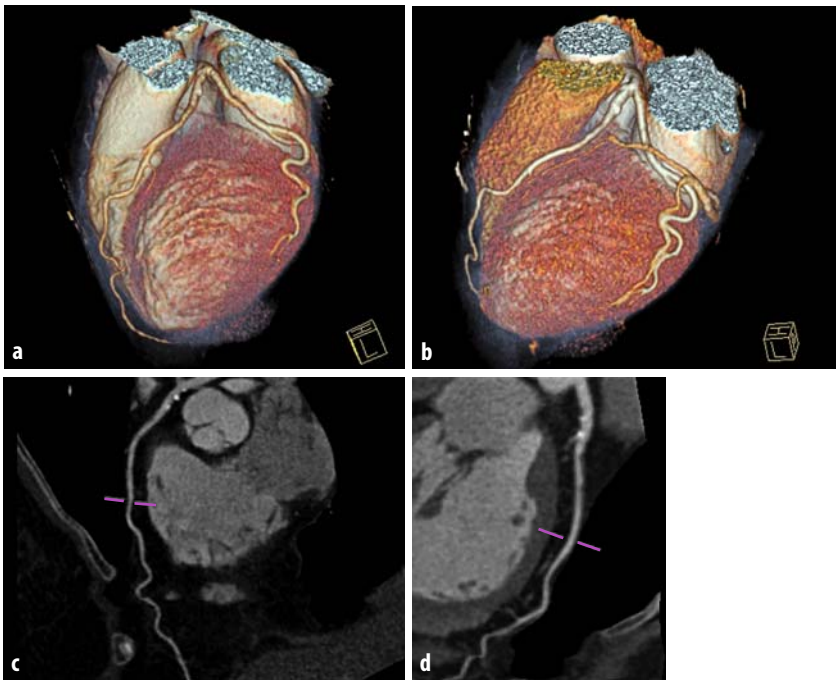

Fig. 14.3 a-d. A 74 -year-old female patient. Data acquisition using (**a, c**) snap and shoot technique (2 mSv exposure) and (**b, d**) spiral acquisition (12 mSv exposure). Image quality is basically the same. **a, b** Three-dimensional volume-rendering image. **c, d** Bi-dimensional images of the same data sets

attempt to use alternative diagnostic procedure, e.g., magnetic resonance imaging and ultrasound.

In elderly patients, damage due to ionizing radiations is statistically less relevant and the statistical incidence of oncological problems is correspondingly lower. In the evaluation of the heart by coronary CTA, only a limited area of the body is exposed and X-ray emission is controlled and collimated, with protection of contiguous anatomic areas through the use of more effective diaphragms, which exclude irradiation of nearby tissues. Thus, in coronary CTA, irradiation is limited to the portion of the lungs surrounding the heart, and, for female patients, the breast tissues. To further reduce unwanted irradiation, bismuth-based mildly radio-opaque breast shields are available.

Conclusion

In considering the relationship between coronary CTA and the tissue damage ensuing from the radiation exposure that is an integral part of this examination, several points must be mentioned:

Firstly, there is the option of using less radiation. Initial techniques employed a high dose of X-ray radiation, with exposures similar to those incurred with cardiac catheterization and nuclear medicine procedures. Nowadays, prospective gating procedures have allowed a dose reduction of

60–80%, resulting in the controlled and limited exposure of a defined anatomic area and to exposure amounts that are similar to those of other current and widely used CT diagnostic procedures.

Secondly, there is the matter of exam repetition. In the USA, patients are frequently and repeatedly exposed to X-rays due to repetitions of diagnostic examinations (this is particularly true in traumatology and oncology). It has been calculated that, during a patient's recovery in the hospital, the total X-ray radiation exposure is 20–40 mSv. CTA, however, is an examination that is performed only once, to evaluate the anatomic status of the coronary arteries. If repetition of the exam is deemed necessary, it will not be until many years later.

Thirdly, the patient's age must be considered. Coronary CTA is indicated for the evaluation of atherosclerotic disease; thus, that the patients are older, usually 55–65 years. In this population, the radiosensitivity of the organs is reduced and the potential oncological risk due to ionizing-radiation exposure is limited if not irrelevant, when careful exposure is performed.

Finally, there are risk-benefit considerations. When proposing CTA to a patient, the cardiologist and the radiologist have to evaluate the benefit that may come from a proper evaluation of the atherosclerotic burden on the coronary arteries, the advantage gained by properly characterizing a plaque in terms of the correct pharmaceutical approach, and the possibility to identify vascular stenosis, which may be amenable to stenting or re-vascularization procedures. Therefore, the proper, limited use of ionizing radiation is to be proposed in the presence of well-defined clinical indications for this procedure.

15

Use of MSCT Scanning in the Emergency-Room Evaluation of Patients with Chest Pain

Giulio Speciale, Vincenzo Pasceri

Acute chest pain is one of the most frequent symptoms reported by patients evaluated in emergency departments. Annually, about 6 million people with acute chest pain visit emergency rooms (ERs) throughout the USA. Diagnosis of an acute coronary syndrome (ACS) is often difficult: studies have suggested that 2–6% of patients with an ACS are inappropriately sent home from the ER, leading to increased morbidity and mortality. This is also an increasing motive for malpractice claims. Protocols for the evaluation of ACS patients include ECG and assessment of markers of myocardial damage (including CK-MB and troponin). Unfortunately, there is a minority of patients with normal ECG and cardiac enzymes at admission who still have ACS. These patients require a time-consuming and expensive protocol, with serial ECG and cardiac-enzyme assessments. Patients with persistently negative results often undergo a stress test, while sometimes additional tests are also performed to rule out other, possibly fatal causes of chest pain (including aortic dissection and lung embolism). Yet, mistakes are still possible even after this complex protocol, which has an estimated annual cost of $10–13 billion in the USA alone. Finally, a large number of patients with no serious disease are held for many hours in the ER, leading to overwork, the need for larger staff, and longer waiting times for other ER patients.

Recently, multi-slice computed tomography (MSCT) scanning was introduced into the diagnostic assessment of acute chest pain in ER patients. The technology is used to obtain an anatomic assessment of the coronary arteries, which may allow a quick diagnosis and early patient discharge. MSCT may also help in identifying patients with other serious conditions, including aortic dissection and lung embolism. In this chapter, we review the current evidence on the use of MSCT scanning in this setting and its pro and cons compared with other widely used diagnostic techniques.

P. Pavone, M. Fioranelli, D.A. Dowe, *CT Evaluation of Coronary Artery Disease*.

Causes of Acute Chest Pain

In clinical practice, the large majority of patients coming to medical attention for acute chest pain do not have cardiac disease. In published registries, only 15–20% of patients seeking the help of a general practitioner for acute chest pain have heart disease. Heart disease is a more common cause of chest pain in patients seen in the ER (Table 15.1), although the majority of patients still have non-cardiac causes of chest pain. Furthermore, data from a US registry (> 10 000 patients who visited the ERs of 10 different US hospitals) showed that, in patients with chest pain who visited the ER, only 17% ultimately met the criteria for cardiac ischemia (8% with myocardial infarction and 9% with unstable angina). More disturbingly, 2.1% of patients with acute myocardial infarction and 2.3% of those with unstable angina were mistakenly discharged. Not surprisingly, mortality among patients with acute myocardial infarction who were discharged home was about twice as high as expected. Most of these patients had a non-diagnostic or normal ECG. Indeed, the ECG is non-diagnostic in many patients with acute myocardial infarction and in most patients with unstable angina. Thus, according to ACC/AHA guidelines, all patients presenting in the ER with acute chest pain should be assessed by ECG and for cardiac biomarkers (preferably, cardiac-specific troponin, i.e., troponin-I or troponin T). Patients with negative ECG should undergo a serial ECG assessment to evaluate dynamic ECG changes (initially at 15- to 30-min intervals), whereas in patients with normal cardiac biomarkers the test should be repeated 8–12 h after symptom onset. Negative ECG and normal troponin identify a low-risk population; however, even patients with persistently normal troponin may have significant coronary disease. In these patients, a diagnosis of coronary disease may require other functional tests, such as ECG stress test, stress-echocardiogram, or nuclear imaging. None of these tests has optimal sensitivity or specificity (Table 15.2). Accordingly, up to 10–15% of patients with a diagnosis of ACS who undergo coronary angiography have normal coronary arteries. This confirms the limits of the current diagnostic methods.

A number of risk assessment tools have been introduced to predict the global risk of the patient by taking into account not only ECG findings and biomarkers, but also clinical presentation, previous history, risk factors, age, etc. However, their predictive ability for detecting patients at risk of clinical events is at best only moderate. In particular, although it can be relatively

Table 15.1. Final diagnosis of patients with acute chest pain who were seen by a general practitioner and at emergency departments. Modified from Erhardt L. et al (2002)

	General practitioner (%)	Emergency department (%)
Cardiac	20	45
Musculoskeletal	43	14
Gastrointestinal	5	6
Psychiatric	11	8
Pulmonary	4	5
Other	16	26

Table 15.2. Diagnostic accuracy of 64-slice CT scan for identifying coronary stenosis > 50%. Modified from Rubinstein R. et al (2007)

Study (year)	Number of patients	Specificity (%)	Sensitivity (%)	Negative predictive value (%)
Leschka (2005)	67	94	97	99
Raff (2005)	70	86	95	98
Leber (2005)	59	73–88	97	99
Mollet (2005)	52	99	95	99
Ropers (2006)	82	95	93	99
Fine (2006)	66	95	96	95

easy to identify subgroups of patients at high risk, it is quite difficult to identify correctly those at low risk (and, ideally, zero risk). The most widely used risk score for patients presenting with chest pain and ACS is the TIMI risk score, validated in the TIMI 11B trial and recently studied in an unselected ER population, with results similar to those reported in the original paper (Fig. 15.1). A modified score, the TIMI risk index (including also systolic blood pressure, age, and heart rate), can be useful in predicting 30-day mortality not only in patients with unstable angina and non-ST-elevation myocardial infarction, but also in patients with ST-elevation myocardial infarction (the TIMI risk calculator is available at www.timi.org). Other risk scores have

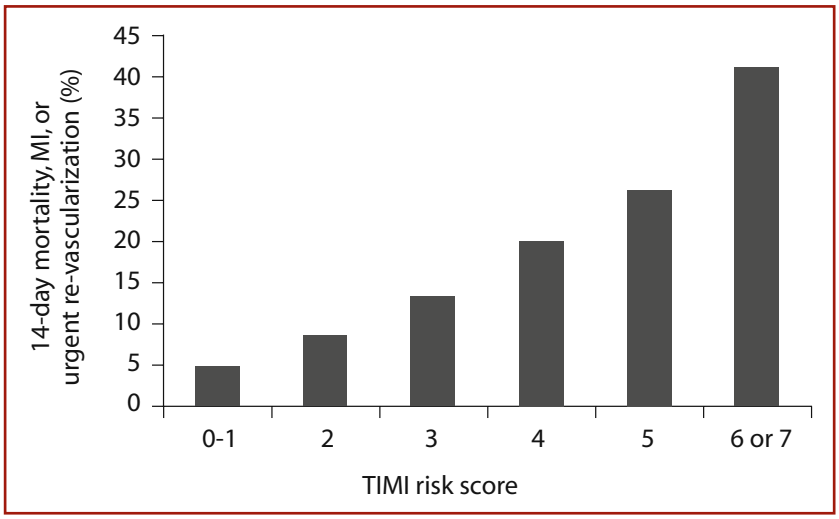

Fig. 15.1. The TIMI risk score for unstable angina and non-ST-elevation myocardial infarction (MI) is determined by the sum of seven factors present at admission (1 point for each variable): age 65 or older, at least three risk factors for coronary disease, evidence of prior coronary stenosis ≥ 50%, use of aspirin in the 7 days before admission, elevated serum biomarkers, ST-segment deviation on ECG at presentation, at least two episodes of angina in the previous 24 h. It is important to note that the risk of serious cardiac events is not negligible even in the lowest risk subgroup. Data from Antman E.M. et al (2000)

been developed from the database of the PURSUIT and GRACE trials. PURSUIT identified factors associated with increased risk of death at 30 days: age, heart rate, systolic blood pressure, ST-segment depression, signs of heart failure, and abnormal cardiac biomarkers (in order of relative strength). The GRACE clinical model can be used to predict mortality 6-months after patient discharge from the ER. However, although these risk scores can be helpful to identify the very-high-risk patient requiring aggressive treatment, they are less helpful in the screening of the large population of ER patients with chest pain, in whom it is important to rule out the presence of significant disease and to identify patients who can be safely discharged. Patients with a previous history of coronary disease, signs of heart failure, ECG changes or positive biomarkers, high heart rate, and low blood pressure are clearly at increased risk and are usually admitted to the hospital to undergo invasive treatment. By contrast, in apparently healthy patients with no previous history of heart disease, brief episodes of chest pain at rest are more difficult to manage.

Multislice CT Scanning in Acute Chest Pain

There are over 30 published studies assessing the diagnostic accuracy of CT scanning in identifying coronary disease, enrolling over 2,000 patients. Studies using a per-patient analysis (1,329 patients, examined by 16- or 64-slice CT scan) reported a mean sensitivity and specificity of 97 and 84%, respectively, with a sensitivity and specificity of 98 and 93%, respectively, for studies using 64-slice CT (Table 15.3). As shown in a recent meta-analysis, compared with previous scanner generations, 64-slice CT significantly improved the accuracy of detection of coronary artery stenoses. The weighted mean sensitivity for the detection of coronary artery stenoses increased from 84% for 4-slice CT and 83% for 16-slice CT to 93% for 64-slice CT, whereas the respective specificities were 93, 96, and 96%. However, the most interesting result was the negative predictive value of > 97%, much better than that reported for any other non-invasive diagnostic test. This excellent negative predictive value makes CT scan very attractive as an ER tool to rule out coronary disease. CT scan may have a lower diagnostic accuracy in patients with pre-existing coronary disease, who often have extensive coronary calcifications and coronary stents (which may produce artifacts on CT scan). However these patients are already included in a high-risk group when they come to the ER, because of their previous history of coronary disease. CT scan may be an invaluable asset for low to intermediate-risk patients with acute chest pain (i.e., the large majority of ER patients).

Table 15.3. Diagnostic accuracy of non-invasive tests for identifying coronary disease. Modified from Rubinstein R. et al (2007)

	Specificity (%)	Sensitivity (%)
ECG-stress test	50–77	68–90
Echo-stress test	90	90
Nuclear imaging	87	64

This hypothesis has led to several studies aimed at assessing the specific role of CT scan in patients with acute chest pain. Six studies on 64-slice CT scan, enrolling a total of 376 ER patients, have been published. All of them included low- to intermediate-risk patients with acute chest pain but normal cardiac biomarkers and no ischemic ECG changes (two studies actually excluded patients with a previous history of coronary disease). CT scan results correctly ruled out significant coronary disease, with a mean negative predictive value of 99%. These findings strongly support the use of CT scan to identify low-risk patients who can be safely discharged from the ER.

In a blinded study, were made attempted to rule out ACS in 103 patients with acute chest pain who presented to the ER (none of the patients had ischemic ECG-confirmed changes and negative initial biomarkers). The absence of both significant coronary artery stenosis and non-stenotic coronary atherosclerotic plaque accurately predicted the absence of an ACS (negative predictive value 100%). However, in this study, the positive predictive value was rather low, indicating false-positive results (47% for the detection of significant stenoses, 14/30 positive scans), and only a small percentage of patients with acute chest pain were actually included in the study (103 of 305 initially screened patients). The group from William Beaumont Hospital (Royal Oak, MI) reported a trial on 197 patients randomized to early CT scan in the ER vs. standard diagnostic protocol (ECG, serial cardiac biomarkers, and nuclear stress test). Of the patients undergoing CT scan, those who had coronary arterial stenosis < 25% were eligible for immediate discharge, while those with stenosis > 70% were referred for invasive coronary angiography, and patients with intermediate lesions (stenosis 26%–70%) or non-diagnostic scans (severe coronary calcifications, excessive motion artifact, or poor contrast-to-noise signals) underwent nuclear stress testing. In patients randomized to the standard diagnostic protocol, those with normal serial ECG, cardiac biomarkers, and stress test were discharged, whereas patients who developed ECG changes, had increased biomarkers, or abnormal nuclear stress studies were referred for invasive angiography. In the CT-scan group, two-thirds of patients were discharged immediately after the scan and none of these patients suffered an adverse event at 6-months follow-up (negative predictive value 100%). CT scan was non-diagnostic (because of the presence of intermediate lesions or suboptimal imaging) in 24% of the patients, while in 8% it identified significant coronary lesions (with a positive predictive value of 85%). The approach with CT scan was much quicker (time to diagnosis 3.4 h vs. 15.0 h in the standard diagnosis group) and significantly reduced costs (–15%) (Table 15.4). This study also obtained a good positive predictive

Table 15.4. Comparison of 64-slice CT scan vs. standard diagnostic protocol in the ER. Modified from Goldstein J.A. et al (2007)

	64-slice CT scan	Standard diagnostic protocol	*P*
Time to diagnosis	3.4 h	15.0 h	< 0.001
Total cost	$US 1586	$US 1872	< 0.001
Re-evaluation at 6 months	2%	7%	0.10

value, but it should be noted that patients with intermediate stenosis or with non-diagnostic scans underwent nuclear imaging (24% of all patients randomized to CT scan).

Conversely, simple assessment of calcium score by CT is insufficient to correctly identify ER patients with coronary disease, since patients with acute chest pain have mostly non-calcified coronary plaques, which can be identified only by MSCT.

The possible limits of MSCT (as reported in other chapters) include fast heart rate (> 65 beats/min) and arrhythmias (in particular, atrial fibrillation). Although it is common to treat patients undergoing MSCT with beta-blockers to reduce heart rate to < 65 beats/min, in up to 15% of ER patients these drugs are contraindicated. Finally, all patients should be screened for a history of iodine allergy and for renal failure.

The "Triple Rule Out" Protocol

MSCT (64-slice and over) allows rapid scanning not only of the heart and coronary arteries, but also of the entire lung and thoracic aorta; indeed, a complete scan of all these areas can be performed in < 20 s. These technical improvements have led to the use of MSCT to identify coronary disease, aortic dissection, and lung embolism. Thus, a single scan can rule out three potentially fatal causes of acute chest pain (the so-called triple rule out). These scans can be technically challenging because they require optimal and simultaneous contrast intensity in both the left (coronary and aorta) and the right (pulmonary) circulation, while avoiding artifacts generated by the presence of contrast in the right atrium and ventricle (which may reduce the accuracy of coronary imaging). Use of a dedicated protocol of contrast injection with two contrast boluses (one for the coronary arteries and one for the pulmonary arteries) followed by saline injection (to clear contrast material from the right heart chambers) yields good imaging of all three arteries in a single scan. This approach seems very attractive and it has been introduced in several hospitals, although it has yet to be tested in clinical trials. In particular, since aortic dissection and lung embolism are much less frequent than coronary disease, it is unclear whether the large-scale use of this protocol (which requires an increased radiation dose) has a positive risk/benefit ratio in an unselected population, while it may be a truly important asset for patients with clinical suspicion of aortic dissection or lung embolism.

Conclusion

Multislice CT scan is an ideal diagnostic test to rule-out coronary disease (and possibly other vascular thoracic disease) in low-risk patients. Diagnostic assessment in the ER of acute chest pain seems to be one of the best settings to use this new diagnostic method. Randomized studies have confirmed that integrating MSCT in the diagnostic protocols of the ER not only results in excellent diagnostic accuracy, but also in shorter hospital stay and reduced costs. Although ACC/AHA guidelines for the assessment of patients with

acute chest pain do not include yet MSCT scan, recent studies have indicated how this new diagnostic tool could become part of ER protocols.

Clearly, patients coming to the ER with acute chest pain should first undergo a complete clinical assessment, with ECG and cardiac biomarkers. High-risk patients with ischemia, as indicated by ECG and/or positive biomarkers, do not require MSCT and should be immediately admitted and treated; patients with negative ECG and biomarkers at admission could receive a diagnostic CT scan (avoiding the wait for serial ECG and biomarkers). This approach would allow the early identification of patients with no coronary disease who could be discharged (Fig. 15.2). The traditional diagnostic protocol with serial ECG, biomarkers, and possible stress testing should be reserved for patients with suboptimal imaging at MSCT scan or with evidence of intermediate stenosis.

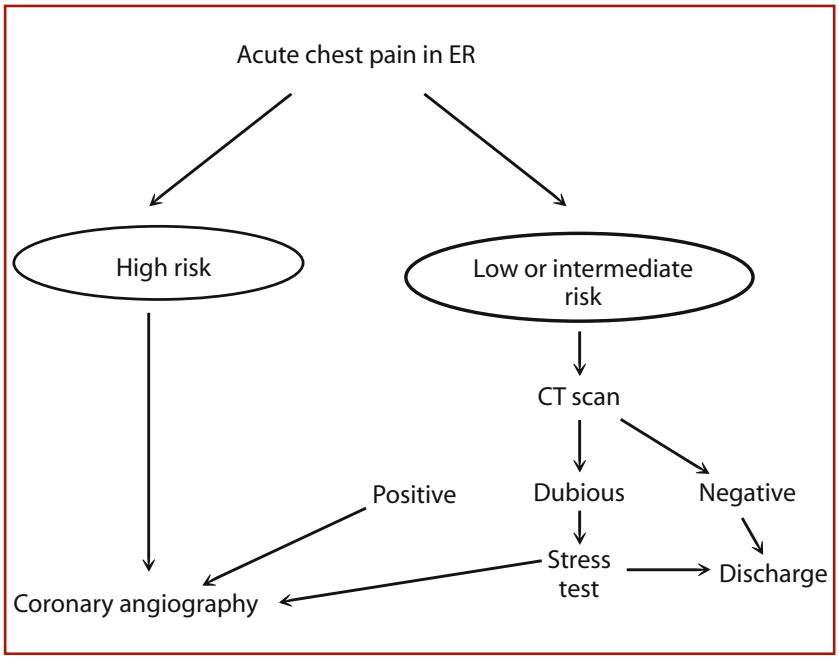

Fig. 15.2. Flow chart for the ER diagnosis of acute chest pain. The approach integrates CT scan with current clinical practice

16

Current Recommendations for Coronary CT Angiography

Massimo Fioranelli, Francesca Sbandi

In 2006, criteria for cardiac computed tomography and cardiac magnetic resonance imaging were published by the American College of Cardiology (ACC). Since then, technological developments and the results of the most recent studies have led to the review of these recommendations and to previously drawn conclusions.

On June 27, 2008, a Scientific Statement from the American Heart Association Committee was published online (Circulation 2008; 118:586-606). Here, we refer to this statement in analyzing the ACC/AHA's classification of recommendations and levels of evidence:

According to the ACC/AHA, there are three classes (and two subclasses) and three levels of evidence:

- Class I: Conditions for which there is evidence for and/or general agreement that the procedure or treatment is beneficial, useful, and effective.
- Class II: Conditions for which there is conflicting evidence and/or a divergence of opinion about the usefulness/efficacy of a procedure or treatment.
- Class IIa: Weight of evidence/opinion is in favor of usefulness/efficacy.
- Class IIb: Usefulness/efficacy is less well-established by evidence/opinion.
- Class III: Conditions for which there is evidence and/or general agreement that the procedure/treatment is not useful/effective and in some cases may be harmful.
- Level of Evidence A: Data derived from multiple randomized clinical trials.
- Level of Evidence B: Data derived from a single randomized trial or nonrandomized studies.
- Level of Evidence C: Only consensus opinion of experts, case studies, or standard of care.

Although no codified indications on coronary computed tomography (CT) are available, the major practical applications thus far include:

- Diagnosis of stenosis in patients with low and intermediate risk of cardiovascular disease.
- Evaluation of bypass patency.

P. Pavone, M. Fioranelli, D.A. Dowe, *CT Evaluation of Coronary Artery Disease*.

– Unsolved diagnostic situations in patients who have undergone intracardiac catheter angiography.

Technical Considerations

Some technical aspects need to be taken into consideration regarding the clinical usefulness of coronary CT. The minimal technical prerequisite for the application of contrast-enhanced multidetector-row CT (MDCT) to coronary CT angiography (CTA) is a 16-slice CT device with a gantry rotation time of 500 ms and slice collimation of 1.0 mm. Most CT scanners currently in use are 64-slice, with a spatial resolution of 0.4 mm and a temporal resolution of 165 ms. The spatial resolution of the machines used in catheter coronary angiography is 0.2 mm, which is twice the CT value, and the temporal resolution is around 8 ms, corresponding to 12–30 images per second. Therefore, even though images are captured by sophisticated software, the CT images are not as detailed as those obtained during catheter coronary angiography. Furthermore, a regular cardiac rhythm is a primary requirement to capture images with an adequate resolution.

CT analysis is only applicable to coronary segments > 1.5–2 mm in diameter. The spatial resolution of CT restricts quantitative analysis of the severity of coronary stenosis, even if the sensitivity to identify a hemodynamically significant stenosis is 73–100%. The percentage of coronary segments that cannot be screened is between 0 and 12%. In the literature, a high negative predictive value (95–100%) has been consistently reported. A description of coronary CT results should include any factors that have limited the technical quality of the examination, as well as the size of the vessels, the presence of coronary anomalies, left or right dominance, coronary stenosis, the presence of non-calcified and/or calcified plaque, presence, location and size of any coronary aneurysmal or pseudoaneurysmal dilatation, and significant non-cardiac findings (class I, level of evidence A).

Evaluation of Coronary Stenosis in Patients at Low or Intermediate Risk of Cardiovascular Disease

Many studies have demonstrated that coronary CT angiography (CTA) is a viable diagnostic option to detect the presence of coronary plaques (calcific and non-calcific) and to rule out significant stenosis. Meta-analyses of 64-slice MDCT studies found a sensitivity of 86–93% and a specificity of about 96%.

Coronary CTA provides useful information about positive coronary remodeling, which has a relevant role in atherogenesis and offers insight into the tissue composition of the coronary atherosclerotic plaque. However, compared to intravascular ultrasound, coronary CTA substantially overestimates plaque volume per segment in a calcific plaque, but underestimates plaque volume in a non-calcific plaque. The potential benefit of non-invasive coronary CTA is likely to be greatest and is reasonable for symptomatic patients who are at intermediate risk for coronary artery disease after initial risk stratification. This includes patients with equivocal stress-test results (class IIa, level of evidence B).

A patient with chest pain and low cardiovascular risk can be dismissed from the ER, without further invasive tests, if a coronary CT of good quality excludes the presence of an atherosclerotic lesion.

Coronary CTA is useful in the peri-operative cardiovascular evaluation and care of patients undergoing non-cardiac surgery; a rapid and non-invasive test does not delay surgery. In patients with syncope or ventricular arrhythmias, coronary CTA is a useful, non-invasive test to detect or to exclude the presence of coronary disease.

In the presence of a chronic coronary atherosclerotic plaque, coronary CTA can provide information about the composition (calcific and non-calcific) of the plaque and then the success of a coronary angioplasty.

Evaluation of Coronary Artery Bypass Patency

Coronary bypass grafts are larger, extracardiac, and less mobile than native coronary arteries; this has the advantage of allowing a better quality analysis. Multislice CT is emerging as a realistic investigative tool in patients with grafted coronary arteries. One of its major advantages is that it is a non-invasive diagnostic approach, which is desirable in patients with bypass grafts as they are at high risk for complications arising from invasive angiography. Indeed, the incidence of so-called major adverse events (death, myocardial infarction, or stroke) during or within 24 h of selective coronary angiography is reported to be 0.2–0.3%, and the incidence of so-called minor complications (most of which are related to problems with the peripheral vessels through which the catheters are inserted) is 1–2%.

The complex course of coronary grafts makes three-dimensional imaging a valuable method to assess the status of the graft as it travels parallel and perpendicular to the axial images. These advances, as well as the capacity for integrated functional cardiac assessment, may change the referral patterns in patients who have had previous bypass surgery. Bypass conduits typically have a luminal diameter of 4–6 mm. Since they are wider than most native coronary arteries, this allows good spatial resolution, vital to an accurate evaluation. Assessment of anastomosis is improved with three-dimensional technologies, as they offer the ability to view the anastomosis from multiple angles.

High-density surgical clips may cause partial-volume and beam-hardening effects, image-quality degradation, and unreliability in determining stenosis grade. Clip artifacts vary with surgical technique but are generally greater around arterial grafts and may increase if the slice thickness is very small. CT evaluation of coronary artery bypass grafts yields consistently excellent image quality, but the clinical value is limited by difficulties in assessing the native coronary arteries downstream of the graft anastomosis. However, the occlusion and patency of arterial and venous bypass grafts can be determined with high accuracy (sensitivity of 100% for detection of bypass occlusion in three studies performed with 16-slice MDCT).

Coronary CT is also a viable diagnostic modality in symptomatic patients with previous bypass surgery but whose stress-test results are non-diagnostic.

Sometimes, catheter coronary angiography cannot visualize a bypass conduit; in this setting, coronary CT is a useful alternative.

Other Frequent Uses of Coronary CT Angiography

Coronary CTA is sometimes applied in situations in which catheter coronary angiography is non-diagnostic. It is very useful in identifying the origin and anatomic course of a coronary segment in case of suspected coronary anomalies (class IIa, level of evidence B).

Assessment of complex congenital heart disease, including anomalies of the coronary circulation, great vessels, and cardiac chambers and valves, are areas in which coronary CTA has had good results. In addition, it is useful in the evaluation of specific cardiomyopathies (amyloidosis, hypertrophic cardiomyopathy, drug toxicity), cardiac and pericardiac neoplasms, aortic dissection, and identification of pulmonary veins before ablative procedures.

In patients with aortic dissection, including those with Marfan syndrome, a coronary CTA is a valid alternative to catheter coronary angiography.

Contraindications to Coronary CT Angiography

It is of pivotal importance to identify those conditions in which coronary CTA is not appropriate. For example, it cannot be used in patients with ACS, in patients with high probability of coronary artery disease, and or those with ECG or biochemical markers indicating myocardial necrotic modifications (class III, level of evidence C).

Catheter angiography remains the gold standard for the detection of coronary arteries stenosis during an ACS or in patients at high risk for cardiovascular diseases.

Arrhythmias, a heart rate > 70 beats per minute (for 64-slice equipment), an adverse reaction to contrast agent, renal or respiratory insufficiency, pregnancy, and heart failure are other contraindications for coronary CTA.

Future Directions in Non-invasive Coronary Artery Imaging with Coronary CT Angiography

Coronary CTA is a rapidly evolving technology and the indications for its use are changing at nearly the same speed.

The evaluation of coronary vessels in re-vascularized patients, either following PTCA or surgery, is now a clinical option. It is possible to evaluate the patency of stents with good accuracy and thus to follow up these patients.

At present, assessment of non-calcified plaque remains limited to studies in which very high image quality is possible. However, the clinical applications of the technique will no doubt soon expand to include the detection of unstable plaques, and, more generally, the characterization and measurement of atherosclerotic plaque burden, as well as its changes over time or in response to therapy.

Continued innovations in coronary CTA will rapidly change our view of this technology. The new 128-slice machines speed the acquisition of heart images from the current 10–15 s for 64 slice machines to 4 s. This velocity can better “freeze” the heart. The gantry rotation of the 128-slice CT is 0.3 s,

and the temporal resolution 150 ms, allowing acquisition of the entire heart in 4–5 s. With a spatial resolution of 0.24 mm, very small anatomic structures can be analyzed. Moreover, the tunnel is larger (78 vs. 65 cm) so that it will also be possible to evaluate obese or claustrophobic patients. By applying a few technical "tricks" (step and shoot, adaptive techniques, ECG-controlled tube-current modulation, protective filters, etc.), radiation exposure can be reduced to a range of 2–3 to 6–12 mSv instead of 15–20 mSv.

While coronary CTA is still an emerging technology, in the next decade it will no doubt become a major cardiovascular imaging option.

17

Prognostic Value of Coronary CT

Massimo Fioranelli, Antonio Lucifero

The majority of acute coronary syndromes (ACSs) are the result of a complication in an atherosclerotic plaque that had not caused a reduction in the blood stream prior to the episode. The presence of a stenosis, even if appreciable, does not necessarily lead to ischemia in the area supplied by the stenotic vessel. Even the presence of a complete obstruction does not automatically imply that the area downstream will become necrotic. Therefore, the stenosis is, in itself, of little diagnostic value in the assessment of perfusion or of contractile function; in other words, the anatomic aspect is often irrelevant with respect to the functional one. In two-thirds of ACS patients, however, there is fragmentation of the plaque. Those plaques that are highly likely to deteriorate are called "vulnerable plaques" and their histopathological characteristics are well-visualized with intravascular ultrasound (IVUS) imaging. About three-quarters of plaques complicated by rupture involve 50% of the vessel diameter, and in approximately half of the cases more than 75%. In two-thirds, the lipidic core occupies > 25% of the volume of the lesion, and in 80% of cases it expands to occupy > 50% of the thickness of the vessel wall. Most vulnerable plaques (95%) are located in the proximal segments of the epicardial branches and only rarely in the distal vessels. Furthermore, the necrotic core in ruptured lesions is significantly larger (2–22 mm in length, average 9 mm) than in the intact vulnerable plaque, suggesting that progressive enlargement of the necrotic core is associated with a higher probability of rupture. Indeed, when the area of the necrotic core exceeds a critical threshold (25% of the plaque area) the plaque is vulnerable to rupture. It has also been shown that the necrotic cores associated with plaque rupture occupy > 60° of the vessel circumference.

These observations underline the diagnostic importance of being able to non-invasively identify the characteristics that make a plaque vulnerable.

In the 1990s, Agatston proposed the use of a CT electron beam to quantify coronary calcium. Many studies demonstrated that a high Agatston score, i.e., a high calcium content, was associated with a high incidence of coronary episodes. The annual incidence of adverse episodes in individuals without

P. Pavone, M. Fioranelli, D.A. Dowe, *CT Evaluation of Coronary Artery Disease*.

significant calcium content in the coronary tree is approximately 2 out of 1,000. With a coronary artery calcium (CAC) score > 400, the incidence of coronary episodes rises ten-fold, which translates into 20–50 episodes for every 1,000 such patients.

In a recent primary prevention study (JACC, 2006), the impact of the CAC score on the prognosis of 25,000 asymptomatic patients was analyzed with an average follow-up period of about 7 years. Six score classes, 0, 1–10, 11–100, 101–400, 401–1,000, and > 1000, were defined, with a patient distribution of 44, 14, 20, 13, 6, and 4%, respectively. At the end of the follow-up period, total mortality was 2% (510 deaths). CAC proved to be an independent predictor of mortality and the relative risk of cardiovascular mortality was 2.2, 4.5, 6.4, 9.2, 10.4, and 12.5 times per score of 11, 100, 101, 299, 300–399, 400–699, 700–999 and > 1,000, respectively ($p < 0.0001$), compared with a CAC score of 0. The survival rate after 10 years was 99.4% for a score of 0 and of 87.8% for a score >1,000 ($p < 0.0001$).

The capabilities of coronary CT are not limited to the quantification of coronary calcium but also include the identification and measurement of parietal calcium. More importantly, coronary CT can be used to determine the size of the arterial stenosis and its composition as well as to monitor its evolution and possible regression. Coronary CT presently has an adequate sensitivity (83–99%), a high specificity (93–98%), and a high negative predictive power (95–100%) in its ability to diagnose a coronary stenosis. However, a review of the literature showed that, in the studies in which these values were reported, patients suffering from arrhythmia, kidney failure, congenital ischemic cardiomyopathy, etc., i.e., conditions that may have altered the population of tested patients, were excluded.

In a recent study, coronary CT evaluation of plaques responsible for ACS registered the following characteristics: the presence of vascular remodeling, reduced CT density of the plaque (< 30 HU), and the presence of micro-calcifications. The simultaneous presence of these three elements was shown to have a positive predictive power of 95%, while the absence of all three characteristics had a negative predictive power of 100%.

To date, the predictive value of coronary CT remains unproven. Some minor studies have assessed the prognostic value in patients with chest pain. For example, a coronary CT negative for stenosis had significant prognostic value; after one year, the possibility of suffering a coronary episode was almost none, corresponding to a negative predictive power of 100%. This high negative predictive power, noted in many studies, suggests that coronary CT is a diagnostic technique capable of excluding the presence of coronary stenosis in a subgroup of patients with a low pre-test probability of a coronary condition. However, CT has limitations, in that with the present technology (64-slice scanner) the spatial resolution is 0.4 mm and the temporal resolution 165 ms. A high spatial and temporal resolution is a prerequisite for visualization of the coronary arteries. A more invasive technique, catheter coronary angiography has a spatial resolution of 0.2 mm, twice that of CT angiography, and a temporal resolution of ~8 ms, corresponding to the acquisition of 12–30 images per second. The implication is that quantification of a stenosis by means of coronary CT cannot be as precise as obtained through catheter angiography. However, as discussed in other chapters in this volume, it is the

composition of the plaque in a stenosis rather than the degree of the stenosis that yields the most significant prognostic information.

The new 128-slice machines speed the acquisition of cardiac images to 4 s compared to 10–15 s for 64-slice machines. The gantry rotation is 0.3 s and the temporal resolution 150 ms; thus, the entire heart can be imaged in 4–5 s. A spatial resolution of 0.24 mm is sufficient to reveal small anatomic structures.

It is well-established that the likelihood of plaque rupture depends on plaque composition rather than on plaque volume. Unstable plaques generally have a higher lipid content than stable plaques, and most ruptures occur in plaques containing a soft, lipid-rich core that is covered by a thin, inflamed fibrous cap. A cap with a thickness < 65 μm is a major characteristic of a vulnerable plaque; however this measurement is ten times beyond the present in-plane resolution of either multidetector-row CT (750 μm) or magnetic resonance imaging (500–780 μm).

In the evaluation of coronary artery disease, we need to move away from the concept of luminal occlusion and instead focus on the morphological characteristics of the atherosclerotic plaque. Current disease management strategy is based on the demonstration of critical luminal obstruction, which is able to identify the extent of the lesion responsible for symptomatic disease, but this approach says very little about the prognosis, for which both the lumen and the vessel wall must be considered. The advent of high-resolution multi-slice CT (MSCT) imaging allows, for the first time, the composition of the plaque to be characterized. MSCT is able to detect the large necrotic core, a major aspect of plaque vulnerability. The larger the plaque volume and necrotic core, the higher the likelihood of plaque rupture. Recent MSCT investigations have demonstrated that hypodense areas in the plaque represent the necrotic lipid cores, and thus so-called soft plaques.

Preliminary studies have confirmed that CT is able to distinguish between fat tissue, fibrous tissue, and calcium. There is a good correlation between lowest CT density values and the lipid-laden plaque, as seen on IVUS, whereas intermediate densities correlate with fibrous lesions. However, overlap between densities makes the distinction between fibrous and soft plaques problematic. At present, assessment of a non-calcified plaque remains limited to studies of very high image quality, beyond that available in daily clinical applications.

Some plaques with large necrotic cores and outward remodeling should be characterized by MSCT. Density-based software is able to define the features of the plaque and identify the necrotic core. The best currently available low-contrast, high-resolution, and minimum slice-thickness (64 × 0.5) hardware should allow better differentiation of the fibrous plaque from the soft plaque.

Cardiovascular risk is currently determined by the Framingham score, according to which around half the population is at low risk. This means that the chance of a coronary episode is < 5% over 10 years (< 0.5% per year); 40% of the population is considered at intermediate risk (5–20% in 10 years, 0.5–2% per year); and 10% is at high risk (> 20%, > 2% per year).

The concept of "vulnerable patient" has developed alongside the concept of "vulnerable plaque." This is a person at high risk, with multiple pathologies and suffering from coronary, peripheral, and cerebral vasculopathy, diabetes

mellitus, or kidney failure. In this population, the challenge is to adequately diagnose vulnerable plaques through non-invasive techniques and to adjust the therapy on the basis of the information obtained, thereby reaping a tremendous clinical benefit. Coronary CT has the potential to diagnose vulnerable plaques in these vulnerable patients.

Suggested Readings

Abbate A, Bonanno E, Mauriello A et al (2004) Widespread myocardial inflammation and infarct-related artery patency. Circulation 110(1):46–50

Achenbach S (2006) Top 10 indications for coronary CTA. Applied Radiology 35:22–31

Airoldi F, Colombo A, Morici N et al (2007) Incidence and predictors of drug-eluting stent thrombosis during and after discontinuation of thienopyridine treatment. Circulation 116:745–754

Alderman EL, Stadius ML (1992) The angiographic definitions of the Bypass Angioplasty Revascularization Investigation (BARI). Coron Artery Dis 3:1189–1120

André P, Nannizzi-Alaimo L, Prasad SK, Phillips DR (2002) Platelet-derived CD40L: the switch-hitting player of cardiovascular disease. Circulation 106(8):896–899

Antman EM, Cohen M, Bernink PJ et al (2000) The TIMI risk score for unstable angina/non-ST elevation MI: a method for prognostication and therapeutic decision making. JAMA 284:835–842

Arbustini E, Grasso M, Diegoli M et al (1993) Coronary thrombosis in non cardiac death. Coron Artery Dis 4:751–759

Ardissino D, Cavallini C, Bramucci E et al (2004) Sirolimus-eluting vs uncoated stents for prevention of restenosis in small coronary arteries: a randomized trial. JAMA 292:2727–2734

Ardissino D, Merlini PA, Bauer KA et al (2003) Coagulation activation and long-term outcome in acute coronary syndromes. Blood 102(8):2731–2735

Associazione Nazionale Medici Cardiologi Ospedalieri (2000) Trattato di Cardiologia. Excerpta Medica, San Donato Milanese, Milan

Austen WG, Edwards JE, Frye RL et al (1975) A reporting system on patients for coronary artery disease: report of the ad hoc Committee for Grading of Coronary Artery Disease, Council on Cardiovascular Surgery, American Heart Association. Circulation 51 (Suppl 4):5–40

Baim DS, Cutlip DE, Midei M et al (2001) Final results of a randomized trial comparing the MULTI-LINK stent with the Palmaz-Schatz stent for narrowings in native coronary arteries. Am J Cardiol 87:157–162

Baim DS, Cutlip DE, O'Shaughnessy CD, et al (2001) Final results of a randomized trial comparing the NIR stent to the Palmaz-Schatz stent for narrowings in native coronary arteries. Am J Cardiol 87:152–156

Bayes-Genis A, Conover CA, Overgaard MT et al (2001) Pregnancy-associated plasma protein A as a marker of acute coronary syndromes. N Engl J Med 345(14):1022–1029

Biasucci LM, Liuzzo G, Ciervo A et al (2003) Antibody response to chlamydial heat shock protein 60 is strongly associated with acute coronary syndromes. Circulation 107(24):3015–3017

Biasucci LM, Liuzzo G, Grillo RL et al (1999) Elevated levels of C-reactive protein at discharge in patients with unstable angina predict recurrent instability. Circulation 99(7):855–860

Braunwald E (1989) Unstable angina. A classification. Circulation 80:410–414

Braunwald E (1997) Heart disease: a textbook of cardiovascular medicines. 5th ed. W.B. Saunders Company, Philadelphia

Brenner DJ, Hall EJ (2007) Computed tomography. An increasing source of radiation exposure. N Engl J Med 357:2277–2284

Briguori C, De Gregorio J, Nishida T et al (2000) Polytetrafluoroethylene-covered stent for the treatment of narrowings in aorticocoronary saphenous vein grafts. Am J Cardiol 86:343–346

Briguori C, Sarais C, Pagnotta P et al (2002) In-stent restenosis in small coronary arteries: impact of strut thickness. J Am Coll Cardiol 40:403–409

Budoff MJ, Shaw LJ, Liu ST et al (2007) Long-term prognosis associated with coronary calcification: observations from a registry of 25,253 patients. J Am Coll Cardiol 49:1860–1870

Budoff MJ, Shinbane JS (2006) Cardiac CT imaging: diagnosis of cardiovascular disease. Springer Berlin Heidelberg New York

Buffon A, Biasucci LM, Liuzzo G et al (2002) Widespread coronary inflammation in unstable angina. N Engl J Med 347(1):5–12

Cademartiri F, Casolo G, Midiri M (2007) La TC del cuore nella pratica clinica. Springer Milano

Cademartiri F, Mollet N, Lemos PA et al (2005) Usefulness of multislice computed tomographic coronary angiography to assess in-stent restenosis. Am J Cardiol 96:799–802

CathSAP II, American College of Cardiology, Society for Cardiac Angiography and Interventions. http://www.acc.org/education/products/suite_core.htm

Chevalier B (2008) NOBORI 1-long term results: two years phase 1, one year phase 2. Scientific Session, Late Breaking Trials, Euro PCR, Barcelona

Chevalier B, Serruys PW, Silber S et al (2007) Randomised comparison of Nobori TM, biolimus A9-eluting coronary stent with Taxus, paclitaxel-eluting coronary stent in patients with stenosis in ntive coronary arteries: the Nobori 1 trial. EuroIntervention 2:426–434

Chiurlia E, Menozzi M, Ratti C et al (2005) Follow-up of coronary artery bypass graft patency by multislice computed tomography. Am J Cardiol 95:1094–1097

Cohen MC, Hartnell GG, Finn JP (1994) Magnetic resonance angiography of congenital pulmonary vein anomalies. Am Heart J 127:954–955

Colombo A, Drzewiecki J, Banning A et al (2003) Randomized study to assess the effectiveness of slow- and moderate-release polymer-based paclitaxel-eluting stents for coronary artery lesions. Circulation 108:788–794

Colombo A, Hall P, Nakamura S et al (1995) Intracoronary stenting without anticoagulation accomplished with intravascular ultrasound guidance. Circulation 91:1676–1688

Colombo A, Stankovic G, Moses JW (2002) Selection of coronary stents. J Am Coll Cardiol 40:1021–1033

Coronary Artery Disease, ACCSAP-6, American College of Cardiology, http://www.acc.org/education/products/suite_core.htm. Cited in March 2005

Daemen J, Wenaweser P, Tsuchida K et al (2007) Early and late coronary stent thrombosis of sirolimus-eluting and paclitaxel-eluting stents in routine clinical practice: data from a large two-institutional cohort study. Lancet 369:667–678

Davies MJ, Thomas A (1984) Thrombosis and acute coronary-artery lesions in sudden cardiac ischemic death. N Engl J Med 310(18):1137–1140

De Palma R, Del Galdo F, Abbate G et al (2006) Patients with acute coronary syndrome show oligoclonal T-cell recruitment within unstable plaque: evidence for a local, intracoronary immunologic mechanism. Circulation 113(5):640–646

Dewey M, Lembcke A, Enzweiler C et al (2004) Isotropic half-millimeter angiography of coronary artery bypass grafts with 16-slice computed tomography. Ann Thorac Surg 77:800–804

Eagle KA, Guyton RA (2004) ACC/AHA 2004 Guideline update for coronary artery by-pass graft surgery. J Am Coll Cardiol

Ehara S, Kobayashi Y, Yoshiyama M et al (2004) Spotty calcification typifies the culprit plaque in patients with acute myocardial infarction. An intravascular ultrasound study. Circulation 110:3424–3429

Engelmann MG, Knez A, von Smekal A et al (2000) Non-invasive coronary bypass graft imaging after multivessel revascularization. Int J Cardiol 76:65–74

Engelmann MG, von Smekal A, Knez A et al (1997) Accuracy of spiral computed tomography for identifying arterial and venous coronary graft patency. Am J Cardiol 80:569–574

Erbel R, Di Mario C, Bartunek J et al (2007) Temporary scaffolding of coronary arteries with bioabsorbable magnesium stents: a prospective, non-randomised multicentre trial. Lancet 369:1869–1875

Erhardt L, Herlitz J, Bossaert L et al (2002) Task force on the management of chest pain. Eur Heart J 23:1153–1176

Fischman DL, Leon MB, Baim DS et al (1994) A randomized comparison of coronary-stent placement and balloon angioplasty in the treatment of coronary artery disease. Stent Restenosis Study Investigators. N Engl J Med 331:496–501

Gallagher MJ, Raff GL (2008) Use of multislice CT for the evaluation of emergency room patients with chest pain: the so-called "triple rule-out". Catheter Cardiovasc Interv 71:92-99

Garasic JM, Edelman ER, Squire JC et al (2000) Stent and artery geometry determine intimal tickening independent of artery injury. Circulation 101:812–818

Gershlick A, De Scheerder I, Chevalier B et al (2004) Inhibition of restenosis with a paclitaxel-eluting, polymer-free coronary stent: the European evaLUation of pacli-Taxel Eluting Stent (ELUTES) trial. Circulation 109:487–493

Gilard M, Cornily JC, Pennec PY et al (2005) Assessment of coronary artery stents by 16-slice computed tomography. Heart 92:58–61

Gilard M, Cornily JC, Rioufol G et al (2005) Noninvasive assessment of left main coronary stent patency with 16-slice computed tomography. Am J Cardiol 95:110–112

Goldstein JA, Demetriou D, Grines CL et al (2000) Multiple complex coronary plaques in patients with acute myocardial infarction. N Engl J Med 343(13):915–922

Goldstein JA, Gallagher MJ, O'Neill WW et al (2007) A randomized controlled trial of multi-slice coronary computed tomography for evaluation of acute chest pain. J Am Coll Cardiol 49:863-871

Grube E, Silber S, Hauptmann KE et al (2004) TAXUS I: six- and twelve-month results from a randomized, double-blind trial on a slow-release paclitaxel-eluting stent for de novo coronary lesions. Circulation (2003) 107:38–42

Grundy SM, Pasternak R, Greenland P et al (1999) Assessment of cardiovascular risk by use of multiple-risk-factor assessment equations. Circulation 100:1481–1492

Guazzi MD, Bussotti M, Grancini L et al (1997) Evidence of multifocal activity of coronary disease in patients with acute myocardial infarction. Circulation 96(4):1145–1151

Gurbel PA, Callahan KP, Malinin AI et al (2002) Could stent design affect platelet activation? Results of the Platelet Activation in STenting (PAST) Study. J Invasive Cardiol 14:584–589

Han Y (2008) Multicenter Registry of Excel Biodegradable Polymer Drug Eluting Stent (CREATE) , 9-months angiographic and 12-months clinical results. American College of Cardiology 2008 Scientific Sessions/i2 Summit-SCAI Annual Meeting) March 31, Chicago, IL. Late-breaking clinical trials 3

Hansson GK, Holm J, Jonasson L (1989) Detection of activated T lymphocytes in the human atherosclerotic plaque. Am J Pathol 135:169–175

Heeschen C, Dimmeler S, Fichtlscherer S et al. CAPTURE Investigators (2004) Prognostic value of placental growth factor in patients with acute chest pain. JAMA 291(4):435–441

Hendel RC, Patel MR, Kramer CM et al (2006) ACCF/ACR/SCCT/SCMR/ASNC/NASCI/SCAI/SIR 2006 appropriateness criteria for cardiac computed tomography and cardiac magnetic resonance imaging. J Am Coll Cardiol 48:1475–1497

Henneman MM, Schuijf JD, Pundziute G et al (2008) Noninvasive evaluation with multislice computed tomography in suspected acute coronary syndrome: plaque morphology on multislice computed tomography versus coronary calcium score. J Am Coll Cardiol 52:216-222

Henschke CI, Yankelevitz DF, Libby DM et al (2006) Survival of patients with stage I lung cancer detected on CT screening. N Engl J Med 355:1763–1771

Hoffmann U, Millea R, Enzweiler C et al (2004) Acute myocardial infarction: contrast-enhanced multi-detector row CT in a porcine model. Radiology 231:697–701

Hoffmann U, Nagurney JT, Moselewski F et al (2006) Coronary multidetector computer tomography in the assessment of patients with acute chest pain. Circulation 114:2251–2260

Hong C, Chrysant GS, Woodard PK et al (2004) Coronary artery stent patency assessed with in-stent contrast enhancement measured at multi-detector row CT angiography: initial experience. Radiology 233:286–291

Hwang CW, Wu D, Edelman ER (2001) Physiological transport forces govern drug distribution for stent-based delivery. Circulation 104:600–605

Iakovou I, Schmidt T, Bonizzoni E et al (2005) Incidence, predictors, and outcome of thrombosis after successful implantation of drug-eluting stents. JAMA 293:2126–2130

Ishikawa T, Hatakeyama K, Imamura T et al (2003) Involvement of C-reactive protein obtained by directional coronary atherectomy in plaque instability and developing restenosis in patients with stable or unstable angina pectoris. Am J Cardiol 91(3):287–292

Kaartinen M, Penttila A, Kovanen (1994) Accumulation of activated mast cells in the shoulder region of human coronary atheroma, the predilection site of atheromatous rupture. Circulation 90:1669–1678

Kalushi E, Tsai S, Klapholz M (2008) Coronary stenting with MGuard: from conception to human trials. Cardiovasc Revasc Med 9(2):88–94

Kastrati A, Dirschinger J, Boekstegers P et al (2000) Influence of stent design on 1-year outcome after coronary stent placement: a randomized comparison of five stent types in 1,147 unselected patients. Catheter Cardiovasc Interv 50:290–297

Kastrati A, Mehilli J, Dirschinger J et al (2001) Intracoronary stenting and angiographic results: strut thickness effect on restenosis outcome (ISAR-STEREO) trial. Circulation 103:2816–21

Kastrati A, Schomig A, Dirschinger J et al (2000) Increased risk of restenosis after placement of gold-coated stents: results of a randomized trial comparing gold-coated with uncoated steel stents in patients with coronary artery disease. Circulation 101:2478–2483

Kim RJ, Fieno DS, Parrish TB et al (1999) Relationship of MRI delayed contrast enhancement to irreversible injury, infarct age, and contractile function. Circulation 100:1992–2002

Kirklin JW, Brian G, Barratt-Boyes BG (1993) Cardiac Surgery. Churchill Livingstone

Kol A, Sukhova GK, Lichman AH, Libby P (1998) Chlamydial heat shock protein 60 localizes in human atheroma and regulates macrophage tumor necrosis factor-alpha and matrix metalloproteinase expression. Circulation 98:300–307

Kollum M, Farb A, Schreiber R et al (2005) Particle debris from a nanoporus stent coating obscures potential antiproliferative effects of tacrolimus-eluting stents in a porcine model of restenosis. Catheter Cardiovasc Interv 64(1):85–90

Koolen JJ, De Vita MR (2007) LEONARDO – Clinical evaluation of a last generation coronary stent in a real world typical Non-DES population – A prospective, single-centre registry. Report, Interventional Cardiology, pp 1–3

Koyama Y, Mochizuki T, Higaki J (2004) Computed tomography assessment of myocardial perfusion, viability, and function. J Magn Reson Imaging 19:800–815

Lansky AJ, Roubin GS, O'Shaughnessy CD et al (2000) Randomized comparison of GR-II stent and Palmaz-Schatz stent for elective treatment of coronary stenoses. Circulation 102:1364–1368

Leber AW, Knez A, von Ziegler F et al (2005) Quantification of obstructive and nonobstructive coronary lesions by 64-slice computed tomography. A comparative study with quantitative coronary angiography and intravascular ultrasound. J Am Coll Cardiol 46:147–154

Leon MB, Baim DS, Popma JJ et al (1998) A clinical trial comparing three antithrombotic-drug regimens after coronary-artery stenting. Stent Anticoagulation Restenosis Study Investigators. N Engl J Med 339:1665–1671

Libby P, Theroux P (2005) Pathophysiology of coronary artery disease. Circulation 111:3481–3488

Lin WS, Prakash VS, Tai CT et al (2000) Pulmonary vein morphology in patients with paroxysmal atrial fibrillation initiated by ectopic beats originating from the pulmonary veins: implications for catheter ablation. Circulation 101:1274–1281

Liuzzo G, Biasucci LM, Gallimore JR et al (1994) The prognostic value of C-reactive protein and serum amyloid a protein in severe unstable angina. N Engl J Med 331(7):417–424

Liuzzo G, Biasucci LM, Trotta G et al (2007) Unusual CD4+CD28null T lymphocytes and recurrence of acute coronary events. J Am Coll Cardiol 50(15):1450–1458

Maintz D, Juergens KU, Wichter T et al (2003) Imaging of coronary artery stents using multislice computed tomography: in vitro evaluation. Eur Radiol 13:830–835

Maintz D, Seifarth H, Flohr T et al (2003) Improved coronary artery stent visualization and in-stent stenosis detection using 16-slice computed-tomography and dedicated image reconstruction technique. Invest Radiol 38:790–795

Maseri A (2000) Ischemic heart disease. Churchill Livingstone and Saunders, New York

Mauri L, Hsieh WH, Massaro JM et al (2007) Stent thrombosis in randomized clinical trials of drug-eluting stents. N Engl J Med 356:1020–1029

McFadden EP, Stabile E, Regar E et al (2004) Late thrombosis in drug-eluting coronary stents after discontinuation of antiplatelet therapy. Lancet 364:1519–1521

Mehran R, Aymong ED, Ashby DT et al (2003) Safety of an aspirin-alone regimen after intracoronary stenting with a heparin-coated stent: final results of the HOPE (HEPACOAT and an Antithrombotic Regimen of Aspirin Alone) study. Circulation 108:1078–1083

Miketic S, Carlsson J, Tebbe U (2001) Randomized comparison of J&J Crown stent versus NIR stent after routine coronary angioplasty. Am Heart J 142:E8

Min JK (2006) Coronary CTA versus cardiac catheterization: where do we stand today? Applied Radiology 35(12):32–40

Moreno PR, Bernardi VH, Lopez-Cuellar J et al (1996) Macrophages, smooth muscle cells, and tissue factor in unstable angina. Implications for cell-mediated thrombogenicity in acute coronary syndromes. Circulation 94(12):3090–3097

Morgan-Hughes GJ, Roobottom CA, Marshall AJ (2002) Aortic valve imaging with computed tomography: a review. J Heart Valve Dis 11:604–611

Morice MC, Serruys PW, Sousa JE et al (2002) A randomized comparison of a sirolimus-eluting stent with a standard stent for coronary revascularization. N Engl J Med 346:1773–80

Moses JW, Leon MB, Popma JJ et al (2003) Sirolimus-eluting stents versus standard stents in patients with stenosis in a native coronary artery. N Engl J Med 349:1315–1323

Nageh T, de Belder AJ, Thomas MR et al (2001) A randomised trial of endoluminal reconstruction comparing the NIR stent and the Wallstent in angioplasty of long segment coronary disease: results of the RENEWAL Study. Am Heart J 141:971–976

Naghavi M, Libby P, Falk E et al (2003) From vulnerable plaque to vulnerable patient: a call for new definitions and risk assessment strategies: Part I. Circulation 108:1664–1672

Narducci ML, Grasselli A, Biasucci LM et al (2007) High telomerase activity in neutrophils from unstable coronary plaques. J Am Coll Cardiol 50(25):2369–2374

Naruko T, Ueda M, Hake K et al (2002) Neutrophil infiltration of culprit lesions in acute coronary syndromes. Circulation 106:2894–2900

Neri Serneri GG, Abbate R, Gori AM et al (1992) Transient intermittent lymphocyte activation is responsible for the instability of angina. Circulation 86(3):790–797

Nieman K, Pattynama PM, Rensin BJ et al (2003) Evaluation of patients after coronary artery bypass surgery: CT angiographic assessment of grafts and coronary arteries. Radiology 229:749–756

Nikolaou K, Knez A, Sagmeister S et al (2004) Assessment of myocardial infarctions using multirow-detector computed tomography. J Comput Assist Tomogr 28:286–292

Nikolaou K, Poon M, Sirol M et al (2003) Complementary results of computed tomography and magnetic resonance imaging of the heart and coronary arteries: a review and future outlook. Cardiol Clin 21:639–655

Ong AT, McFadden EP, Regar E et al (2005) Late angiographic stent thrombosis (LAST) events with drug-eluting stents. J Am Coll Cardiol 45:2088–2092

Ormiston JA, Serruys PW, Regar E et al (2008) A bioabsorbable everolimus-eluting coronary stent system for patients with single de-novo coronary artery lesions (ABSORB): a prospective open-label trial. Lancet 371:899–907

Pache G, Saueressig U, Frydrychowicz A et al (2006) Initial experience with 64-slice cardiac CT: non-invasive visualization of coronary artery bypass grafts. Eur Heart J 27:880–976

Pache J, Kastrati A, Mehilli J et al (2003) Intracoronary stenting and angiographic results: strut thickness effect on restenosis outcome (ISAR-STEREO-2) trial. J Am Coll Cardiol 41:1283–1288

Park SJ, Lee CW, Hong MK et al (2002) Comparison of gold-coated NIR stents with uncoated NIR stents in patients with coronary artery disease. Am J Cardiol 89:872–875

Park SJ, Shim WH, Ho DS et al (2003) A paclitaxel-eluting stent for the prevention of coronary restenosis. N Engl J Med 348:1537–1545

Perez-Lugones A, Schvartzman PR, Schweikert R et al (2003) Three-dimensional reconstruction of pulmonary veins in patients with atrial fibrillation and controls: morphological characteristics of different veins. Pacing Clin Electrophysiol 26:8–15

Perisinakis K, Theocharopoulos N, Karkavitsas N, Damilakis J (2002) Patient effective radiation dose and associated risk from transmission scans using 153Gd line sources in cardiac spect studies. Health Phys 83:66–74

Pilleul F, Merchant N (2000) MRI of the pulmonary veins: comparison between 3D MR angiography and T1-weighted spin echo. J Comput Assist Tomogr 24:683–687

Pope, JH, Aufderheide TP, Ruthazer R et al (2000) Missed Diagnoses of Acute Cardiac Ischemia in the Emergency Department. N Engl J Med 342:1163–1170

Rajtar A, Kaluza GL, Yang Q et al (2006) Hydroxyapatite-coated cardiovascular stents. Euro Intervention, pp 113–115

Rastogi A, Stavchansky S (2008) Drug eluting stents and beyond. Curr Pharm Des 14(21):2111–2120

Redberg R (2006) Computed tomographic angiography. More than just a pretty picture? J Am Coll Cardiol 49:1827–1829

Reifart N, Morice MC, Silber S et al (2004) The NUGGET study: NIR ultra gold-gilded equivalency trial. Catheter Cardiovasc Interv 62:18–25

Rioufol G, Finet G, Ginon I et al (2002) Multiple atherosclerotic plaque rupture in acute coronary syndrome: a three-vessel intravascular ultrasound study. Circulation 106(7):804–808

Rogacka R, Chieffo A, Latib A, Colombo A (2008) Bioabsorbable and biocompatible stents. Is a new revolution coming? Minerva Cardioangiol 56:483–491

Ropers D, Ulzheimer S, Wenkel E et al (2001) Investigation of aortocoronary artery bypass grafts by multislice spiral computed tomography with electrocardiographic-gated image reconstruction. Am J Cardiol 8:792–795

Rubinstein R, Halon DA, Gaspar T et al (2007) Usefulness of 64-slice cardiac computed tomographic angiography for diagnosing acute coronary syndromes and predicting clinical outcome in emergency department patients with chest pain of uncertain origin. Circulation 115:1762-1768

Sangiorgi GM, Clementi F, Cola C, Biondi-Zoccai G (2007) Plaque vulnerability and related coronary event prediction by intravascular ultrasound with virtual histology: "it's a long way to tipperary"? Catheter Cardiovasc Interv 70:203-210

Sangiorgi G, Melzi G, Agostoni P (2007) Engineering aspects of stents design and their translation into clinical practice. Annali dell'Istituto Superiore Sanità 43:89–100

Sano T, Tanaka A, Namba M et al (2003) C-reactive protein and lesion morphology in patients with acute myocardial infarction. Circulation 108(3):282–285

Schachinger V, Hamm CW, Munzel T et al (2003) A randomized trial of polytetrafluoroethylene-membrane-covered stents compared with conventional stents in aortocoronary saphenous vein grafts. J Am Coll Cardiol 42:1360–1369

Schampaert E, Cohen EA, Schluter M et al (2004) The Canadian study of the sirolimus-eluting stent in the treatment of patients with long de novo lesions in small native coronary arteries (C-SIRIUS). J Am Coll Cardiol 43:1110–1115

Schofer J, Schluter M, Gershlick AH et al (2003) Sirolimus-eluting stents for treatment of patients with long atherosclerotic lesions in small coronary arteries: double-blind, randomised controlled trial (E-SIRIUS). Lancet 362:1093–1099

Schomig A, Neumann FJ, Kastrati A et al (1996) A randomized comparison of antiplatelet and anticoagulant therapy after the placement of coronary-artery stents. N Engl J Med 334:1084–1089

Schonbeck U, Libby P (2001) CD40 signaling and plaque stability. Circ Res 89:1092–1103

Schroeder S, Achenbach S, Bengel F et al (2008) Cardiac computed tomography: indications, applications, limitations, and training requirements: report of a Writing Group deployed by the Working Group Nuclear Cardiology and Cardiac CT of the European Society of Cardiology and the European Council of Nuclear Cardiology. Eur Heart J 29:531-556

Schueller G, Schima W, Schueller-Weidekamm C et al (2006) Multidetector CT of pancreas: effects of contrast material flow rate and individualized scan delay on enhancement of pancreas and tumor contrast. Radiology 241:441–448

Schuijf JD, Bax JJ, Jukema JW et al (2004) Feasibility of assessment of coronary stent patency using 16-slice computed tomography. Am J Cardiol 94:427–430

Schultz RK. REVA Medical Inc (2007) Bioabsorbable stent. scientific session, late breaking trials, CRT, Washington DC

Schwartzman D, Lacomis J, Wigginton W (2003) Characterization of left atrium and distal pulmonary vein morphology using multidimensional computed tomography. J Am Coll Cardiol 41:1349–1357

Seifarth H, Raupach R, Schaller S et al (2005) Assessment of coronary artery stents using 16-slice MDCT angiography: evaluation of a dedicated reconstruction kernel and a noise reduction filter. Eur Radiol 15:721–726

Serruys PW, de Jaegere P, Kiemeneij F et al (1994) A comparison of balloon-expandable-stent implantation with balloon angioplasty in patients with coronary artery disease. Benestent Study Group. N Engl J Med 331:489–495

Sheiban I, Villata G, Bollati M et al (2008) Next-generation drug-eluting stents in coronary artery disease: focus on everolimus-eluting stent (Xience V) Vasc Health Risk Manag 4(1):31–38

Silber S (2003) Final results of the NIRTOP trial. Euro PCR Symposium, Paris, France

Solomon SB, Dickfeld T, Calkins H (2003) Real-time cardiac catheter navigation on three-dimensional CT images. J Interv Card Electrophysiol 8:27–36

Spagnoli LG, Bonanno E, Mauriello A et al (2002) Multicentric inflammation in epicardial coronary arteries of patients dying of acute myocardial infarction. J Am Coll Cardiol 40(9):1579–1588

Stabile E, Cheneau E, Kinnaird T et al (2004) Late thrombosis in cypher stents after the discontinuation of antiplatelet therapy. Cardiovasc Radiat Med 5:173–176

Stoeckel D, Bonsignore C, Duda S (2002) A survey of stent designs. Min Invas Ther & Allied Technol 11:137–147

Stone GW, Ellis SG, Cox DA et al (2004) A polymer-based, paclitaxel-eluting stent in patients with coronary artery disease. N Engl J Med 350:221–231

Tamai H, Igaki K, Kyo E et al (2000) Initial and 6-month results of biodegradable poly-l-lactic acid coronary stents in humans. Circulation 102:399–404

Tanajura LF, Abizaid AA, Feres F et al (2003) Randomized intravascular ultrasound comparison between patients that underwent amorphous hydrogenated silicon-carbide coated stent deployment versus uncoated stents (abstr). J Am Coll Cardiol 41:58A

Taylor AJ, Burke AP, Tang AL et al (2000) A comparison of the Framingham risk index, coronary artery calcification, and culprit plaque morphology in sudden cardiac death. Circulation 101:1243–1248

Thuesen L, Andersen HR, Krusell LR et al (2003) Randomized comparison of the coil-design Crossflex and the tubular NIR stent. Catheter Cardiovasc Interv 59:8–12

Tin Hay E, Hou XM, Lim J et al (2007) A novel drug-eluting stent using bioabsorbable polymer technology: Two-year follow-up of the CURAMI registry. Int J Cardiol

Unverdorben M, Sippel B, Degenhardt R et al (2003) Comparison of a silicon carbide-coated stent versus a noncoated stent in human beings: the Tenax versus Nir Stent Study's long-term outcome. Am Heart J 145:e17

van der Giessen WJ, Lincoff AM, Schwartz RS et al (1996) Marked inflammatory sequelae to implantation of biodegradable and nonbiodegradable polymers in porcine coronary arteries. Circulation 94:1690–1697

Vanhoenacker PK, Heijenbrok-Kal MH, Van Heste R et al (2007) Diagnostic performance of multidetector CT angiography for assessment of coronary artery disease: meta-analysis. Radiology 244:419–428

Virmani R, Kolodgie FD, Burke AP et al (2005) Atherosclerotic. plaque progression and vulnerability to rupture angiogenesis as a source of intraplaque hemorrhage. Arterioscler Thromb Vasc Biol 25:2054–2061

Willerson JT, Cohn J (2000) Cardiovascular medicine. 2nd ed, Churchill Livingstone and Saunders, New York

Windecker S, Simon R, Lins M et al (2005) Randomized comparison of a titanium-nitride-oxide-coated stent with a stainless steel stent for coronary revascularization: the TiNOX trial. Circulation 111:2617–2622

Wohrle J, Al-Khayer E, Grotzinger U et al (2001) Comparison of the heparin coated vs the uncoated Jostent – no influence on restenosis or clinical outcome. Eur Heart J 22:1808–1816

Wong P, Lau KW, Lim YL, Oesterle SN (2000) Stent placement for non-STRESS/BENESTENT lesions: a critical review. Catheter Cardiovasc Interv 51:223–233

Yasojima K, Schwab C, McGeer EG, McGeer PL (2001) Generation of C-reactive protein and complement components in atherosclerotic plaques. Am J Pathol 158(3):1039–1051

Yoo KJ, Choi D, Choi BW et al (2003) The comparison of the graft patency after coronary artery bypass grafting using coronary angiography and multi-slice computed tomography. Eur J Cardiothorac Surg 24:86–91